

**Manipulating the Sleeping Beauty Mutase
Operon in Engineered *Escherichia coli* for
Controlled Biosynthesis of 1-Propanol and Other
Value-Added Chemicals**

by

Kajan Srirangan

A thesis

presented to the University of Waterloo

in fulfillment of the

thesis requirement for the degree of

Doctor of Philosophy

in

Chemical Engineering

Waterloo, Ontario, Canada, 2016

©Kajan Srirangan 2016

AUTHOR'S DECLARATION

I hereby declare that I am the sole author of this thesis. This is a true copy of the thesis, including any required final revisions, as accepted by my examiners.

I understand that my thesis may be made electronically available to the public.

Abstract

A great fraction of the world's energy requirements are presently met through the unrestricted use of fossil-derived fuels. However, due to the anticipated demise of these energy sources and the environmental and socioeconomic concerns associated with their use, a recent paradigm shift is to displace conventional fuels with renewable energy sources. Although most resources in biofuels have been directed towards the implementation of bioethanol platforms, the advanced alcohol 1-propanol has recently received significant attention as a promising alternative biofuel. Compared to that of ethanol, 1-propanol has an energy density that is more comparable to gasoline and is far less hygroscopic and volatile. Nevertheless, no microorganism has been identified as a natural 1-propanol producer. Accordingly, in this thesis, we manipulated a novel metabolic pathway for the synthesis of 1-propanol in the genetically tractable bacterium *Escherichia coli*. *E. coli* strains capable of producing 1-propanol were engineered by extending the dissimilation of the tricarboxylic acid intermediate succinate to the C3 biogenic precursor propionyl-CoA. This was accomplished by activation of the dormant yet extant Sleeping beauty mutase operon genes (i.e. *sbm-ygfD-ygfG*).

In our initial studies, we developed propanogenic *E. coli* strains by episomally expressing selection of key genes, i.e. (1) three native genes in the sleeping beauty mutase (Sbm) operon (2) the genes encoding bifunctional aldehyde/alcohol dehydrogenases (ADHs) from various microbial sources, and (3) the *sucCD* gene encoding succinyl-CoA synthetase from *E. coli*. Using these triple-plasmid expression systems in *E. coli*, production titers up to 150 mg/L of 1-propanol were obtained in laboratory shake-flask growths under strict anaerobic conditions using glucose as the major carbon source.

Following the development of these plasmid-harboring propanogenic *E. coli* hosts, we systematically explored various biochemical, genetic and metabolic/physiological factors to potentially enhance 1-propanol production and productivity. It was found that 1-propanol production can be significantly improved in a bioreactor under anaerobic conditions by using glycerol as a carbon source using a single-plasmid system solely expressing the Sbm operon genes. This may in part be due to the high reductance degree of glycerol compared with the microbial cell biomass. Equally important, we also alleviated plasmid-induced metabolic burden by chromosomally activating the Sbm operon genes. This plasmid-free propanogenic strain allowed high-level coproduction of 1-propanol and ethanol (accounting for 85 % of dissimilated carbon) under anaerobic fed-batch cultivation using glycerol as the major carbon source.

To expand the chemical diversity and utility of our plasmid-free propanogenic *E. coli* strains, we explored the possibility of producing other value-added chemicals of biotechnological relevance derived from propionyl-CoA. We first examined the possibility of producing butanone, an important commodity ketone. To produce butanone, we developed a modular CoA-dependent chain elongation platform to fuse Sbm-derived propionyl-CoA and endogenous acetyl-CoA to form the C5 biogenic precursor 3-ketovaleryl-CoA. Next, 3-ketovaleryl-CoA was channeled into the clostridial acetone-formation pathway for thioester hydrolysis and subsequent decarboxylation. In also manipulating initial glycerol dissimilation in the engineered ketogenic *E. coli* strains, we achieved co-production of 1.3 g/L butanone and 2.9 g/L acetone under semi-aerobic batch cultivation with glycerol as the major carbon source.

In our final study we investigated the feasibility of using our developed propanogenic strains for the production of the bio(co)polymer poly(3-hydroxybutyrate-co-3-hydroxyvalerate) using unrelated carbon sources glycerol or glucose. (i.e. without exogenous supplementation of propionate or valerate). P(3HB-co-3HV) producing propanogenic strains were developed by first fusing two acetyl-CoA moieties or acetyl-CoA and propionyl-CoA generate the C4 and C5 thioesters 3-hydroxybutyryl-CoA and 3-ketovaleryl-CoA, respectively via a CoA-dependent chain elongation platform. Next, the resulting C4 and C5 thioesters intermediates were channeled into a polyhydroxyalkanoate biosynthetic pathway for subsequent thioester reduction and polymerization. In modulating various carbon sources, aeration regimes, and host-gene deletions, copolymers with 3HV fractions ranging from ~3 mol% to ~19 mol% were obtained.

Taken together, we have demonstrated that activating the Sbm operon not only transforms *E. coli* to be propanogenic, but also introduces an intracellular “flux competition” between the traditional C2-fermentative pathway (i.e. acetate and ethanol) and the novel C3-fermentative pathway (i.e. propionate and 1-propanol). Harnessing this flux and employing various modular chain elongation and pathway enzymes can open the avenue for the controlled production of various odd-chain organic acids, medium chain ketones, bio(co)polymers and other oleochemicals. Accordingly, the developed propanogenic *E. coli* strains and associated genetic and metabolic tools reported here expands the classes of chemicals that can be produced microbially via propionyl-CoA.

Keywords: Metabolic engineering, synthetic biology, Sleeping beauty mutase operon, value-added chemicals, biofuels, propionyl-CoA, 1-propanol, propionate, butanone, methyl ethyl ketone, poly(3-hydroxybutyrate-co-3-hydroxyvalerate), bio(co)polymers, glycerol

Acknowledgements

First and foremost, I would like to thank the University of Waterloo for providing me with a perfect environment for my undergraduate and graduate studies. I would like to also acknowledge the following people for their support during my doctoral studies.

I would like to extend my deepest gratitude to my supervisors Drs. C. Perry Chou and Murray Moo-Young for their support and guidance throughout my graduate studies. Professor Chou, you have been a wonderful mentor and friend over the past six years. Thank you for your faith in me, for your endless encouragement, and extraordinary patience. You are an inspiring engineer and scientist, and I have learnt many life-long lessons from you. It has been an honour to be your student and I will miss our conversations.

I would also like to take this opportunity to thank Dr. Marc Aucoin from the Department of Chemical Engineering. Professor Aucoin, thank you for providing me with the opportunity to work as an undergraduate student in your laboratory, serving as my teaching project supervisor, and your thought provoking suggestions and valuable contributions to my research.

I am immensely grateful to my PhD committee members – Professors Marc Aucoin, Bill Anderson and the late Jenö Scharer from the Department of Chemical Engineering and Professor Bernie Duncker from the Department of Biology – thank you for attending my comprehensive examination and thesis defense, and for also providing me with valuable suggestions and comments. Dr. Duncker, part of the reason I pursued this line of work was due to your undergraduate molecular techniques course. Thank you for also providing our laboratory with yeast genomic DNA over the past few years. I am also honored to have had Professor Akihiko Kondo from Kobe University serve as my external examiner and share his expertise at my thesis defense.

From the Faculty of Science, I would like to thank Drs. Barbara Moffatt, Christine Dupont, and Mario Coniglio, for being wonderful advisors during my undergraduate years at Waterloo and guiding me in the right direction. Dr. Moffatt, thank you for also providing me with the opportunity to work in your laboratory as a work-study student. Your early encouragement and enthusiasm not only set me on the right path but also fueled my love for molecular biology. I would also like to thank Dr. Cheryl Duxbury, for providing me with the opportunity to become a teaching assistant for many of her courses.

I would also like to thank the hard-working staff of the Department of Chemical Engineering, especially Rose Guderian, Ingrid Scherrer, Liz Bevan, Berthold Habicher, Rick Hecktus, Tom Dean, Judy

Caron and Ralph Dickhout. Judy, thank you for being a wonderful graduate advisor and helping me stay on track during my graduate studies. Ralph, I am grateful for all the techniques you have tirelessly taught me over the years.

In the Chou lab, I want to first and foremost thank Ian (Xuejia) for collaborating with me over the past three years to cultivate and characterize all our recombinant strains. I would also like to thank Michael for showing me various experimental techniques, for his guidance, and the friendship from him and his wife Summer. This work would also not have been possible without the help of all my other past and present lab mates – Karan, Daryoush, Victoria (Lin), Michelle (Yali), Lamees, Mark, Fred (Fan), Luyang, Valerie, Adam, Nimhani, Aaqil, Saideh, Bahram, Shane and Dragan. I am also deeply indebted for the hard work provided by all of our co-op students, especially Jane (Ying), Pulkit, Aleisha, Aprana, Kelly, Tina, Chinmayee, Kumar (Varun), Luvneet and Uchenna.

I would also like to extend my thanks to all past and present members of the Aucoin lab – Steve, David, Jimmy, Hanan, Stan, Eric, Anup, Ian, Dushanth, Joseph, Ben, Altamash, Jann, Sandi, Jian, Andreas, Meagan, and Julia. Specifically, I would like to thank David for introducing me to the Aucoin lab and for also brainstorming with me on my senior honor's thesis. Also a special thanks to Eric and Stan for their NMR work and metabolic profiling of our recombinant strains. And finally, Steve – it would take the writings of another thesis to highlight what an incredible friend (and roommate) you are.

On a personal note, I would like to thank my family and friends in Waterloo, Guelph and Scarborough for their constant love and support. I cannot thank my parents and my sister enough for all the sacrifices they have made to make this possible. To my father, for all the hard-work you have done over the years and for driving each week to see me in Waterloo. To my mother for not only working hard over the years to provide for us but for also always taking the time to talk to me about my thoughts, life, and school work. Thank you for encouraging me to always follow my dreams. There's no way I can pay you back – but I hope this thesis can serve as a thank you note for all that you have done. And of course Pranavy, one cannot ask for a better sister.

Lastly, and most importantly – I would like to acknowledge all my propanogenic *E. coli* strains. For without their contribution, I could not have done anything.

*I dedicate my dissertation work to my parents, and my loving sister
Pranavy.*

Table of Contents

AUTHOR'S DECLARATION.....	ii
Abstract.....	iii
Acknowledgements	v
Table of Contents	viii
List of Figures.....	xii
List of Tables	xiv
Abbreviations	xv
Chapter 1 Introduction.....	1
1.1 Research Objectives.....	3
1.2 Thesis organization	3
Chapter 2 Literature Review	5
2.1 Background.....	5
2.2 Biomass feedstock	8
2.2.1 First-generation feedstock.....	8
2.2.2 Starch crops.....	11
2.2.3 Sugar crops.....	11
2.2.4 Oilseed crops.....	12
2.3 Second-generation feedstock	12
2.3.1 Organic waste residues.....	13
2.3.2 Dedicated energy crops.....	13
2.4 Third-generation feedstock	14
2.5 Biomass conversion routes for the production of clean energy carriers	14
2.5.1 Biorefineries.....	14
2.5.2 Thermo-chemical conversion routes	15
2.5.3 Biochemical conversion routes	17
2.6 Clean energy carriers derived from acetyl-CoA	20
2.6.1 Bioethanol.....	22
2.6.2 Biodiesels.....	26
2.6.3 Biomethane	27
2.6.4 Biobutanol / 1-butanol	28

2.6.5 Other energy carriers.....	29
2.7 Harnessing propionyl-CoA metabolism for the production of biological fuels.....	31
2.7.1 Overview of propionyl-CoA metabolism.....	31
2.7.2 1-Propanol as a prospective biofuel	35
2.7.3 Overview of the Sleeping beauty mutase operon pathway genes	40
Chapter 3 Development of host-vector systems for 1-propanol production	44
3.1 Background.....	44
3.2 Methods.....	49
3.2.1 Plasmid construction	49
3.2.2 Bacterial strains and chromosomal manipulation	50
3.2.3 Media and cultivation.....	50
3.2.4 Analytical procedures	55
3.3 Results.....	56
3.3.1 Construction of propanogenic <i>E. coli</i> strains for 1-propanol production.....	56
3.3.2 Manipulation of cultivation conditions and NMR studies	59
3.3.3 Effects of various ADHs on 1-propanol production	63
3.3.4 Effects of host-gene deletions on 1-propanol production	64
3.4 Discussion.....	68
Chapter 4 Biochemical, genetic and metabolic engineering strategies to enhance co-	
production of 1-propanol and ethanol in engineered propanogenic <i>E. coli</i>	72
4.1 Background.....	72
4.2 Methods.....	76
4.2.1 Bacterial strains and plasmids.....	76
4.2.2 Media and cultivation conditions	77
4.2.3 Analyses.....	78
4.3 Results.....	83
4.3.1 Biosynthesis of 1-propanol using engineered <i>E. coli</i> strains	83
4.3.2 Glycerol serves as a superior carbon source for enhanced solventogenesis	86
4.3.3 Fedbatch cultivation for high-level coproduction of 1-propanol and ethanol.....	88
4.3.4 Derivation of plasmid-free propanogenic <i>E. coli</i> strains	93
4.4 Discussion.....	95

Chapter 5 <i>De novo</i> engineering of a recursive CoA-dependent carbon chain elongation platform for biosynthesis of butanone (methyl ethyl ketone) in propanogenic <i>E. coli</i>.....	101
5.1 Background.....	101
5.2 Methods.....	104
5.2.1 Bacterial strains and plasmids.....	104
5.2.2 Media and cultivation conditions.....	109
5.2.3 Offline analyses and metabolite detection.....	110
5.2.4 RNA extraction, microarray hybridization, and gene expression analyses.....	110
5.3 Results.....	111
5.3.1 Implementation of synthetic pathway for ketone production in <i>E. coli</i>	111
5.3.2 Engineering of <i>E. coli</i> to enhance ketone biosynthesis.....	114
5.3.3 Manipulating glycerol dissimilation to enhance ketone biosynthesis.....	116
5.4 Discussion.....	117
Chapter 6 Engineering propanogenic <i>E. coli</i> for direct biosynthesis of poly(3-hydroxybutyrate-co-3-hydroxyvalerate) using unrelated carbon sources	121
6.1 Background.....	122
6.2 Methods.....	125
6.2.1 Bacterial strains and plasmids.....	125
6.2.2 Media and cultivation conditions.....	129
6.2.3 Offline analyses and polymer extraction.....	130
6.3 Results.....	131
6.3.1 Direct biosynthesis of P(3HB-co-3HV) in <i>E. coli</i>	131
6.3.2 Cultivation conditions for P(3HB-co-3HV) biosynthesis.....	134
6.3.3 Metabolic engineering of fermentative pathways to enhance P(3HB-co-3HV) biosynthesis..	136
6.3.4 Manipulation of glycerol dissimilation to enhance P(3HB-co-3HV) biosynthesis.....	138
6.4 Discussion.....	140
Chapter 7 Original contributions and recommendations	145
7.1 Original contributions.....	145
7.1.1 Activation of the <i>Sbm</i> operon for the production of 1-propanol.....	145
7.1.2 Identification of glycerol as an efficient carbon source for the production of 1-propanol and the development of a plasmid-free propanogenic <i>E. coli</i> strain.....	145
7.1.3 Extending the <i>Sbm</i> pathway in engineered <i>E. coli</i> for the production of butanone.....	146

7.1.4 Extending the Sbm pathway in engineered <i>E. coli</i> for direct biosynthesis of poly(3-hydroxybutyrate-co-3-hydroxyvalerate)	146
7.2 Recommendations and future prospects	146
Appendix A Chapter 5 supplementary materials	150
Appendix B Chapter 6 supplementary materials	161
Bibliography	170

List of Figures

Figure 2.1: Model of carbon cycle illustrating how energy carriers are derived from biomass	6
Figure 2.2: Summary of various major biomass feedstock, conversion processes, and final products associated with biorefinery	9
Figure 2.3 The acetyl-CoA metabolic nexus	22
Figure 2.4: Major metabolic pathways for ethanol production from hexose and pentose sugars	24
Figure 2.5: Natural pathways associated with propionyl-CoA metabolism found in microorganisms	32
Figure 2.6: Propionyl-CoA acting as a precursor	35
Figure 2.7: Metabolic pathways for 1-propanol production in engineered <i>E. coli</i>	38
Figure 2.8: The Sleeping beauty mutase biosynthetic pathway and proposed 1-propanol production strategy in <i>E. coli</i>	42
Figure 2.9: The Sbm operon in <i>E. coli</i>	42
Figure 3.1: Metabolic engineering of <i>E. coli</i> for 1-propanol production.	47
Figure 3.2: A schematic representation of the triple-plasmid expression systems utilized for 1-propanol production.	48
Figure 3.3: The effect of cyanocobalamin concentration on 1-propanol production in strain WT-adhE2(CA) ³	60
Figure 3.4: End point secretion profile of major end products from anaerobic fermentations of WT-adhE2(CA) ³ at five optical densities (OD ₆₀₀), profiled by 1D- ¹ H-NMR.	61
Figure 3.5: Single dimension hydrogen NMR spectra scanned at 600 MHz from samples of <i>E. coli</i> supernatant from strain WT-adhE2(CA) ³	62
Figure 4.1: Schematic representations of the anaerobic 1-propanol production pathway (A).....	75
Figure 4.2: Genomic engineering for deriving the plasmid-free propanogenic strain CPC-PrOH3.	82
Figure 4.3: Time profiles of glucose, biomass, and major metabolites during batch cultivation of (A) CPC-CNTRL1 and (B) CPC-PrOH1 with glucose as the major carbon source.	84
Figure 4.4: Time profiles of glucose, biomass, and major metabolites during batch cultivation of (A) CPC-CNTRL2 and (B) CPC-PrOH2 with glucose as the major carbon source.	85
Figure 4.5: Time profiles of glycerol, biomass, and major metabolites during batch cultivation of (A) CPC-CNTRL2 and (B) CPC-PrOH2 with glycerol as the major carbon source.	87
Figure 4.6: Time profiles of the concentrations glycerol, biomass, and major metabolites during fedbatch cultivation of CPC-PrOH2 with glycerol as the major carbon source.	89

Figure 4.7: Time profiles of the concentrations glycerol, biomass, and major metabolites during fedbatch cultivation of CPC-PrOH3 with glycerol as the major carbon source.	94
Figure 4.8: Average metabolite excretion fluxes during each stage of CPC-PrOH3 cultivation.....	97
Figure 5.1: Schematic representation of the butanone biosynthetic pathway.	104
Figure 5.2: Synthetic biology strategies used for heterologous production of butanone in engineered <i>E. coli</i>	112
Figure 5.3: Constructing the biosynthetic pathway for ketone production in <i>E. coli</i>	113
Figure 5.4: Enhancing ketone production in engineered <i>E. coli</i>	115
Figure 6.1: Schematic representation of the synthetic biology and metabolic strategies used to establish the P(3HB-co-3HV) biosynthetic pathway in engineered propanogenic/propionogenic <i>E. coli</i>	125
Figure 6.2.: Establishing the biosynthetic pathway for P(3HB) and P(3HB-co-3HV) copolymer formation in propanogenic/propionogenic <i>E. coli</i>	133
Figure 6.3.: Cultivation conditions for enhancing 3HV incorporation in the copolymer.	135
Figure 6.4.: Metabolic engineering strategies enhance copolymer formation.	137
Figure 6.5.: Linking glycerol metabolism to P(3HB-co-3HV) biosynthesis in propanogenic/propionogenic <i>E. coli</i>	139
Figure 7.1: Putative metabolic pathways for the production of small chain volatile esters, C2-C4 alk(a/e)nes, and advanced ketones using propionyl-CoA as a key precursor.	148

List of Tables

Table 2.1: Potential benefits and technical limitations of biofuels	7
Table 2.2: Major characteristics of globally available biomass feedstock.....	10
Table 2.3: Major metabolic engineering approaches to enhance the production of bioethanol.....	25
Table 2.4: Major metabolic engineering approaches to enhance the production of 1-butanol	29
Table 2.5: A comparison of 1-propanol to other energy carriers	37
Table 2.6: Major metabolic engineering approaches to enhance the production of 1-propanol in engineered microbial platforms	39
Table 3.1: Hosts strains, plasmids and primers used in this study	51
Table 3.2: <i>E. coli</i> strains containing variants of the synthetic 1-propanol pathway used in this study.....	54
Table 3.3: 1-Propanol and other metabolite titers (mg/L) in reduced M9 minimal media using <i>E. coli</i> strain BW25141 transformed with appropriate plasmids.....	58
Table 3.4: Comparison of 1-propanol production titers and other metabolites (mg/L) by expression of several ADHs in <i>E. coli</i> strain BW25141, transformed with appropriate plasmids.....	66
Table 3.5: Secretion profile of the metabolites produced (mg/L) by various knock out strains..	67
Table 4.1: List of <i>E. coli</i> strains, plasmids, and primers used in this study..	79
Table 4.2: Culture performance (i.e. overall glycerol consumption and final biomass and metabolite concentrations) of fedbatch cultivation in a bioreactor for (A) CPC-PrOH ₂ and (B) CPC-PrOH ₃ using glycerol as the major carbon source.....	90
Table 5.1: Strains and plasmids used for butanone production in engineered <i>E. coli</i>	105
Table 6.1: List of <i>E. coli</i> strains, plasmids, and oligonucleotides used in this study.	126

Abbreviations

Δ :	Deletion
[]:	Denotes plasmid-carrier state
ABE:	Acetone-butanol-ethanol
<i>accAB</i> :	Genes encoding acetyl acetyl-CoA carboxylase
<i>ackA</i> :	Gene encoding acetate kinase
AD:	Anaerobic digestion
ADH(s):	Alcohol dehydrogenase(s)
<i>adhE</i> :	Gene encoding acetaldehyde dehydrogenase/alcohol dehydrogenase
<i>adhE1</i> :	Gene encoding bifunctional acetaldehyde-CoA/alcohol dehydrogenase
<i>adhE2</i> :	Gene encoding bifunctional acetaldehyde-CoA/alcohol dehydrogenase
<i>adhP</i> :	Gene encoding alcohol/acetaldehyde dehydrogenase, 1-propanol preferring
<i>aldBA</i> :	Genes encoding aldehyde dehydrogenase
Ap:	Ampicillin
<i>argK/ygfD</i> :	Gene encoding arginine kinase
ATF(s):	Alcohol- <i>O</i> -acetyltransferase(s)
<i>bdhB</i> :	Gene encoding butanol dehydrogenase
<i>bla</i> :	Gene encoding ampicillin resistance (Ap ^R) gene
<i>cI857</i> :	Gene encoding temperature-sensitive λ repressor
CB:	Consolidated bioprocessing
Cm:	Chloramphenicol
CSI:	Chemical shape indicator
DO:	Dissolved oxygen
DHA:	Dihydroxyacetone
<i>dhaKLM</i> :	Genes encoding dihydroxyacetone kinase
ED:	Entner–Doudoroff pathway
FAEEs:	Fatty acid ethyl esters
<i>fbxB</i> :	Gene encoding fructose-bisphosphate aldolase
<i>flp</i> :	Gene encoding <i>Saccharomyces cerevisiae</i> F1p recombinase
<i>frdABCD</i> :	Genes encoding fumarate reductase subunits
FRT:	F1p recombination target
<i>fumABC</i> :	Genes encoding fumarate hydratase subunits
FTS	Fischer-Tropsch Synthesis
G3P:	Glycerol-3-phosphate
<i>gapA</i> :	Gene encoding glyceraldehyde-3-phosphate dehydrogenase
GC:	Gas chromatography
<i>gldA</i>	Gene encoding glycerol dehydrogenase
<i>glk</i> :	Gene encoding glucokinase
<i>gloAB</i> :	Gene encoding glyoxalase I
<i>glpABC</i> :	Genes encoding the fermentative glycerol-3-phosphate dehydrogenase
<i>glpD</i> :	Gene encoding respiratory glycerol-3-phosphate dehydrogenase

<i>glpK</i> :	Gene encoding glycerol kinase
<i>gltA</i> :	Gene encoding citrate synthase
<i>gpmA</i> :	Gene encoding phosphoglyceromutase I
<i>gpsA</i> :	Gene encoding glycerol-3-phosphate dehydrogenase
HPLC:	High-performance liquid chromatography
<i>icd</i> :	Gene encoding isocitrate dehydrogenase
IPTG:	Isopropyl β -D-thiogalactopyranoside
<i>kan</i> :	Gene encoding Km ^R
Km:	Kanamycin
Km ^R -FRT:	Cassette carrying Km ^R marker
LB:	Lysogeny broth
<i>ldhA</i> :	Gene encoding lactate dehydrogenase
<i>mdh</i> :	Gene encoding malate dehydrogenase
MEK:	Methyl ethyl ketone (2-butanone or butanone)
<i>mgr</i> :	Gene encoding glyceraldehyde 3-phosphate reductase
<i>mgsA</i> :	Gene encoding methylglyoxal synthase
NMR:	Nuclear magnetic resonance
OAA:	Oxaloacetate
ORF:	Open reading frame
PEP:	Gene encoding phosphoenolpyruvate
<i>pepC</i> :	Gene encoding phosphoenolpyruvate carboxylase
<i>ppc</i> :	Phosphoenolpyruvate carboxylase
<i>pfkAB</i> :	Genes encoding 6-phosphofructokinase subunits A and B
<i>pflB</i> :	Gene encoding pyruvate formate lyase I
<i>pgi</i> :	Gene encoding glucosephosphate isomerase
<i>pgk</i> :	Gene encoding phosphoglycerate kinase
PHBV	Poly(3-hydroxybutyrate-co-3-hydroxyvalerate) also referred to as P(3HB-co-3HV)
<i>poxB</i> :	Gene encoding pyruvate dehydrogenase
<i>prpC</i> :	Gene encoding 2-methylcitrate synthase
<i>pta</i> :	Gene encoding phosphate acetyltransferase
<i>ptc</i> :	Gene encoding phosphoenolpyruvate carboxylase
<i>ptsG</i> :	Gene encoding glucose-specific phosphotransferase permease
<i>pyc</i> :	Gene encoding pyruvate carboxylase
<i>pykFA</i> :	Gene encoding pyruvate kinase
^R :	Resistant/resistance
^S :	Sensitive/sensitivity
<i>sbm/scpA</i> :	Gene encoding methylmalonyl-CoA mutase in <i>E. coli</i>
<i>sdhAB</i> :	Gene encoding succinate dehydrogenase
SHF:	Separate hydrolysis and fermentation
SSF:	Simultaneous saccharification and fermentation
SOE PCR:	Splicing by overlap extension PCR
<i>sucCD</i> :	Gene encoding succinyl-CoA synthetase subunits

Tc:	Tetracycline
TCA:	Tricarboxylic acid cycle
<i>tpiA</i> :	Gene encoding triosephosphate isomerase
<i>tetAR</i> :	Genes encoding Tc ^R and Tc repressor
<i>iktAB</i> :	Genes encoding transketolase
^{ts} :	Temperature sensitive
WT:	Wild type
<i>ygfG/scpB</i> :	Gene encoding methylmalonyl-CoA decarboxylase
<i>ygfH/scpC</i> :	Gene encoding propionyl-CoA:succinate-CoA transferase
<i>yqhD</i> :	Gene encoding aldehyde reductase

Chapter 1

Introduction

Due to the prognosticated demise of fossil fuel reserves in the years to come and the increasing environmental concerns associated with petrochemical-based processes, there is an ever-growing need for the development of whole-cell biocatalysts for the production of platform chemicals and fuels (1, 2). In addition to alleviating global reliance on fossil fuels, whole-cell biocatalytic platforms offer several technological advantages, such as providing absolute enantio- and regio-control on the configuration of the target compound and the ability to catalyze reactions with multiple chemical steps under ambient conditions (3). However, the applicability of natural biological systems is often limited due to inefficient or incompetent metabolic pathways. Accordingly, a present focus in metabolic engineering and systems biology is to expand the metabolic repertoire of genetically tractable host platforms (1, 4, 5). To improve the catalytic capacity and efficacy of microbial systems, it is often necessary to rewire host metabolism to ensure adequate supply of endogenous precursors and intermediary metabolites of the target compound. To date, significant progress has been made through the development of novel genetic and metabolic engineering strategies for efficient conversion of carbonaceous feedstock into acetyl coenzyme A (acetyl-CoA) (6, 7). Given that acetyl-CoA is ubiquitous as an acetyl transfer agent of the central metabolism in all living systems, it serves as a key intermediate for the production of numerous even-chain products. On the other hand, the endogenous production of propionyl-CoA, the three-carbon biogenic counterpart to acetyl-CoA, is uncommon and restricted to a limited number of phylogenetically diverse soil-dwelling microorganisms and commensals of the mammalian gut (8). In these organisms, propionyl-CoA is an intermediary molecule derived from a variety of pathways, such as thioesterification of propionate and dissimilation of odd-chain fatty acids or α -amino acids (e.g. L-threonine) (9). Accordingly, metabolic engineering approaches for implementation and overexpression of pathways for high-level propionyl-CoA biosynthesis in model microorganisms are still in their infancy. However, it is well recognized that tapping and harnessing propionyl-CoA metabolism can greatly expand the capacity for microbial synthesis of a wide variety of odd-chain compounds.

The primary focus of this thesis is to investigate an alternative biological production pathway toward 1-propanol from propionyl-CoA in the genetic tractable microorganism *Escherichia coli* by manipulating the endogenous sleeping beauty mutase (Sbm) operon genes. While ethanol, one of the most common and successful biofuels today, possesses established economic niches within energy markets, significant attention is being directed towards the production of longer-chain alcohols, such as 1-butanol

and 1-propanol (10, 11). These longer-chain alcohols tend to have a higher energy content, lower hygroscopicity, and water solubility; and are compatible with existing transportation infrastructures and pipelines (12).

The Sbm operon is a four-gene cluster (*sbm-ygfD-ygfG-ygfH*) that encodes various enzymes involved in a cobalamin-dependent metabolic pathway for decarboxylation of succinate into propionate (13). The metabolic context of the Sleeping beauty pathway remains ambiguous, but is suspected to be involved in the assimilation of unusual carbon sources, such as succinate and propionate. Moreover, eponymous to its name, the operon genes are hardly expressed possibly due to an inactive or weak promoter-operator system (14, 15). Three of the encoded proteins from this operon are identified to be members of the crotonase superfamily, namely (1) *sbm* encoding a cobalamin-dependent methylmalonyl-CoA mutase (or Sbm; Sleeping beauty mutase), which catalyzes the isomerization of succinyl-CoA to L-methylmalonyl-CoA; (2) *ygfG* encoding a methylmalonyl-CoA decarboxylase (YgfG), which catalyzes the decarboxylation of methylmalonyl-CoA to propionyl-CoA; and (3) *ygfH* encoding a propionyl-CoA:succinate transferase (YgfH) (16). The *ygfD* gene encodes a protein kinase (YgfD/ArgK) whose function remains unclear. Although the structure, function, and relationship of these enzymes have been characterized, hardly any work has been performed for their practical application.

The second portion of this thesis investigates the applicability of the Sbm-activated propanogenic *E. coli* strains for the production of other commodity chemicals of biotechnological relevance. The production of these target metabolites is made possible via molecular fusion (i.e. a Claisen condensation) of native acetyl-CoA and heterologous propionyl-CoA using highly promiscuous thiolases to generate the C5 biogenic precursor 3-ketovaleryl-CoA. Intracellular presence of 3-ketovaleryl-CoA expands the chemical diversity of the propanogenic *E. coli* strains and opens several possible avenues for the production of other longer-chain molecules, such as butanone (a medium chain ketone) and polyhydroxyalkanoate-based biopolymers.

1.1 Research Objectives

The chief objectives of this research can be described as follows:

- 1) Develop expression vector systems in *E. coli* to facilitate the production of 1-propanol.
- 2) Activation of the Sbm operon genes in the *E. coli* genome to generate plasmid-free propanogenic strains capable of high-level production of 1-propanol.
- 3) Optimize culture performance and 1-propanol productivity whilst suppressing by-product formation by investigating the application of established *E. coli* genetic tools for targeted gene knockout and knockin.
- 4) Establishing a CoA-dependent chain elongation platform in the propanogenic *E. coli* strains to enable *in vivo* biological synthesis of other higher-chain value-added chemicals.

1.2 Thesis organization

This thesis is comprised of six technical manuscripts corresponding to **Chapters 2-6**.

Chapter 2 provides a comprehensive literature review on current biomass transformation technologies and biofuel platforms, and an overview of the Sbm pathway and propionyl-CoA metabolism.

Following Chapter 2 – the thesis is presented in two parts. **Part I** details the use of engineered *E. coli* for the production of 1-propanol whereas **Part II** investigates the use of the engineered propanogenic *E. coli* strains for the production of other long-chain chemicals such as ketones and biological copolymers.

Chapter 3 encompasses the first step towards 1-propanol production in engineered *E. coli*. Here, a triple-plasmid expression system was used to express the Sbm operon genes and other essential genes for *de novo* synthesis of 1-propanol in *E. coli*. In addition to developing a host-vector system for 1-propanol synthesis, other genetic factors critically affecting the levels of 1-propanol are discussed.

Chapter 4 discusses the various biochemical, genetic and metabolic factors that were systematically explored to enable high-level anaerobic production of 1-propanol. Most importantly, this chapter discusses the work involved in the development of a plasmid-free propanogenic strain by activating the Sbm operon on the *E. coli* genome using a modified λ -Red recombination system. Systematic improvements were also made to improve the culture performance of these propanogenic strains in a bioreactor by fine-tuning the culture parameters and tailoring the cultivation media. It was found that

glycerol, with a higher-degree of reductance compared to that of glucose, was a far superior carbon source for the production of 1-propanol under anaerobiosis.

Chapter 5 details the development of a modular CoA-dependent chain elongation platform to enable molecular fusion of acetyl-CoA and propionyl-CoA to generate the C5 biogenic precursor 3-ketoaleryl-CoA in the engineered propanogenic *E. coli* strains. 3-Ketoaleryl-CoA was then channeled via the canonical clostridial acetone-formation pathway to enable production of butanone (also referred to as methyl ethyl ketone, or MEK). In this chapter, a comparative transcriptome analysis is also presented of propanogenic *E. coli* cultivated using glycerol and glucose. Using transcriptome analysis as a guide, several key genes in glycerol metabolism were targeted and knocked out to better link glycerol dissimilation and ketogenesis.

Chapter 6 investigates the applicability of the propanogenic *E. coli* strains and the CoA-dependent chain elongation platform for the direct production of the bio(co)polymer poly(3-hydroxybutyrate-co-3-hydroxyvalerate) using an unrelated carbon source of glycerol and glucose.

Chapter 7 concludes this thesis by providing an overview of the biochemical, genetic, and metabolic work performed throughout the entirety of this work. Recommendations and future prospects are provided as a means of further developing whole-cell biocatalytic platforms based on propionyl-CoA metabolism for the production of other products of biotechnological relevance.

Chapter 2

Literature Review

2.1 Background

Conventional fuels, primarily including coal, oil, and gas, are invaluable resources whose availability has been integral to the rapid technological progresses over the past few centuries. Currently, it is estimated that more than 85% of the world's energy requirements are supplied based on the utilization of conventional fuels (17). In addition to supplying energy, they are also an important feedstock for the majority of commodity products produced today (e.g., plastics and fabrics) (18). However, conventional fuels are non-sustainable and currently having two major issues, i.e. (1) the prognosticated demise of natural reserves in the years to come, (2) the substantial environmental impacts associated with their use. In light of the uncertainties, the recent fluctuating prices, and the environmental disturbances associated with the use of conventional fuels, a recent paradigm shift is to displace conventional fuels with sustainable, renewable, and environmentally-friendly/clean energy sources, among which biomass-derived energy appears to be the most attractive (18, 19). Interconversion of various biomass and energy forms in the carbon cycle is schematically illustrated in **Figure 2.1**. While biomass can be directly burned to obtain energy, it can also serve as a feedstock to be converted to various liquid or gas fuels for practical applications. Hence, a recent emerging strategy is to develop biorefinery and biotransformation technologies to convert renewable biomass feedstock into clean energy fuels and other commodities (20-22).

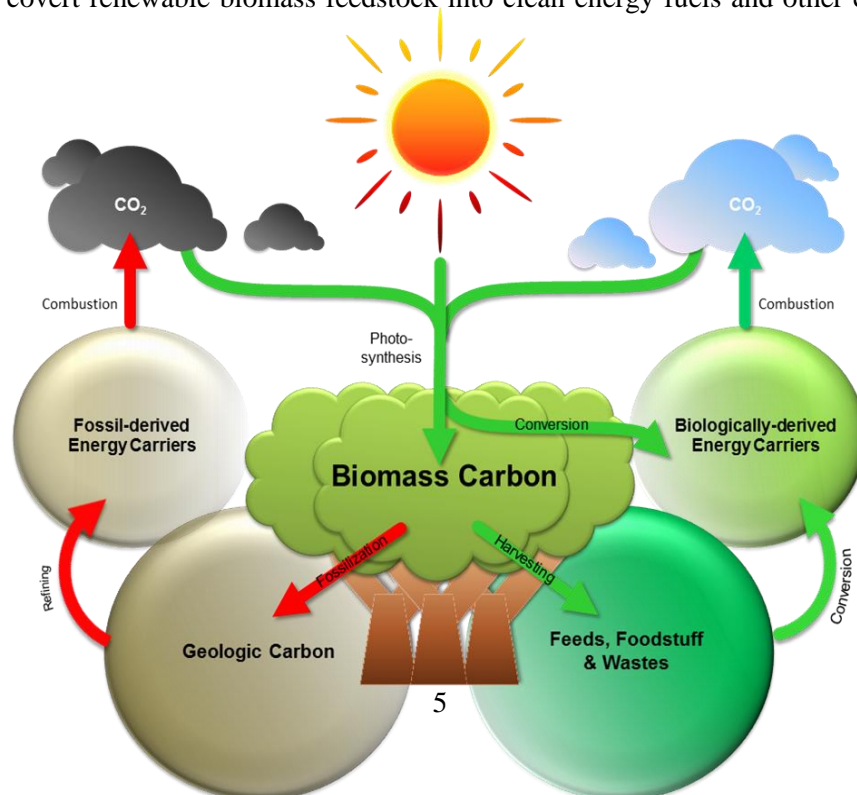


Figure 2.1 Model of carbon cycle illustrating how energy carriers are derived from biomass (*on previous page*)

Biomass carbon is generated via photosynthesis upon fixing atmospheric CO₂ with a simultaneous conversion of solar energy into chemical energy stored in biomass. Biomass carbon could be transformed into several energy carriers through either an environmentally amicable route (shown in green) or environmentally unfriendly route (shown in red). If biomass carbon, harvested crops, or wastes are converted into fuel, the process is renewable with no atmospheric CO₂ build-up. Conversely, biomass decomposed over several epochs (geologic carbon) can also be partially recovered and utilized. However, the later process is lethargic, non-sustainable, and potentially deleterious to the natural environment.

Biomass feedstock are energy sources derived from plants, microbial cells, and the wastes and residues associated with their processing (e.g. agricultural residues, forestry and municipal wastes). They are generally formed through photosynthesis, whereby plants (and some microbial cells) garner atmospheric CO₂ and sunlight to produce high energy carbonaceous compounds (i.e. biomass) and oxygen (19, 23). The dry biomass is a carbohydrate polymer containing carbon, hydrogen and oxygen in a ratio of approximately 1:1.4:0.6 (24). When the energy constrained within biomass is released, the carbon is oxidized to CO₂, which can be recycled to produce new biomass. Theoretically, no additional greenhouse gas is produced since the emitted CO₂ is part of the current carbon cycle. Therefore, if efficiently utilized, biomass is regarded as an alternative clean and renewable source for energy and other commodities due to its abundance (~100 and 50 billion tons of land and aquatic biomass, respectively, is produced on the Earth), high energy content, sustainability, biodegradability, and generation of recyclable exhaust gases. Moreover, the utilization of biomass-derived fuels will also greatly mitigate current energy security and trade balance issues, and foster socioeconomic developments for many rural communities in developing nations (**see Table 2.1**) (18, 19, 24). Nevertheless, given the recalcitrant nature of certain biomass feedstock and the current technological bottlenecks associated with various transformation processes, the economical feasibility of biomass-derived fuels are far too low to compete with the existing fossil fuel technologies. Therefore, recent advances in biotechnology and bioengineering are synergistically attempting to develop efficient biocatalysts (e.g. microbial fuel platforms) for the transformation of biomass into usable energy carriers.

Table 2.1: Potential benefits and technical limitations of biofuels

Potential Benefits	Technical Limitations
<p>Environmental gains</p> <ul style="list-style-type: none"> • Reduced dependency on environmentally damaging fossil fuels and petroleum products • Lowered levels of greenhouse gas (GHG) emissions • Reduced smog and toxic chemical emissions • Use of waste materials reducing the need for landfill sites <p>Economic benefits:</p> <ul style="list-style-type: none"> • Relatively inexpensive resources • Locally distributed energy sources provide constancy and reliability • More widely distributed access to energy • Price stability • Generation of employment opportunities in rural communities • Biomass and bio-energy technology export opportunities • Use of underutilized biomass resources as a renewable and inexhaustible fuel source 	<p>Environmental threats:</p> <ul style="list-style-type: none"> • Use of protected land for biomass production • Depleting local water supplies • High demand for fertilizers, herbicides and pesticides leading to an increase in air and soil pollution • Possibility of global climate change with increased atmospheric CO₂ production • Use of genetically engineered crops and microorganisms can possibly affect ecosystems • Reduced biodiversity due to soil pollution and/or industrial cultivation of favoured crop species • Increased particulate carbon emissions from wood burning <p>Associated technologies:</p> <ul style="list-style-type: none"> • Collection storage of feed stock • Pre-treatment of biomass • Enzyme production • Cost of technology manufacturing and maintenance

2.2 Biomass feedstock

Currently, biomass-derived energy sources supply ~50 EJ (exajoules) of the world's energy, which represents 10% of global annual primary energy consumption and ~75% of the energy derived from alternative renewable energy sources (25). Moreover, it is expected that biomass-derived energy may have to contribute ~1500 EJ by 2050. At this time, only 2% of the biomass-derived energy sources are utilized in the transportation sector whilst the rest is generally for household uses (26, 27). Transportation fuels derived from biomass (i.e. biofuels) can be produced using the feedstock of conventional agricultural crops (first-generation), lignocellulosic crops and unused agricultural wastes (second-generation) or microscopic organisms (third-generation) (28). Feedstock are categorized on the basis of the type of raw materials and transformation processes, and their features are compared in **Table 2.2** and **Figure 2.2**.

2.2.1 First-generation feedstock

First-generation feedstock are edible feedstock from the agricultural sector such as corn, wheat, sugarcane, and oilseeds. These basic feedstock are generally harvested with a high carbohydrate or oil content, and transformed into fuels such as biodiesel (bio-esters), alcohols, and biogas (mixture of CH₄ and CO₂). The biofuels based on the first-generation feedstock are normally derived through conventional technologies (delineated further in section 3). Conventional crops are already available in high quantities as these crops are produced in a large scale for human consumption and animal feed. Currently, three most popular edible feedstock that are exploited for biofuel production are sugar canes (in Brazil for bioethanol), corn (in the United States for bioethanol) and lastly rapeseed (in various European nations for biodiesel). While the use of edible feedstock content may potentially enhance the conversion and yield of biofuels from biomass, it tends to impact food prices (29).

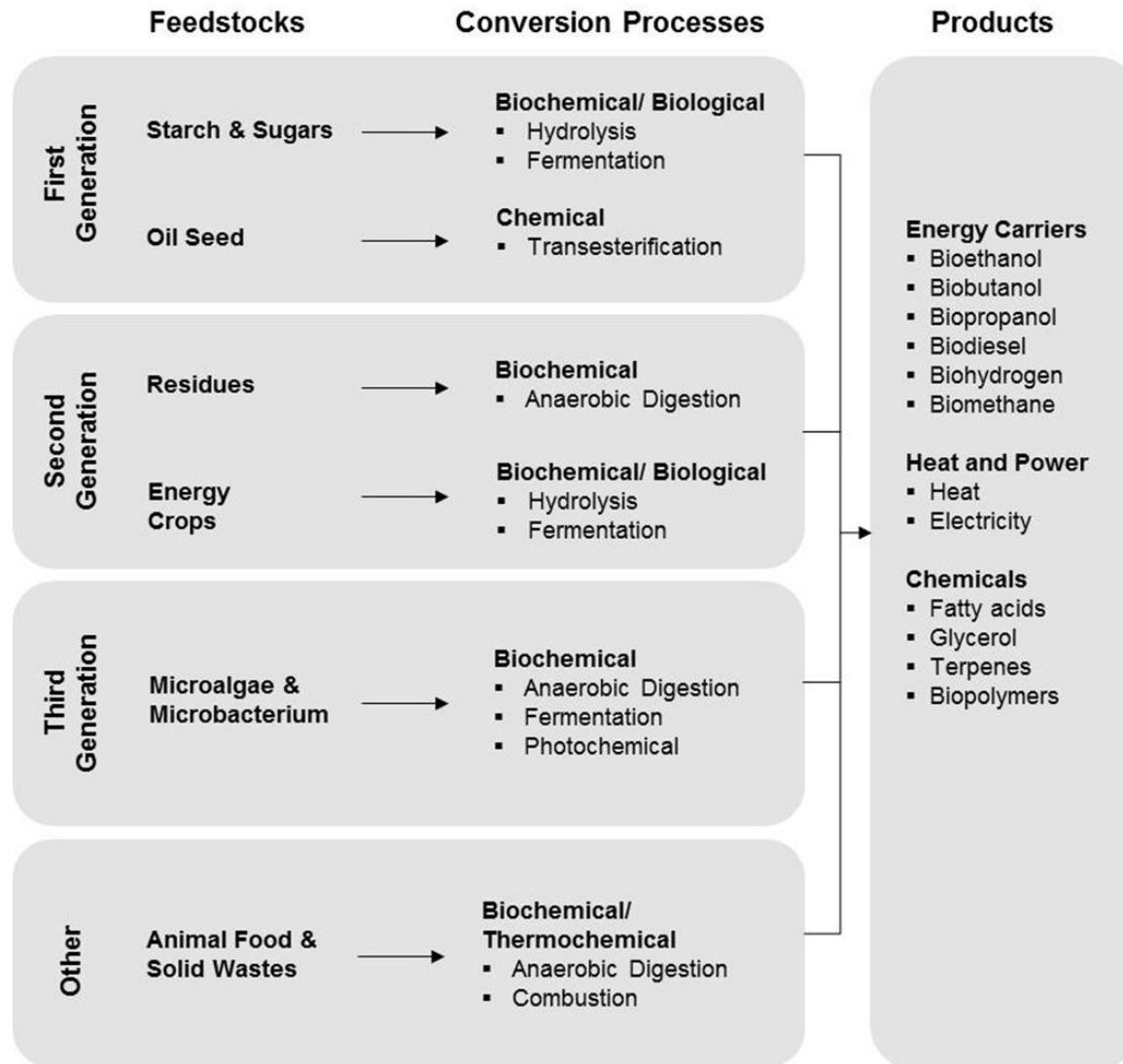


Figure 2.2: Summary of various major biomass feedstock, conversion processes, and final products associated with biorefinery

Table 2.2: Major characteristics of globally available biomass feedstock

Feedstock	Advantage	Development of Associated Technology	Limitation	Share of Total Renewable Energy in the World (%)	Share of Total Energy in the World (%)
First-generation (e.g.: food crops)	Excellent energy content	Relatively mature (e.g.: Bioethanol refineries)	Requires tropical arable land	~9	~1
Second-generation (e.g.: energy crops)	Devoid of competition with food industries	Relatively immature	Laborious and costly treatment technologies	~87	~10
Third-generation (e.g.: microbial cells)	Devoid of farming and land inputs	Immature	Low yield of energy carriers	~0	~0
Other (e.g.: municipal solid wastes)	No cost associated with feedstock	Mature (e.g.: Anaerobic digestion)	Size of feedstock inconsistent	~4	~0.5

2.2.2 Starch crops

Domesticated cereal grains and cultivated crops such as corn (maize), wheat, sorghum, cassava, and potatoes possess a high starch content and can be obtained in high yields if cultivated properly. Corn is the largest fuel crop for producing bioethanol and one of the most important agricultural crops globally principally because it utilizes a unique and highly efficient 'C4' photosynthesis system for carbon fixation. This photosynthesis system, in contrast to the conventional 'C3' one for most plants, yields a higher starch content (19, 28). The annual global production of corn grain is ~822 million MT (metric tons) annually with major producers being the United States, China, and some nations in southern Africa. Through genetic modifications, numerous desirable traits have been obtained to enhance of the crop production, such as resistance to various pathogens (e.g. *Bacillus thuringiensis* endotoxins) and stresses (e.g. drought and high salinity) (19, 28, 30). While wheat and rice are also important grains with a high starch content, their use to produce biofuels is uncommon as these crops are harvested primarily for human food consumption (28).

Two other important cultivated crops that may potentially be used for biofuel production are cassava and sorghum. Cassava is a perennial plant cultivated as an annual crop in the tropical and subtropical countries. The largest producers of cassava are currently various African and south Asian nations. It also possesses a high starch content, and is recognized as an alternative to corn and sugarcane for the production of bioethanol (28). Moreover, the cassava ethanol production schemes are compatible with current corn ethanol technologies and infrastructures. However, cassava cultivation is rather labor-intensive and the ethanol yield obtained from cassava is substantially lower than those from sugarcane and corn (28). Sorghum is cultivated in temperate-to-hot and dry regions and is the one of the most widely grown cereal crop in the world. It contains ~30 species providing human food, animal feed and forage, and sugar. As a 'C4 plant', it also has a high grain, starch, and biomass content, and thus is now being developed as a potential bioenergy crop (31). Its conversion process for biofuel production depends on the type and part of sorghum to be used. Multiple systems are available for biofuel production using starch from grain sorghum, stalk sugar from sweet sorghum, and cellulose from the crop residue. The properties of sorghum are also improved by conventional breeding and genetic approaches (31, 32).

2.2.3 Sugar crops

Sugarcane is a perennial grass commonly cultivated in the tropics and subtropics, with a annual worldwide production of ~1.74 billion MT. The largest producer of sugarcane is Brazil, followed by Australia, India, South Africa, and Thailand (19, 28). As a 'C4 plant' with a fast growth rate, fecundity,

and high sucrose content (~20%), it is the preeminent choice for biofuel production by supplying more than 40% of all fuel ethanol. With the advantages from its vast arable land, cheap feedstock price, and advanced agricultural technologies, Brazil has developed a green and sustainable sugarcane ethanol industry. Stem cutting has been the reproduction method for propagation with subsequent milling and biorefinery process to produce ethanol (19, 33). The byproduct and residue (bagasse and molasses) from sugarcane milling process are also useful for ethanol fermentation and power generation, making the net energy ratio of sugarcane ethanol relatively higher than corn ethanol. Other alternatives to sugarcanes are sugar beets and sweet sorghums. However these crops are generally not utilized for biofuel production owing to their low harvest yields and labor-intensive cultivation schemes (19, 33).

2.2.4 Oilseed crops

Oilseed crops such as rapeseed, soybean, sunflower, peanut, palm, coconut, safflower, linseed and hemp are valuable feedstock for the production of liquid biofuels (34). Aside from fuels, these oils may also be used for culinary purposes, as well as for deriving other commodities such as soaps, skin products, and perfumes. The unsaturated oils from these crops can be transformed by hydrogenation into fat with high melting points. More importantly, the vegetable oils yielded by these crops can be directly used in conventional or modified diesel engines, or can be refined via transesterification with a short-chain alcohol to produce alkyl (methyl, ethyl or propyl) esters, namely, biodiesels (35, 36).

2.3 Second-generation feedstock

Although the first-generation feedstock are attractive options for biofuel production in terms of their high sugar and starch composition, abundance in nature and combined ease of cultivation and processing, this production scheme is considered unsustainable. As the demand for renewable energy increases exponentially, the practicability of the production first-generation feedstock becomes tentative and limited since large arable croplands in tropical and temperate regions are required for their cultivation. Moreover, the direct competition of biofuels with human food and animal feed results in significant price increases of these crops. Second-generation feedstock are non-edible and comprise of raw materials derived from lignocellulosic biomass and crop waste residues from various agricultural and forestry processes (37, 38). These raw materials are far more ideal for fuel production since their utilization will not impact the food industry. Accordingly, second-generation feedstock can be cultivated in a large scale solely for the purpose of energy production. Cellulosic biomasses are also far more versatile than conventional energy crops and can be cultivated in a much wider range of soils and environments with comparable yields. Finally, if accrued crude agricultural and forestry residues are processed efficiently for biofuel

production, it will greatly reduce the current disposal problems associated with these materials. However, the conversion processes (i.e. thermo-chemical and biochemical conversions, see section 3) are far more complex and sophisticated because of the recalcitrant nature of cellulosic biomass, which is associated with the composition of tenaciously complex polysaccharides such as cellulose, hemicelluloses and lignins. Moreover, due to the present bottlenecks in the production scheme, second-generation feedstock are not cost-competitive with existing petroleum-derived fuels. In general, the second-generation feedstock can be categorized into two major groups, i.e. organic waste residues and dedicated energy crops (37, 39, 40).

2.3.1 Organic waste residues

Every year, approximately 40 dry tons per hectare of lignocellulosic residues are produced, most of which are underutilized. These lignocelluloses derived from an assortment of agricultural processes include corn cobs, corn stover, wheat straw, rice hulls, and cane bagasse. In many developing nations, these wastes are currently combusted for the generation of heat and electricity or for forage, or are ploughed back into croplands (28, 41). Considering their distributive variety, large quantity available, and high carbohydrate content, the energy potential of these residues is enormous. Nevertheless, it should be noted that the energy content of waste residues greatly varies from one crop to another. Among organic waste residues, woody wastes, i.e. the byproducts from logging operations, sawmill processes, pulp- and plywood factories, and the lumber industry, are also excellent feedstock for fuel production. Although biofuel production from woody biomass is still in its infancy, the importance of these feedstock has been perceived because of their high cellulose and low hemicelluloses composition (28, 41, 42).

2.3.2 Dedicated energy crops

With the substantially increasing demand for producing biofuels from the lignocellulosic feedstock in recent years, it becomes important to identify and cultivate crops exclusively for generating energy. Desired merits of energy crops include: fast growth rate, fecundity, high tolerance to various environmental stresses, high energy content, and relative ease of cultivation in comparison to grain crops. To date, the following energy crops are of great interest: perennial grasses (such as switch grass and *Miscanthus*) and woody energy crops (such as poplars, willows, and eucalyptus) (19, 33). Compared to conventional grain crops, these ‘short-rotation’ and fast-growing crops are excellent feedstock largely due to their superior growth on cold, wet or temperate soils with high annual biomass yield and their ability to be co-produced with grain crops in the same soil, a cultivation strategy known as “double-cropping” (19, 33).

2.4 Third-generation feedstock

While a wide collection of fermentative and photosynthetic bacteria and algae are currently being explored as biocatalysts, they are also recognized as excellent feedstock, so-called “third-generation feedstock”, primarily due to their high oil/lipid, carbohydrate, or protein contents. In comparison to the first- and second- generation feedstock, microbial cells can be obtained in high yields via bioreactors with no requirement of arable crop lands and other farming inputs (i.e. fertilizers, water, and pesticides) (38, 43). The impetus for exploring microalgae as an alternative energy source stems from its highly efficient photosynthetic systems for carbon fixation and carbohydrate production, and high lipid content (20-40% dry weight). Algal strains are capable of accruing oils through three types of production schemes, i.e. phototrophic (via photosynthesis), heterotrophic (via dissimilation of carbonaceous substrates such as glucose), or mixtropic (a mixture of phototrophic and heterotrophic). While the current algal-based oil production platform is technologically immature, a few genetically modified algal strains can produce oil with an extremely high yield (up to 75% dry weight). It is estimated that microalgae may produce ~10-300 times more oil (used for biodiesel production) than conventional and dedicated energy crops in near future (38).

2.5 Biomass conversion routes for the production of clean energy carriers

2.5.1 Biorefineries

Akin to petroleum-based refineries, bio-based refineries are facilities that integrate conversion processes based on the use of biomass feedstock to produce transportation fuels, direct power, high-value chemicals, and other useful commodities with minimal wastes and emissions. It is expected that in the future the product palette of a biorefinery will be significantly broadened. Three major types of conversion are often included in a typical biorefinery process, i.e. (1) thermo-chemical and mechanical conversions, (2) biochemical and biological conversions, and (3) physicochemical conversions. All these conversion routes are aiming to concomitantly deoxygenize and depolymerize the biomass feedstock to release monomeric sugar for subsequent conversions (29). Many of these conversion routes demand extensive pretreatment or upgrading of the feedstock (e.g. heat generated via combustion) due to the complex and recalcitrant nature of biomass, particularly lignocelluloses. Biorefineries are categorized into three groups, i.e. phase I, II, and III. Phase I biorefineries are of limited value as they utilize a single feedstock for the production of a single product. Phase II biorefineries also handle a single feedstock, but transform it through several conversion processes to produce multiple products. Phase III biorefineries are the most advanced ones aiming at employing numerous conversion processes to produce multiple

products with the use of a selection of feedstock (e.g. whole-crop biorefineries). Nevertheless, current biorefinery operations are not cost-competitive with traditional petroleum-based refineries since the costs of biomass feedstock and their transportation and processing are extremely high in comparison to crude oil. Strenuous research and development in biorefinery is also needed to improve the performance of transformation processes (21).

2.5.2 Thermo-chemical conversion routes

Thermo-chemical conversion involves treating the biomass with high temperatures in either an oxygenic or anoxygenic condition to promote structural degradation. There are four main thermo-chemical routes for the production of fuels, i.e. direct combustion, gasification, pyrolysis, and liquefaction; each differing in the temperature, heating rate, and oxygen level present during the treatment.

2.5.2.1 Direct combustion

The burning of biomass in an oxygen-rich environment has been one of the traditional methods for the generation of heat (and/or electricity) from biomass with the aid of a steam cycle (e.g. combustion boilers, steam turbines, power plants). Through combustion, the chemical energy from the biomass feedstock, such as fuelwood, agricultural (bagasse) and wood residues from the pulp and paper industry, and municipal solid wastes, can be harnessed. These feedstock are cheap, exist in large quantities, and generally contain a low water content for combustion (44, 45). Presently, different combustion systems, such as grate boilers and underfeed stokers, are available for the production of heat for large-scale industrial use (100-3000 MW) or for district heating (<100 MW). In regions that may demand both heat and electricity, cogeneration systems are also available through the use of steam turbines. With the advent of more advanced technologies such as fluidized bed combustion systems, the efficacy for power generation can be greatly enhanced with reduced emissions and increased tolerance to different types of biomass (42, 45). Although these advanced combustion systems may offer power outputs comparable to traditional carbonaceous fuels, the technology is currently not economically feasible due to the costs involved in the distribution networks and processing of high-moisture-content biomass. Moreover, direct combustion systems may not be a clean technology per se, as toxic emissions are potentially released from certain contaminated wastes (e.g. municipal solid wastes). Accordingly, future research and development should be geared towards improving energy outputs, broadening the range of usable feedstock, and reducing the release of harmful pollutants.

2.5.2.2 Gasification

Gasification is a thermo-chemical process where biomass is converted into a combustible gaseous mixture (e.g. syngas) under partial oxidation at high temperatures (800-900 °C) with gasification media such as air, oxygen or steam (45). The process is optimized to increase combustible gaseous components of CO, H₂, CH₄, and other gaseous hydrocarbons while minimizing char and tar formation (46). Four types of gasifiers are currently available for commercial use, i.e. fixed bed (counter-current and co-current), fluidized bed, and entrained flow. The performance of gasification processes is affected by different operation conditions, such as biomass flow rate, biomass properties, gasifying agent flow rate, and gasification temperature profile (47, 48). The generated gas mixtures are intermediate energy carriers that are either combusted for heat and power generation or processed further to synthesize transportation fuels (49). The conversion of syngas to liquefied fuels is referred as Fisher-Tropsch Synthesis (FTS) and dates back to the 1920s when coal syngas was used to produce hydrocarbons (e.g. gasoline and diesel). Syngas can be also used as a feedstock for the production of high-value chemicals (e.g. olefins and formaldehyde). Products derived via FTS vary greatly, depending on the catalyst types and process conditions (46, 50). One obstacle that limits large-scale application of gasification conversion technologies is the formation of tars and other undesired byproducts, thus gas cleaning is important to prevent catalyst poisoning before fuel synthesis (51).

2.5.2.3 Pyrolysis

Pyrolysis is a thermal process for biomass decomposition in the absence of oxygen with temperatures ranging from 350 °C to more than 800 °C (52). Temperature and residence time are key factors to control the composition of pyrolysis products. Three types of pyrolysis are applied, i.e. slow pyrolysis, fast pyrolysis, and flash pyrolysis (53), depending on the operation parameters such as heating rate, temperature, particle size, and residence time. Slow pyrolysis (also referred as conventional pyrolysis) of wood has been used to produce wood charcoal, whereas fast and flash pyrolysis are employed to produce bio-oils with various reactor schemes (53, 54). The major composition of bio-oils produced via pyrolysis are organic acids, esters, alcohols, ketones, phenols, aldehydes, alkenes, furfurals, sugars and some inorganic species (54). They are easier to transport and store than solid biomass and can also be converted into valuable chemicals, fuels, and distillates used in engines and turbines for power generation. However, there are numerous technical bottlenecks associated with the utilization of bio-oils as transportation fuels because of their crude and inconsistent nature, thermal instability, and corrosive properties. As a result, several strenuous upgrading steps are required to ensure the applicability of these bio-oils as

transportation fuels. Hydrodeoxygenation, catalytic cracking, emulsification, steam reforming, and chemical extraction are relevant techniques developed to improve the bio-oil quality (55).

2.5.2.4 Liquefaction

Liquefaction is a conversion process under a liquid phase with a low temperature (250-350 °C) and a high pressure (10-20 MPa), whereby biomass is catalytically broken down into fragments of light molecules in the presence of hydrogen. These unstable and active light fragments are subsequently re-polymerized into heavier oily compounds with appropriate molecular weights (56, 57). The process and products are analogous to pyrolysis except the use of lower temperatures and higher pressures. To prevent undesired side reactions and heavy solid char formation during re-polymerization, hydrogen and organic solvents are added into the reaction system (57, 58). Catalysts (e.g., alkaline hydroxides and carbonates) are crucial to lower the solid residue and improve the yield of bio-oils (58). To date, technological advances in liquefaction are still in its infancy and its economic feasibility is uncertain due to the high cost associated with the complex reactor and feeding system (59, 60).

2.5.3 Biochemical conversion routes

Biochemical conversions include a variety of chemical reactions catalytically mediated inside microorganisms as whole-cell biocatalysts and/or enzymes to convert fermentable feedstock substrates (e.g., monosugars) into fuels or other high-value commodities (39). They are one of the few conversion technologies that enable energy production in an environmentally friendly manner. While biochemical conversions are generally slow (taking days to weeks or even months) in comparison to the rapid thermo-chemical reactions (taking minutes to hours), these reactions produce less byproducts and pollutants. Thermo-chemical reactions, on the other hand, lack specificity and generally yield multiple and complex products. If implemented for large-scale biofuel production, biochemical conversions are considered more sustainable than thermo-chemical conversions, as these processes can be operated at a lower temperature with the use of a broader range of biomass feedstock. Feedstock for thermo-chemical processes often contain a low moisture content, whereas biological-derived processes can utilize both dry feedstock as well as those with a high moisture content such as herbaceous sugar and starch plants or livestock manures (29, 39). The two main biochemical processes for harnessing chemical energy from biomass are anaerobic digestion and microbial/enzymatic processes.

2.5.3.1 Anaerobic digestion

Anaerobic digestion (AD) is a biological process in which various bacterial species mediate in the decomposition of organic matters under anoxic conditions. The product from this process is biogas, which is a gas mixture containing mainly methane (60-70%) and carbon dioxide (20-40%). This process also occurs in many natural anoxic environments, such as watercourses, soils, animal intestines, and landfills. Currently, biogas is naturally produced in landfills and contributes greatly to accruing greenhouse gases in the troposphere. Such an environmental issue can be greatly ameliorated if naturally emitted biogas from anoxic reservoirs is efficiently harvested and processed. The crude biogas from AD can be burned for heat generation, and it is an invaluable and inexpensive energy source particularly in developing nations (61, 62). In addition to heat generation, purified methane can also be directly used in gas turbines for electricity generation or for use as a transportation fuel, similar to natural gas. In addition, AD produces a solid and liquid residue known as digestate, which can be used for soil conditioning and fertilizing (63).

A wide range of biodegradable waste materials can be applied to the versatile AD process (64, 65), such as agricultural waste, industrial waste, animal manure, sewage sludge, leftover food, municipal solid waste, pulp and paper residues, even microalgae waste after oil extraction (66). However, wood residues are less favorable in this process due to the difficulty in lignin degradation. Many of these feedstock are processed in anaerobic containers known as digesters, where feedstock and water are mixed. Digesters can range from 1 m³ for domestic units to as large as 2000 m³ for large-scale industrial installations (42, 62). Many considerations are crucial for optimization of AD (67), including reactor design, pretreatment, mixing, temperature, pH, buffering capacity, fatty acid concentrations, number of stages, monitoring and control systems. AD is a well-established technology widespread in numerous countries, such as China which is the largest biogas producer and user in the world (68, 69). While in Europe and North America, AD is less common, certain countries like Germany and the UK hold several thousand operation units (70). Ultimately, the sustainability and reliability of AD will greatly depend on the transportation costs of feedstock, the energy production efficiency, and the accessibility of biomass feedstock.

2.5.3.2 Microbial/enzymatic processes

2.5.3.2.1 Pretreatment

Feedstock costs often represent the largest portion (~40-70%) of the selling prices of biofuels. Although lignocellulosic feedstock are cheap and abundant, these recalcitrant feedstock contain complex chains of polysaccharides and other carbonaceous polymers that must be depolymerized prior to enzymatic hydrolysis. Depolymerization of lignocellulosic materials can be carried out physically (e.g., steam treatment), chemically (e.g., hydrolysis by acid or alkali), enzymatically or via a combination of these methods (71). Enzymes employed for the degradation of lignocelluloses include cellulase, hemicellulase, accessory enzymes (debranching enzymes), and lignin modifying enzymes. After the hemicellulose and lignin barriers to cellulose microfibrils are mitigated by physical and chemical pretreatments, crystalline cellulose is exposed for hydrolysis by cellulase enzymes, which generally include three classes of endo-cellulase, exo-cellulase, and cellobiase (72). The cellulases derived from cellulose-utilizing microorganisms are divided into two major categories: individual non-complex cellulases produced by aerobic bacteria and fungi and complex cellulase (or cellulosome) secreted by anaerobic bacteria and fungi (73). The efficiency of cellulose hydrolysis relies largely on the synergistic coordination of these enzyme activities to produce soluble sugar substrates.

2.5.3.2.2 Enzymatic hydrolysis

The production of cellulases is rather costly and thus has been identified as a potential bottleneck limiting the commercialization of lignocellulose biorefineries. Most commercially available cellulases are produced by *Trichoderma* or *Aspergillus* species. Being widely regarded as a model strain and industrial source of cellulases and hemicellulases (74, 75), *Trichoderma* has a high protein secretion ability and its genome has been sequenced recently (76). To enhance industrial biodegradation of cellulosic raw materials, recent research initiatives in cellulase-engineering have focused on improving specificity, catalytic activities, temperature and pH stability, and environmental tolerance. Rational design and directed evolution are two genetic strategies widely applied to improve cellulase activity (77). Since the information of the protein structure and catalytic mechanisms of cellulases remains limited, random mutagenesis followed by elaborate screening has been commonly employed to identify novel lignocellulose-degrading enzymes (78, 79). Recombinant cellulosomes, in which various complexes of heterologous cellulases are artificially assembled as scaffolding constructs, may also prove to be a breakthrough for cellulosic conversion (80). Advances arising from these genetic and protein engineering approaches have led to a great improvement in the enzymatic hydrolysis of lignocelluloses, reflected by a significant reduction in the cellulase cost associated with lignocellulosic ethanol production from more

than \$5 to approximately \$0.2 per gallon ethanol with more cost-effective expectation of less than \$0.1 per gallon ethanol (81).

2.5.3.2.3 Microbial fermentation

Monosugars derived from the hydrolysis of lignocellulosic materials or agricultural crops can be converted to various biofuels or high-value commodities via different fermentative and/or synthetic pathways using microbial cell factories. The first-generation feedstock are still the major feedstock source because of numerous unresolved technical issues associated with the utilization of lignocellulosic biomass (38). As a result, no industrial-scale microbial fermentation plant currently exists for the production of lignocellulosic biofuels. On the other hand, sugarcane- and corn starch-based bioethanol production plants were widely implemented in the United States and Brazil during the stagflation of the 1970s (71). Other clean biofuels produced based on microbial fermentation include methane, butanol, and hydrogen. These biofuels and the microorganisms associated with their production are detailed in Section 4.

Enzymatic hydrolysis and microbial fermentation are carried out either sequentially, i.e. separate hydrolysis and fermentation (SHF) process, or in parallel as a single-stage operation, i.e. simultaneous saccharification and fermentation (SSF) process. While the enzymes and microorganisms can function at their own optimal conditions in SHF processes, the operation is laborious and enzymatic hydrolysis may be incomplete due to the inhibition from the end products. As a result, the strategy of combining the two stages via SSF is adopted to reduce process complexity and overall cost and to increase process yield (82). Recently, a novel strategy has been proposed by combining cellulosic enzyme production and SSF, leading to a so-called consolidated bioprocessing (CBP) technology for simultaneous cellulase production, cellulose breakdown, and fermentation in a single bioreactor (83).

2.6 Clean energy carriers derived from acetyl-CoA

As mentioned in Chapter 1, given that acetyl-CoA is ubiquitous as a biogenic precursor of central metabolism in all living systems, it serves as a key intermediate of most biologically-derived energy carriers (see **Figure 2.3**). Accordingly, in this subsection, an overview is first presented of energy carriers derived from acetyl-CoA (e.g. ethanol and 1-butanol). Biohydrogen (derived from pyruvate) production strategies are also briefly highlighted. Next, an overview is presented of propionyl-CoA metabolism and biocatalytic platforms which utilize the propionyl-CoA nexus.

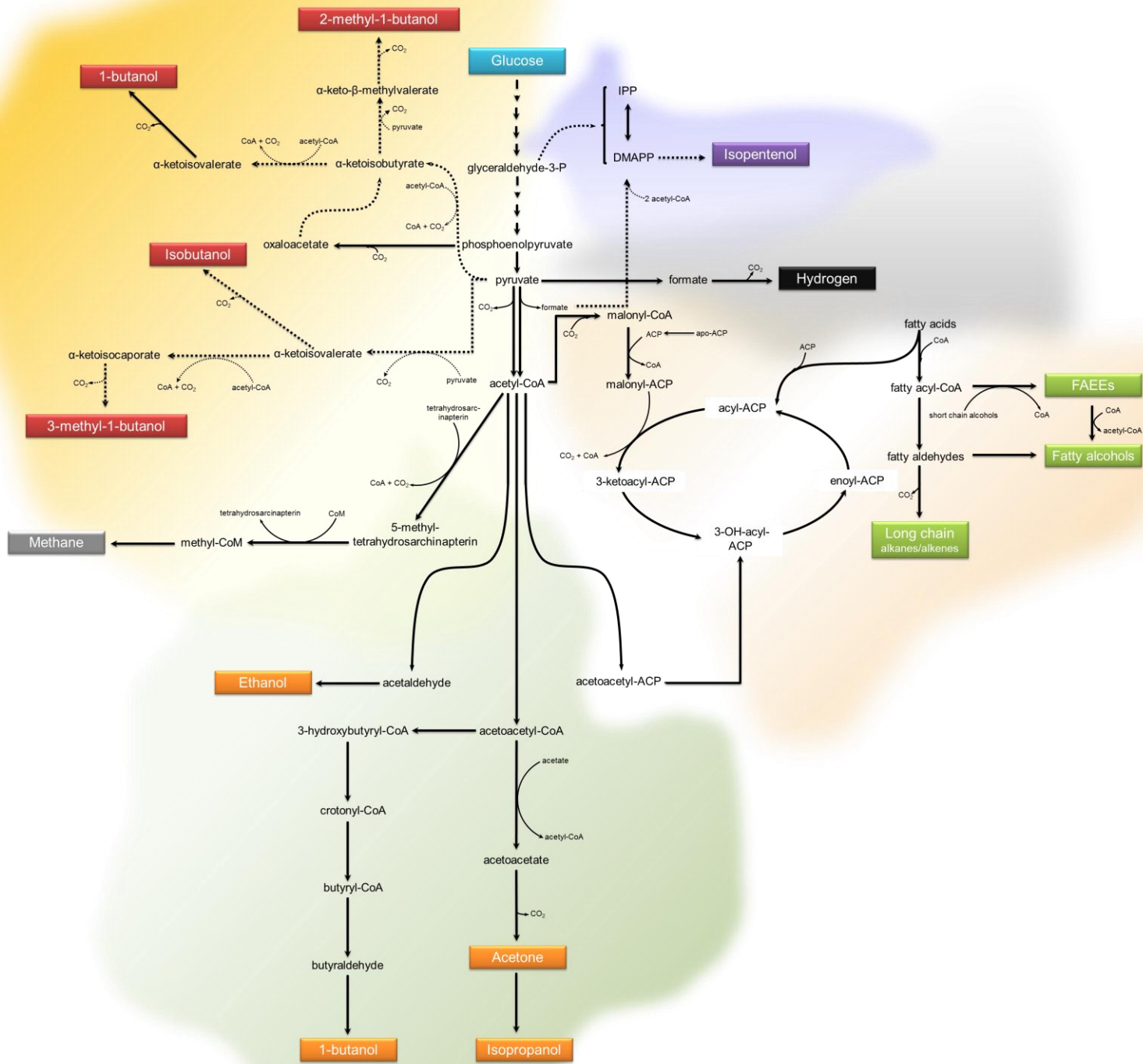


Figure 2.3 The acetyl-CoA metabolic nexus (*on previous page*).

General pathways for the production of several advanced liquid and gaseous biofuels from acetyl-CoA, adapted from (84, 85). (1) 2-ketoacid metabolic pathway for the production of various fuel alcohols (highlighted in red); (2) methanogenesis for the production of methane (highlighted in grey) from acetyl-CoA ; (3) clostridial pathway for the production of ethanol, and several fuel alcohols (highlighted in orange) from acetyl-CoA; (4) fatty acid pathway for the biosynthesis of FAEEs, fatty alcohols, and long chain alkanes and alkenes (highlighted in green); (5) hydrogen evolution (highlighted in black) from formate, an aspect of microbial dark fermentation; (6) isoprenoid (highlighted in purple) biosynthesis pathway. Abbreviations: ACP, acyl carrier protein; CoA, Coenzyme A; CoM, Coenzyme M; DMAPP, dimethylallyl pyrophosphate; FAEEs, fatty acids ethyl esters; IPP, isopentenyl pyrophosphate

2.6.1 Bioethanol

A major impetus for ethanol production through fermentation was initiated largely in response to the oil embargo of 1970's. Currently, two major fermentation platforms for ethanol production exist, i.e. the corn-ethanol program in the United States and the sugarcane-ethanol program in Brazil, with annual production of ~13 and ~7 billion gallons, respectively. Attractiveness of bioethanol as a transportation fuel stems from its high production efficiency, high octane rating (108), and GHG benefits. However, ethanol possesses several applicative limitations, i.e. the relatively low energy density and vapor pressure, the corrosive nature as a result of its hygroscopicity, and the incompatibility with existing fuel transportation infrastructures. Hence, bioethanol is not targeted as a key competitor to petroleum-derived fuels per se, but rather as a gasoline extender and an octane enhancer (19, 39).

Common feedstock harnessed for ethanol production comprise of the first-generation feedstock derived from sugar and starch crops and the second-generation lignocellulosic feedstock. While it is advantageous to convert lignocelluloses to ethanol, this production scheme is presently unrealistic because of the limited substrate spectrum for most microbial species and the recalcitrant nature of lignocellulosic materials. The genetically tractable baker's yeast, *Saccharomyces cerevisiae*, has become the preeminent choice to convert sugars derived from biomass for the production of ethanol based on its robust growth, high ethanol yield, and ethanol tolerance. Like most microbial species, wild-type *S. cerevisiae* is only capable of fermenting mono- and disaccharides of hexose sugars, such as glucose, sucrose, maltose, and fructose via glycolysis (**Figure 2.4**), but does not possess enzymes for hydrolyzing cellulose/hemicellulose or for fermentation of pentose sugars present in hemicellulose (i.e. xylose and arabinose) (86). Consequently, the first-generation feedstock are presently used for industrial production of bioethanol (71) with three primary operating stages: (1) mono- and disaccharides are released through either chemical or enzymatic hydrolysis, (2) ethanol fermentation using microbial cell factories such as *S.*

cerevisiae and other yeast, fungi or bacteria, (3) distillation for ethanol separation and concentration (71, 86).

The ethanologenic bacterium *Zymomonas mobilis* is another attractive cell factory for industrial production of ethanol. While *Z. mobilis* also lacks the ability to ferment pentose sugars, it has several appealing properties, including the ability to anaerobically metabolize glucose via the Entner-Duodoroff (ED) pathway (**Figure 2.4**), as opposed to glycolysis, and high tolerance to ethanol (~120 g/L). As a result, the bacterium produces ethanol with minimal byproduct formation, leading to ~5-10% higher ethanol yield in comparison to the traditional yeast-based microbial platform. Because the ED pathway has a lower ATP yield than glycolysis, *Z. mobilis* constitutively maintains a high glucose flux and produces less biomass than yeasts (86).

Enteric bacteria (e.g. *Escherichia coli*) and certain types of yeast (e.g. *Pachysolen tannophilus* and *Pichia stipites*) are potentially capable of metabolizing pentose sugars. However, pentose-fermenting yeasts are not suitable for large-scale bioethanol production due to the organisms' low ethanol yield, heightened sensitivity to ethanol (~ 40g/L), inability to ferment xylose in acidic environments, and strict requirement for microaerophilic conditions (86, 87). Enteric bacteria and yeasts possess different metabolic pathways for xylose dissimilation. In bacteria, xylose is first converted into xylulose by xylose isomerase (XI). In xylose-utilizing fungi and yeasts, xylose is converted to xylulose through a two-step conversion by xylose reductase (XR) and xylitol dehydrogenase (XDH). In both cases, xylulose is phosphorylated and dissimilated via the pentose phosphate pathway (PPP) (**Figure 2.4**) (71, 86-88).

Over the past two decades, metabolic engineering and genetic engineering strategies have played a pivotal role in broadening the substrate range of *S. cerevisiae*, *Z. mobilis*, and *E. coli* for more effective dissimilation of the pentose sugars and ethanol production (**Table 2.3**). Popular strategies that have been explored include: heterologously grafting the xylose catabolic pathway from *P. stipitis* into *S. cerevisiae*, incorporation of various pentose dissimilation genes from *E. coli* into *Z. mobilis*, and enhancing the ethanol competence of *E. coli* via knocking out various diverting pathways (e.g. lactate and formate formation pathways) and displacing the native fermentation pathway with the homoethanol pathway of *Z. mobilis* (40, 71, 86, 87). Other microbial candidates that may prove to be efficient ethanol producers in the future include genetically modified *Klebsiella oxytoca* strains and various *Clostridium* species (e.g. *C. thermocellum* and *C. thermosaccharolyticum*) that possess the ability to metabolize treated or even untreated lignocellulosic substrates (40, 71).

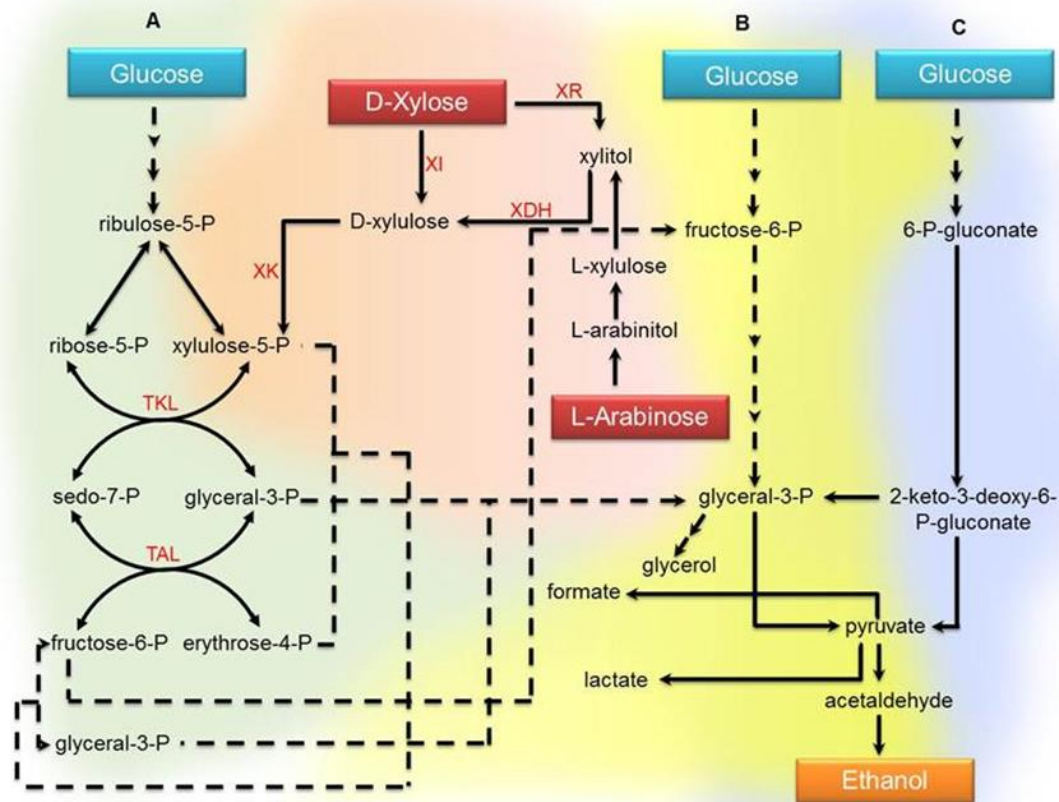


Figure 2.4 Major metabolic pathways for ethanol production from hexose and pentose sugars

(A) pentose phosphate pathway (PPP) with the inclusion of the xylose and arabinose dissimilation pathways, (B) glycolysis; and (C) Entner-Doudoroff (ED) pathway (87). Abbreviations: sedo-7-P, sedoheptulose-7-P; glycerol-3-P, glyceraldehyde-3-P; TKL, transketolase; TAL, transaldolase; XI, xylose

Table 2.3: Major metabolic engineering approaches to enhance the production of bioethanol

Cell factory	Carbon source	Genetic approach	Maximum ethanol titer (g l ⁻¹)	References
<i>S. cerevisiae</i> NRRL Y-50463	Glucose (50 g l ⁻¹) and xylose (50 g l ⁻¹)	Overexpression of key genes responsible for xylose utilization from <i>P. stipitis</i>	~38	Ma et al., 2012 (89)
<i>S. cerevisiae</i> MT8-1XS	Glucose (50 g l ⁻¹) and xylose (50 g l ⁻¹)	Overexpression of key genes responsible for xylose uptake and utilization from <i>P. stipitis</i>	~40	Katahira et al., 2008 (90)
<i>Z. mobilis</i> CP4	Glucose (25 g l ⁻¹) and xylose (25g l ⁻¹)	Overexpression of two genes responsible for xylose catabolism from <i>E. coli</i>	~24	Zhang et al., 1995 (91)
<i>Z. mobilis</i> A3	Glucose (25 g l ⁻¹) and xylose (25g l ⁻¹)	Overexpression of four <i>E. coli</i> xylose metabolic genes; strain further enhanced for xylose utilization via adaptive evolution	~50	Agrawal et al., 2011 (92)
<i>E. coli</i> KO11	Xylose (10 g l ⁻¹)	Replacement of the native fermentation pathway with a homo-ethanol pathway from <i>Z. mobilis</i>	~45	Tao et al., 2001 (93)
<i>K. oxytoca</i> M5A1	Glucose (20 g l ⁻¹) or xylose (20 g l ⁻¹)	Replacement of the native fermentation pathway with a homo-ethanol pathway from <i>Z. mobilis</i>	~46	Ohta et al., 1991 (94)
<i>K. oxytoca</i> P2	Microcrystalline cellulose (100 g l ⁻¹)	Chromosomally integrated genes responsible for homo-ethanol production from <i>Z. mobilis</i>	~36	Golias et al., 2002 (95)

For more sustainable production of bioethanol in the future, it is imperative to displace the first-generation feedstock with lignocellulosic biomass or other cheap non-food materials. Major operating stages for lignocellulosic ethanol production are similar to those for starch- or sugarcane-based ethanol production except lignocellulosic feedstock require tedious pretreatment prior to chemical/enzymatic hydrolysis. Barriers limiting industrial-scale production of lignocellulosic ethanol include the technical difficulties associated with the pretreating and hydrolytic steps as well as the ineptness of most microbial species for the assimilation of the pentose sugars. The pretreatment issues can be addressed by optimizing the operating conditions for effective breakdown of the lignocelluloses structure whilst minimizing the release of byproduct inhibitors. Also, the catalytic efficiency of cellulolytic and saccharolytic enzymes should be enhanced with the enzyme production cost being minimized.

2.6.2 Biodiesels

Biodiesels have properties closer to gasoline and petrodiesel so that they can be blended at high levels up to 30% (v/v) or even completely displace petrodiesels in certain vehicles. Currently, biodiesel-powered flexible-fuel vehicles are widely available in many countries (96). Similar to bioethanol, the production cost of biodiesel varies significantly, depending on the feedstock source and the scale of the plant. Biodiesel production from the first-generation feedstock (i.e., oilseeds which are abundant) is technically mature and commercially viable. The conversion is conducted through two main routes, i.e., transesterification, which is a simple catalytic process with oils and short-chain alcohols as reactants and hydrogenation, which is a process resembling oil refining. While hydrogenation produces renewable diesels of superior quality and free of particulates and byproducts (such as glycerol, which is a byproduct associated with the transesterification process), this process is technically limited by the degradation of hydrogenation catalysts (97). In addition to oils, fatty acids can serve as a potential reactant for biodiesel production. Since fatty acid biosynthesis is a natural pathway for energy storage in microorganisms, fatty acyl coenzyme A or fatty acyl carrier protein can be used as a starting molecule for the intracellular accumulation of fatty acids, which can be further esterified *in vivo* to form fatty acid ethyl esters (FAEEs; **Figure 2.3**) known as microdiesels with similar properties to biodiesels (98). Such a production pathway has been demonstratively implemented in *E. coli* for novel biodiesel production in a pilot scale (99, 100).

In addition to the land oil crops, algae represent a nascent platform to be actively exploited for biodiesel production as their harvested oils can be extracted for conversion into biodiesels. This production scheme is particularly attractive on the basis of the microorganisms' rapid growth rate, high photosynthetic efficiency, and high biomass production. The use of algal oils as a feedstock appears to be more effective in biodiesel production than land oil crops (38). The cultivation of algae can be conducted

in either open (e.g. ponds) or closed systems (e.g. bioreactors). Open systems are advantageous in that they are economical to operate and are scalable for mass cultivation. However, the risk of contamination allows the growth of only a few hardy algal strains with a low lipid content. In addition, the open process can suffer from evaporative losses, low photosynthetic efficiencies, and inadequate mixing, leading to low biomass yields. Closed systems, on the other hand, are expensive to establish and operate though they offer far superior biomass productivities. The three main types of closed systems are flat plate bioreactors, vertical bioreactors and tubular bioreactors (101, 102). A technical limitation for algal cultivation is that the high cell density often compromises the growth rate due to reduced illumination. To extract oil, algae cells are first harvested and disrupted through various mechanical and chemical treatments, which represent a major portion of the production costs. There are still many technical challenges to be overcome for the large-scale production of algal biofuels. In particular, genetic tools may lead to the construction of strains with desired characteristics, such as high oil contents. Nevertheless, the economic feasibility of algal biofuels might be achieved progressively by combining the fuel production with high-value byproducts for food and feed ingredients to hopefully meet the growing energy demand in the future (103, 104).

2.6.3 Biomethane

Biogas, with methane as the major component, is produced via anaerobic digestion based on the use of a wide range of feedstock, including agricultural wastes, municipal wastes, food wastes, and industrial and municipal waste waters. The conversion of methane from organic waste residues is carried out by a mixed community of microbes capable of catabolizing complex biopolymers and polysaccharides to form acetate, hydrogen, and formate via acetogenesis. Acetate is further converted to methane by methanogenic archaea, such as *Methanosarcina* spp. and *Methanosaeta* spp. (**Figure 2.3**) (71, 105). Apart from being a combusting source for heat and electricity generation, biogas can also be upgraded to refined biomethane, which can be injected into the natural gas networks for various alternative uses (106). While economical production of biogas is often limited by inconsistent quantity and quality of the feedstock, this conversion route has been experiencing significant development and deployment, particularly in light of more common use of biogas as a vehicle fuel in many countries like Sweden, Germany, India, China, USA (107). Nevertheless, the incentives for biogas as a vehicle fuel can be strengthened by reducing the production cost, improving the pertinent technology, and building the industry and commercial standards.

2.6.4 Biobutanol / 1-butanol

While bioethanol appears to be the most popular and successful biofuel in the market, it has numerous unfavorable attributes such as low energy content, incompatibility with the existing storage and distribution infrastructures, and hygroscopicity. Hence, various liquid biofuels, in particular C3-C8 fuels, are recently under exploration and 1-butanol seems to be an attractive alternative among them. 1-Butanol is a linear C4 alcohol potentially superior to ethanol as a transportation fuel due to its immiscible property, higher energy content, lower volatility, low hygroscopicity, and low corrosibility (108). While 1-butanol is primarily produced through chemical processes in commercial scales, biological routes based on microbial fermentation have been actively investigated over the past few decades. Microbial anaerobes, such as *Clostridium acetobutylicum* and other solventogenic *Clostridia*, are native 1-butanol producers owing to the microorganisms' unique pathway for ABE (acetone-butanol-ethanol) fermentation (**Figure 2.3**). ABE fermentation by *C. acetobutylicum* was previously explored as a potential production platform in the early 20th century, but was determined to be economically unfavorable as compared to chemical processes. In light of recent biotechnological advances and growing attention on biofuels, the applicative potential of this biological route is being reevaluated with the following major disadvantages to be overcome. First, similar to bioethanol production, the ABE fermentation platform suffers from the high cost of biomass feedstock. Second, conducting anaerobic cultivation is tedious, inconvenient, and expensive, particularly for large-scale production, and the associated 1-butanol recovery (e.g. distillation) is energy-intensive and costly. Third, *Clostridium* species often have a complex physiology that is not well understood and genetic tools and strategies for improving the productivity of these species are still under development (108-110).

Technological advances in genetic engineering and metabolic engineering have offered a promise to genetically tailor *Clostridium* species to overcome the aforementioned limitations. Among various solventogenic *Clostridia*, *C. acetobutylicum* and *C. beijerinckii* strains have served as model microorganisms for metabolic engineering because of the establishment of key genetic tools, such as transformation techniques, integrative and shuttle vectors, and targeted gene disruption methods (108). Rational metabolic engineering approaches (**Table 2.4**) include the disruption of pathways diverting the 1-butanol flux (e.g. butyrate, acetone, lactate, and acetate formation pathways), overexpression of genes encoding key enzymes to enhance 1-butanol yield, genetic manipulation to improve 1-butanol tolerance, and lastly the introduction of exogenous genes to broaden substrate specificity (108, 109).

Table 2.4: Major metabolic engineering approaches to enhance the production of 1-butanol

Cell factory	Genetic approach	Maximum 1-butanol titer (g l ⁻¹)	References
<i>C. acetobutylicum</i> EA 2018	Disruption of the acetone pathway via Targetron gene knockdown system	~14	Jiang et al., 2009 (111)
<i>C. acetobutylicum</i> M5	Overexpression of several key genes responsible for butanol production in a solvent-negative strain	~11	Lee et al., 2009 (112)
<i>C. acetobutylicum</i> ATCC 824	Thiolase/alcohol dehydrogenase overexpression and down-regulation of key gene involved in acetone-formation pathway	~13	Sillers et al., 2008 (113)
<i>C. beijerinckii</i> NCIMB 8052	Overexpression of two exogenous glycoside hydrolases to broaden substrate specificity	~5	López-Contreras et al., 2001 (114)
<i>C. acetobutylicum</i> ATCC 824	Overexpression of several heat-shock proteins to improve butanol tolerance	~17	Tomas et al., 2003 (115)

To circumvent the innate limitations of *Clostridium* species, numerous synthetic biology strategies based on heterologously grafting the 1-butanol production pathway into the genetically amenable host of *E. coli*, which is a non-native 1-butanol producer. These approaches appear to be powerful enough, particularly in tandem with metabolic engineering strategies, to develop novel production strains with 1-butanol titers up to 30g/L (12, 116, 117). On the other hand, reconstructing the clostridial 1-butanol pathway in other non-native host producers, such as *Pseudomonas putida* (118), *Bacillus subtilis* (118), *Lactobacillus brevis* (119), and *S. cerevisiae* (120), often leads to low titers.

2.6.5 Other energy carriers

2.6.5.1 Biohydrogen

In addition to being an important material in the chemical industries, hydrogen is also an excellent and clean energy carrier with a high heating content (i.e., 141.8 kJ/g, which is almost 3 times that of gasoline) and with no CO₂ emission upon burning. Currently, more than 95% of the hydrogen is derived from fossil fuels and electrolysis. The use of abundant biomass feedstock, including dedicated energy crops and organic wastes, for hydrogen production has garnered tremendous interests (121, 122). Transformation for biohydrogen production is often carried out via biophotolysis (in green algae and cyanobacteria), photo-

fermentation (in purple non-sulfur bacteria), and dark fermentation (in anaerobic bacteria, **Figure 2.3**) (123, 124). Though the biological platforms are considered more environmentally friendly and less energy intensive for hydrogen production, they are not technically mature and economically feasible to compete with traditional chemical or electrochemical processes (125). So far, gasification and fermentation of waste biomass are two practical systems for biohydrogen production and further development is needed to overcome the efficiency and economic challenges, particularly in the aspect of identifying cheaper feedstock (121).

2.6.5.2 Butanol isomers and other advanced fuels

Other synthetic biology strategies based on biocatalytic rearrangement of 2-keto acid intermediates from the amino acid biosynthetic pathways (**Figure 2.3**) via decarboxylase and dehydrogenase have been applied to engineer *E. coli* strains for the production of non-native short-chain alcohols, including 1-butanol, isobutanol, 3-methyl-1-butanol, and 2-methyl-1-butanol (10). Similar strategies have also been implemented in other microbial cell factories, such as *Corynebacterium glutamicum*, *Clostridium cellulolyticum*, and *Synechococcus elongatus*, for the production of longer chain alcohols (10, 11, 126). Isoprenoid compounds are generally synthesized from isoprenyl pyrophosphate and dimethylallyl pyrophosphate (**Figure 2.3**) (127) and isoprenoid-derived fuels or precursors, such as branched-chain and cyclic alkanes, alkenes and alcohols, could be produced in *E. coli* through isoprenoid biosynthesis pathways (11, 127). Several clostridial species are also natural producers of isopropanol (e.g. *C. isopropylicum*) (**Figure 2.3**), but these microorganisms are not suitable for large-scale production due to the low isopropanol yield. Akin to the above synthetic biology strategies, recent efforts have concentrated on heterologously transplanting the clostridial isopropanol pathway into *E. coli* to enhance the production of isopropanol with reported titers as high as 140 g/L (11, 128-130).

2.6.5.3 Biomethanol and its derivatives

Due to its abundance over other conventional biofuels such as bioethanol and 1-butanol, biologically-derived methanol has also garnered tremendous interest from researchers. Although traditionally biomethanol is produced via a non-sustainable and cost-intensive chemical process involving catalytic steam reforming of natural gas, it is also possible to produce this fuel in an environmentally benign manner using biomass resources. Biologically, methanol can be produced through either the distillation of woody material via pyrolysis, gaseous products (i.e. biohydrogen and CO) from bio-oil, or syn-gas from cheap waste biomass and woody material. Nonetheless, given that the yield obtained from these resources is quite low (particularly biohydrogen), biomethanol production processes are not economically viable at

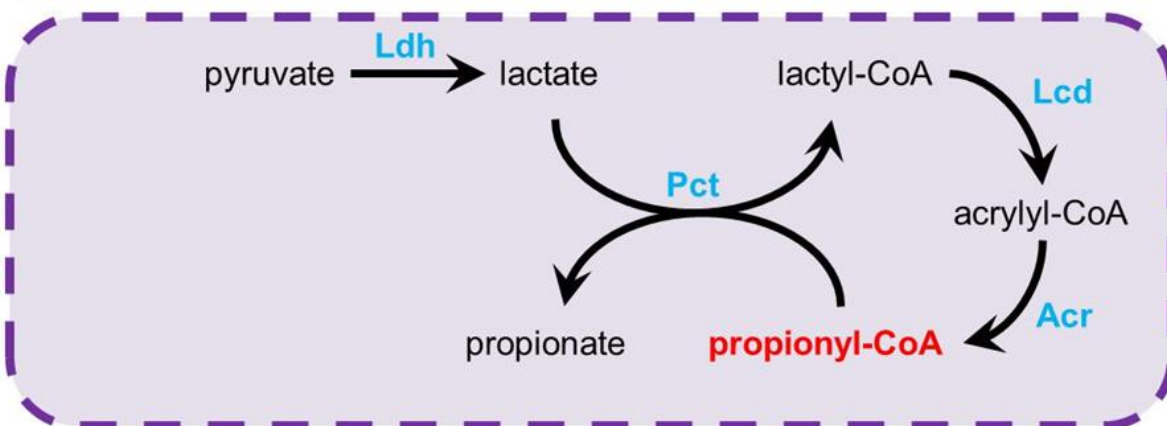
an industrial-scale as of yet. If these production processes for biomethanol production can be improved in the foreseeable future, it can be a valuable fuel with multiple applications. First and foremost, it can be used as a motor fuel in conventional engines in its pure form or as a blend with gasoline with an excellent emission profile. It is also possible to directly convert methanol to gasoline as well. Second, it can be converted to MTBE (methyl tert-butyl ether), an additive to gasoline. While MTBE is a formidable fuel additive and enhancer, its production process involves using isobutylene, a product derived from fossil fuels. Third, it can be dehydrated to produce DME (dimethyl ether), a suitable replacement for natural gas. Lastly, owing to its reactivity, it can be used as a raw material in the production of biodiesel (as FAME, fatty acid methyl esters).

2.7 Harnessing propionyl-CoA metabolism for the production of biological fuels

2.7.1 Overview of propionyl-CoA metabolism

In prokaryotes, two canonical routes toward propionyl-CoA formation exist. In the first one, i.e. the acrylate pathway (**Figure 2.5A**), lactoyl-CoA (activated from lactate) is dehydrated by lactoyl-CoA dehydratase to acryloyl-CoA, and subsequently reduced by the acryloyl-CoA reductase complex to propionyl-CoA. This pathway is endogenous to selected amino-acid utilizing clostridia, such as *Clostridium propionicum*. The second route involves the methylmalonyl-CoA pathway (**Figure 2.5B**) (131). This cyclic pathway is generally confined to Gram-positive propionic acid bacteria (of the genus *Propionibacterium*) and relies on the synthesis of oxaloacetate by one of two enzymes, i.e. pyruvate carboxylase and methylmalonyl-CoA carboxytransferase, which catalyze the transfer of the carboxyl moiety from (*S*)-methylmalonyl-CoA to pyruvate, concomitantly generating oxaloacetate and propionyl-CoA (132). It is still unclear as to why these pathways for propionyl-CoA synthesis are not conserved among microbial communities. As propionyl-CoA is toxic at high concentrations, most organisms have evolved to prevent intracellular accumulation of propionyl-CoA (8, 133). Furthermore, one of the key enzymes for the conversion of succinyl-CoA to propionyl-CoA is methylmalonyl-CoA mutase (**Figure 2.5B**), whose activity requires a vitamin B₁₂-derived prosthetic group, adenosylcobalamin, to function. Given that most microbial systems do not possess the ability for *de novo* synthesis of cobalamin, exogenous provision of it as the vitamin precursor is required to utilize this pathway (16).

(A) Acrylate pathway



(B) Methylmalonyl-CoA pathway

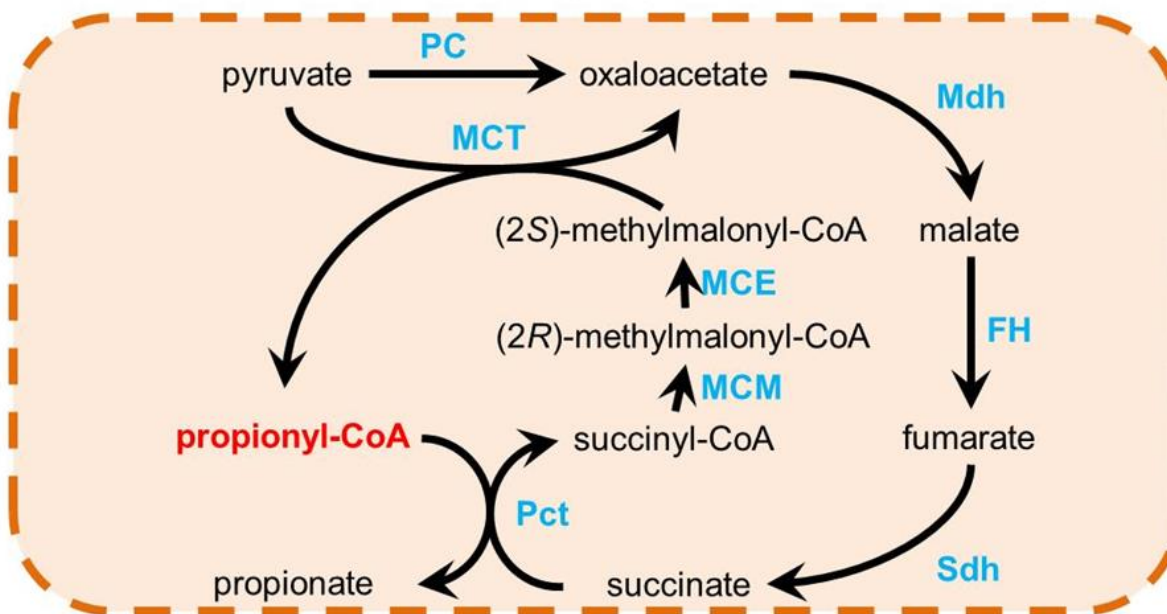


Figure 2.5: Natural pathways associated with propionyl-CoA metabolism found in microorganisms
(A) The acrylate pathway of *Clostridium propionicum*. (B) The methylmalonyl-CoA pathway of propionic bacteria. Key enzymes in the pathways are: Ldh, lactate dehydrogenase; Pct, propionyl-CoA transferase; Lcd, lactyl-CoA dehydratase; Acr, acrylyl-CoA reductase; PC, pyruvate carboxylase; Mdh, malate dehydrogenase; FH, fumarate hydratase; Sdh, succinate dehydrogenase; MCM, methylmalonyl-CoA mutase; MCE, methylmalonyl-CoA epimerase/isomerase; MCT, methylmalonyl-CoA carboxytransferase.

Various strategies have been developed to increase the intracellular level of propionyl-CoA as a precursor for biosynthesis of not only 1-propanol but a range of other value-added products (e.g. propionate, polyketides, and biological co-polymers) (**Figure 2.6**), particularly in genetically tractable hosts with propionyl-CoA as a non-native metabolite such as *E. coli*. As a biochemical approach, propionate or odd-chain fatty-acid-rich feedstocks have been exogenously supplemented in the culture medium for their direct conversion to propionyl-CoA (84). However, the high costs associated with these feedstocks potentially limit practical application of this approach. Alternatively, a popular approaches based on extended dissimilation of 2-ketobutyrate (i.e. the L-threonine biosynthetic pathway (134)) have been explored to enable biosynthesis of propionyl-CoA from unrelated carbon sources in *E. coli*. Such explorations have opened an avenue for novel biosynthesis. In the next section, these metabolic engineering pathways used for the production of 1-propanol are reviewed.

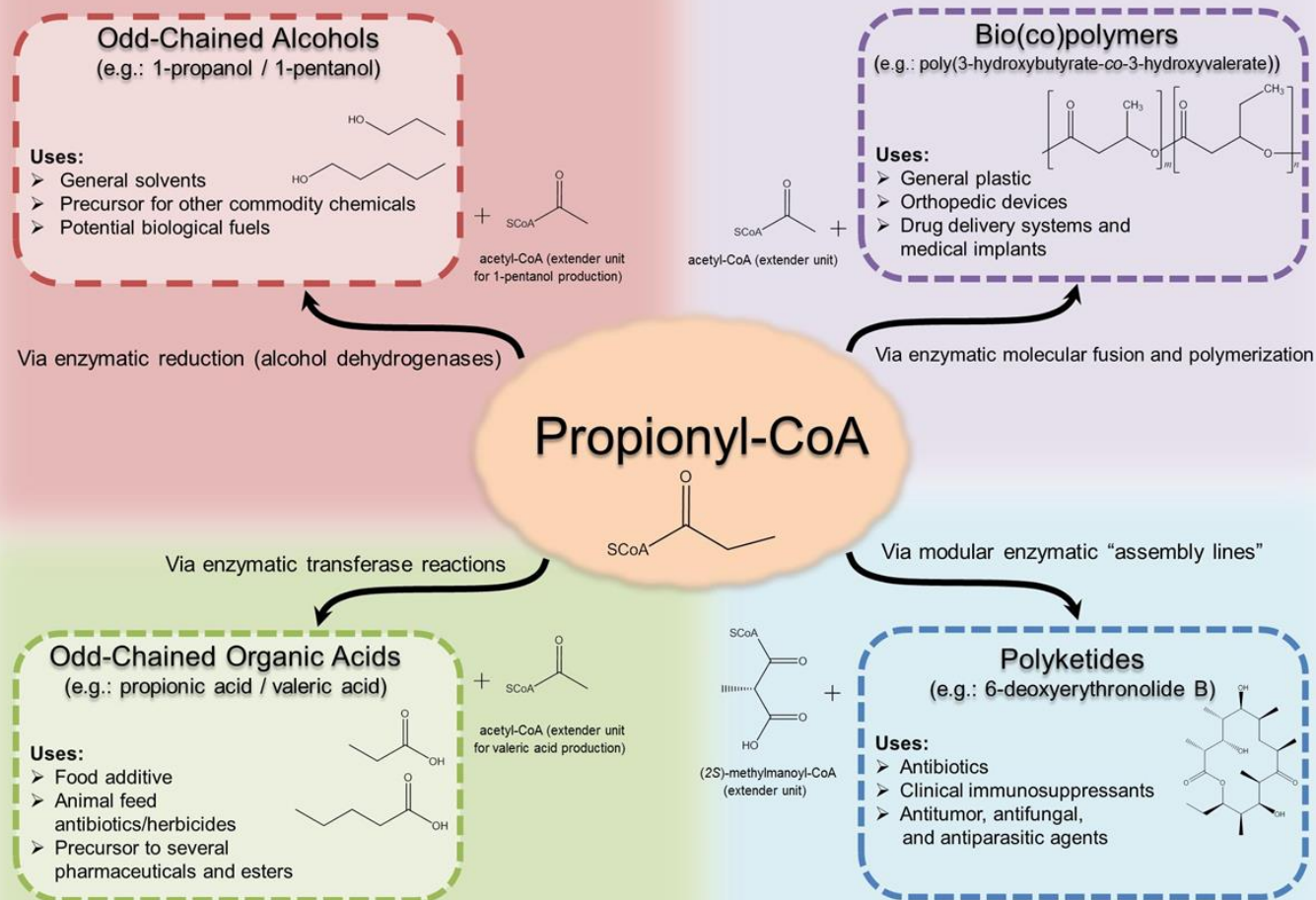


Figure 2.6: Propionyl-CoA acting as a precursor (*on previous page*)

Propionyl-CoA can act as a key biogenic precursor for the production of several value-added chemicals and biofuels of industrial importance.

2.7.2 1-Propanol as a prospective biofuel

2.7.2.1 Overview of 1-propanol and current strategies toward its production

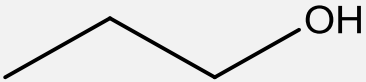
As mentioned previously, compared to the most popular biofuel ethanol, 1-propanol and other higher-chain alcohols are considered to be better energy carriers because of their potentially favorable physicochemical properties, including higher energy density, octane number, and lower hygroscopicity (see **Table 2.5** for a comparative overview of 1-propanol and other fuels). Additionally, 1-propanol has found its use as a multi-purpose solvent for a multitude of industrial applications, including paints, cleaning products, and cosmetics (135, 136). However, due to insignificant titers achieved so far, large-scale microbial production of 1-propanol has been economically unfeasible. Because no native microbial 1-propanol producer has been identified so far, rational synthetic biology and metabolic engineering strategies to enhance 1-propanol production in microbial hosts, particularly genetically tractable *E. coli*, have been developed. To this end, recent studies aimed at modulating the intracellular pool of propionyl-CoA and/or other key intermediates through introduction of heterologous synthetic pathways as well as engineering endogenous metabolic pathways (**Figure 2.7** and **Table 2.6**), with promising 1-propanol titers beyond the g/L threshold.

In addition to propionyl-CoA, 2-ketobutyrate can be another key precursor to 1-propanol production. In many microorganisms, including *E. coli*, 2-ketobutyrate is an endogenous product associated with L-threonine degradation and a reductive pathway (such as alcohol production) can be unusually used to dispose of electrons generated during amino acid metabolism (137). Nonetheless, production of 1-propanol from L-threonine has been previously detected in *Clostridium* sp. strain 17cr1, demonstrating the synthesis of higher-chain alcohols via non-fermentative pathways (137). Alternative to L-threonine degradation, 2-ketobutyrate can be synthesized via citramalate biosynthesis in select microorganisms, including *Methanococcus jannaschii* (138). These observations formed the basis for the production of higher-chain alcohols in *E. coli* via non-fermentative pathways (10, 136, 139). Specifically, production of 1-propanol was achieved through promoting 2-ketobutyrate synthesis via the L-threonine pathway (136) (**Figure 2.7A**) and citramalate pathway (139) (**Figure 2.7B**). In these studies, the concerted feedback inhibition exerted by L-threonine biosynthesis was overcome through directed mutagenesis of *thrA*, which encodes the bifunctional aspartokinase/homoserine dehydrogenase and is the target for allosteric feedback inhibition by L-threonine. In addition, by overexpression of the genes

involved in 2-ketobutyrate synthesis as well as elimination of other biosynthetic competing pathways, production titers of up to ~2 g/L 1-propanol was achieved in the engineered strains (136, 140).

Alternatively, 2-ketobutyrate can be derived through the condensation of acetyl-CoA and pyruvate via the citramalate pathway (**Figure 2.7B**). By overexpression of the heterologous *cimA* gene from *M. jannaschii* to form citramalate and then the endogenous *leuABCD* operon to form 2-ketobutyrate with inactivation of several competing pathways, approximately 0.5 g/L 1-propanol was produced. The propanol titer can be significantly increased by overexpressing an evolved *cimA* (*cimA3.7*) derived through multiple rounds of error-prone PCR (139). Note that a promiscuous 2-ketoacid decarboxylase (i.e. Kivd from *Lactococcus lactis*) and a broad-range alcohol dehydrogenase (i.e. ADH2 from *S. cerevisiae*) were used for direct conversion of 2-ketobutyrate to 1-propanol (136, 139). While 2-ketobutyrate can be converted endogenously to 1-propanol through the carboxylic intermediates of propionate and propionyl-CoA, the aforementioned direct conversion of 2-ketobutyrate to 1-propanol can potentially circumvent the production of propionate as a byproduct. Furthermore, by synergistically combining the strategies of deregulated L-threonine biosynthetic pathway (136) and evolved *cimA* (139), as well as more extensive inactivation of pathways competing for the essential precursor 2-ketobutyrate, the production of 1-propanol was significantly enhanced based on the use of glucose and glycerol as the feedstock (134, 140). The L-threonine biosynthetic pathway activity was enhanced to increase the intracellular 2-ketobutyrate pool through directed-evolution of the *ilvA* gene encoding L-threonine dehydratase and overexpression of the endogenous L-threonine synthetic operon *thrABC* (134). Alternative to direct conversion of 2-ketobutyrate to 1-propanol via promiscuous 2-ketoacid decarboxylase and alcohol dehydrogenase, various genes in the other 1-propanol-formation pathway, i.e. *ackA* encoding acetate kinase A/propionate kinase II, *atoDA* encoding acetyl-CoA:acetoacetyl-CoA synthase, and an aerobic-tolerant *adhE* encoding alcohol/aldehyde dehydrogenase, were overexpressed (134). Interestingly, inactivation of *rpoS* encoding the stationary-phase sigma factor can increase the expression of enzymes involved in the TCA cycle and L-threonine metabolism, as well as the accumulation of pyruvate, phosphoenolpyruvate (PEP) and oxaloacetate (OAA) during the stationary growth phase, resulting in enhanced 1-propanol production under aerobic culture conditions with glucose as the carbon source (134). Previously, it has been demonstrated that inactivating the stationary-phase sigma factor RpoS deregulates global expression of genes involved in stress response. Although mutant *E. coli* strains lacking the *rpoS* gene exhibit growth characteristics similar to that of the wild-type, acetate production is significantly hampered, thus enhancing carbon flux toward other fermentative end-products (141).

Table 2.5: A comparison of 1-propanol to other energy carriers

Properties	1-propanol		1-propanol structure		
	Melting point (°C)	-126.0			
Boiling point (°C)	97.5				
Ignition temperature (°C)	371.0				
Flash point (°C)	22.0				
Density at 20°C (g/ml)	.80				
Critical pressure (MPa)	51.7				
Critical temperature (°C)	263.5				
	Fuels				
	1-pentanol	1-butanol	1-propanol	Gasoline	Ethanol
Energy density (MJ/kg)	37.7	36.1	33.6	42.7	29.7
Air-fuel ratio	12.5	11.2	21.4	14.6	9
Vapor Pressure (psi)	0.04	0.08	0.29	0.1-30	1.1
Average Octane (AKI rating/RON)	84/113	97/103	108/118	85-96/90-105	99.5/108.6

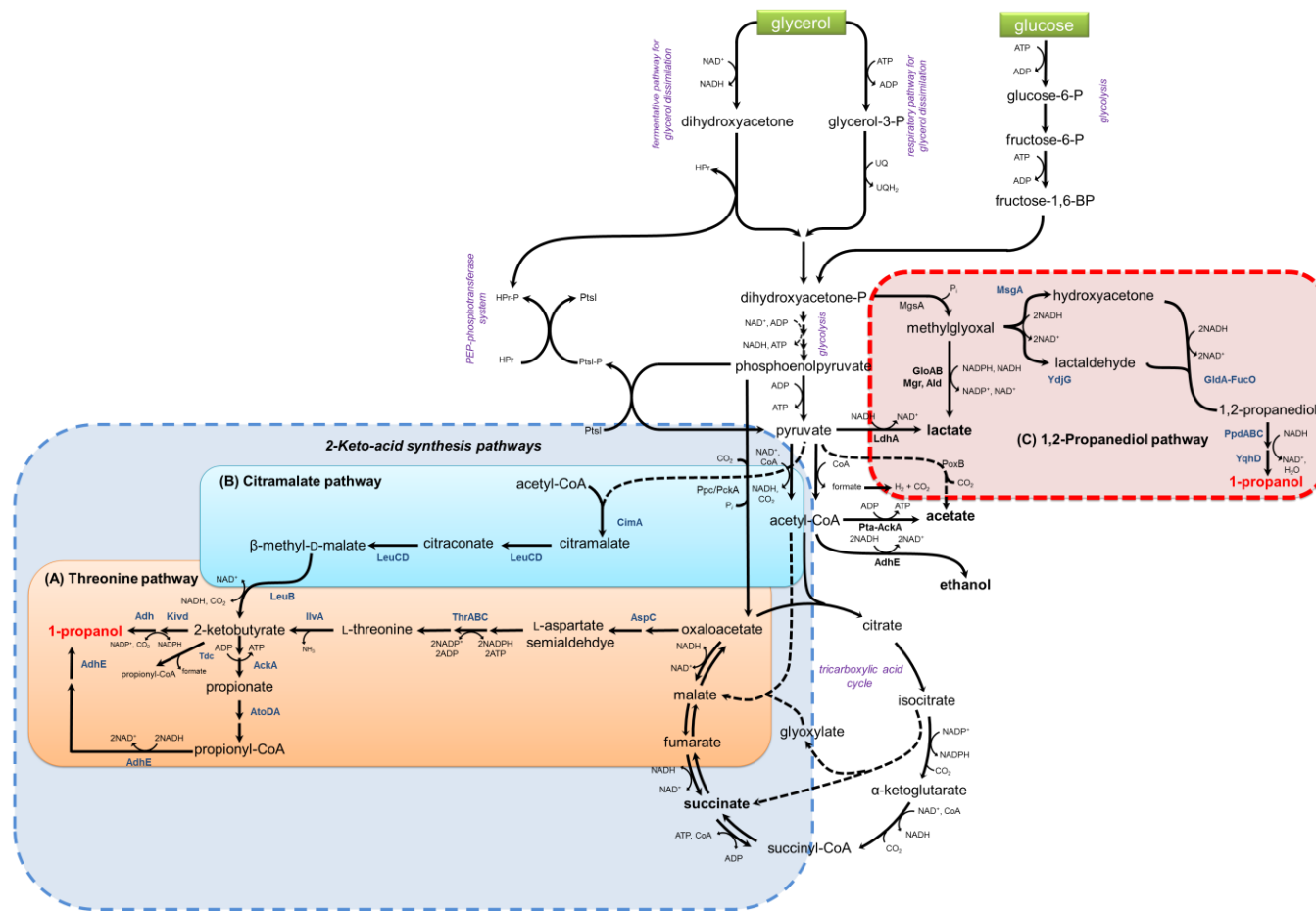


Figure 2.7: Metabolic pathways for 1-propanol production in engineered *E. coli*.

Pathways include the non-fermentative pathways via (A) l-threonine and (B) citramalate biosynthesis, as well as the fermentative ones via (C) synthetic extension of 1,2-propanediol. Key enzymes in the pathways are: AspC, aspartate aminotransferase; LeuB, 3-isopropylmalate dehydrogenase; LeuCD, 3-isopropylmalate isomerase A and B; ThrA, homoserine dehydrogenase; ThrB, homoserine kinase; ThrC homoserine deaminase; IlvA, l-threonine deaminase; AdhE, bifunctional alcohol/aldehyde dehydrogenase. Heterologous enzymes are represented in blue, whereas native *E. coli* enzymes are represented in green.

Table 2.6: Major metabolic engineering approaches to enhance the production of 1-propanol in engineered microbial platforms

Cell factory	Carbon source	Genetic approach	Pathway legend	Maximum 1-propanol titer (g l ⁻¹)	References
<i>E. coli</i> JCL16	Glucose (50 g l ⁻¹)	<i>E. coli</i> strain was modified to assimilate L-threonine into 1-propanol	Figure 2.7A	~0.03	Atsumi et al., (10)
<i>E. coli</i> KS145	Glucose (72 g l ⁻¹)	<i>E. coli</i> strain with an engineered citramalate pathway	Figure 2.7B	~2.7	Atsumi et al.,(139)
<i>E. coli</i> JCL16	Glucose (30 g l ⁻¹) and l-threonine (8 g l ⁻¹)	Modified L-threonine overproducing <i>E. coli</i> strain	Figure 2.7A	~1.6	Shen and Liao(142)
<i>E. coli</i> BW25113	Glucose (20 g l ⁻¹)	<i>E. coli</i> strain with an engineered with a novel and expanded 1,2 propanediol pathway	Figure 2.7C	~0.3	Jain and Yan(143)
<i>Thermobifida fusca</i> B6	Switchgrass (0.48 g l ⁻¹)	Chromosomally engineered <i>Thermobifida fusca</i> strain with an alcohol dehydrogenase gene from <i>C. acetobutylicum</i>	N/A	~0.6	Deng and Fong(144)
<i>E. coli</i> PRO2	Glycerol (40 g l ⁻¹)	<i>E. coli</i> strain was modified to assimilate L-threonine into 1-propanol with feedback inhibitions removed	Figure 2.7A	~10.3	Choi et al., (134)
<i>E. coli</i> CRN SYN 12	Glucose (36 g l ⁻¹)	<i>E. coli</i> strain engineered with two pathways: 1) L-threonine into 1-propanol and 2) citramalate pathway	Figure 2.7A and B	~8	Shen and Liao (145)

2.7.3 Overview of the Sleeping beauty mutase operon pathway genes

In addition to the 2-keto-acids pathways, an alternative approach to generate the required propionyl-CoA for 1-propanol production is via the Sbm operon (**Figure 2.8**). Although the metabolic and mechanistic role of pathways similar to the Sleeping beauty pathway (i.e. the methylmalonyl-CoA pathway) has been elucidated in most Gram-positive prokaryotes (e.g. propionic bacteria), its role in *E. coli* is still rather ambiguous. It should be noted that while *E. coli* possess an intact pathway (found as a four-gene cluster at ~ 62.8 min on the *E. coli* genome – see **Figure 2.9**), the pathway genes are thought to be silent for two reasons, (1) it is hypothesized that the operon genes are hardly expressed possibly due to an inactive or weak promoter-operator system (14, 15); and (2) while *E. coli* encodes several cobalamin-dependent mutases and possesses receptors specifically for uptake of vitamin B₁₂ (which is the active form of cyanocobalamin) (146), the organism neither produces cyanocobalamin *de novo* nor does it require it for cell growth (147). Thus, cyanocobalamin must be supplemented exogenously in the cultivation medium in order to activate Sbm from its apo-form to its holo-form. Moreover, while Haller et al.(16), demonstrated that three of the genes from this operon [i.e. (1) *sbm* encoding a cobalamin-dependent methylmalonyl-CoA mutase (or Sbm; sleeping beauty mutase); (2) *ygfG* encoding a methylmalonyl-CoA decarboxylase (YgfG) and (3) *ygfH* encoding a propionyl-CoA::succinate transferase (YgfH)] encode proteins that are necessary and sufficient for the decarboxylation of succinate to propionate, the role of the second gene within the operon (*ygfD* encoding a putative arginine kinase, ArgK/YgfD) remains to be elucidated. However, recently it was discerned that YgfD could potentially interact with Sbm to form a multi-subunit complex (148).

We hypothesize that it is feasible to produce 1-propanol using engineered *E. coli* strains with an activated Sbm operon for extended dissimilation of succinate (see **Figure 2.8** for relevant pathways). In order to do so, the first three genes from the operon (i.e. *sbm*, *ygfD*, and *ygfG*) are required for conversion of succinyl-CoA to propanoyl-CoA. Moreover, a bifunctional alcohol dehydrogenase (endogenous or heterologous) is also required for the reduction of propanoyl-CoA into propanaldehyde and finally into 1-propanol.

A major limitation in the implementation of this pathway in *E. coli* is the limitation of succinyl-CoA, an important precursor. Under standard aerobic conditions, succinyl-CoA is not produced as an end product, given that most of it is siphoned into the production of the tricarboxylic acid cycle intermediate, succinate(149). Conversely, under anoxic conditions (**Figure 2.8**), *E. coli* produces both succinate and succinyl-CoA, via a reductive reverse tricarboxylic acid (TCA) cycle as fermentative end-products. Thus,

this bioprocess can be performed under anaerobic conditions, with succinate and succinyl-CoA as the precursors for their extended conversion into 1-propanol.

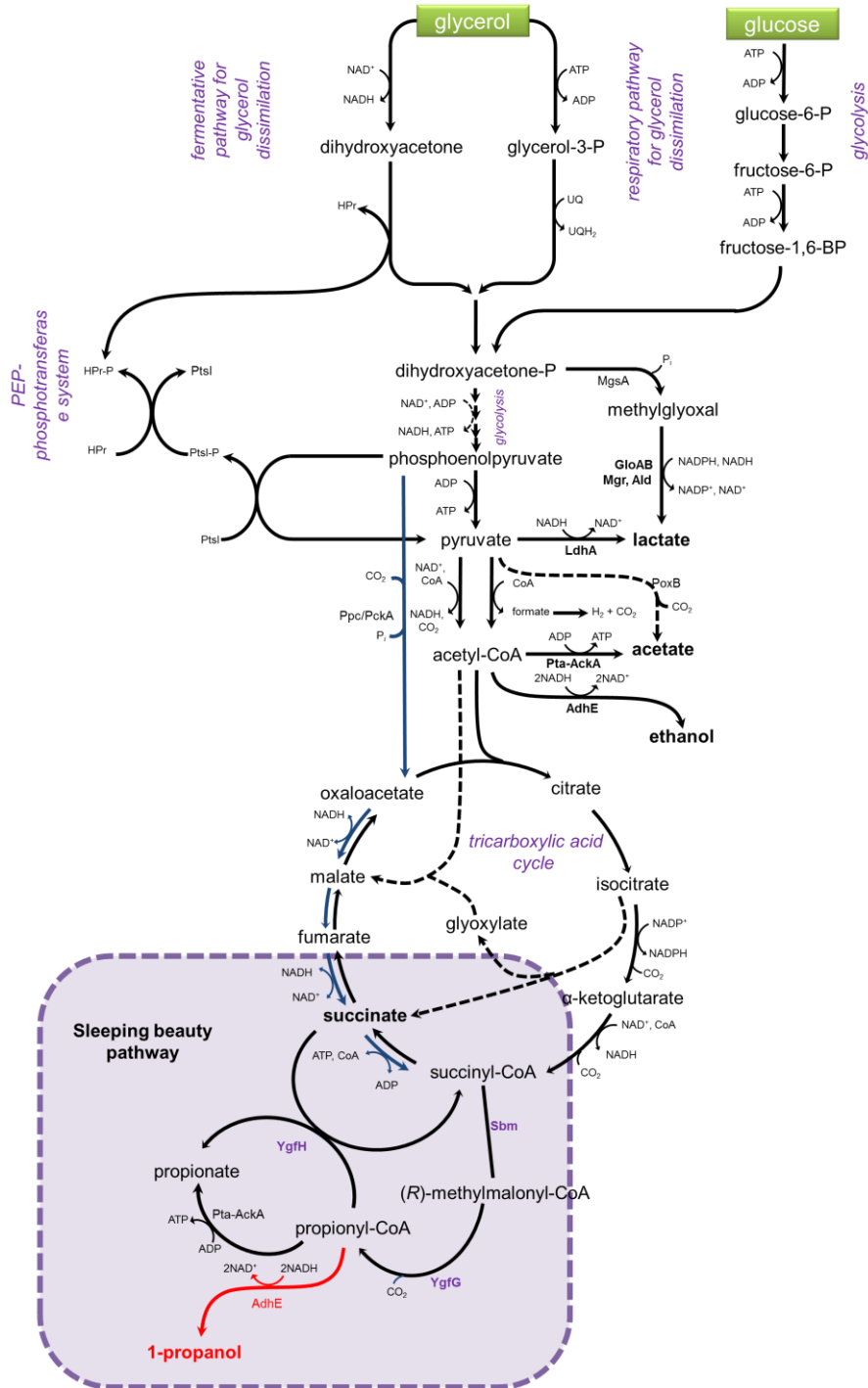


Figure 2.8: The Sleeping beauty mutase biosynthetic pathway and proposed 1-propanol production strategy in *E. coli* (on previous page).

The genetically engineered central metabolic pathway showing an activated Sbm operon (*Sbm*, *YgfD*, and *YgfG*, see purple text), and the expression of an endogenous alcohol dehydrogenase (*AdhE*) for the production of 1-propanol (in red text and arrows). Note the reductive TCA cycle (from the glycolytic trunk to oxaloacetate) toward succinyl-CoA is shown in blue arrows.

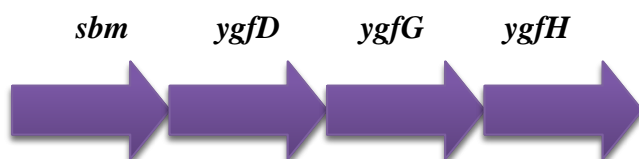


Figure 2.9: The Sbm operon in *E. coli*

sbm codes for methylmalonyl-CoA mutase, *ygfD* (or *argK*) codes for a protein kinase that catalyses the phosphorylation of two periplasmic binding proteins involved in cationic amino acid transport, *ygfG* codes for methylmalonyl-CoA decarboxylase and *ygfH* codes for propionyl-CoA: succinyl-CoA transferase. Figure and caption adapted from Kannan(14). Operon genes not to scale.

PART I

ACTIVATING THE SLEEPING BEAUTY PATHWAY IN *ESCHERICHIA COLI* FOR PRODUCTION OF 1-PROPANOL

Chapter 3

Development of host-vector systems for 1-propanol production

Chapter Abstract

While most resources in biofuels are directed towards implementing bioethanol programs, 1-propanol has recently received attention as a promising alternative biofuel. Nevertheless, no microorganism has been identified as a natural 1-propanol producer. In this chapter, we manipulated a novel metabolic pathway for the synthesis of 1-propanol in the genetically tractable bacterium *Escherichia coli*. *E. coli* strains capable of producing heterologous 1-propanol were engineered by extending the dissimilation of succinate via propionyl-CoA. This was accomplished by expressing a selection of key genes, i.e. (1) three native genes in Sbm operon, i.e. *sbm-ygfD-ygfG* from *E. coli*, (2) the genes encoding bifunctional aldehyde/alcohol dehydrogenases (ADHs) from several microbial sources, and (3) the *sucCD* gene encoding succinyl-CoA synthetase from *E. coli*. Using the developed whole-cell biocatalyst under anaerobic conditions, production titers up to 150 mg/L of 1-propanol were obtained. In addition, several genetic and chemical effects on the production of 1-propanol were investigated, indicating that certain host-gene deletions could abolish 1-propanol production as well as that the expression of a putative protein kinase (encoded by *ygfD/argK*) was crucial for 1-propanol biosynthesis. This portion of the study showcases a novel route for 1-propanol production in *E. coli*, which is subjected to further improvement by identifying limiting conversion steps, shifting major carbon flux to the productive pathway, and optimizing gene expression and culture conditions.

3.1 Background

The majority of the world's energy requirements are currently met through unfettered use of carbonaceous fossil fuels. However, mounting environmental and socioeconomic concerns associated with exploiting these resources have led to the exploration of more sustainable and environmentally friendly energy forms, in particular biofuels (2). While ethanol, one of the most common and successful biofuels today, almost possesses established economic niches within energy markets, significant attention is being directed towards the production of longer-chain alcohols, such as 1-butanol and 1-propanol (10,

11). These longer-chain alcohols tend to have a higher energy content, lower hygroscopicity, and water solubility; and are compatible with existing transportation infrastructures and pipelines (12).

In addition to being a potential biofuel, 1-propanol serves as an important solvent and chemical for relevant industrial applications (143). Up to now, the production of 1-propanol primarily relies on chemical synthesis and no microbial cells have been identified as a natural 1-propanol producer. Nevertheless, recent advances in synthetic biology and metabolic engineering have enabled biological production of 1-propanol using various non-natural but genetically tractable microorganisms, among which *E. coli* is the most common. It is critical to identify potential synthetic pathways and enzymes relevant to the target metabolite (i.e. 1-propanol) heterologously produced in a non-native microbial host. For example, Atsumi et al., (10) devised a synthetic approach to convert 2-ketobutyrate to produce 1-propanol in a genetically engineered *E. coli* strain through a non-fermentative biosynthetic pathway mediated by a promiscuous 2-ketoacid decarboxylase and an aldehyde/alcohol dehydrogenase (ADH). The conversion bioprocess was further enhanced using an evolved citramalate pathway (139). On the other hand, Choi et al., (134) demonstrated the production of 1-propanol by grafting a pathway containing several key genes for further conversion of L-threonine into 1-propanol in an engineered L-threonine overproducing *E. coli* strain. Jain and Yan (143) reported the production of 1-propanol in *E. coli* by expanding the 1,2-propanediol pathway with two steps mediated by a novel 1,2-propanediol dehydratase and an ADH. More recently, Shen and Liao (145) combined the native threonine pathway and a heterologous citramalate pathway for synergistic production of 1-propanol in *E. coli*. In addition to the aforementioned *E. coli* platforms, Deng and Fong (144) explored direct conversion of untreated plant biomass to 1-propanol using an engineered *Thermobifida fusca* strain.

Herein, we present an alternative novel biosynthesis of 1-propanol by manipulating the sleeping beauty mutase (Sbm) operon in *E. coli*. This four-gene operon (*sbm-ygfD-ygfG-ygfH*) encodes various enzymes involved in a cobalamin-dependent metabolic pathway for decarboxylation of succinate into propionate (13). The metabolic context of the Sbm-pathway remains ambiguous, but is suspected to be involved in the assimilation of unusual carbon sources, such as succinate and propionate. Moreover, eponymous to its name, the operon genes are hardly expressed possibly due to an inactive or weak promoter-operator system (14, 15). Three of the encoded proteins from this operon are identified to be members of the crotonase superfamily, namely (1) *sbm* encoding a cobalamin-dependent methylmalonyl-CoA mutase (or Sbm; sleeping beauty mutase), which catalyzes the isomerization of succinyl-CoA to L-methylmalonyl-CoA; (2) *ygfG* encoding a methylmalonyl-CoA decarboxylase (YgfG), which catalyzes the decarboxylation of methylmalonyl-CoA to propionyl-CoA; and (3) *ygfH* encoding a propionyl-

CoA::succinate transferase (YgfH) (16). The *ygfD* gene encodes a putative protein kinase (YgfD/ArgK) whose function remains unclear. However, YgfD could potentially interact with Sbm to form a multi-subunit complex (148). Although the structure, function, and relationship of these enzymes have been characterized, hardly any work has been performed for their practical application.

In this study, we demonstrated the production of 1-propanol using engineered *E. coli* strains with an activated Sbm operon for extended dissimilation of succinate (see **Figure 3.1** for relevant pathways). First, three *E. coli* genes of *sbm*, *ygfD*, and *ygfG* were assembled as a single operon and then were expressed to convert succinyl-CoA to propionyl-CoA. Second, the genes encoding bifunctional ADHs from various microorganisms were cloned and expressed to convert propionyl-CoA to 1-propanol. We further channeled carbon flux towards the 1-propanol-producing pathway by expressing *sucCD* (encoding succinyl-CoA synthetase) from *E. coli*. These biosynthetic strategies were implemented into *E. coli* based on the construction of triple-plasmid expression systems (**Figure 3.2**) to facilitate the evaluation of suitable pathways. The 1-propanol-producing capacity of these metabolically engineered *E. coli* strains were evaluated under anaerobic cultivation conditions. The exometabolome of the culture was analyzed using 1-dimensional hydrogen nuclear magnetic resonance (1D-¹H-NMR) spectroscopy with more than thirty metabolites being identified. In addition, we investigated several genetic and chemical effects associated with 1-propanol production in engineered *E. coli*.

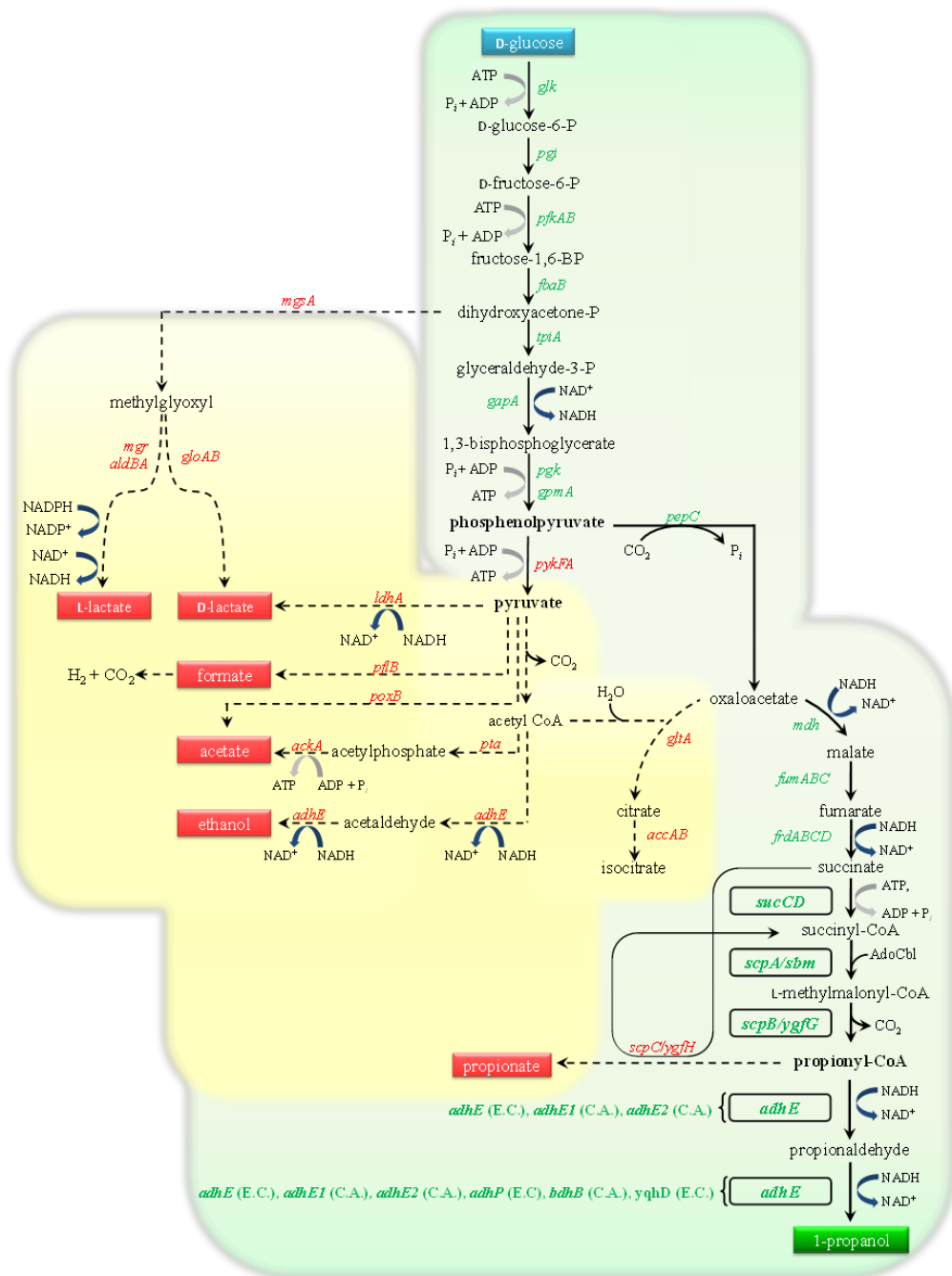


Figure 3.1: Metabolic engineering of *E. coli* for 1-propanol production.

The genetically engineered central metabolic pathway under anaerobic conditions showing the activation of the Sbm operon (*sbm*, *ygfD*, and *ygfG*), and the expression of various *adhE*s used in this study. Red colored gene names above or beside dashed lines represent diverting pathways; metabolites in red boxes are unwanted. Genes in green represent the necessary genes for 1-propanol conversion from glucose; those that are in bold font and boxed represent genes expressed via episomal plasmids.

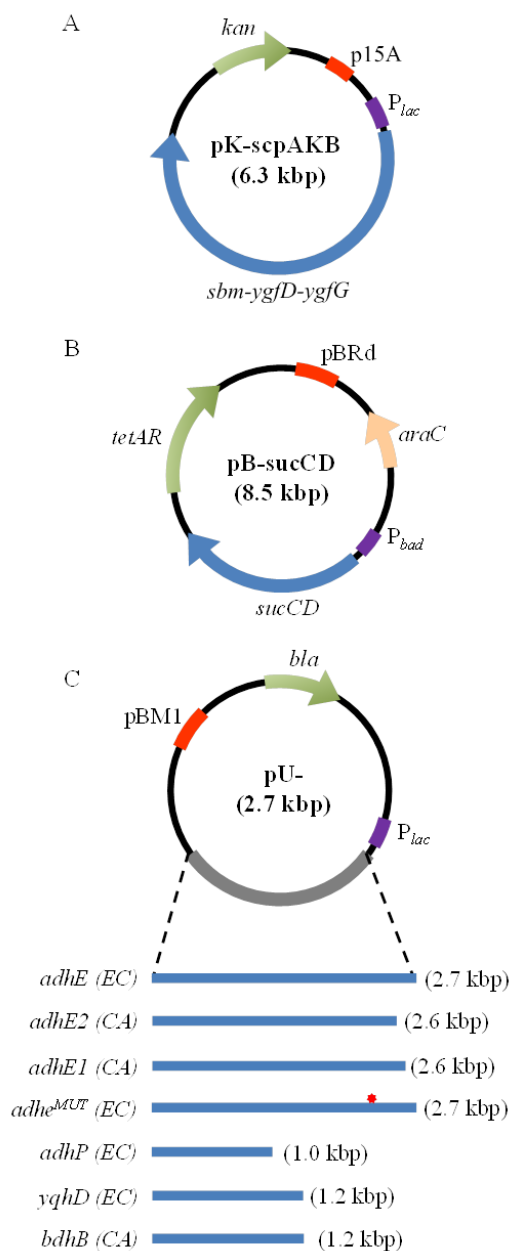


Figure 3.2: A schematic representation of the triple-plasmid expression systems utilized for 1-propanol production.

All strains have *sbm-ygfD-ygfG* cloned into pK184 under the control of P_{iac} as well as *sucCD* cloned into pBR1MCS-3 under the control of the arabinose inducible p_{araB} . In addition to these, each strain has pUC19 containing one of the seven listed alcohol dehydrogenases. The red star in the *adhE^{MUT}* (EC) represents the E (glu)→K (lys) mutation at amino acid residue 568.

3.2 Methods

3.2.1 Plasmid construction

All plasmids and primers used in this study are listed in **Table 3.1**. Genomic DNA from various bacterial strains was isolated using the Blood & Tissue DNA Isolation Kit (Qiagen, Hilden, Germany). Standard recombinant DNA technologies for gene cloning (150) were applied. Various DNA polymerases, restriction endonucleases, T4 DNA ligase, and Antarctic phosphatase were obtained from New England Biolabs (Ipswich, MA). All oligonucleotides were obtained from Integrated DNA Technologies (Coralville, IA). DNA sequencing was conducted in the Centre for Applied Genomics at the Hospital for Sick Children (Toronto, Canada).

The succinyl-CoA synthetase gene (*sucCD*) from *E. coli* was cloned into the plasmid pBBR1MCS-3 for its expression under the regulation of the inducible P_{araB} promoter. To make this construct, *sucCD* was PCR-amplified from *E. coli* BW25141 genomic DNA using the c-sucCD primer set, whereas the *araC*- P_{araB} fragment was PCR-amplified from pKD46 using the c-paraB primer set. The two DNA fragments were then transcriptionally fused with splice overlap extension PCR (151) using the forward primer c-paraB and the reverse primer c-sucCD. The resulting *araC*- P_{araB} ::*sucCD* fragment was directionally cloned into the XhoI and XbaI restriction sites of pBBR1MCS-3, yielding pB-sucCD.

The fusion containing the three genes of *sbm-ygfD-ygfG* from the Sbm operon was PCR-amplified from *E. coli* BW25141 genomic DNA using the c-scpAB primer set. The amplified DNA fragment was non-directionally cloned into the EcoRI restriction site of pK184. A clone with the correct transcriptional orientation of the *sbm-ygfD-ygfG* fragment with respect to the inducible P_{lac} promoter was selected and verified by DNA sequencing, yielding pK-scpAKB. To test the essentialness of YgfD/ArgK, PCR was used to amplify the entire pK-scpAKB construct, with the exception of *ygfD*, using the c-argK primer set. This resulted in the addition of a flanking XbaI site downstream of *sbm* and upstream of *ygfG*. XbaI digestion and relegation of this PCR product rendered plasmid pK-scpAB.

A selection of genes encoding alcohol/aldehyde dehydrogenases from various sources were respectively cloned into pUC19 as transcriptional fusions under the control of the inducible P_{lac} promoter. To do this, the *adhE*, *ydhD*, and *adhP* genes were amplified from *E. coli* BW25141 genomic DNA using the c-adhE(EC), c-yqhD(EC), and c-adhP(EC) primer sets, respectively. The resulting PCR products were individually fused with the BamHI-linearized pUC19 using the In-Fusion PCR Cloning System (Clontech Laboratories Inc., Mountainview, CA) to yield pU-adhE(EC), pU-yqhD(EC), and pU-

adhP(EC), respectively. Similarly, the *adhE2*, *adhE1*, and *bdhB* genes were PCR-amplified from *Clostridium acetobutylicum* ATCC 824 genomic DNA using the c-adhE2(CA), c-adhE1(CA), and c-bdhB primer sets, respectively. The resulting PCR products were individually fused with the BamHI-linearized pUC19 to yield pU-adhE2(CA), pU-adhE1(CA), and pU-bdhB(CA), respectively. Plasmid pU-adhE^{MUT}(EC) was derived from pU-adhE(EC) by generating a Glu568Lys mutation within the *adhE* coding sequence using the Phusion Site-directed Mutagenesis Kit (New England Biolabs) with the m-adhE primer set and the point-mutation was screened based on the loss of a unique SapI restriction site. Similar to a previous approach (84), pU-adhE^{MUT}(EC) was used to express an aero-tolerant *E. coli* alcohol/acetaldehyde dehydrogenase mutant.

3.2.2 Bacterial strains and chromosomal manipulation

A selection of *E. coli* host strains and host/vector systems used in this study are listed in **Tables 3.1 and 3.2**, respectively. BW25141 was used to provide wild-type (WT) genetic backgrounds for 1-propanol production. HST08 was used for molecular cloning. Various host gene deletions (e.g. *adhE*, *pta*, and *ldhA*) were introduced to BW25141 by P1-phage transduction (150) using proper Keio Collection strains (CGSC, Yale University) as donors (152). The co-transduced Km^R-FRT gene cassette was removed using pCP20 (153). *E. coli* strain MC4100 was used as a control strain for all P1 phage transductions. The genotypes of derived knockout strains were confirmed with colony PCR using appropriate primer sets (e.g. v-adhE, v-pta, and v-ldhA).

3.2.3 Media and cultivation

All chemicals for medium components were obtained from Sigma-Aldrich Co. (St Louis, MO) except yeast extract and tryptone, which were obtained from BD Diagnostic Systems (Franklin Lakes, NJ). When required, antibiotics at a proper concentration were used: 100 µg/mL carbenicillin, 50 µg/mL kanamycin, and 20 µg/mL tetracycline. For multi-plasmid systems, the concentration of each antibiotic was reduced to half to avoid negative impacts on growth. Isopropyl-β-D-thiogalactopyranoside (IPTG) (1 mM) and L-arabinose (10 mM) were used to induce gene expression respectively regulated by the P_{lac} and P_{araB} promoters

Table 3.1: Hosts strains, plasmids and primers used in this study

Name	Description, relevant genotype or primer sequence (5'→3')	Reference
<i>E. coli</i> host strains		
HST08	F-, <i>endA1</i> , <i>supE44</i> , <i>thi-1</i> , <i>recA1</i> , <i>relA1</i> , <i>gyrA96</i> , <i>phoA</i> , $\Phi 80d$ <i>lacZ</i> Δ <i>M15</i> , Δ(<i>lacZYA</i> – <i>argF</i>) <i>U169</i> , Δ(<i>mrr</i> – <i>hsdRMS</i> – <i>mcrBC</i>), Δ <i>mcrA</i> , λ–	Takara Bio, Shiga, Japan
MC4100	F-, [<i>araD139</i>]B/τ, Del(<i>argF-lac</i>)169, λ–, <i>e14-</i> , <i>flhD5301</i> , Δ(<i>fruK-yeiR</i>)725(<i>fruA25</i>), <i>relA1</i> , <i>rpsL150</i> (strR), <i>rbsR22</i> , Del(<i>fimB-fimE</i>)632(::IS1), <i>deoC1</i>	(154)
BW25141	F-, Δ(<i>araD-araB</i>)567, Δ <i>lacZ4787</i> :: <i>rrnB-3</i> , Δ(<i>phoB-phoR</i>)580, λ-, <i>galU95</i> , Δ <i>uidA3</i> :: <i>pir+</i> , <i>recA1</i> , <i>endA9</i> (<i>del-ins</i> ::FRT, <i>rph-1</i> , Δ(<i>rhaD-rhaB</i>)568, <i>hsdR514</i>	(153)
BW25113	F-, Δ(<i>araD-araB</i>)567, Δ <i>lacZ4787</i> :: <i>rrnB-3</i> , λ-, <i>rph-1</i> , Δ(<i>rhaD-rhaB</i>)568, <i>hsdR514</i>	(153)
WT-Δ <i>adhE</i>	<i>adhE</i> null mutant of BW25113	This study
WT-Δ <i>ldhA</i>	<i>ldhA</i> null mutant of BW25113	This study
WT-Δ <i>pta</i>	<i>pta</i> null mutant of BW25113	This study
Plasmids		
pCP20	FLP ⁺ , λ <i>cI857</i> ⁺ , λ p _R Rep(pSC101 ori) ^{ts} , Ap ^R , Cm ^R	(155)
pKD46	RepA101 ^{ts} , Ap ^R , <i>araC</i> -P _{araB} :: <i>gam-bet-exo</i>	(153)
pK184	p15A ori, Km ^R , P _{lac} :: <i>lacZ'</i>	(156)

pBBR1MCS-3	broad host range ori, Tc ^R , P _{lac} :: <i>lacZ</i> '	(157)
pUC19	ColE1 ori, Ap ^R , P _{lac} :: <i>lacZ</i> '	Invitrogen, Corp., Carlsbad, CA
pK-scpAKB	From pK184, P _{lac} :: <i>sbm-ygfD-ygfG</i>	This study
pK-scpAB	From pK184, P _{lac} :: <i>sbm-ygfG</i>	This study
pB-sucCD	From pBBR1MCS-3, <i>araC-P_{araB}::sucCD</i>	This study
pU-adhE(EC)	From pUC19, P _{lac} :: <i>adhE</i> (EC)	This study
pU-adhE2(CA)	From pUC19, P _{lac} :: <i>adhE2</i> (CA)	This study
pU-adhE1(CA)	From pUC19, P _{lac} :: <i>adhE1</i> (CA)	This study
Pu-adhE ^{MUT} (EC)	From pUC19, P _{lac} :: <i>adhE</i> Glu568Lys(EC)	This study
pU-adhP(EC)	From pUC19, P _{lac} :: <i>adhP</i> (EC)	This study
pU-yqhD(EC)	From pUC19, P _{lac} :: <i>yqhD</i> (EC)	This study
Primers		
v-adhE	AATCTTGCTTACGCCACCTGGAAGTG; CGAACGGTCGCATGAGCAGAAAGCG	This study

v-pta	GGCATGAGCGTTGACGCAATCAACA; GATCCTGAGGTTAATCCTTCAAACG	This study
v-ldhA	TCATCAGCAGCGTCAACGGC; ATCGCTGGTCACGGGCTTACCGTT	This study
m-adhE	CATCCGGAAACTCACTTCGAAAAGCTGGCGCTG; CAGCGCCAGCTTTTCGAAGTGAGTTTCCGGA	This study
c-scpAB	CCATGATTACGAATTCGCAACAGCTTGCCAACAAGGA; TACCGAGCTC <u>GAAATTC</u> TTAATGACCAACGAAATTAGGTTTA	This study
c-argK	GCTCTAG <u>AATGTCTT</u> ATCAGTATGTTAAGG; GCTCTAG <u>ATTAATCATGATGCTGGC</u>	This study
c-paraB	CCGCTCTAGATATTTAGAAAAATAAACAAATAGGGGTTCC; TTGTTTTGCCTGATATTCATGTAAGTTCATTTTTTATAACCTCCTTAGAGCTCGAATTCC	This study
c-sucCD	ATGAACTTACATGAATATCAGGCAAAACAA; CCCCC <u>TCGAGT</u> TATTTTCAGAACAGTTTTTCAGTGCTTCACC	This study
c-adhE(EC)	CGACTCTAGAGGATCCCATGGCTGTTACTAATGTCGCTGAAC; CTCGGTACCCGGGGATCGATCGGTCAACTAATCCTTAACTGATCG	This study
c-adhE2(CA)	CGACTCTAGAGGATCCCATGAAAGTTACAAATCAAAAAGAACTAAAACAAAAGC; CTCGGTACCCGGGGATCATAGTCTATGTGCTTCATGAAGCTAATATAATGAAGCAAA	This study
c-adhE1(CA)	CGACTCTAGAGGATCCCATGAAAGTCACAACAGTAAAGGAATTAGATGAAAA; CTCGGTACCCGGGGATCTTAAGGTTGTTTTTTAAAACAATTTATATACATTTCTTTTATC	This study
c-adhP(EC)	CGACTCTAGAGGATCCCATGAAGGCTGCAGTTGTTACGAAGG; CTCGGTACCCGGGGATCTTAGTGACGGAAATCAATCACCATGC	This study
c-yqhD(CA)	CGACTCTAGAGGATCCCATGAACAACTTTAATCTGCACACCC; CTCGGTACCCGGGGATCTTAGCGGGCGGCTTCGTATATACGG	This study
c-bdhB(CA)	CGACTCTAGAGGATCCCGTGGTTGATTTTCGAATATTCAATACCAACTAGAAT; CTCGGTACCCGGGGATCTTACACAGATTTTTTTGAATATTTGTAGGACTTCGGA	This study

Table 3.2: *E. coli* strains containing variants of the synthetic 1-propanol pathway used in this study.

Strain	<i>E. coli</i> host	Plasmid 1	Plasmid 2	Plasmid 3
WT2	BW25141	pK-scpAKB	pB-sucCD	—
WT-adhE2(CA) ²	BW25141	pK-scpAKB	—	pU-adhE2(CA)
WT-adhE2(CA) ³	BW25141	pK-scpAKB	pB-sucCD	pU-adhE2(CA)
WT-adhE2(CA) ³ - Δ ygfD	BW25141	pK-scpAB	pB-sucCD	pU-adhE2(CA)
WT-adhE1(CA)	BW25141	pK-scpAKB	pB-sucCD	pU-adhE1(CA)
WT-adhE ^{MUT} (EC)	BW25141	pK-scpAKB	pB-sucCD	pU-adhE ^{MUT} (EC)
WT-adhP(EC)	BW25141	pK-scpAKB	pB-sucCD	pU-adhP(EC)
WT-yqhD(EC)	BW25141	pK-scpAKB	pB-sucCD	pU-yqhD(EC)
WT-bdhB(CA)	BW25141	pK-scpAKB	pB-sucCD	pU-bdhB(CA)
Δ ldhA-adhE(EC)	WT- Δ ldhA	pK-scpAKB	pB-sucCD	pU-adhE(EC)
Δ ldhA-adhE2(CA)	WT- Δ ldhA	pK-scpAKB	pB-sucCD	pU-adhE2(CA)
Δ ldhA-adhE1(CA)	WT- Δ ldhA	pK-scpAKB	pB-sucCD	pU-adhE1(CA)
Δ ldhA-adhE ^{MUT} (EC)	WT- Δ ldhA	pK-scpAKB	pB-sucCD	pU-adhE ^{MUT} (EC)
Δ ldhA-adhP(EC)	WT- Δ ldhA	pK-scpAKB	pB-sucCD	pU-adhP(EC)
Δ ldhA-yqhD(EC)	WT- Δ ldhA	pK-scpAKB	pB-sucCD	pU-yqhD(EC)
Δ ldhA-bdhB(CA)	WT- Δ ldhA	pK-scpAKB	pB-sucCD	pU-bdhB(CA)

For all cultivation experiments, *E. coli* strains (stored as glycerol stocks at -80 °C) were streaked on LB plates with appropriate antibiotics and incubated for 16 h at 37 °C. Single colonies were picked from LB plates to inoculate 25-mL LB media with appropriate antibiotics in 125-mL conical flasks. The cultures were grown in a rotary shaker at 250 rpm and 37 °C to reach an optical cell density at 600 nm (OD₆₀₀) of 0.7. Four milliliter of the seed culture was used to inoculate 400-mL LB media with appropriate antibiotics in 1-L conical flasks. This second seed culture was also shaken at 250 rpm and 37 °C to reach an OD₆₀₀ of 0.7. Cells were collected by centrifugation at 6,000 × g and 4 °C for 20 min and the cell pellets were transferred into a controlled anaerobic atmosphere (85% N₂, 10% H₂, and 5% CO₂) in an anaerobic chamber (Plas-Labs, Inc.; Lansing, MI, USA). Cell pellets were washed and resuspended in reduced modified M9 minimal media [6 g/L Na₂HPO₄, 3 g/L KH₂PO₄, 0.5 g/L NaCl, 1g/L NH₄Cl, 1 mM MgSO₄, 0.1 mM CaCl₂, 10 mM NaHCO₃, 10 mg/L vitamin B₁, and 0.2 μM cyanocobalamin (vitamin B₁₂)] containing appropriate carbon sources, 5 g/L yeast extract, appropriate antibiotics and inducers, and 1000X trace metal mix A5 (2.86 g/L H₃BO₃, 1.81 g/L MnCl₂•4H₂O, 0.222 g/L ZnSO₄•7H₂O, 0.39 g/L Na₂MoO₄•2H₂O, 0.079 g/L CuSO₄•5H₂O, 49.4 mg/L Co(NO₃)₂•6H₂O). Cells were resuspended to a final OD₆₀₀ of 15 unless specified otherwise. While most oxygen in the modified M9 minimal media was purged by autoclaving, trace oxygen was reduced using a palladium catalyst attached to the heating unit of the anaerobic chamber. The anaerobic condition of the medium was monitored using resazurin, which was added at 1mg/L. Suspended cultures were then transferred into 50-mL screw-capped conical flasks and sealed with Parafilm, before being removed from the anaerobic chamber and placed in a rotary shaker running at 250 rpm 37 °C. Cultures were unsealed and analyzed after 3 days.

3.2.4 Analytical procedures

Culture samples were appropriately diluted with an isotonic saline solution for measuring the optical cell density (OD₆₀₀) using a spectrophotometer (DU520, Beckman Coulter, Fullerton, CA). For HPLC and NMR analyses, culture samples were centrifuged for 3 min at 13,000 × g to recover the supernatant fraction which was filtered with a 0.2 μM syringe filter prior to being stored at -20 °C.

3.2.4.1 HPLC analysis

Extracellular metabolites were analyzed using HPLC (LC-10ATVP, Shimadzu, Kyoto, Japan) equipped with an Aminex HPX87 column (BioRad Laboratories, Hercules, CA) and a refractive index detector (RID-10A, Shimadzu, Kyoto, Japan). The column temperature was maintained at 65 °C when conducting analysis. The mobile phase was 5 mM H₂SO₄ (pH 2.0) running at 0.6 mL/min. The RID was connected to an integrator (C-R8A, Shimadzu, Kyoto, Japan) for chromatographic data processing. Pure samples of

various metabolites with concentrations ranging from 0.02 to 12.0 g/L were used as standards for calibration. Cell-free fermentation samples were subjected to filtration treatment prior to their injection for HPLC analysis.

3.2.4.2 NMR analysis

3.2.4.2.1 NMR sample preparation

Extracellular medium samples were diluted in 10% v/v with an internal standard composed of 99.9% D₂O with 5 mM 2,2-Dimethyl-2-silapentane-5-sulfonate (DSS) serving as a chemical shift indicator (CSI) and 0.2% w/v sodium azide (NaN₃) to inhibit bacterial growth. The diluted samples were subsequently transferred to 5-mm NMR tubes (NE-UL5-7, New Era Enterprises Inc., Vineland, NJ). Spectra were acquired by a 1D NOESY pulse sequence on a Bruker Avance 600.13 MHz spectrometer with a TXI 600 Probe (Bruker Canada Ltd., Milton, ON).

3.2.4.2.2 Spectra processing and compound identification

Following acquisition, spectra were imported into Chenomx NMR Suite 7.5 (Chenomx Inc., Edmonton, Alberta, Canada) for data processing with phase, baseline, shim, and shape corrections being carried out. An average sample pH of 5.2 measured during fermentation was applied as a reference for metabolite identification. Following spectral processing, various extracellular metabolites were identified by targeted profiling. Since the compound database associated with Chenomx NMR Suite 7.5 software did not include 1-propanol or propionaldehyde, the ‘compound builder’ application was used to implement the hydrogen spectra and unique peaks of these compounds.

3.3 Results

3.3.1 Construction of propanogenic *E. coli* strains for 1-propanol production

Based on the proposed novel pathway for the production of 1-propanol (**Figure 3.1**), the intracellular pool of propionyl-CoA, a rare metabolite in *E. coli*, should be first increased to promote its subsequent conversion to 1-propanol. To do this, genes encoding methylmalonyl-mutase (Sbm), arginine kinase (YgfD/ArgK), and methylmalonyl-CoA decarboxylase (YgfG) from the Sbm operon were cloned and expressed under the control of the P_{lac} promoter from plasmid pK-scpAKB. To convert the increased pool of propionyl-CoA to 1-propanol, the gene encoding a common bifunctional ADH from *C. acetobutylicum* was cloned and expressed under the control of the P_{lac} promoter from plasmid pU-adhE2(CA). While the wild-type strain of BW25141 showed no sign of propionate or 1-propanol production, approximately 47

mg/L of 1-propanol was detected for WT-adhE2(CA)² when glucose was used as the sole carbon source (**Table 3.3**), implying that the implemented 1-propanol production pathway was functioning. A potential factor limiting the overall production of 1-propanol was perceived to be the abundance of various precursors, such as succinate and succinyl-CoA. To investigate this, the gene encoding *E. coli* succinyl-CoA synthetase (*sucCD*) gene was cloned and expressed under the control of the P_{araB} promoter from plasmid pB-sucCD. Compared to WT-adhE2(CA)², a significant increase in both propionate and 1-propanol production was observed for WT-adhE2(CA)³ (**Table 3.3**), implying that the conversion catalyzed by succinyl-CoA synthetase can limit the production of 1-propanol under shake flask culture conditions. On the other hand, the production of propionate and 1-propanol was further extended for WT-adhE2(CA)³ when 4 g/L succinate was supplemented in the cultivation medium (**Table 3.3**), implying that succinate could also be a key precursor limiting 1-propanol production.

To further characterize this pathway, we investigated the dispensability of YgfD/ArgK, a gene product from the Sbm operon, for 1-propanol production. To do this, we excised the YgfD/ArgK coding region from plasmid pK-scpAKB. The resulting plasmid pK-scpAB was used to replace pK-scpAKB in WT-adhE2(CA)³ to form WT-adhE2(CA)³-ΔygfD. While 1-propanol production was detected in the WT-adhE2(CA)³-ΔygfD culture, the titer was approximately one third that of WT-adhE2(CA)³ (**Table 3.3**). Interestingly, the propionate concentrations from the two strains of WT-adhE2(CA)³ and WT-adhE2(CA)³-ΔygfD were approximately the same. From these results, we assume that the presence of YgfD/ArgK can be crucial for 1-propanol production.

Table 3.3: 1-Propanol and other metabolite titers (mg/L) in reduced M9 minimal media using *E. coli* strain BW25141 transformed with appropriate plasmids. Cultures were induced at an O.D600 of 15. Strains were cultivated anaerobically at 37 °C for 72 h. Carbon sources: 20 g/L glucose and 4 g/L succinate where indicated. All experiments were performed in triplicate.

Strain	Carbon source	Metabolite titers (mg/L)					
		Succinate	Lactate	Acetate	Propionate	Ethanol	1-Propanol
Control							
BW25141	Glucose	307 ± 36	128 ± 11	4436 ± 250	—	3021 ± 156	—
Experimental							
WT-adhE2(CA) ²	Glucose	264 ± 8	2601 ± 642	2961 ± 72	Trace	2640 ± 170	47 ± 2
WT-adhE2(CA) ³	Glucose	231 ± 11	1877 ± 303	2653 ± 55	51 ± 14	3199 ± 283	103 ± 16
WT-adhE2(CA) ³	Glucose and succinate	2200 ± 172	2293 ± 2970	3699 ± 352	123 ± 21	2774 ± 297	168 ± 39
WT-adhE2(CA) ³ -ΔygfD	Glucose	269 ± 94	3970 ± 1367	2527 ± 142	52 ± 8	1999 ± 104	37 ± 1

3.3.2 Manipulation of cultivation conditions and NMR studies

As mentioned above, the production of 1-propanol can be limited by the structural rearrangement of succinyl-CoA into L-methylmalonyl-CoA. The catalytic activity of the enzyme responsible for this conversion, Sbm, is dependent on the availability of cyanocobalamin (132). While *E. coli* encodes several cobalamin-dependent mutases and possesses receptors specifically for uptake of vitamin B₁₂ (which is the active form of cyanocobalamin) (146), the organism neither produce cyanocobalamin *in vivo* nor require it for cell growth (147). Using WT-adhE2(CA)³ as the host/vector system, it was observed that 1-propanol can be produced only when a threshold concentration of cyanocobalamin of 0.2 μM was supplemented in the cultivation medium. Using several cyanocobalamin concentrations less than 0.2 μM either significantly reduced or even abolished 1-production (**Figure 3.3**). As a result, this cyanocobalamin concentration of 0.2 μM was used for all cultivations.

Studies were conducted to investigate the effects of various operating parameters on cultivation performance, particularly 1-propanol titer. WT-adhE2(CA)³ was grown aerobically and then resuspended in five different optical cell densities for anaerobic fermentation and 1-propanol production. Typical major fermentation metabolites, including ethanol, lactate, and acetate, as well as those relevant to the proposed pathway, including fumarate, succinate, 1-propanol, and propionate, were detected in extracellular medium samples and their titer distributions under various culture conditions are summarized in **Figure 3.4**. While the distribution of two major metabolites of acetate and lactate appears to be affected by suspension cell density, the sum of their titers remained rather constant at approximately 8 g/L. Such high levels of major metabolites can potentially inhibit cell growth during anaerobic fermentation. Interestingly, the titer of the other major metabolite ethanol was minimally affected by suspension cell density by maintaining at approximately 2 g/L. Metabolites associated with the 1-propanol-producing pathway were considered minor and their titer distribution was also affected by suspension cell density. 1-Propanol titer reached a peak level at approximately 150 mg/L when suspension cell density was higher than 10 OD₆₀₀. Considering the above effects, suspension cell density at 25 OD₆₀₀ was chosen for all characterization experiments in this study. In addition to HPLC analysis, metabolites of interest were also analyzed by NMR, either qualitatively or quantitatively, based on their unique spectral signature and the results of a representative culture sample are summarized in **Figure 3.5**. In particular, the spectral signature associated with 1-propanol, i.e. the three peak clusters, was mapped to verify the production of 1-propanol (**Figure 3.5C**).

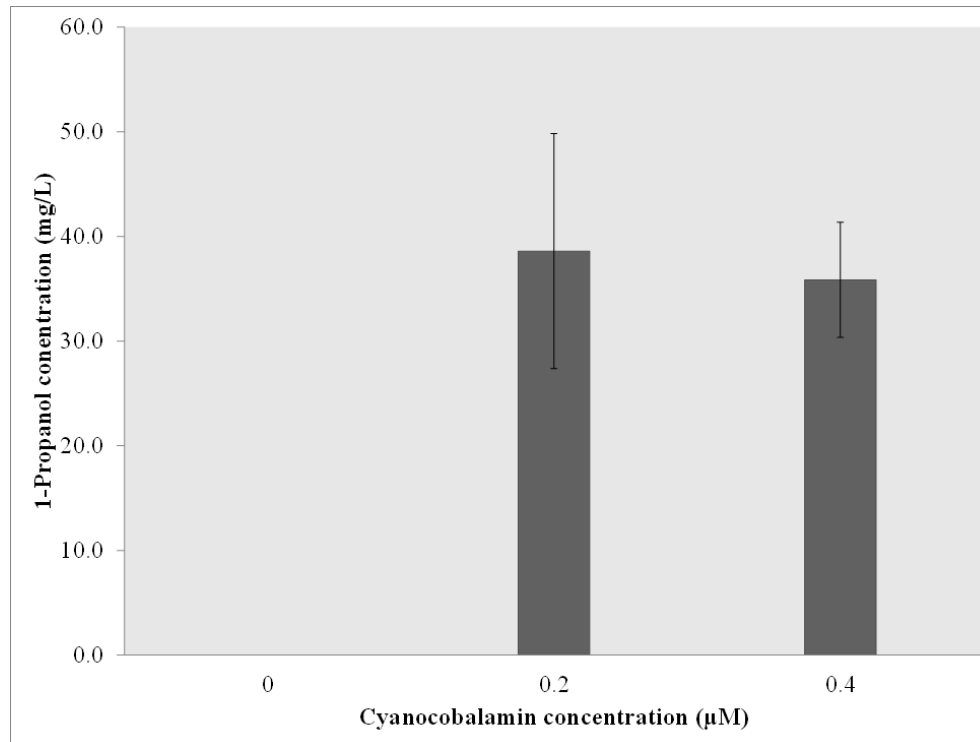


Figure 3.3: The effect of cyanocobalamin concentration on 1-propanol production in strain WT-adhE2(CA)³.

1-Propanol production is dependent on the exogenous supplementation of cyanocobalamin and saturation occurs at concentrations above 0.2 µM. Strains were cultivated anaerobically in reduced M9 minimal media with 20 g/L of glucose at 37 °C for 72 h. All experiments were performed in triplicate.

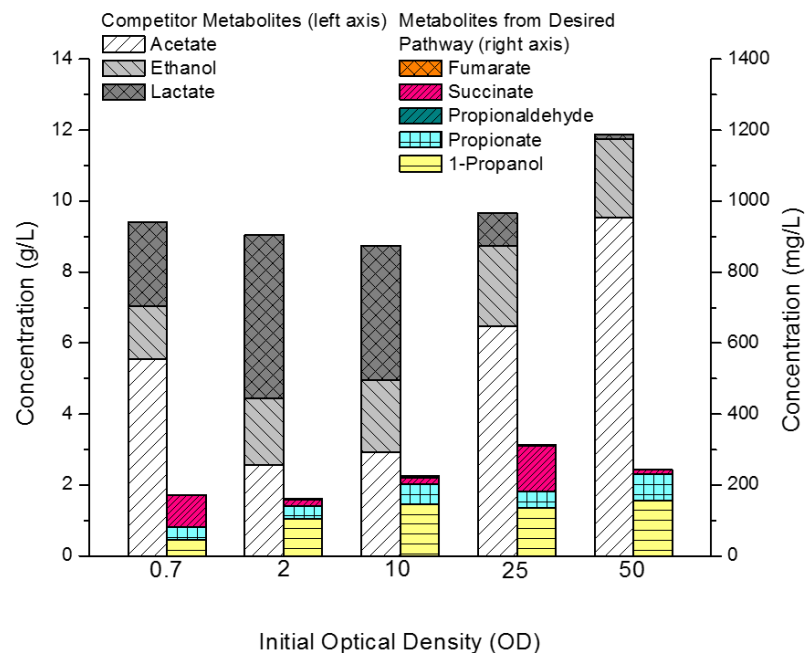


Figure 3.4: End point secretion profile of major end products from anaerobic fermentations of WT-adhE2(CA)³ at five optical densities (OD₆₀₀), profiled by 1D-¹H-NMR.

Major end products that are competitor metabolites to the production of 1-propanol are quantified by the left axis. Products detected along the desired metabolic pathway towards formation of 1-propanol are quantified by the right axis. Strain was cultivated anaerobically in reduced M9 minimal media with 20 g/L of glucose at 37 °C for 72 h.

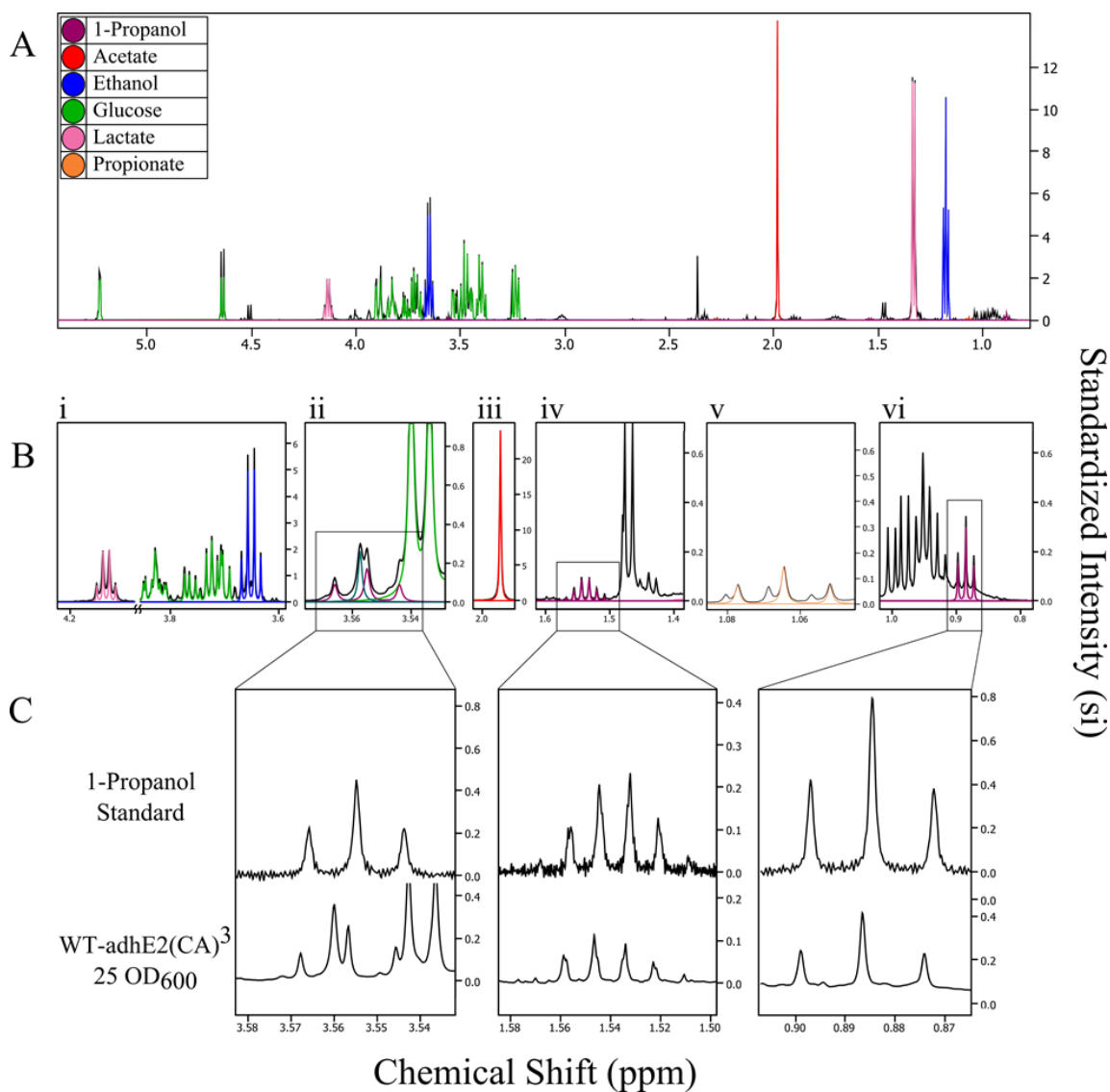


Figure 3.5: Single dimension hydrogen NMR spectra scanned at 600 MHz from samples of *E. coli* supernatant from strain WT-adhE2(CA)³.

Strain was cultivated anaerobically in reduced M9 minimal media with 20 g/L of glucose at 37 °C for 72 h. Culture samples were then centrifuged for 3 min at 13,000 × g to recover the supernatant fraction for analysis. A) The 25 OD₆₀₀ spectrum profiled for metabolites using Chenomx Suite 7.5. B) Zoomed in panels from part A, identifying the three peak clusters of 1-propanol and major end-product metabolites. From left to right the panels show: i. lactate, glucose and ethanol peaks, ii. convolution of glycine spectra with that of the first 1-propanol peak cluster, iii. acetate, iv. the unobscured second peak cluster of 1-propanol, v. propionate, vi. the third peak cluster of 1-propanol. C) Zoomed in panels from part B of the three 1-propanol peak clusters from pure solution standard and supernatant of WT-adhE2(CA)³ grown at 25 OD₆₀₀.

3.3.3 Effects of various ADHs on 1-propanol production

Based on reported biosynthetic pathways of several alcohols (particularly long-chain alcohols) (116, 158), the sequential reduction of propionyl-CoA to propionaldehyde and then to 1-propanol via a bifunctional ADH can represent a key step limiting the overall production of 1-propanol. In addition to *C. acetobutylicum* bifunctional ADH (AdhE2), various other ADHs were investigated in this study. *E. coli* has several ADHs, including AdhE, AdhP, YqhD, EutG, and YiaY (158). To evaluate the effects of these endogenous ADHs on 1-propanol production, an *E. coli* strain of WT2, similar to WT-adhE2(CA)³ but without episomal expression of AdhE2, was derived. This strain, though harboring its native ADHs, failed to produce any detectable amount of 1-propanol after 72 h of cultivation (data not shown). The results suggest that 1-propanol production was primarily mediated by *C. acetobutylicum* AdhE2 in WT-adhE2(CA)³. In principle, 1-propanol should be detected in WT2, since bioinformatics databases such as BRENDA (159) report that certain *E. coli* ADHs also possess affinity for either propionyl-CoA and/or propionaldehyde as potential substrates. The abolishment of 1-propanol production in WT2 may be attributed to the very low basal levels of the native ADHs present in the cell with higher affinities for other substrates.

To further study the effects of various *E. coli* ADHs on 1-propanol production, we respectively cloned the *adhE*, *adhP*, and *yqhD* genes for episomal expression (**Figure 3.2**) and the results are summarized in **Table 3.4**. Amongst the native ADHs, YqhD and AdhP were of particular interest because of their affinity for medium-to-long chain substrates (158). Titers of 1-propanol detected in the WT-adhP(EC) and WT-yqhD(EC) cultures were ~25% less than that in WT-adhE2(CA)³. Note that both YqhD and AdhP are unifunctional ADHs and thus lack an acetaldehyde dehydrogenase domain at the carboxyl end. The bifunctional AdhE of *E. coli* (encoded by the *adhE* gene) was also evaluated. However, the plasmid containing the *E. coli adhE* gene cannot be transformed into *E. coli* cells since episomal expression of the endogenous AdhE appears to be physiologically toxic. To circumvent this limitation, we derived an aerotolerant mutant of AdhE, which was previously documented to be less toxic to *E. coli* cells (160), and the corresponding propanogenic strain, i.e. WT-AdhE^{MUT}(EC), could produce 1-propanol, but only at a level similar to WT-adhP(EC) and WT-yqhD(EC) (Table 2). These results

suggest that the activities of *E. coli* ADHs towards propionyl-CoA or propionaldehyde are less than *C. acetobutylicum* AdhE2 under similar cultivation conditions. Moreover, the utilization of a unifunctional or bifunctional ADH seems to have no major effects on 1-propanol biosynthesis. In addition to AdhE2, two alternative ADHs from *C. acetobutylicum*, i.e. AdhE1 and BdhB, which are involved in butanol production during Clostridia solventogenesis phase (161), were examined for their effects on 1-propanol production using WT-adhE1(CA) and WT-bdhB(CA) (Table 2). The 1-propanol titer of the WT-adhE1(CA) culture was ~25% lower than that of WT-adhE2(CA)³, whereas WT-bdhB(CA) demonstrated a 1-propanol capacity similar to WT-adhE2(CA)³ (**Table 3.4**). The results suggest that 1-propanol biosynthesis in *E. coli* can be mediated by a variety of ADHs and the intracellular levels of these ADHs appear to be critical to drive 1-propanol production under shake flask culture conditions.

3.3.4 Effects of host-gene deletions on 1-propanol production

While 1-propanol production based on this novel pathway in *E. coli* is feasible, the titer and yield can be potentially limited by the accumulation of major metabolites of lactate, acetate, and ethanol (**Figure 3.4**). Hence, we also explored deletion of several host genes involved in the production of these metabolites, specifically *adhE* encoding AdhE, *pta* encoding phosphotransacetylase, and *ldhA* encoding lactate dehydrogenase, and the results are summarized in Table 3. Deletion of *adhE* (in WT- Δ *adhE*) reduced the production of ethanol significantly compared to wild-type BW25141. However, the 1-propanol-producing capacity of WT- Δ *adhE* appears to be completely abolished, even after being transformed with the triple-plasmid expression system for activation of the Sbm pathway (data not shown). On the other hand, deleting *pta* (in WT- Δ *pta*) resulted in marked growth retardation though the acetate levels were significantly reduced, compared to wild-type BW25141, with the main fermentative byproduct being lactate. Similar to WT- Δ *adhE*, WT- Δ *pta* was also incapable of producing 1-propanol when being transformed with the triple-plasmid expression system (data not shown). Deletion of *ldhA* (in WT- Δ *ldhA*) did not significantly reduce lactate titers, yet superior cell growth was observed compared to wild-type BW25141 under aerobic conditions. In contrast to the previous two mutant strains, WT- Δ *ldhA* retained the 1-propanol-producing capacity upon its transformation with the triple-plasmid expression system. Nevertheless, the 1-propanol titers for these

expression systems were approximately half of that for WT-adhE2(CA)³ (**Table 3.5**). Note that both ethanol and acetate titers for these WT- Δ ldhA expression systems were significantly higher than WT-adhE2(CA)³, implying that the carbon flux was not properly channeled into the 1-propanol-producing pathway. Furthermore, while WT- Δ ldhA expression systems were competent producers of 1-propanol, certain double (i.e. Δ ldhA Δ adhE) and triple mutant (i.e. Δ ldhA Δ adhE Δ pta) counterparts failed to produce the target metabolite under shake flask culture conditions (data not shown).

Table 3.4: Comparison of 1-propanol production titers and other metabolites (mg/L) by expression of several ADHs in *E. coli* strain BW25141, transformed with appropriate plasmids. Cultures were suspended in reduced M9 minimal media and induced at an O.D600 of 15. Strains were cultivated anaerobically at 37 °C for 72 h. Glucose (20 g/L) was used as the sole carbon source and all experiments were performed in triplicate.

Strain	Metabolite titers (mg/L)					
	Succinate	Lactate	Acetate	Propionate	Ethanol	1-Propanol
Control						
BW25141	307 ± 36	128 ± 11	4436 ± 250	—	3021 ± 156	—
Experimental						
WT-adhE2(CA) ³	231 ± 11	1877 ± 303	2653 ± 55	51 ± 14	2774 ± 297	103 ± 16
WT-adhP(EC)	239 ± 57	2986 ± 498	2545 ± 89	100 ± 18	3192 ± 80	84 ± 7
WT-yqhD(EC)	Trace	3322 ± 920	3818 ± 826	29 ± 67	3469 ± 538	69 ± 10
WT-adhE ^{MUT} (EC)	Trace	3762 ± 393	2164 ± 64	Trace	4016 ± 83	74 ± 6
WT-adhE1(CA)	Trace	411 ± 120	4247 ± 198	71 ± 10	4397 ± 403	76 ± 11
WT-bdhB(CA)	150 ± 131	2139 ± 474	2329 ± 21	67 ± 22	3455 ± 169	109 ± 6

Table 3.5: Secretion profile of the metabolites produced (mg/L) by various knock out strains. Cultures were suspended in reduced M9 minimal media and induced at an O.D₆₀₀ of 15. Strains were cultivated anaerobically at 37 °C for 72 h. Glucose (20 g/L) was used as the sole carbon source and all experiments were performed in triplicate.

Strain	Metabolite titers (mg/L)					
	Succinate	Lactate	Acetate	Propionate	Ethanol	1-Propanol
Controls						
BW25141	307 ± 36	128 ± 11	4436 ± 250	—	3021 ± 156	—
WT- $\Delta adhE$	Trace	99 ± 17	4646 ± 705.2	—	1936 ± 741.9	—
WT- Δpta	776 ± 57	7259 ± 14	694 ± 196	—	3927 ± 691	—
WT- $\Delta ldhA$	187 ± 7	195 ± 14	3960 ± 151	—	6128 ± 80	—
Experimental						
WT-adhE2(CA) ³	231 ± 11	1877 ± 303	2653 ± 55	51 ± 14	2774 ± 297	103 ± 16
$\Delta ldhA$ - adhE(EC)	206 ± 49	63 ± 3	4181 ± 550	—	6209 ± 183	42 ± 4
$\Delta ldhA$ - adhE2(CA)	247 ± 64	77 ± 4	4210 ± 292	—	6713 ± 270	57 ± 1
$\Delta ldhA$ - adhE1(CA)	256 ± 106	81 ± 10	3696 ± 652	—	5863 ± 9	45 ± 10
$\Delta ldhA$ - adhE ^{MUT} (EC)	243 ± 8	79 ± 7	3814 ± 26	—	6021 ± 104	60 ± 9
$\Delta ldhA$ - adhP(EC)	208 ± 115	190 ± 16	4488 ± 126	—	6124 ± 119	65 ± 2
$\Delta ldhA$ -yqhD(EC)	145 ± 49	99 ± 16	4145 ± 14	—	5732 ± 77	38 ± 1
$\Delta ldhA$ - bdhB(CA)	212 ± 50	89 ± 12	4351 ± 204	—	5652 ± 195	41 ± 4

3.4 Discussion

To date, metabolic engineering of *E. coli* for 1-propanol biosynthesis has been conducted through two major pathways, i.e. (1) the keto-acid biosynthetic pathway (134, 139, 145) and (2) the extended 1,2-propanediol pathway (143). Unlike these approaches, our strategy focused on activation of the endogenous but often silent Sbm operon for extended conversion of succinate into 1-propanol. The 1-propanol-producing capacity was implemented by transforming a wild-type *E. coli* strain, BW25141, with three plasmids respectively harboring the Sbm operon genes (with the exception of *ygfG*), *sucCD*, and *adhE2* for expression of these key genes. Using the metabolically engineered strains for anaerobic fermentation, we obtained 1-propanol titers up to 150 mg/L which is comparable to those of other studies (143, 144). In addition, we identified several potential factors limiting 1-propanol production, in particular the abundance of precursors and the conversion step catalyzed by a bi-functional alcohol/aldehyde dehydrogenase. While it is possible to perform this biotransformation aerobically, anaerobic cultivation was chosen for two reasons. Firstly, the two TCA intermediates of succinate and succinyl-CoA are the precursors for 1-propanol biosynthesis and their abundance can potentially limit 1-propanol production. Under anaerobic, but not aerobic, conditions, *E. coli* generates both succinate and succinyl-CoA as fermentation end products via a reductive reverse TCA pathway (**Figure 3.1**). Secondly, potential oxygen-sensitivity of AdhE2 and other ADHs is another limitation for oxygenic production of 1-propanol.

While the expression of enzymes encoded by the Sbm operon is potentially detectable, their levels are far too low to form a functional pathway (16, 148, 162). Moreover, due to *E. coli*'s inability to produce coenzyme B₁₂, the expressed Sbm remains as an inactive apo-enzyme, but nano-molar supplementation of cyanocobalamin can result in the formation of active Sbm (163, 164). Our observations of no detectable titers of propionate and 1-propanol for wild-type BW25141 as well as the production of 1-propanol upon heterologous expression of the Sbm operon genes with proper supplementation of cyanocobalamin was associated with the activation of the Sbm-pathway. While the activated Sbm-pathway can result in 1-propanol production, the expression of SucCD was deemed crucial to increase the succinyl-CoA pool and consequently the 1-propanol titer. In addition, 1-propanol production was enhanced by exogenous supplementation of succinate. These results suggest that 1-propanol production can be limited by the availability of various precursors and key enzymes along this 1-propanol-producing pathway.

While the metabolic context for the three enzymes encoded by the four-gene Sbm operon, i.e. Sbm, YgfG, and YgfH, has been unraveled, the biological role of the other member, i.e. YgfD/ArgK,

remains ambiguous. Earlier studies determined that YgfD/ArgK is a putative arginine kinase interacting with Sbm *in vivo* and *in vitro* (148) and involved in the phosphorylation of periplasmic binding proteins for amino acid translocation (14). The activity of YgfD/ArgK was shown to be potentially essential for 1-propanol biosynthesis since the 1-propanol titer was significantly reduced by the *ygfD/argK* deletion. Interestingly, propionate production was hardly affected by the *ygfD/argK* deletion, and this result is consistent with a previous report (84), where propionate was derived from fatty acids by expressing the Sbm-operon genes excluding *ygfD/argK* in an engineered *E. coli* strain.

A selection of native and non-native ADHs were heterologously expressed for evaluation of their effects on 1-propanol-producing capacity of various metabolically engineered *E. coli* strains, with AdhE2 and BdhB being identified as the most prominent ones for 1-propanol production. Nevertheless, our consistent observation that ethanol titers were significantly higher than 1-propanol implies that propionyl-CoA or propionaldehyde might have less affinity towards ADHs than acetyl-CoA or acetaldehyde. Several native *E. coli* ADHs (e.g. YqhD, AdhP, and AdhE^{MUT}) were also active in driving 1-propanol production, but in a much lower titer. In particular, the generation of the aerotolerant AdhE mutant (AdhE^{MUT}) opens an avenue for aerobic production of 1-propanol. Under anaerobic conditions, the maximum theoretical yield (on the molar basis) of 1-propanol from glucose is less than one due to limited NADH availability. Thus, developing an oxygenic production system would be beneficial as it increases the carbon throughput whilst improving cell growth and physiology.

Under anoxic conditions for anaerobic fermentation in *E. coli*, the carbon flux at the PEP node favors reduction into pyruvate rather than carboxylation into oxaloacetate (OAA), with lactate, acetate, and ethanol as major metabolites (**Figure 3.1**). Note that there are four NADH-consuming steps along the 1-propanol-producing pathway downstream of phosphoenolpyruvate (PEP), whereas only one or two NADH-consuming steps for the other pathways associated with the major metabolites. The anaplerotic reactions within the metabolic network are optimized in order to balance the cell's energy budget and electrons. Consequently, only ~10% of glucose consumed is channeled towards succinate and cell mass (165). Our results suggest that the production of 1-propanol was potentially hampered by the inherent limitation in succinate production and a metabolic deficiency in NADH generation. Interestingly, propionate was also concomitantly produced with 1-propanol in our metabolically engineered strains (**Table 3.3 and 3.4**). Additional studies are needed to elucidate the dichotomy between 1-propanol and propionate accumulation.

There is an apparent need to reduce the amounts of major metabolites, i.e. ethanol, acetate, and lactate. This could be achieved by knocking out relevant native genes in the hope to redirect the carbon flux into the 1-propanol-producing pathway. While deletions of both *adhE* and *pta* were previously found to improve succinate titers (166), these mutations abolished 1-propanol production in our study (data not shown). Deletion of *pta* resulted in the channeling of the carbon flux towards lactate accumulation. In addition, heterologous expression of *E. coli* AdhE or other ADH homologs failed to complement the *adhE* genomic knockout in terms of restoring 1-propanol production, potentially due to unknown perturbations in the metabolite pool or gene regulation. While the lactate level was significantly reduced for the *ldhA* null mutants, they produced considerable levels of both acetate and ethanol, thus reducing the carbon flux towards 1-propanol production (**Table 3.5**). Nonetheless, the *ldhA* mutation was deemed beneficial since it offers an additional NADH source and greatly reduces the acidification of the medium, thus improving cell growth.

Another critical factor limiting the production of 1-propanol (and other desired metabolites, such as succinate (166) and malate (167)) is the energetically favored diversion of carbon flux at the node of PEP towards pyruvate, resulting in the production of the major metabolites ethanol, lactate, and acetate. Blocking the production of one of these major metabolites (i.e. lactate, acetate, or ethanol) causes the accumulation of the others without improving the overall production of 1-propanol since these major metabolites all share the same precursor of pyruvate. Therefore, the implementation of a “driving force” diverting the carbon flux from pyruvate to OAA appears to be inevitable. Several metabolic engineering strategies to improve this are currently under our investigation. Since a considerable amount of succinate accumulated in the extracellular medium potentially due to the poor affinity of succinate to SucCD (K_m of ~0.25 mM with succinyl-CoA as the substrate in comparison to K_m of ~4 mM with succinate as the substrate (168)), we are also identifying novel succinyl-CoA synthetases with a higher affinity for succinate to alleviate this limitation in 1-propanol production.

In conclusion, in this chapter, we demonstrated the manipulation of the homologous Sbm operon for extended dissimilation of succinate in *E. coli*, leading to 1-propanol production. Using the engineered *E. coli* strains for anaerobic cultivation in a shaker, 1-propanol titers up to 150 mg/L could be obtained. However, ethanol, acetate, and lactate represented the major metabolites, potentially limiting the productivity of 1-propanol. To improve the efficiency and applicability of this biocatalytic system, further studies have to be conducted to derive superior production strains by eliminating key conversion

bottlenecks, metabolic imbalances, and undesirable byproducts as well as to optimize gene expression and culture conditions.

Chapter 4

Biochemical, genetic and metabolic engineering strategies to enhance co-production of 1-propanol and ethanol in engineered propanogenic *E. coli*

Chapter Abstract

In the previous chapter, the heterologous production of 1-propanol was demonstrated in *Escherichia coli* via extended dissimilation of succinate under anaerobic conditions through expression of the endogenous Sbm operon. In this portion of the study, we demonstrate high-level coproduction of 1-propanol and ethanol by further developing novel engineered *E. coli* strains with effective cultivation strategies. Various biochemical, genetic, metabolic, and physiological factors affecting relative levels of acidogenesis and solventogenesis during anaerobic fermentation were investigated. In particular, CPC-PrOH3, a plasmid-free propanogenic *E. coli* strain derived by activating the Sbm operon on the genome, showed high levels of solventogenesis accounting for up to 85% of dissimilated carbon. Anaerobic fed-batch cultivation of CPC-PrOH3 with glycerol as the major carbon source produced high titers of nearly 7 g/L 1-propanol and 31 g/L ethanol, implying its potential industrial applicability. Note, the activated Sbm pathway served as an ancillary channel for consuming reducing equivalents upon anaerobic dissimilation of glycerol, resulting in an enhanced glycerol dissimilation and a major metabolic shift from acidogenesis to solventogenesis.

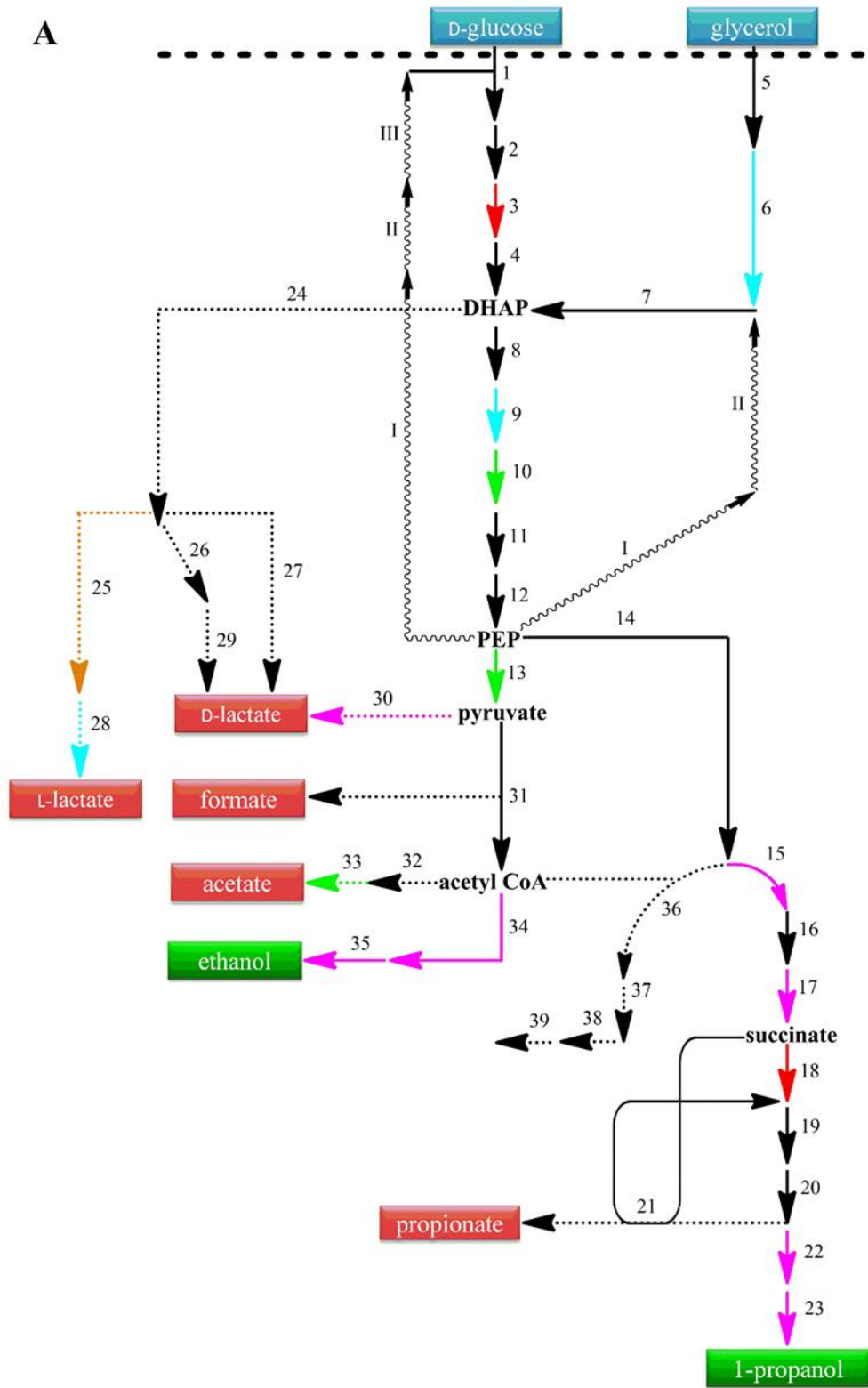
4.1 Background

1-Propanol is a C3-primary alcohol with broad industrial applicability, serving as a precursor for the production of several commodity chemicals (e.g. diesel fuels and propylene) and a general solvent in the pharmaceutical and textile industries for the formulation of drugs, antiseptic solutions, cosmetics, and dyes (169). In addition, several physical and chemical properties make 1-propanol superior to ethanol as an alternative biofuel (170). 1-Propanol is produced primarily by petrochemical processes, such as Oxo synthesis, which is currently the most cost-effective approach (171). Due to rising environmental concerns and finite crude oil reserves, a recent paradigm is the development of biotechnological (particularly, microbial) platforms for the production of biofuels, high-value commodities, and fine chemicals (2, 170-172). Cultivation of engineered microorganisms with low-cost renewable feedstock for sustainable biofuel production may eventually displace existing fossil fuel technologies.

While no microorganisms have been identified as natural producers of 1-propanol, technological advances in synthetic biology and metabolic engineering have enabled the production of 1-propanol using engineered strains of *E. coli*. For example, the L-threonine (10, 134, 136) and citramalate (12) pathways have been exploited for 1-propanol biosynthesis. Subsequently, synergistic coupling of the two pathways was shown to further enhance the production (145). Furthermore, expansion of the canonical 1,2-propanediol pathway was explored by dehydrating and subsequently reducing 1,2-propanediol to 1-propanol (143). Alternatively, Deng and Fong (144) reported the production of 1-propanol from a selection of lignocellulosic feedstocks using metabolically engineered *Thermobifida fusca*. Recently, we proposed a novel approach for 1-propanol production through extended dissimilation of the tricarboxylic acid (TCA) cycle intermediate of succinate (173) (**Figure 4.1**). This was accomplished by converting succinate first to succinyl-CoA via succinyl-CoA synthase, subsequently to propionyl-CoA via enzymes associated with the sleeping beauty mutase (Sbm) operon (16), and finally to 1-propanol via bifunctional alcohol/aldehyde dehydrogenases. Specifically, the Sbm operon contains three key genes: (1) *sbm*, encoding a vitamin B₁₂-dependent methylmalonyl-CoA mutase for the isomerization of succinyl-CoA to L-methylmalonyl-CoA, (2) *ygfG*, encoding a methylmalonyl-CoA decarboxylase for decarboxylation of L-methylmalonyl-CoA to propionyl-CoA, and (3) *ygfH*, encoding a propionyl-CoA:succinate transferase facilitating the interconversion between succinyl-CoA and propionyl-CoA. The operon also contains a putative protein kinase (encoded by *ygfD*) whose molecular function remains largely unclear (14, 16). The Sbm operon exists in the wild-type *E. coli* genome, but its expression remains minimal due to an inherently weak or inactive promoter (16, 148), such that wild-type *E. coli* strains do not produce 1-propanol. Using our engineered *E. coli* strains, production titers up to 150 mg/L of 1-propanol were achieved in shake-flask cultures. However, the culture performance was limited due to a disproportionate channeling of central metabolic intermediates for the production of byproducts such as lactate, acetate, and ethanol (173).

In the present study, we extended our exploration in strain engineering and cultivation strategies to identify various biochemical and genetic factors limiting 1-propanol production. The physiological and metabolic effects associated with host genotype and the expression of the Sbm operon under different culture conditions were investigated. In particular, based on an overall redox balance with respect to the fermentative metabolic network, the selection of a major carbon source for cultivation was identified to critically affect relative levels of acidogenesis and solventogenesis with a significant implication on 1-propanol production. On the other hand, while heterologous genes can be conveniently introduced into host cells via plasmids for cellular manipulation, the presence of multicopy plasmids often imposes a

A



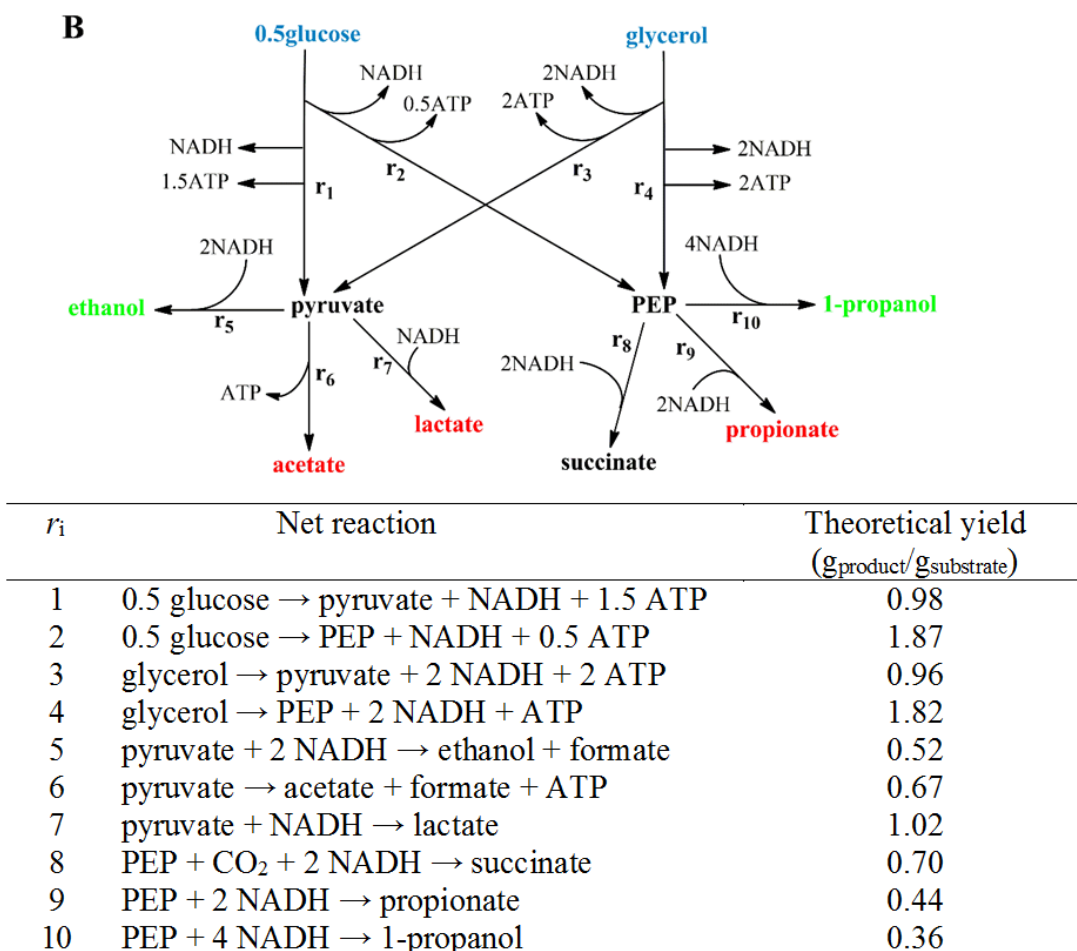


Figure 4.1: Schematic representations of the anaerobic 1-propanol production pathway (A) (on previous page)

Major metabolic pathways for anaerobic fermentation and the activated Sbm pathway for extended dissimilation of succinate to form 1-propanol. Enzymes catalyzing primary (solid lines) and divergent (dashed lines) reactions and the corresponding products are listed. I) phosphotransferase system (PTS) enzyme I (*ptsI*), II) histidine-containing protein (*ptsH*), III) PTS enzyme IIA^{glucose} (*crr*), 1) PTS enzyme IIBC^{glucose} (*ptsG*): D-glucose-6-P, 2) glucosephosphate isomerase (*pgi*): D-fructose-6-P, 3) 6-phosphofruktokinase I/II (*pfkAB*): fructose-1,6-BP, 4) fructose-bisphosphate aldolase (*fbpA*), 5) glycerol channel protein (*glpF*), 6) glycerol dehydrogenase (*gldA*): dihydroxyacetone, 7) dihydroxyacetone kinase (*dhaKLM*), 8) triosephosphate isomerase (*tpiA*): glyceraldehyde-3-P, 9) glyceraldehyde-3-phosphate dehydrogenase A (*gapA*): 1,3-bisphosphoglycerate, 10) phosphoglycerate kinase (*pgk*): 3-phosphoglycerate, 11) phosphoglyceromutase 1 (*gpmA*): 2-phosphoglycerate, 12) enolase (*eno*), 13) pyruvate kinase I/II (*pykFA*), 14) phosphoenolpyruvate carboxylase (*pepC*): oxaloacetate, 15) malate dehydrogenase (*mdh*): malate, 16) fumarase A, B, and C (*fumABC*): fumarate, 17) fumarate reductase (*frdABCD*), 18) succinyl-CoA synthetase (*sucCD*): succinyl-CoA, 19) methylmalonyl-CoA mutase (*scpA*): L-methylmalonyl-CoA, 20) methylmalonyl-CoA decarboxylase (*scpB*): propionyl-CoA, 21)

propionyl-CoA/succinate CoA transferase (*scpC*): succinyl-CoA and propionate, 22) alcohol dehydrogenase (*adhE*): propionaldehyde, 23) alcohol dehydrogenase (*adhE*), 24) methylglyoxal synthase (*mgsA*): methylglyoxal, 25) methylglyoxal reductase (*mgr*): L-lactaldehyde, 26) glyoxalase I (*gloA*): S-lactoyl-glutathione, 27) glyoxalase III (*hchA*), 28) lactaldehyde dehydrogenase (*aldA*), 29) S-lactoylglutathione hydrolase (*yeiG*) and glyoxalase II (*gloB*), 30) D-lactate dehydrogenase (*ldhA*), 31) pyruvate formate lyase I (*pflB*), 32) phosphate acetyltransferase (*pta*), 33) acetate kinase A (*ackA*), 34) alcohol dehydrogenase (*adhE*): acetaldehyde, 35) alcohol dehydrogenase (*adhE*), 36) citrate synthase (*gltA*): citrate, 37) aconitate hydratase/2-methylisocitrate dehydratase (*acnB*): *cis*-aconitate, 38) aconitate hydratase/2-methylisocitrate dehydratase (*acnB*): *D-threo*-isocitrate, 39) isocitrate dehydrogenase (*icd*): 2-oxoglutarate. Green lines indicate ATP-generating reactions, red lines indicate ATP-consuming reactions, blue lines indicate NADH-generating reactions, pink lines indicate NADH-consuming reactions, and orange lines indicate NADPH-consuming reactions. Compounds highlighted in blue represent primary carbon sources, compounds highlighted in green represent target solvents, and compounds highlighted in red represent undesirable metabolites. Wavy lines represent intermediate reactions of the PTS for glucose and glycerol metabolism. **(B)** *On previous page* - Overall reactions (r_1 - r_{10}) connecting major metabolic nodes. Theoretical yields are calculated based on stoichiometric ratio of the product to the initial substrate (i.e. glucose or glycerol). Products: pyruvate (r_1), PEP (r_2), pyruvate (r_3), PEP (r_4), ethanol (r_5), acetate (r_6), lactate (r_7), succinate (r_8), propionate (r_9), and 1-propanol (r_{10}).

severe metabolic burden to cells and/or may result in various technical issues arising from structural and segregational plasmid instability, ultimately leading to retarded cell growth and diminished product formation. With recent technological advances in genomic engineering, plasmid-free systems can be more suitable for biomanufacturing purposes, particularly from the standpoint of metabolic engineering applications for which gene dosage is unlikely a limiting factor (174-176). Herein, we also report the derivation of a plasmid-free propanogenic *E. coli* strain by activating the chromosomal *Sbm* operon for high-level coproduction of 1-propanol and ethanol.

4.2 Methods

4.2.1 Bacterial strains and plasmids

E. coli strains, plasmids and DNA primers used in this study are listed in **Table 4.1**. Standard recombinant DNA technologies for molecular cloning were applied (150). *Pfu* and *Taq* DNA polymerases, T4 DNA ligase, and large (Klenow) fragment of DNA Polymerase I were obtained from New England Biolabs (Ipswich, MA). All synthesized oligonucleotides were obtained from Integrated DNA Technologies (Coralville, IA). DNA sequencing was conducted by the Centre for Applied Genomics at the Hospital for Sick Children (Toronto, Canada).

E. coli BW25141 was used to provide the parental genetic background for 1-propanol production. *E. coli* HST08 was used for molecular cloning. Gene knockouts were introduced to BW25141 strains by

P1-phage transduction (150) using proper Keio Collection strains (The Coli Genetic Stock Center, Yale University) as donors (152). The co-transduced Km^R-FRT gene cassette was removed using pCP20 (153). The genotypes of derived knockout strains were confirmed by colony PCR using appropriate primer sets.

To fuse the strong promoter (P_{trc}) with the Sbm operon in the *E. coli* genome, we used a modified λ Red-mediated recombination protocol (177) (**Figure 4.2**). The FRT-Cm^R-FRT cassette was PCR-amplified from pKD3 using the c-frt primer set, whereas the P_{trc} promoter-operator fragment was PCR-amplified from pTrc99a using the c-ptrc primer set. The two DNA fragments were fused by splice overlap extension (SOE) PCR (151) using the forward primer of the c-frt primer set and the reverse primer of the c-ptrc primer set to generate the FRT-Cm^R-FRT- P_{trc} cassette. To generate the DNA cartridge for genomic integration, the FRT-Cm^R-FRT- P_{trc} cassette was PCR-amplified using the r-frt:ptrc primer set containing the 36-bp homology arms of H1 and H2, respectively. To derive the plasmid-free strain of CPC-PrOH3, 0.5 μ g of the amplified/purified DNA cassette was electro-transformed, using a Gene Pulser (BioRad Laboratories, Hercules, CA) set at 2.5 kV, 25 μ F, and 200 Ω , to WT- Δ ldhA- Δ pykF harboring the λ -Red recombinase expression plasmid pKD46 for DNA recombination to replace the 204-bp upstream region of the Sbm operon (**Figure 4.2**). Expression of the λ -Red recombination enzymes and preparation of competent cells were carried out as described by Datsenko and Wanner (153). After electroporation, cells were resuspended in 500 μ L of SOC (super optimal broth with catabolite repression) medium (3.6 g/L glucose, 20 g/L tryptone, 5 g/L yeast extract, 0.6 g/L NaCl, 0.19 g/L KCl, 4.8 g/L MgSO₄) (178) and recuperated at 37 °C for 1 h in a rotatory shaker at 250 rpm (New Brunswick Scientific, NJ). Cells were then plated on lysogeny broth (LB) agar containing 12 μ g/mL chloramphenicol for incubation at 37 °C for 16 h to select chloramphenicol-resistant recombinants. The fusion of the FRT-Cm^R-FRT- P_{trc} cassette with the Sbm operon was verified by colony PCR using the v-frt:ptrc primer set as well as DNA sequencing.

4.2.2 Media and cultivation conditions

All media components were obtained from Sigma-Aldrich Co. (St Louis, MO) except glucose, yeast extract, and tryptone which were obtained from BD Diagnostic Systems (Franklin Lakes, NJ). Media was supplemented with antibiotics as required (30 μ g/mL kanamycin and 12 μ g/mL chloramphenicol). For 1-propanol production, propanogenic *E. coli* strains (stored as glycerol stocks at -80 °C) were streaked on LB agar plates with appropriate antibiotics and incubated at 37 °C for 16 h. Single colonies were picked from LB plates to inoculate 30-mL SB medium (32 g/L tryptone, 20 g/L yeast extract, and 5 g/L NaCl) with appropriate antibiotics in 125 mL conical flasks. Overnight cultures

were shaken at 37 °C and 280 rpm in a rotary shaker (New Brunswick Scientific, NJ) and used as seed cultures to inoculate 200 mL SB media at 1% (v/v) with appropriate antibiotics in 1 L conical flasks. This second seed culture was shaken at 37 °C and 280 rpm for approximately 16 h. Cells were then harvested by centrifugation at $6,000 \times g$ and 20 °C for 15 min and resuspended in 100-mL fresh LB media. The suspended culture was used to inoculate a 1-L stirred-tank bioreactor (Omni-Culture, VirTis, NY) operated anaerobically at 30 °C and 430 rpm. The production medium in the bioreactor contained 30 g/L carbon source (i.e. glucose or glycerol), 0.23 g/L K_2HPO_4 , 0.51 g/L NH_4Cl , 49.8 mg/L $MgCl_2$, 48.1 mg/L K_2SO_4 , 1.52 mg/L $FeSO_4$, 0.055 mg/L $CaCl_2$, 2.93 g/L NaCl, 0.72 g/L tricine, 10 g/L yeast extract, 10 mM $NaHCO_3$, 0.2 μM cyanocobalamin (vitamin B_{12}), trace elements (2.86 mg/L H_3BO_3 , 1.81 mg/L $MnCl_2 \cdot 4H_2O$, 0.222 mg/L $ZnSO_4 \cdot 7H_2O$, 0.39 mg/L $Na_2MoO_4 \cdot 2H_2O$, 79 $\mu g/L$ $CuSO_4 \cdot 5H_2O$, 49.4 $\mu g/L$ $Co(NO_3)_2 \cdot 6H_2O$), and appropriate antibiotics (179). Anaerobic conditions were maintained by constant bubbling of nitrogen. The pH of the production culture was maintained at 7.0 ± 0.1 with 30% (v/v) NH_4OH and 15% (v/v) HNO_3 . The feeding solution for fedbatch cultivation contained 500 g/L glycerol only and 50 mL of it was added manually when the glycerol concentration in the production culture fell below 5 g/L. IPTG was supplemented in the cultivation medium for induction purposes since it was observed that IPTG supplementation had negligible effects on the 1-propanol production for all propanogenic strains in this study.

4.2.3 Analyses

Culture samples were appropriately diluted with saline for measuring the optical cell density (OD_{600}) using a spectrophotometer (DU520, Beckman Coulter, Fullerton, CA). Cell-free supernatant was collected and filter sterilized for titer analysis of glucose, glycerol, and various metabolites using an HPLC (LC-10AT, Shimadzu, Kyoto, Japan) with a refractive index detector (RID-10A, Shimadzu, Kyoto, Japan) and a chromatographic column (Aminex HPX-87H, Bio-Rad Laboratories, CA, USA). The column temperature was maintained at 65 °C and the mobile phase was 5 mM H_2SO_4 (pH 2.0) running at 0.6 mL/min. The RID signal was acquired and processed by a data processing unit (Clarity Lite, DataApex, Prague, The Czech Republic).

Table 4.1: List of *E. coli* strains, plasmids, and primers used in this study. Notation for primers: v- verification primer, r- recombining primer and c- cloning primer. Underlined sequences within the primers denote the homology arms (H1 and H2).

Name	Description, relevant genotype or primer sequence (5'→3')	Reference
<i>E. coli</i> host strains		
HST08	F-, <i>endA1</i> , <i>supE44</i> , <i>thi-1</i> , <i>recA1</i> , <i>relA1</i> , <i>gyrA96</i> , <i>phoA</i> , $\Phi80d$ <i>lacZ</i> Δ <i>M15</i> , Δ (<i>lacZYA</i> – <i>argF</i>) <i>U169</i> , Δ (<i>mrr</i> – <i>hsdRMS</i> – <i>mcrBC</i>), Δ <i>mcrA</i> , λ -	TaKaRa Bio Inc.
MC4100	F-, [<i>araD139</i>]B/r, Δ (<i>argF-lac</i>)169, λ -, <i>e14</i> -, <i>flhD5301</i> , Δ (<i>fruK-yeiR</i>)725(<i>fruA25</i>), <i>relA1</i> , <i>rpsL150</i> (strR), <i>rbsR22</i> , Δ (<i>fimB-fimE</i>)632(::IS1), <i>deoC1</i>	(154) (CGSC#: 6152)
BW25141	F-, Δ (<i>araD-araB</i>)567, Δ <i>lacZ4787</i> (:: <i>rrnB-3</i>), Δ (<i>phoB-phoR</i>)580, λ -, <i>galU95</i> , Δ <i>uidA3</i> :: <i>pir+</i> , <i>recA1</i> , <i>endA9</i> (del-ins)::FRT, <i>rph-1</i> , Δ (<i>rhaD-rhaB</i>)568, <i>hsdR514</i>	(153) (CGSC#: 7635)
BW25113	F-, Δ (<i>araD-araB</i>)567, Δ <i>lacZ4787</i> (:: <i>rrnB-3</i>), λ -, <i>rph-1</i> , Δ (<i>rhaD-rhaB</i>)568, <i>hsdR514</i>	(153) (CGSC#: 7636)
WT- Δ <i>ldhA</i>	<i>ldhA</i> null mutant of BW25113	(173)
WT- Δ <i>ldhA</i> - Δ <i>pykF</i>	<i>ldhA/pykF</i> double null mutant of BW25113	This study
CPC-CNTRL1	BW25141/pK184	This study
CPC-CNTRL2	WT- Δ <i>ldhA</i> /pK184	This study
CPC-PrOH1	BW25141/pK-scpAKB	This study
CPC-PrOH2	WT- Δ <i>ldhA</i> /pK-scpAKB	This study
CPC-PrOH3	WT- Δ <i>ldhA</i> - Δ <i>pykF</i> , P_{trc} :: <i>sbm</i> (i.e. with the FRT-CmR-FRT- P_{trc} cassette replacing the 204-bp upstream of the <i>Sbm</i> operon)	This study

Plasmids		
pCP20	FLP ⁺ , λ cI857 ⁺ , λ p _R Rep(pSC101 ori) ^{ts} , Ap ^R , Cm ^R	(155)
pKD46	RepA101 ^{ts} ori, Ap ^R , <i>araC</i> -P _{araB} : <i>gam-bet-exo</i>	(153)
pTrc99a	ColE1 ori, Ap ^R , P _{trc}	(180)
pKD3	R6K-γ ori, Ap ^R , FRT-Cm ^R -FRT	(153)
pK184	p15A ori, Km ^R , P _{lac} : <i>lacZ</i> '	(156)
pK-scpAKB	From pK184, P _{lac} : <i>sbm-ygfD-ygfG</i>	(173)
Primers		
v-ldhA	TCATCAGCAGCGTCAACGGC; ATCGCTGGTCACGGGCTTACCGTT	(173)
v-pykF	TAGCAATTGAGCGATGATATATTTATACACCGG; TCGTTGCTCAGCTGGTCAACTTT	This study
c-frt	AGATTGCAGCATTACACGTCTTGAG; CCAGCTGCATTAATGAATCGGGCCATGGTCCATATGAATATCCTCC	This study
c-ptrc	CCGATTCATTAATGCAGCTGG; GGTCTGTTTCCTGTGTGAAATTGTTA	This study
r-frt:ptrc	<u>CTCGATTATGGTCACAAAGTCCTTCGTCAGGATTAAGATTGCAGCATTACACGTCTTGA;</u> <u>GTTGGCAAGCTGTTGCCACTCCTGCACGTTAGACATGGTCTGTTTCCTGTGTGAAATTGT</u>	This study

v-frt:ptrc

GCGCTCGACTATCTGTTCGTCAGCTC; TCGACAGTTTTCTCCCGACGGCTCA

This study

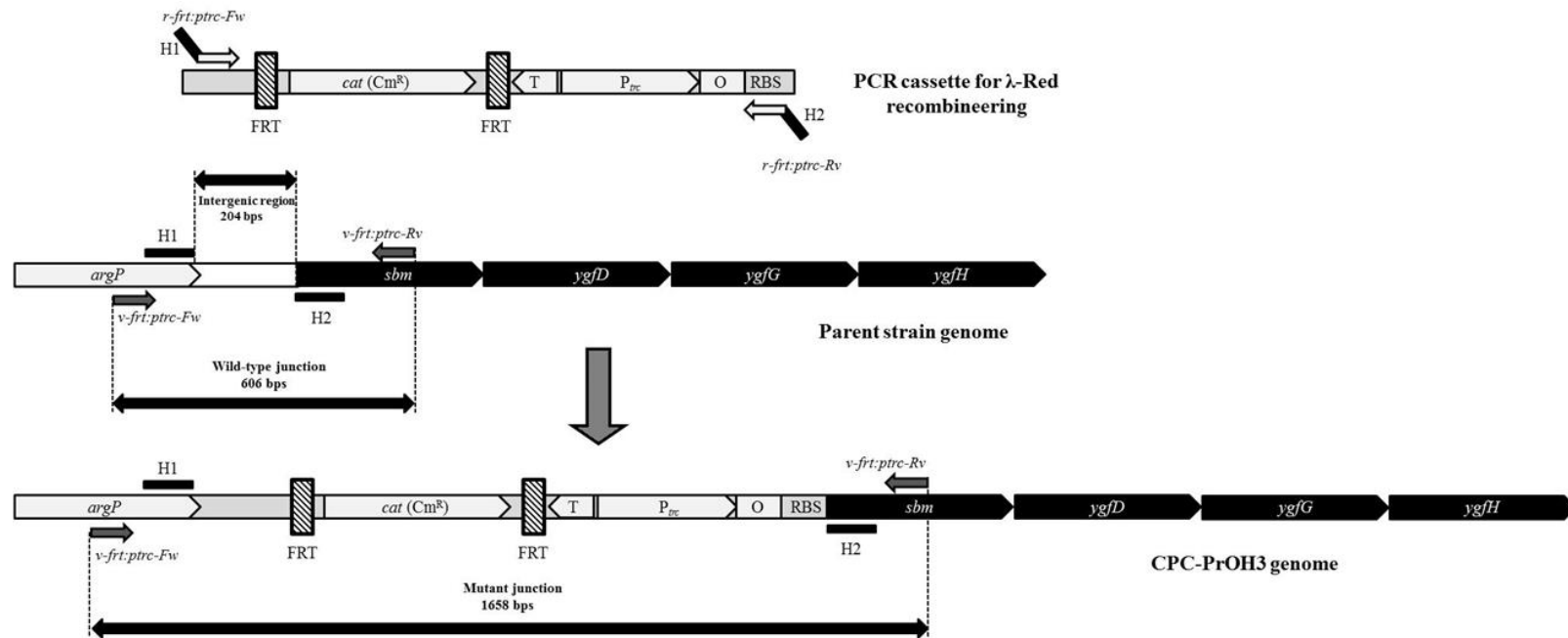


Figure 4.2: Genomic engineering for deriving the plasmid-free propanogenic strain CPC-PrOH3.

In order to activate the naturally silent *Sbm* operon with the strong promoter (P_{ptrc}), the FRT-CmR-FRT- P_{ptrc} fragment was PCR amplified using the primer set of *r-frt:ptrc* with homology extensions (H1 and H2) for λ -Red-mediated recombination to replace the superfluous 204-bp region upstream of the operon. The primer set of *r-frt:ptrc* was used to PCR-verify the genotype of CPC-PrOH3. Genes and regulatory elements [i.e. operator (O), terminator (T) and ribosome binding site (RBS)] are not to scale.

4.3 Results

4.3.1 Biosynthesis of 1-propanol using engineered *E. coli* strains

Anaerobic cultivation of the propanogenic strain CPC-PrOH1 was conducted in a bioreactor using glucose as the major carbon source for the production of 1-propanol (**Figure 4.3B**). The control strain CPC-CNTRL1, harboring an inactive Sbm operon on the genome, had a similar glucose dissimilation pattern to CPC-PrOH1 in terms of cell growth and metabolite production, but showed elevated succinate levels and no 1-propanol production (**Figure 4.3A**). Introducing the Sbm operon genes (i.e. *sbm-ygfD-ygfG*) for episomal expression made the *E. coli* strain propanogenic with a reduced level of succinate, implying 1-propanol was produced through extensive dissimilation of succinate via the Sbm pathway (**Figure 4.1A**). Nevertheless, 1-propanol titer reached only 0.11 g/L with lactate, acetate, and ethanol being the major metabolites (**Figure 4.3B**). Note that previously, in addition to the Sbm operon, two other genes, i.e. *sucCD* (encoding succinyl-CoA synthetase) and *adhE* (encoding the bifunctional aldehyde/alcohol dehydrogenase), were coexpressed episomally to alleviate potential limitation of these conversion steps (173). However, the resulting strains suffered a significant physiological burden associated with the maintenance of multiple plasmids and, consequently, 1-propanol productivity was limited. The physiological limitation appeared minimal for the single-plasmid system of CPC-PrOH1, implying that the aldehyde/alcohol dehydrogenase from *E. coli* was effective in driving 1-propanol production. While glucose dissimilation was complete within 14 h, anaerobic fermentation appeared to significantly lean towards acidogenesis rather than solventogenesis. More than 80% of dissimilated glucose was converted to acetate, lactate, and succinate (**Figure 4.3**), with lactate accounting for more than 60%. On the other hand, only ~15% was diverted to solventogenesis for ethanol and 1-propanol production. It should be noted that formate was not detected in any of the cultures, likely due to active formate dehydrogenases which oxidize this endogenously produced metabolite into CO₂. Since lactate was significantly overproduced, the *ldhA* gene (encoding lactate dehydrogenase) was inactivated with the intention of reducing lactate accumulation as well as shifting carbon flux towards solventogenesis. Culture performance of this mutant strain with glucose as the major carbon source and metabolite profiling are summarized in **Figure 4.4**. Similar to the strains with the parental genetic background, the control *ldhA* mutant strain CPC-CNTRL2 with an inactive Sbm operon on the genome produced elevated levels of succinate (**Figure 4.4A**), whereas the *ldhA* mutant strain CPC-PrOH2 with episomal Sbm expression for extended dissimilation of succinate became propanogenic (**Figure 4.4B**). The efficiency of glucose dissimilation was slightly affected by *ldhA* disruption as total consumption occurred within 18 h

of cultivation. Notably, lactate levels of the *ldhA* mutant strains were significantly reduced to 2 g/L, representing a ~90% reduction compared to the control strains.

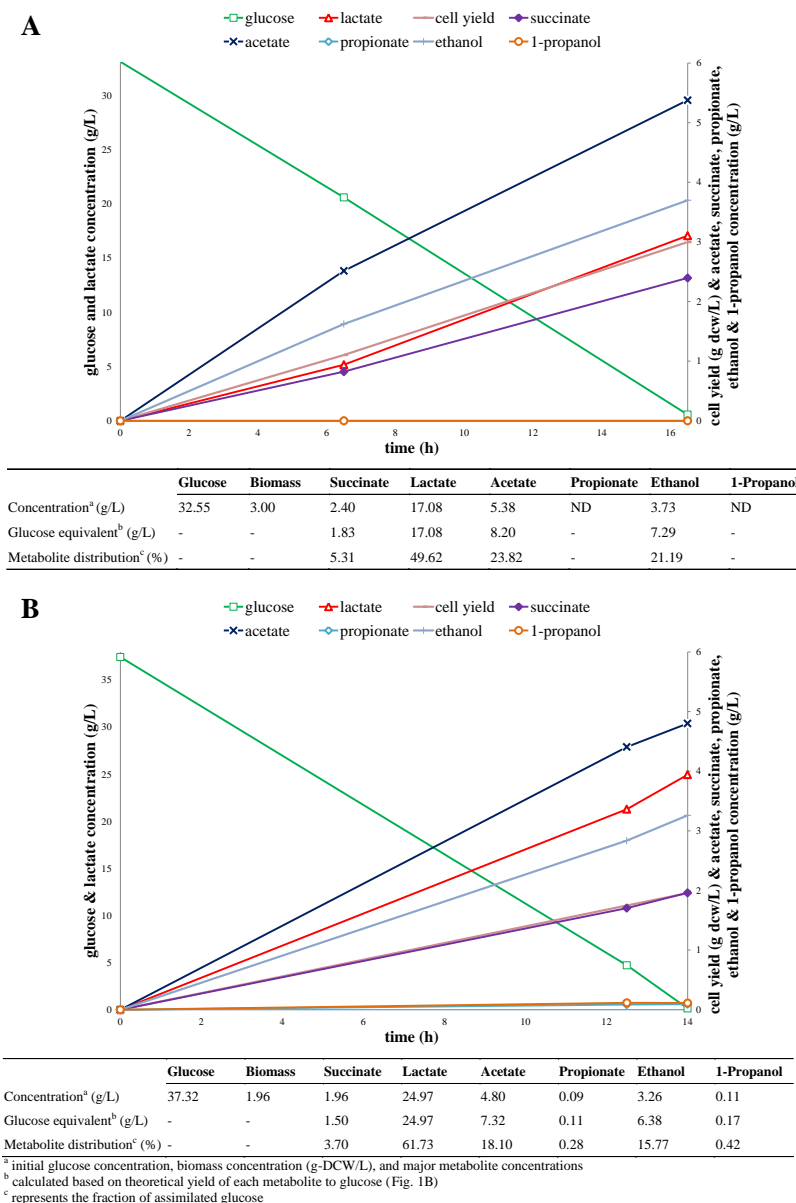
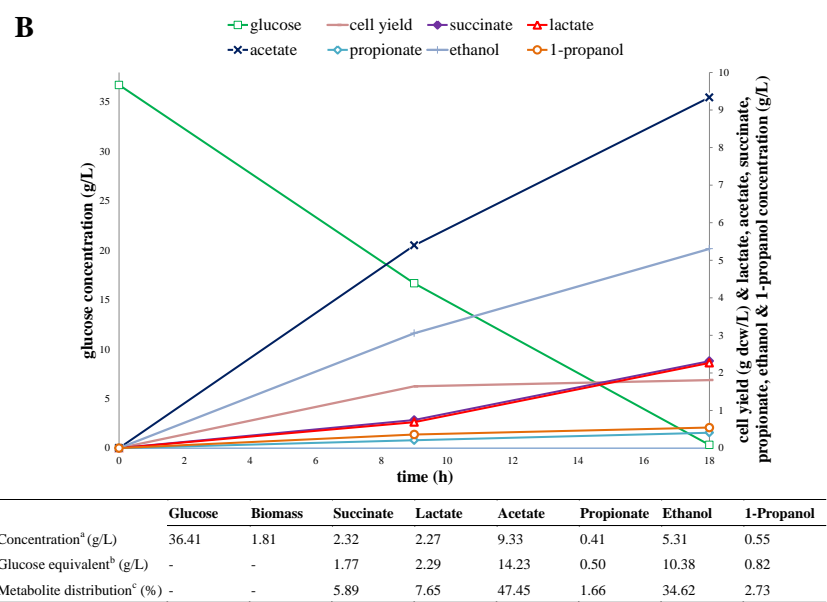
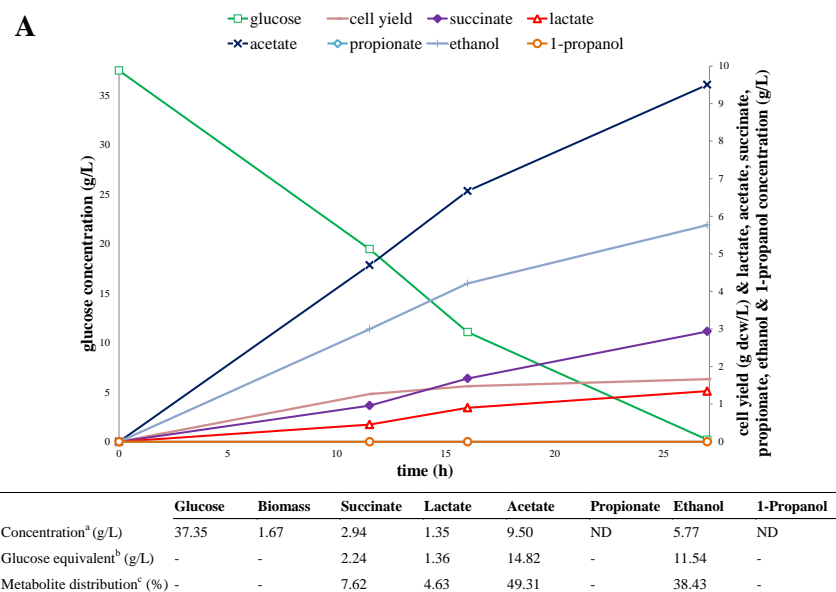


Figure 4.3: Time profiles of glucose, biomass, and major metabolites during batch cultivation of (A) CPC-CNTRL1 and (B) CPC-PrOH1 with glucose as the major carbon source.

Culture performance (i.e. overall glucose consumption and final biomass and metabolite concentrations) of batch cultivation in a bioreactor is summarized in the tables below each time profile. The glucose equivalent for each metabolite is calculated based on the corresponding theoretical yield in **Figure 4.1B**. The metabolite distribution (i.e. the fraction of dissimilated glucose to form a metabolite) is defined as the ratio of the glucose equivalent of a metabolite to the sum of the total glucose equivalents of all metabolites.



^a initial glucose concentration, biomass concentration (g-DCW/L), and major metabolite concentrations
^b calculated based on theoretical yield of each metabolite to glucose (Fig. 1B)
^c represents the fraction of assimilated glucose

Figure 4.4: Time profiles of glucose, biomass, and major metabolites during batch cultivation of (A) CPC-CNTRL2 and (B) CPC-PrOH2 with glucose as the major carbon source.

Culture performance (i.e. overall glucose consumption and final biomass and metabolite concentrations) of batch cultivation in a bioreactor is summarized in the tables below each time profile. The glucose equivalent for each metabolite is calculated based on the corresponding theoretical yield in **Figure 4.1B**. The metabolite distribution (i.e. the fraction of dissimilated glucose to form a metabolite) is defined as the ratio of the glucose equivalent of a metabolite to the sum of the total glucose equivalents of all metabolites.

Low concentrations of lactate were still detected in the cultures of the *ldhA* mutants strains and these small amounts of lactate can be associated with alternative lactate synthetic routes such as the methylglyoxal pathway (**Figure 4.1**) (181). Carbon flux was redirected towards acetate overproduction and enhanced solventogenesis, with acetate and ethanol titers accounting for 47% and 34% of dissimilated glucose, respectively, during CPC-PrOH2 cultivation (**Figure 4.4B**). Most importantly, the 1-propanol titer of the CPC-PrOH2 culture increased significantly to 0.55 g/L, corresponding to 5-fold that of the CPC-PrOH1 culture.

4.3.2 Glycerol serves as a superior carbon source for enhanced solventogenesis

Glycerol is a potentially superior carbon source to glucose, particularly for biofuel production, due to its higher reductance, leading to higher biomass yields and less acidogenesis during fermentation (182). Recent oversupply in the biodiesel industry has made glycerol, a byproduct of biodiesel production, an economically viable feedstock for biomanufacturing (183). Accordingly, glycerol was investigated as a carbon source for anaerobic cultivation of the *ldhA* mutant propanogenic strain, CPC-PrOH2, for 1-propanol production (**Figure 4.5**). Compared with glucose, the glycerol dissimilation rate of CPC-PrOH2 was much slower during batch cultivation, requiring more than 80 h to consume 30 g of glycerol whereas 18 h to consume 30 g of glucose. However, high ethanol titers of 10.9 and 9.3 g/L were obtained for CPC-CNTRL2 and CPC-PrOH2, respectively, when glycerol was used as the major carbon source. Most importantly, 1-propanol titer was 2.15 g/L for CPC-PrOH2, representing an approximate 4-fold increase compared to the batch culture of CPC-PrOH2 with glucose as the major carbon source. The results show that more than 70% of glycerol dissimilation was directed towards solventogenesis (**Figure 4.5**). In contrast to cultures with glucose as the major carbon source, acetate production was minimal and lactate was even undetectable when glycerol was used. This can alleviate the physiological impacts associated with the presence of organic acids in *E. coli* cultures (184), which may limit 1-propanol production. Note that the control strain CPC-CNTRL2 accumulated succinate to 3.45 g/L, whereas the succinate concentration was merely 0.62 g/L for CPC-PrOH2 (**Figure 4.5**), implying that the extended dissimilation of succinate via episomal expression of the *Sbm* operon was functional. In addition, glycerol dissimilation appeared more effective upon episomal expression of the *Sbm* operon since it took 134 h and 85 h to consume 30 g glycerol for CPC-CNTRL2 and CPC-PrOH2, respectively.

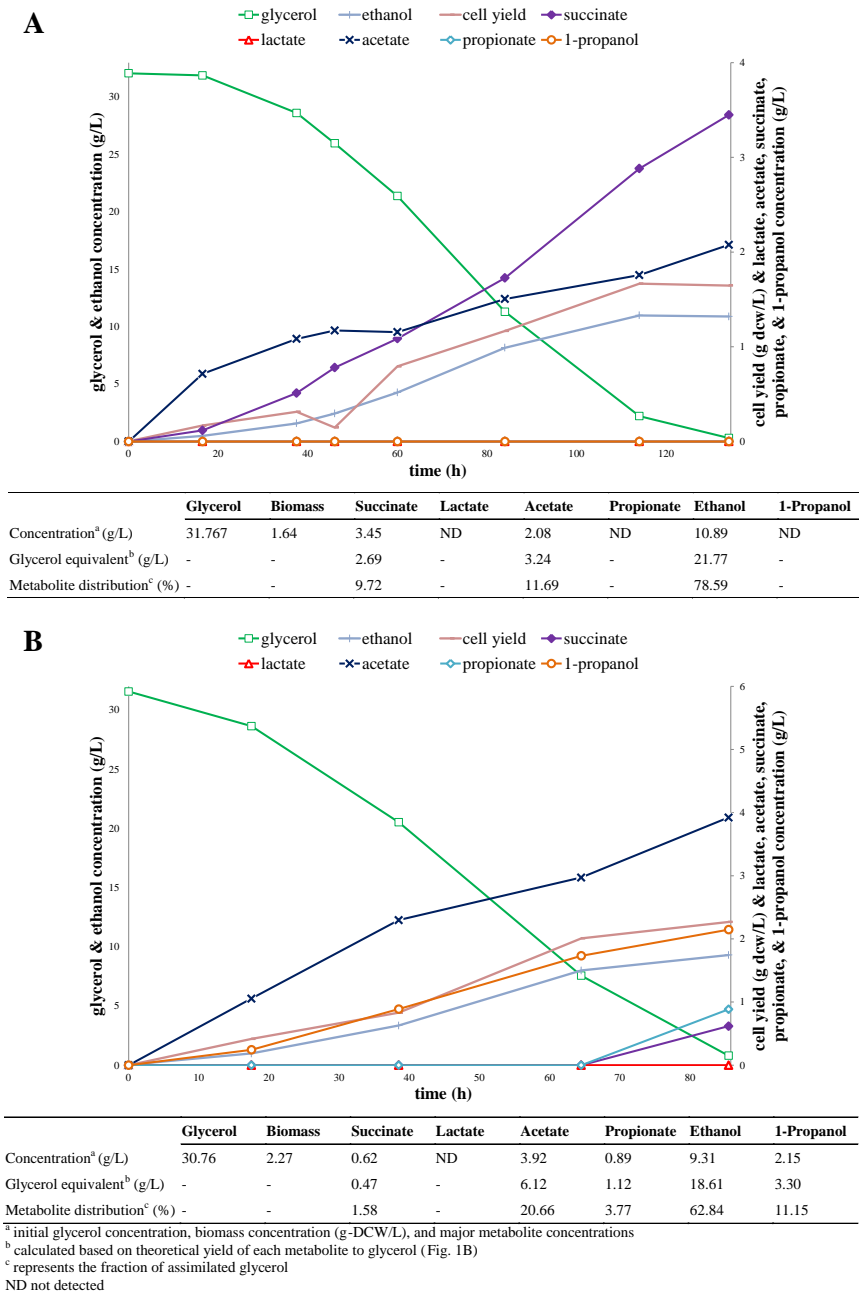


Figure 4.5: Time profiles of glycerol, biomass, and major metabolites during batch cultivation of (A) CPC-CNTRL2 and (B) CPC-PrOH2 with glycerol as the major carbon source.

Culture performance (i.e. overall glycerol consumption and final biomass and metabolite concentrations) of batch cultivation in a bioreactor is summarized in the tables below each time profile. The glycerol equivalent for each metabolite is calculated based on the corresponding theoretical yield in **Figure 4.1B**. The metabolite distribution (i.e. the fraction of dissimilated glycerol to form a metabolite) is defined as the ratio of the glycerol equivalent of a metabolite to the sum of the total glucose equivalents of all metabolites.

4.3.3 Fedbatch cultivation for high-level coproduction of 1-propanol and ethanol

To extend 1-propanol productivity, fedbatch cultivation of CPC-PrOH2 was explored using glycerol as the major carbon source (**Figure 4.6 and Table 4.2A**). Unlike fedbatch cultures using glucose as the major carbon source where a specific glucose feeding profile must be developed to prevent the over-accumulation of organic acids impacting culture performance (185), no glycerol feeding profile was required due to minimal acidogenesis associated with glycerol dissimilation. Instead, a designated amount of glycerol was intermittently fed into the culture as a single inoculum to increase glycerol concentration to 20-25 g/L when depletion of glycerol was observed. The fedbatch culture of CPC-PrOH2 was divided into four stages with glycerol being fed at the start of each stage (**Figure 4.6**) and metabolic analysis was conducted for each stage (**Table 4.2A**). More than 70% of glycerol dissimilation was directed towards solventogenesis, with ethanol and 1-propanol being the two major metabolites, and such high-level solventogenesis was maintained towards the end of the fedbatch culture (**Table 4.2A**). This led to high-level coproduction of ethanol at 25 g/L and 1-propanol at 3.78 g/L. Note that these titers were underestimated due to the dilution by fed glycerol. Given the persistence of high-level solventogenesis throughout the entire fedbatch cultivation, 1-propanol yield steadily decreased and hardly any 1-propanol was produced during the last stage. The results suggest the deterioration of the bioactivity of the Sbm operon, which also resulted in the accumulation of succinate to a high level of 5.44 g/L at the end of the fedbatch cultivation. Glycerol dissimilation rate was increased by approximately 30% upon fedbatch operation (i.e. from 0.35 g/L/h in Stage I to approximately 0.45 g/L/h afterwards) (**Figure 4.6**), presumably due to an increased biomass concentration. While the level of acidogenesis remained low during the entire fedbatch cultivation, acetate steadily accumulated to a final concentration of 8.15 g/L which could potentially impact culture performance. The deterioration in culture performance can also be observed by the decreasing efficiency of glycerol utilization towards metabolite production (**Table 4.2A**), suggesting that a certain amount of glycerol was consumed for cell maintenance and sustained viability in increasingly harsh cultivation conditions during the late stages of fedbatch cultivation.

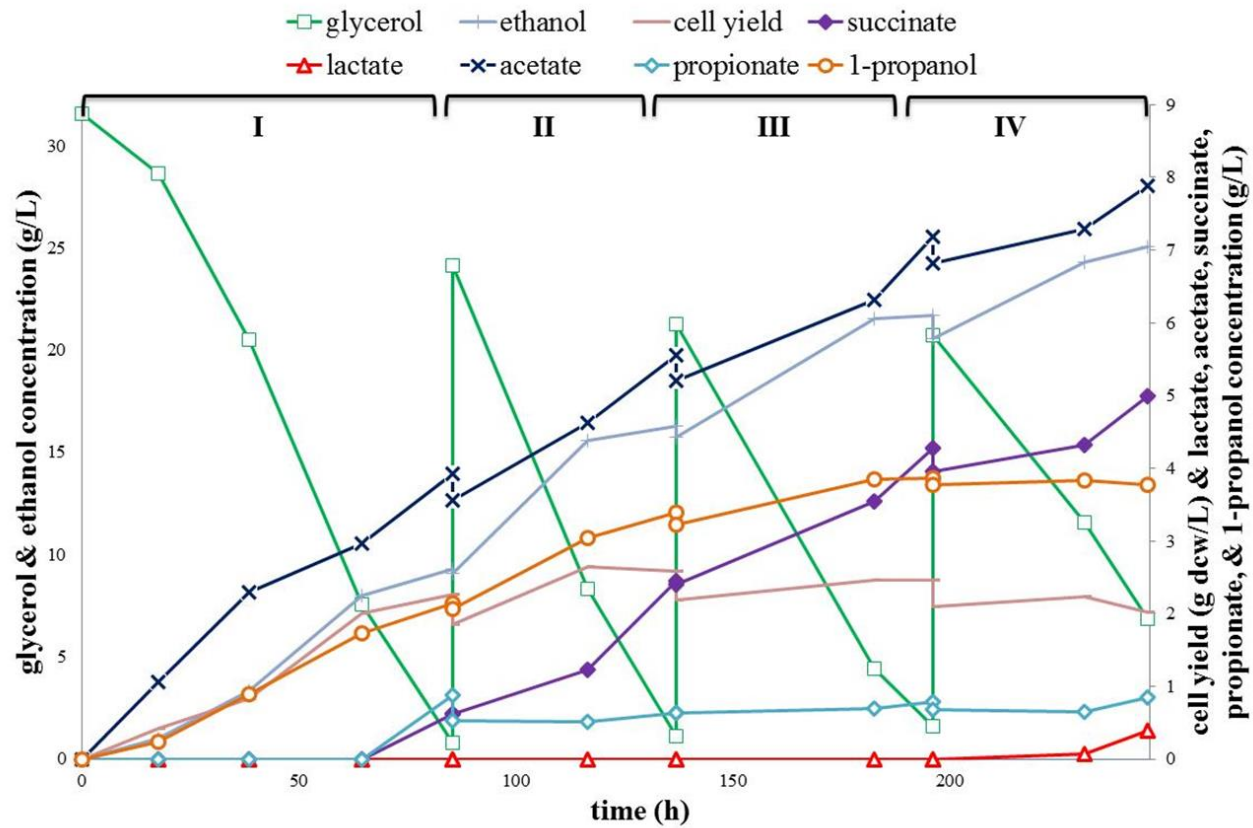


Figure 4.6: Time profiles of the concentrations glycerol, biomass, and major metabolites during fedbatch cultivation of CPC-PrOH2 with glycerol as the major carbon source.
 Approximately 25 g of pure glycerol was fed into the bioreactor in the beginning of each stage and samples were taken before and after the glycerol feeding.

Table 4.2: Culture performance (i.e. overall glycerol consumption and final biomass and metabolite concentrations) of fedbatch cultivation in a bioreactor for (A) CPC-PrOH2 and (B) CPC-PrOH3 using glycerol as the major carbon source.

The glycerol equivalent for each metabolite is calculated based on the corresponding theoretical yield in **Figure 4.1B**. The metabolite distribution (i.e. the fraction of dissimilated glycerol to form a metabolite) is defined as the ratio of the glycerol equivalent of a metabolite to the sum of the total glucose equivalents of all metabolites.

(A) CPC-PrOH2		Glycerol	Biomass	Succinate	Lactate	Acetate	Propionate	Ethanol	1-Propanol
Stage I 0-85.5h	Concentration ^a (g/L)	30.76	2.27	0.62	ND	3.92	0.89	9.31	2.15
	Glycerol equivalent ^b (g/L)	-	-	0.47	-	6.12	1.12	18.61	3.30
	Metabolite distribution ^c (%)	-	-	1.58	-	20.66	3.77	62.84	11.15
	Glycerol efficiency ^d (%)	96.26	-	-	-	-	-	-	-
Stage II 85.5-137h	Concentration ^a (g/L)	23.01	0.73	1.83	ND	2.01	0.11	7.21	1.32
	Glycerol equivalent ^b (g/L)	-	-	1.62	-	3.13	0.14	14.42	2.03
	Metabolite distribution ^c (%)	-	-	7.59	-	14.65	0.67	67.57	9.51
	Glycerol efficiency ^d (%)	92.74	-	-	-	-	-	-	-
Stage III 137-196h	Concentration ^a (g/L)	19.65	0.27	1.88	ND	1.98	0.16	5.96	0.65
	Glycerol equivalent ^b (g/L)	-	-	1.47	-	3.09	0.20	11.92	0.99
	Metabolite distribution ^c (%)	-	-	8.32	-	17.49	1.11	67.47	5.62
	Glycerol efficiency ^d (%)	89.92	-	-	-	-	-	-	-
Stage IV 196-245.5h	Concentration ^a (g/L)	13.84	-0.08	1.04	0.39	1.07	0.17	4.49	0.00
	Glycerol equivalent ^b (g/L)	-	-	0.81	0.40	1.66	0.21	8.98	0.01
	Metabolite distribution ^c (%)	-	-	6.70	3.29	13.77	1.76	74.40	0.05
	Glycerol efficiency ^d (%)	87.21	-	-	-	-	-	-	-

(B) CPC-PrOH3		Glycerol	Biomass	Succinate	Lactate	Acetate	Propionate	Ethanol	1-Propanol
Stage I 0-42.5h	Concentration ^a (g/L)	30.73	2.79	0.59	ND	4.04	0.78	9.51	2.44
	Glycerol equivalent ^b (g/L)	-	-	0.46	-	6.30	0.99	19.03	3.75
	Metabolite distribution ^c (%)	-	-	1.51	-	20.64	3.23	62.34	12.29
	Glycerol efficiency ^d (%)	99.34	-	-	-	-	-	-	-
Stage II 42.5-72h	Concentration ^a (g/L)	22.69	0.38	0.34	ND	1.84	0.37	8.57	2.01
	Glycerol equivalent ^b (g/L)	-	-	0.26	-	2.88	0.46	17.15	3.09
	Metabolite distribution ^c (%)	-	-	1.10	-	12.06	1.94	71.94	12.95
	Glycerol efficiency ^d (%)	105.06	-	-	-	-	-	-	-
Stage III 72-94h	Concentration ^a (g/L)	18.51	0.65	0.30	ND	1.38	0.12	5.68	1.45
	Glycerol equivalent ^b (g/L)	-	-	0.24	-	2.15	0.16	11.36	2.23
	Metabolite distribution ^c (%)	-	-	1.46	-	13.31	0.96	70.43	13.84
	Glycerol efficiency ^d (%)	87.16	-	-	-	-	-	-	-
Stage IV 94-144h	Concentration ^a (g/L)	25.67	0.10	0.85	ND	2.39	0.17	7.33	1.07
	Glycerol equivalent ^b (g/L)	-	-	0.66	-	3.73	0.21	14.65	1.65
	Metabolite distribution ^c (%)	-	-	3.16	-	17.86	1.00	70.08	7.90
	Glycerol efficiency ^d (%)	81.41	-	-	-	-	-	-	-
Stage V 144-210.5h	Concentration ^a (g/L)	18.22	0.02	0.17	ND	1.98	0.21	4.57	0.55
	Glycerol equivalent ^b (g/L)	-	-	0.13	-	3.09	0.26	9.14	0.85
	Metabolite distribution ^c (%)	-	-	0.99	-	22.94	1.95	67.81	6.31

Glycerol efficiency ^d (%)	73.92	-	-	-	-	-	-	-
--------------------------------------	-------	---	---	---	---	---	---	---

^a total concentration of glycerol consumption, biomass concentration (g-DCW/L), and major metabolite concentrations for each specific stage of the fedbatch culture

^b calculated based on theoretical yield of each metabolite to glycerol (Figure 4.1B)

^c represents the fraction of dissimilated glycerol

^d ratio of the sum of the glycerol equivalents associated with all metabolites to overall glycerol consumption

ND not detected

4.3.4 Derivation of plasmid-free propanogenic *E. coli* strains

It has been well perceived that plasmid-free strains outperform recombinant ones in metabolite production for which gene dosage seldom limits the yield of the target metabolite (174). Since wild-type *E. coli* has the silent *Sbm* operon potentially due to an inactive promoter, plasmid-free propanogenic *E. coli* strains were derived by replacing the 204-bp intergenic region upstream of the chromosomal *Sbm* operon with a strong *trc*-promoter (P_{trc}) using our previously developed protocol for genomic engineering (177). A chloramphenicol-resistance cassette flanked by two FRT sites was fused with a P_{trc} promoter-operator fragment via Splicing by Overlap Extension (SOE)-PCR. The DNA fusion (FRT-Cm^R-FRT- P_{trc}) was then used to replace the region upstream of the native *Sbm* operon on the genome to form the engineered strain CPC-PrOH3 (**Figure 4.2**). The 1-propanol production capacity of the plasmid-free strain CPC-PrOH3 was characterized using fedbatch cultivation with glycerol as the major carbon source (**Figure 4.7 and Table 4.2B**). While the levels of solventogenesis for CPC-PrOH3 and CPC-PrOH2 were similar during Stage I for batch cultivation (i.e. the sum of ethanol and 1-propanol titers was approximately equivalent to 74% of dissimilated glycerol for both strains) (**Table 4.2**), the glycerol dissimilation rate for CPC-PrOH3 was approximately 2-fold that for CPC-PrOH2 since it took 42.5 h (**Figure 4.7**) and 85.5 h (**Figure 4.6**) for CPC-PrOH3 and CPC-PrOH2, respectively, to consume 30 g/L glycerol during Stage I. In addition to the higher glycerol dissimilation rate, CPC-PrOH3 produced slightly more 1-propanol than CPC-PrOH2 (2.44 versus 2.15 g/L) during Stage I. Moreover, unlike CPC-PrOH2 which exhibited a low glycerol dissimilation rate and steadily deteriorating 1-propanol yield, the high glycerol dissimilation rate and high 1-propanol yield of CPC-PrOH3 in Stage I (equivalent to 12-13% of dissimilated glycerol) even persisted during Stage II and III of fedbatch cultivation (**Table 4.2B**). The results suggest that a single chromosomal copy of the active *Sbm* operon was sufficient to drive 1-propanol production. The improved culture performance also indicates that there may be some metabolic burden and physiological impact associated with the active *Sbm* operon located in a multicopy plasmid. Using CPC-PrOH3 for fedbatch cultivation with glycerol as the major carbon source, the 1-propanol titer soared to 6.76 g/L. The final ethanol titer also reached a high level of 31.1 g/L which is equivalent to approximately 70% of dissimilated glycerol. Similar to the CPC-PrOH2 fedbatch culture, while the level of acidogenesis remained low during the entire fedbatch cultivation of CPC-PrOH3, acetate steadily accumulated to a final concentration of 9.41 g/L which could potentially impact culture performance. However, the final succinate level was only 2.05 g/L for CPC-PrOH3, as opposed to a much higher level of 5.44 g/L for CPC-PrOH2, implying that carbon is more efficiently channeled into the 1-propanol pathway for CPC-PrOH3.

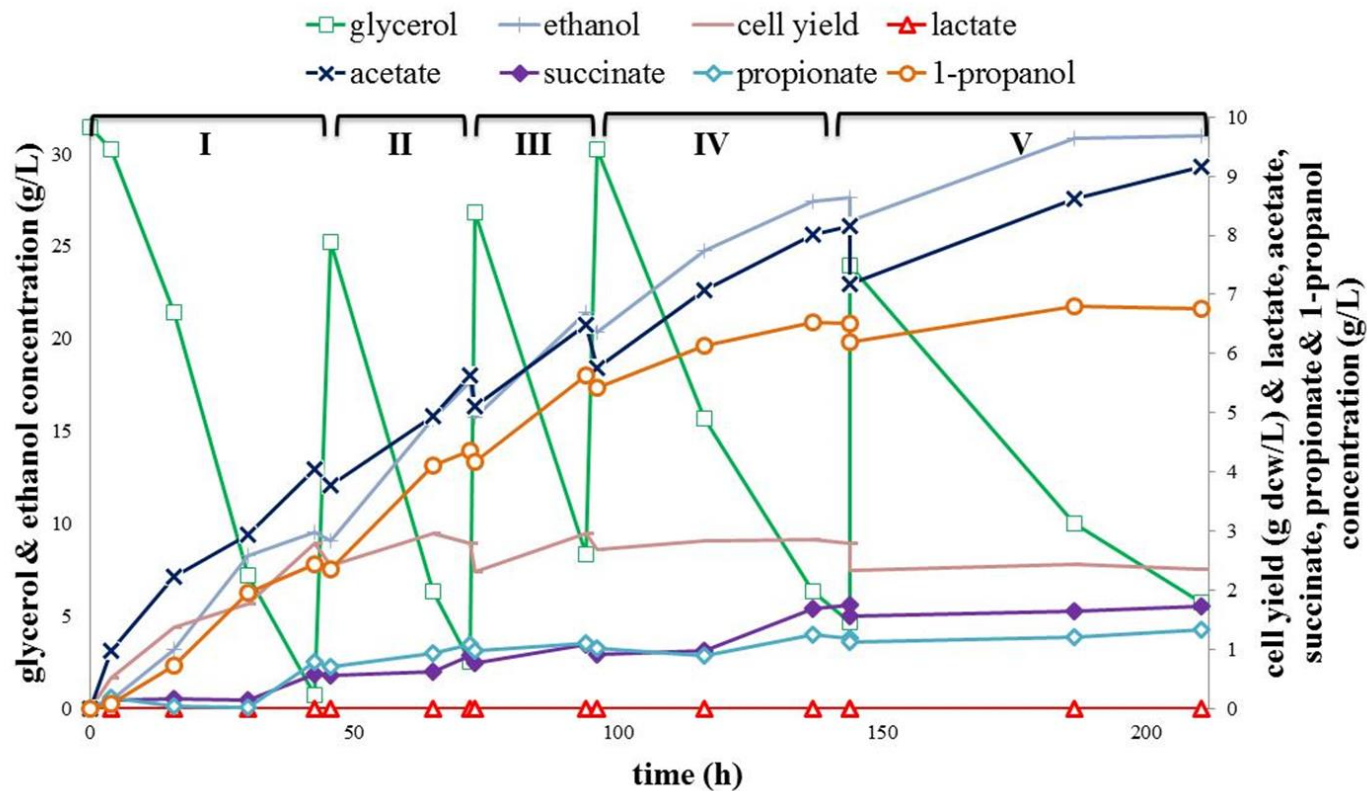


Figure 4.7: Time profiles of the concentrations glycerol, biomass, and major metabolites during fedbatch cultivation of CPC-PrOH3 with glycerol as the major carbon source.

Approximately 25 g of pure glycerol was fed into the bioreactor in the beginning of each stage and samples were taken before and after the glycerol feeding.

4.4 Discussion

While the production of 1-propanol in *E. coli* was previously achieved through activation of the keto-acid (12, 134, 145) or extended 1,2-propanediol (143) pathways, we herein take an alternative approach via extended dissimilation of succinate by activating the endogenous Sbm operon in *E. coli*. Under anaerobic conditions, succinate could accumulate as one of the final fermentation products although activation of the Sbm operon reduced succinate accumulation as 1-propanol was produced (**Figures 4.3-4.5**). Nevertheless, 1-propanol production appeared to be highly dependent on culture conditions, particularly carbon source. The use of glucose as the major carbon source resulted in dominance of acidogenesis over solventogenesis with low yields of 1-propanol. Further inspection of the major active pathways during glucose fermentation reveals inherent constraints of the metabolic network that prevent sufficient diversion of carbon flux from the phosphoenolpyruvate (PEP) node towards the reductive arm of oxaloacetate for 1-propanol biosynthesis. The metabolic deficiency is in part due to the high redox demand for 1-propanol production. As illustrated in **Figure 4.1**, PEP generation from glucose produces only one mole of NADH per mole of PEP produced, whereas subsequent 1-propanol production requires four moles of NADH per mole formed. As a result, a large fraction (up to 95%) of the PEP derived from glucose was channeled into the pyruvate node to prevent such a redox imbalance, forming lactate, acetate, and ethanol as major metabolites. The limitation in the supply of NADH potentially caused the carbon flux to stall at the succinate node, leading to succinate accumulation even when the Sbm operon was expressed (**Figure 4.3B and Figures 4.4B**). For the propanogenic strain CPC-PrOH1 with a parental genetic background, homolactic fermentation dominated, resulting in lactate overproduction and poor 1-propanol yield. Disruption of the major lactate synthesis route by knocking out *ldhA* minimized carbon leakage into the lactate pathway in CPC-PrOH2, but marginally improved 1-propanol production. Upon comparing metabolic profiles for CPC-PrOH1 and CPC-PrOH2 (**Figure 4.3 and 4.4**), it is evident that the pleiotropic effect associated with the *ldhA* gene knockout was to promote the production of pyruvate-derived fermentative products (i.e. acetate and ethanol), rather than diverting carbon flux to metabolites in the PEP branch, such as succinate and 1-propanol. Nevertheless, the results were unsurprising as similar metabolic effects were previously observed (173).

Glycerol has obvious advantages over glucose due to a higher reductance and more reducing equivalents generated upon its dissimilation. Nevertheless, glycerol metabolism in *E. coli* is often restricted to respiratory (aerobic) conditions, as the excess reducing equivalents cannot be well consumed by standard redox-balanced pathways in *E. coli* during anaerobiosis (186). Accordingly, glycerol appears to be a recalcitrant carbon source in the absence of external electron acceptors for CPC-CNTRL2 (**Figure**

4.5A), whereas an approximate 60% increase in the glycerol dissimilation rate was observed for the propanogenic strain CPC-PrOH2 (**Figure 4.5A**), suggesting that utilization of the 1-propanol pathway can be an effective means to dispose of excess reducing equivalents generated by glycerol dissimilation. Most importantly, in stark contrast to glucose, the use of glycerol as the major carbon source significantly favored solventogenesis (accounting for up to 84% of dissimilated glycerol) and minimized acidogenesis, resulting in high-level coproduction of ethanol and 1-propanol. The dramatic switch in the metabolic distribution associated with glycerol fermentation may be in part due to the oxidized nature of metabolites. Incidentally, previous studies reported that *E. coli* produces 1,2-propanediol to attain redox balance during anaerobic fermentation of glycerol (183, 187). While this compound was not detected in the present study, the solventogenic pathways apparently can act as an auxiliary channel for redox balance upon glycerol dissimilation under anaerobic conditions.

During fedbatch cultivation for 1-propanol production, an increase in the rate of glycerol dissimilation was observed after Stage I (**Figure 4.6 and 4.7**). The mechanism associated with this rate increase is unknown, but may entail the induction of genes responsible for glycerol dissimilation (e.g. *gldA*, encoding glycerol dehydrogenase and *dhaKLM*, encoding a PEP-dependent dihydroxyacetone kinase) (188) and/or the formation of certain intermediate metabolites which may act as external electron donors. The glycerol dissimilation pathways (i.e. the respiratory and fermentative arms) and their effect on the C3 metabolite pool are further discussed in **Chapters 5 and 6**. Since synthesis of ethanol and succinate (and 1-propanol/propionate in the present study) are the only pathways readily available for redox-balancing during glycerol fermentation (187), the elevated rate of glycerol consumption was concomitant with the increase in conversion yields of ethanol and succinate during Stage II and III (**Table 4.2**). However, given that the ethanologenic pathway leads to higher ATP output (**Figure 4.1A**) (182), more than 60% (and up to 75%) of dissimilated glycerol was diverted to ethanol production, whereas less than 15% was diverted to succinate and 1-propanol production (**Table 4.2, and Figure 4.8**). Such high-level production of ethanol sustained during almost the entire fedbatch cultivation and, therefore, limited 1-propanol yield. Taken together, these results suggest that further enhancement of 1-propanol production with glycerol as the major carbon source will require sequestering of carbon flux from the ethanologenic pathway. For example, placing an entropic driving force at the PEP node through the expression of a heterologous PEP carboxykinase (PckA) (189) or converting pyruvate back to PEP through the expression of an endogenous phosphoenolpyruvate synthase (Pps) (190) may be feasible approaches to shift carbon flux from ethanologensis towards 1-propanol production.

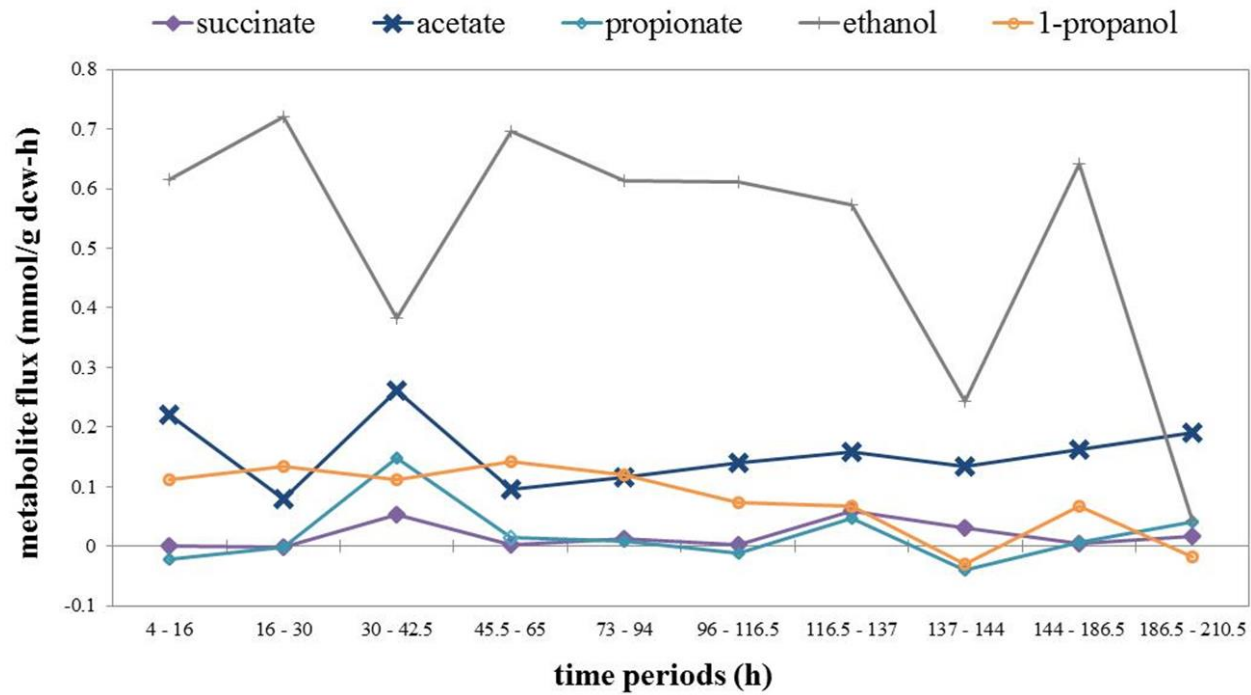


Figure 4.8: Average metabolite excretion fluxes during each stage of CPC-PrOH3 cultivation.

The fluxes were estimated by normalizing the glycerol uptake rate to 1 mmol/g dcw-h. While most carbon flux was channelled into the ethanol fraction, 1-propanol production was stably maintained throughout the entire cultivation.

On the other hand, the recession of 1-propanol production in later stages of fedbatch cultures correlated with heightened levels of acetate and ethanol production (**Figures 4.6, 4.7, and 4.8**), suggesting that the toxicity of these metabolites may mediate physiological stresses on cells and eventually hinder 1-propanol production.

While ethanol can be the exclusive product of glycerol fermentation (accounting for ~98% glycerol equivalents) by wild-type *E. coli* strains (188), our fedbatch cultivation with glycerol as the major carbon source produced acetate in relatively large quantities (**Figure 4.6 and 4.7**). **Figure 4.8** shows that, across all time periods of the fedbatch cultivation, the average carbon flux for acetate production was greater than or approximately equal to that for 1-propanol production. A simple explanation to this observation can be derived from the redox balance associated with glycerol dissimilation. No net NADH is produced when glycerol is converted to ethanol, whereas the overall conversion of glycerol to acetate and 1-propanol will result in 2 NADH accumulation and 2 NADH depletion, respectively. Shifting carbon flux away from ethanol pathway and toward 1-propanol production would cause NADH imbalance, which can be partially compensated by concomitant production of acetate. Note that extra ATP will be released upon acetate production to support potential ATP requirement for cell growth and maintenance. This is evident in the late stages of batch cultivations (**Figure 4.5**), as cultures tend to suffer from overflow metabolism of acetate in order to fulfil cell maintenance requirements.

Multicopy plasmids tend to place metabolic burden and physiological impact on host cells, deteriorating cell growth and product formation. Unlike overexpression of recombinant proteins, gene dosage is seldom a limiting factor for metabolic engineering approaches (174), for which plasmid-free strains are particularly attractive. The *Sbm* operon in *E. coli* is naturally silent, conceivably due to a weak or inactive promoter-operator system (14, 15), thus providing us with a unique opportunity for minor genomic engineering without grafting several heterologous genes or a large operon into the host genome. In the present study, we derived a plasmid-free propanogenic strain CPC-PrOH3 for which expression of the *Sbm* operon was activated by replacing the 204-bp upstream region of the native *Sbm* operon with the strong *trc*-promoter. Compared to CPC-PrOH2, CPC-PrOH3 has the following technical advantages, leading to high-level coproduction of 1-propanol and ethanol. First, CPC-PrOH3 had higher rates for cell growth and glycerol dissimilation (**Figure 4.7**), potentially due to alleviated metabolic burden and more active expression of the *Sbm* operon (even based on a single chromosomal copy). Second, upon glycerol fermentation, CPC-PrOH3 had a higher level of solventogenesis (accounting for up to 85% of dissimilated glycerol), a higher 1-propanol conversion yield (accounting for up to 14% of dissimilated

glycerol), and a prolonged 1-propanol producing capacity during the fedbatch culture (particularly during the first three stages) (**Table 4.2B**). The results suggest that a single chromosomal copy of the active Sbm operon was sufficient to drive extended dissimilation of succinate for effective 1-propanol production. Also, alleviating the metabolic burden associated with the presence of multicopy plasmids can lead to healthy cell physiology and, consequently, improved production of the target metabolite. While the dominance of ethanogenesis upon glycerol fermentation remains the key issue to be tackled, 1-propanol production for CPC-PrOH3 can be potentially limited by the accumulation of acetate and succinate. These limitations along with the decreasing glycerol utilization efficiency for metabolite production (**Table 4.2B**) suggest metabolic burden might still exist in CPC-PrOH3, leading to inactivation of the Sbm operon, particularly towards the late stage of the fedbatch culture. Interestingly, although CPC-PrOH3 had a fully activated Sbm operon (including *ygfH*), propionate production appeared to be minimally affected when compared to the fed-batch culture of CPC-PrOH2 (in which the episomal construct only includes the *sbm*, *ygfD*, and *ygfG* genes). These results suggest that either propionyl-CoA may have a higher substrate affinity towards bifunctional alcohol/aldehyde dehydrogenases than YgfH or other pathways may exist in *E. coli* to facilitate the conversion of propionate to propionyl-CoA. One possibility is the canonical methylcitrate pathway, which is involved in the oxidation of propionate to pyruvate or succinate with propionyl-CoA as an intermediate (191).

PART II

EXTENDING THE SLEEPING BEAUTY PATHWAY IN *ESCHERICHIA COLI* FOR PRODUCTION OF LONG-CHAIN CHEMICALS

Chapter 5

De novo* engineering of a recursive CoA-dependent carbon chain elongation platform for biosynthesis of butanone (methyl ethyl ketone) in propanogenic *E. coli

Chapter Abstract

To expand the chemical and molecular diversity of biotransformation using whole-cell biocatalysts, in this chapter, we genetically engineered a chimeric pathway in *E. coli* for heterologous production of butanone, a highly important commodity ketone. First, a *E. coli* host strain with its inherently Sbm operon in the genome being activated (i.e. a propanogenic *E. coli* strain) was used to establish a high-level intracellular pool of non-native propionyl-CoA. Subsequently, molecular fusion of propionyl-CoA and acetyl-CoA was conducted to form the biogenic C5 moiety 3-ketovaleryl-CoA via a modular CoA-dependent elongation pathway. Lastly, 3-ketovaleryl-CoA was channeled into the canonical clostridial acetone-formation pathway for thioester hydrolysis and decarboxylation to form butanone. Biochemical, genetic, and metabolic factors affecting relative levels of ketogenesis, acidogenesis, and alcohologenesis under selected fermentative culture conditions were investigated. Using the derived engineered *E. coli* strain for batch cultivation, we achieved high-level co-production of butanone (1.3 g/L) and acetone (2.9 g/L), thus demonstrating potential industrial applicability of this microbial production platform.

5.1 Background

Due to waning fossil fuel reserves, the demand for more cost-effective and environmentally conscientious bioprocesses to replace petrochemical processes has increased significantly. Whole-cell biocatalytic platforms offer several technological advantages over traditional synthetic chemical processes, such as high chemo-, stereo-, and regio-selectivity and the ability to catalyze complex multi-step reactions under ambient conditions. However, biological systems are often limited in their applicability for the production of valuable chemicals due to the lack of natural biosynthetic pathways (192, 193). Fortunately, nature has evolved to possess remarkable molecular catalytic processes that can be manipulated and redesigned for *in vivo* chemical synthesis. Accordingly, metabolic engineering has been integrated with synthetic biology to expand the molecular capabilities and chemical diversity of living systems for scalable synthesis of a wider array of value-added chemicals and biofuels.

In this chapter, we report the implementation of a robust metabolic pathway in *Escherichia coli* for heterologous production of butanone (also referred as methyl ethyl ketone or MEK), an advanced aliphatic commodity ketone. Owing to its low boiling point and high dissolution properties, butanone is used as a general solvent in trades extending from printing and textile to domestic uses (194). Currently, butanone is exclusively manufactured using petroleum-derived feedstocks, such as 2-butanol, 2-butene, and various branched alkylbenzenes, with an annual production of 730,000 tons (195). Similar to most value-added chemicals of interest, no natural biosynthetic pathways have been identified to produce butanone. Recently, a biosynthetic approach to produce butanone in engineered *E. coli* was proposed by extending the *meso*-2,3 butanediol synthetic pathway using a promiscuous vitamin B₁₂-dependent glycerol dehydratase (196). A similar strategy was also undertaken by implementing this chimeric pathway in engineered *Saccharomyces cerevisiae* for co-production of butanone and 2-butanol (197); however, the butanone titer/yield for these approaches is considered limited particularly for large-scale industrial adoption.

Our proposed butanone biosynthetic pathway starts with production of the non-native metabolite propionyl-CoA in *E. coli* for use as a substrate for subsequent molecular fusion. Propionyl-CoA metabolism in wild-type *E. coli* is generally confined to selected reactions associated with either the thio-esterification of propionate or the dissimilation of odd-chained fatty acids and several α -amino acids (e.g. L-threonine) (145, 191). Accordingly, to elevate the propionyl-CoA pool in the cell, propionate must be exogenously supplemented in the culture medium or complex genetic approaches have to be undertaken to overcome the concerted feedback inhibition exerted by the amino acid biosynthetic pathways (12, 145, 198). In the previous two chapters, we reported heterologous production of 1-propanol based on genomic activation of the extant yet *Sbm* operon in *E. coli* (173, 199). This four-gene operon (i.e. *sbm-ygfD-ygfG-ygfH*) encodes various enzymes for extended dissimilation of succinate and its functional expression redirects carbon flux toward the propionyl-CoA node, resulting in the production of non-native C3-fermentative products of 1-propanol and propionate (173, 199) (**Figure 5.1**). The presence of propionyl-CoA opens an avenue for novel microbial synthesis of several non-native metabolites, including butanone. Genomic activation of the *Sbm* operon not only transforms *E. coli* to be propanogenic, but also introduces an intracellular “flux competition” between the traditional C2-fermentative pathway (forming acetate and ethanol) and the novel C3-fermentative pathway (forming propionate and 1-propanol). As a result, further biochemical and genetic strategies must be applied in this study to redirect carbon flux and increase the level of the propionyl-CoA pool.

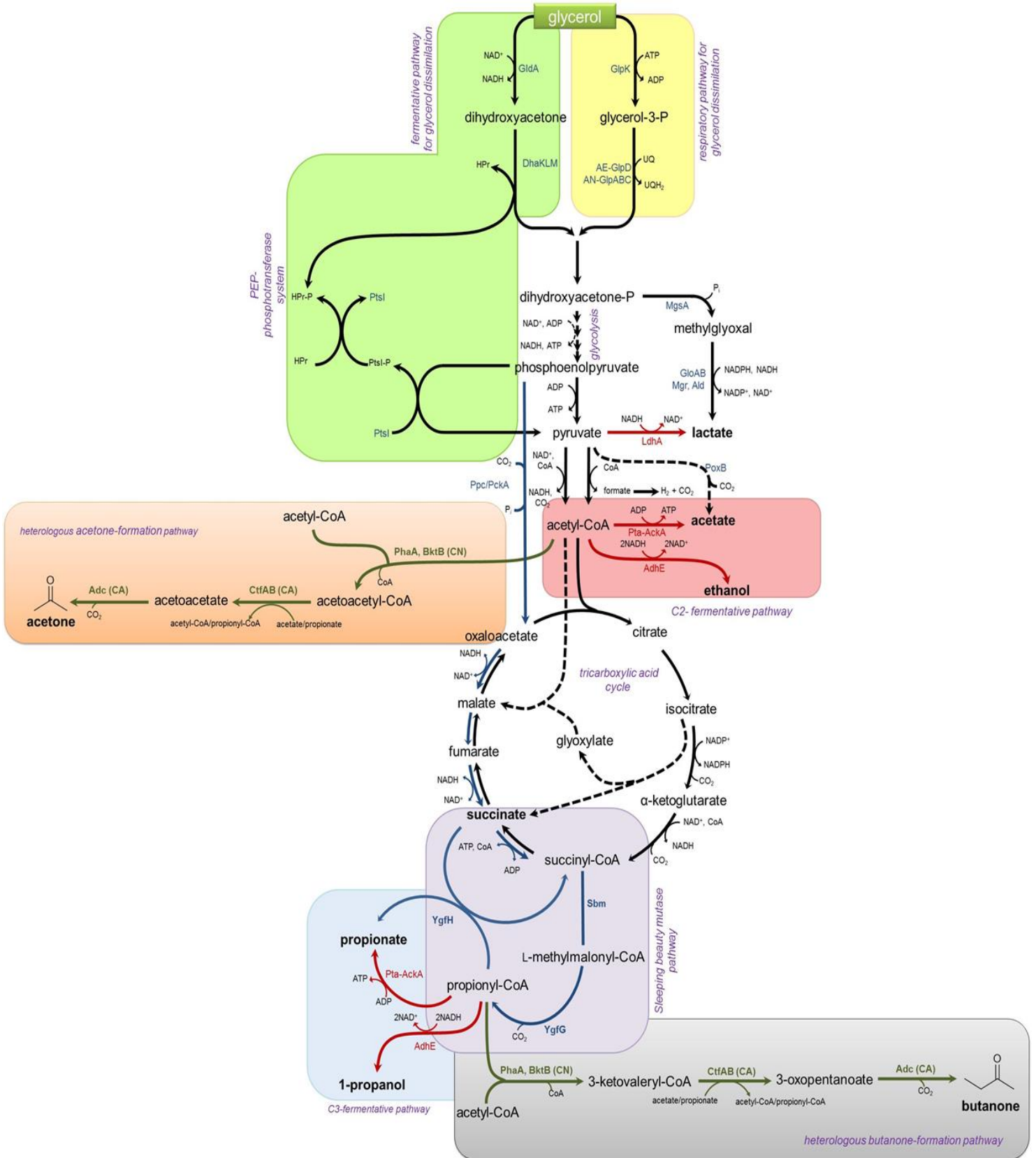


Figure 5.1: Schematic representation of the butanone biosynthetic pathway (on previous page).

Heterologous enzymes from *Cupriavidus necator* (CN) and *Clostridium acetobutylicum* are shown in green text. The fermentative pathway for glycerol dissimilation is presented in a light green box and the respiratory pathway for glycerol dissimilation is presented in a yellow box. The Sleeping beauty mutase (Sbm) pathway is presented in a purple box. The C2-fermentative pathway is presented in a red box, while the C3-fermentative pathway is presented in a blue box. Relevant enzymes for production of various fermentative products as well as the enzymes of the respiratory and fermentative glycerol pathways and the Sbm pathway are in blue text. Competing pathways at the pyruvate/acetyl-CoA and propionyl-CoA nodes are shown in red arrows.

For butanone formation in the propanogenic *E. coli* strain, two major intracellular transformations will be carried out. First, propionyl-CoA is fused with the native intermediate acetyl-CoA, to form 3-ketovaleryl-CoA (also referred to as 3-oxopentanoyl-CoA) via the CoA-dependent elongation pathway, which is implemented by functionally expressing a set of highly promiscuous β -ketothiolases from *Cupriavidus necator* (former *Ralstonia eutropha*) (200). Next, the formed 3-ketovaleryl -CoA is channeled into the clostridial acetone-formation pathway, which is implemented by functionally expressing acetoacetyl-CoA: acetate/butyrate: CoA transferase and acetoacetate decarboxylase from *C. acetobutylicum*, for thioester hydrolysis and decarboxylation. Note that the clostridial acetone-formation pathway was previously expressed in *E. coli* for hydrolysis and decarboxylation of acetoacetyl-CoA, leading to acetone production (201).

In addition to the above synthetic biology approaches, various genetic and metabolic factors and cultivation strategies were also explored to enhance the production of butanone. To our knowledge, our developed engineered *E. coli* strains with high butanone titers up to 1.3 g l⁻¹ represent the most effective microbial platform for butanone production reported to date, and will serve as a basis for future improvement strategies.

5.2 Methods

5.2.1 Bacterial strains and plasmids

E. coli strains and plasmids used in this study are listed in **Table 5.1**. Sequence of all oligonucleotides used for DNA cloning, verification and homologous recombination are found in **Appendix A - Table S1**. Standard recombinant DNA technologies for molecular cloning were applied (150). *Pfu* and *Taq* DNA polymerases, T4 DNA ligase, and large (Klenow) fragment of DNA Polymerase I were obtained from New England Biolabs (Ipswich, MA, USA). All synthesized oligonucleotides were obtained from Integrated DNA Technologies (Coralville, IA, USA). DNA sequencing was conducted by the Centre for Applied Genomics at the Hospital for Sick Children (Toronto, Canada). *E. coli* BW25141 was the

Table 5.1: Strains and plasmids used for butanone production in engineered *E. coli*

Name	Description and relevant genotype	Reference
<i>E. coli</i> host strains		
HST08	F ⁻ , <i>endA1</i> , <i>supE44</i> , <i>thi-1</i> , <i>recA1</i> , <i>relA1</i> , <i>gyrA96</i> , <i>phoA</i> , $\Phi 80d$ <i>lacZ</i> Δ <i>M15</i> , Δ (<i>lacZYA</i> – <i>argF</i>) <i>U169</i> , Δ (<i>mrr</i> – <i>hsdRMS</i> – <i>mcrBC</i>), Δ <i>mcrA</i> , λ^-	Takara Bio, Shiga, Japan
BW25141	F ⁻ , Δ (<i>araD-araB</i>)567, Δ <i>lacZ</i> 4787(:: <i>rrnB-3</i>), Δ (<i>phoB-phoR</i>)580, λ^- , <i>galU95</i> , Δ <i>uidA3</i> :: <i>pir+</i> , <i>recA1</i> , <i>endA9</i> (<i>del-ins</i>)::FRT, <i>rph-1</i> , Δ (<i>rhaD-rhaB</i>)568, <i>hsdR514</i>	Datsenko and Wanner (153)
BW25113	F ⁻ , Δ (<i>araD-araB</i>)567, Δ <i>lacZ</i> 4787(:: <i>rrnB-3</i>), λ^- , <i>rph-1</i> , Δ (<i>rhaD-rhaB</i>)568, <i>hsdR514</i>	Datsenko and Wanner (153)
BW- Δ ldhA	BW25113 Δ <i>ldhA</i> null mutant	Srirangan et al. (173)
CPC-Sbm-Cm ^R	BW- Δ <i>ldhA</i> , P _{<i>trc</i>} :: <i>sbm</i> (i.e. with the FRT-Cm ^R -FRT-P _{<i>trc</i>} cassette replacing the 204-bp upstream of the Sbm operon)	This study
CPC-Sbm	BW- Δ <i>ldhA</i> , P _{<i>trc</i>} :: <i>sbm</i> (i.e. with the FRT -P _{<i>trc</i>} cassette replacing the 204-bp upstream of the Sbm operon)	This study
CPC-Sbm Δ <i>adhE</i>	BW- Δ <i>ldhA</i> , Δ <i>adhE</i> , P _{<i>trc</i>} :: <i>sbm</i> (i.e. with the FRT -P _{<i>trc</i>} cassette replacing the 204-bp upstream of the Sbm operon),	This study
CPC-Sbm Δ <i>pta</i>	BW- Δ <i>ldhA</i> , Δ <i>pta</i> , P _{<i>trc</i>} :: <i>sbm</i> (i.e. with the FRT -P _{<i>trc</i>} cassette replacing the 204-bp upstream of the Sbm operon)	This study
CPC-Sbm Δ <i>glpD</i>	BW- Δ <i>ldhA</i> , Δ <i>glpD</i> , P _{<i>trc</i>} :: <i>sbm</i> (i.e. with the FRT -P _{<i>trc</i>} cassette replacing the 204-bp upstream of the Sbm operon)	This study
CPC-Sbm Δ <i>dhaK</i>	BW- Δ <i>ldhA</i> , Δ <i>dhaK</i> , P _{<i>trc</i>} :: <i>sbm</i> (i.e. with the FRT- P _{<i>trc</i>} cassette replacing the 204-bp upstream of the Sbm operon)	This study
CPC-MEKCon1	CPC-Sbm/pK-PhaA and pCtfAB-Adc	This study

CPC-MEKCon2	CPC-Sbm/pK-BktB and pCtfAB-Adc	This study
CPC-MEKCon3	CPC-Sbm/pK-PhaA-BktB and pCtfAB	This study
CPC-MEKCon4	CPC-Sbm/ pK-PhaA-BktB and pAdc	This study
CPC-MEK	CPC-Sbm/pK-PhaA-BktB and pCtfAB-Adc	This study
CPC-MEK $\Delta adhE$	CPC-Sbm $\Delta adhE$ /pK-PhaA-BktB and pCtfAB-Adc	This study
CPC-MEK Δpta	CPC-Sbm Δpta /pK-PhaA-BktB and pCtfAB-Adc	This study
CPC-MEK $\Delta glpD$	CPC-Sbm $\Delta glpD$ /pK-PhaA-BktB and pCtfAB-Adc	This study
CPC-MEK $\Delta dhaK$	CPC-Sbm $\Delta dhaK$ /pK-PhaA-BktB and pCtfAB-Adc	This study
Plasmids		
pCP20	FLP ⁺ , λ cI857 ⁺ , λ p _R Rep(pSC101 ori) ^{ts} , Ap ^R , Cm ^R	Cherepanov and Wackernagel (155)
pKD46	RepA101 ^{ts} ori, Ap ^R , <i>araC</i> -P _{araB} : <i>gam-bet-exo</i>	Datsenko and Wanner (153)
pTrc99a	ColE1 ori, Ap ^R , P _{trc}	Amann et al. (180)
pKD3	R6K- γ ori, Ap ^R , FRT-Cm ^R -FRT	Datsenko and Wanner (153)

pK184	p15A ori, Km ^R , P _{lac} : <i>lacZ</i> '	Jobling and Holmes (156)
pSOS95	repL ori, ColE1 ori, MLS ^R , Em ^R , Ap ^R , P _{thi} : <i>ctfAB-adc</i>	Soucaille and Papoutsakis, Unpublished work
pK-PhaA	From pK184, P _{lac} : <i>phaA</i>	This study
pK-BktB	From pK184, P _{lac} : <i>bktb</i>	This study
pK-PhaA-BktB	From pK184, P _{lac} : <i>phaA-bktb</i>	This study
pCtfAB	From pTrc99a, P _{thi} : <i>ctfAB</i>	This study
pAdc	From pTrc99a, P _{thi} : <i>adc</i>	This study
pCtfAB-Adc	From pTrc99a, P _{thi} : <i>ctfAB-adc</i>	This study

parental strain for derivation of all mutant strains in this study and *E. coli* HST08 was used for molecular cloning.

Activation of the genomic *Sbm* operon to form propanogenic *E. coli* CPC-Sbm was described previously (199). Briefly, the FRT-Cm^R-FRT cassette from pKD3 was PCR-amplified using the primer set c-frt, whereas the *trc* promoter-operator region was PCR-amplified using the c-ptrc primer set. The two DNA amplicons were fused together by splice overlap-extension (SOE) PCR (151) using the forward primer of the c-frt primer set and the reverse primer of the c-ptrc primer set to generate the FRT-Cm^R-FRT-P_{*trc*} cassette. To generate the DNA cartridge for genomic integration, the FRT-Cm^R-FRT-P_{*trc*} cassette was PCR-amplified using the r-frt:ptrc primer set containing the 5'- and 3'-36-bp homology arms, respectively. The homology arms were chosen so that the FRT-Cm^R-FRT-P_{*trc*} cassette was inserted precisely upstream of the *Sbm* operon. λ -Red genomic recombineering was carried out as described by Datsenko and Wanner (153).

Gene knockouts (i.e. *adhE*, *pta*, *glpD*, and *dhaK*) were introduced into CPC-Sbm by P1 phage transduction (150) using the appropriate Keio Collection strains (The Coli Genetic Stock Center, Yale University, New Haven, CT, USA) as donors (152). To eliminate the co-transduced FRT-Kn^R-FRT cassette, the transductant mutants were transformed with pCP20 (155), a temperature sensitive plasmid expressing a flippase (Flp) recombinase. Upon Flp-mediated excision of the Kn^R cassette, a single Flp recognition site (FRT “scar site”) was left behind. Plasmid pCP20 was then removed by growing cells at 42 °C. The genotypes of derived knockout strains were confirmed by whole-cell colony PCR using the appropriate “verification” primer sets listed in **Appendix A - Table S1**.

The DNA fragment containing the three *C. acetobutylicum* ATCC 824 genes (*cftA-cftB-adc*) under the control of the P_{*thl*} was PCR-amplified from pSOS95 (a kind gift of Dr. E.T. Papoutsakis, Delaware Biotechnology Institute, Newark, DE, USA) using the c-ctf primer set. Note that this 2.3-kb PCR-amplified fragment also contained the rho-independent transcriptional terminator from the clostridial *adc* gene. The amplified DNA fragment was then subcloned into the *EcoRV* and *EcoRI* restriction sites of pTrc99a to generate pCtfAB-*adc*. Similarly, to generate control plasmid pCtfAB, *ctfA-cftB* under the control of the P_{*thl*} was PCR-amplified from pSOS95 using the primer set c-ctf-c3 and the amplified fragment was cloned into the *EcoRV* and *EcoRI* restriction sites of pTrc99a. To generate control plasmid pAdc, P_{*thl*} was PCR-amplified using primer set c-*adc*-c4A whereas *adc* was PCR-amplified using primer set c-*adc*-c4B from pSOS95. The two amplicons were then fused using Gibson enzymatic assembly (202) and cloned into the *EcoRV* and *EcoRI* restriction sites of pTrc99a.

The two β -ketothiolases genes were PCR-amplified from the genomic DNA of the wild-type *C. necator* strain (ATCC 17699) using primer sets c-phaA1 for *phaA* and c-bktb1 for *bktB*. To generate plasmid pK-PhaA harboring the *phaA* gene under the control of the P_{lac} promoter, the *phaA* amplicon was fused with the PCR-linearized pK184 (linearized using primer set c-pK184) using the Gibson enzymatic assembly. A clone with the correct transcriptional orientation of the *phaA* fragment with respect to the P_{lac} promoter was selected and verified by DNA sequencing. The same approach was used to generate plasmid pK-BktB harboring the *bktB* gene under the control of the P_{lac} promoter. To generate the DNA cartridge containing both β -ketothiolases (i.e. PhaA and BktB), the *phaA* and *bktB* were first individually PCR-amplified from *C. necator* ATCC 17699 genomic DNA using primer sets c-phaA2 and c-bktb2, respectively. The two DNA fragments were then transcriptionally fused with splice overlap extension (SOE) PCR (151) using the forward primer of c-phaA2 and the reverse primer of c-bktb2. The resulting fused fragment was cloned into the *EcoRI* restriction site of pK184. A clone with the correct transcriptional orientation of the *phaA-bktB* fragment with respect to the P_{lac} promoter was selected and verified by DNA sequencing, yielding pK-PhaA-BktB.

5.2.2 Media and cultivation conditions

All media components were obtained from Sigma-Aldrich Co. (St Louis, MO, USA) except glucose, yeast extract, and tryptone which were obtained from BD Diagnostic Systems (Franklin Lakes, NJ, USA). Media was supplemented with antibiotics as required ($30 \mu\text{g mL}^{-1}$ kanamycin and $12 \mu\text{g mL}^{-1}$ chloramphenicol). For ketone production, the ketogenic (i.e. ketone-producing) *E. coli* strains (stored as glycerol stocks at $-80 \text{ }^\circ\text{C}$) were streaked on LB agar plates with appropriate antibiotics and incubated at $37 \text{ }^\circ\text{C}$ for 16 h. Single colonies were picked from LB plates to inoculate 30-mL SB medium (32 g l^{-1} tryptone, 20 g l^{-1} yeast extract, and 5 g l^{-1} NaCl) with appropriate antibiotics in 125-mL conical flasks. Overnight cultures were shaken at $37 \text{ }^\circ\text{C}$ and 280 rpm in a rotary shaker (New Brunswick Scientific, NJ, USA) and used as seed cultures to inoculate 200 mL SB media at 1% (v/v) with appropriate antibiotics in 1-L conical flasks. This second seed culture was shaken at $37 \text{ }^\circ\text{C}$ and 280 rpm for approximately 16 h. Cells were then harvested by centrifugation at $6,000 \times g$ and $20 \text{ }^\circ\text{C}$ for 15 min and resuspended in 100-mL fresh LB media. The suspended culture was used to inoculate a 1-L stirred-tank bioreactor (CelliGen 115, Eppendorf AG, Hamburg, Germany) to obtain a target initial optical density at 600 nm of ~ 5.5 (i.e. $\sim 3.5 \text{ g l}^{-1}$) and operated anaerobically, microaerobically, or semi-aerobically at $30 \text{ }^\circ\text{C}$ and 430 rpm. The semi-defined production medium in the bioreactor contained 30 g l^{-1} glycerol or 30 g l^{-1} glucose, 0.23 g l^{-1} K_2HPO_4 , 0.51 g l^{-1} NH_4Cl , 49.8 mg l^{-1} MgCl_2 , 48.1 mg l^{-1} K_2SO_4 , 1.52 mg l^{-1} FeSO_4 , 0.055 mg l^{-1} CaCl_2 ,

2.93 g l⁻¹ NaCl, 0.72 g l⁻¹ tricine, 10 g l⁻¹ yeast extract, 10 mM NaHCO₃, 0.2 μM cyanocobalamin (vitamin B₁₂) and trace elements (2.86 g l⁻¹ H₃BO₃, 1.81 g l⁻¹ MnCl₂•4H₂O, 0.222 g l⁻¹ ZnSO₄•7H₂O, 0.39 g l⁻¹ Na₂MoO₄•2H₂O, 79 μg l⁻¹ CuSO₄•5H₂O, 49.4 μg l⁻¹ Co(NO₃)₂•6H₂O) (179), appropriate antibiotics, and supplemented with 0.1 mM isopropyl β-D-thiogalactopyranoside (IPTG). Anaerobic conditions were maintained by constant bubbling of nitrogen into the bulk culture at 0.1 vvm (volume of air/volume of bioreactor/min). Microaerobic conditions were maintained by purging air into the headspace at 0.1 vvm. Semi-aerobic conditions were maintained by purging air into the bulk culture at 0.1 vvm. The pH of the production culture was maintained at 7.0 ± 0.1 with 30% (v/v) NH₄OH and 15% (v/v) H₃PO₄. All cultivation experiments were performed in duplicate.

5.2.3 Offline analyses and metabolite detection

Culture samples were appropriately diluted with saline for measuring the optical cell density (OD₆₀₀) using a spectrophotometer (DU520, Beckman Coulter, Fullerton, CA). Cell-free supernatant was collected and filter sterilized for titer analysis of glycerol, and various metabolites using an HPLC (LC-10AT, Shimadzu, Kyoto, Japan) with a refractive index detector (RID-10A, Shimadzu, Kyoto, Japan) and a chromatographic column (Aminex HPX-87H, Bio-Rad Laboratories, CA, USA). The column temperature was maintained at 65 °C and the mobile phase was 5 mM H₂SO₄ (pH 2.0) running at 0.6 mL min⁻¹. The RID signal was acquired and processed by a data processing unit (Clarity Lite, DataApex, Prague, The Czech Republic). While HPLC was used as the primary analytic method for quantification, the identity of all volatile metabolites (i.e. acetone, butanone, ethanol and 1-propanol) was also verified by GC equipped with a flame ionization detector (FID). The GC system is a Agilent 6890 series (Agilent Technologies, Santa Clara, CA, USA) with a J & W Scientifics DB Wax column (30 m x 0.53 mm, film thickness 1 μM) (Agilent Technologies, Santa Clara, CA, USA). The oven program was set as following: initial temperature was set at 80 °C for 5 min, then ramped to 230 °C at 7.5 °C min⁻¹, and continued to ramp to 260 °C at a faster rate at 10 °C min⁻¹ followed by maintaining that temperature for the analysis. The FID detector was held at 330 °C. The injection volume was 1 μl, injected at a 15:1 split ratio. Helium was used as the carrier gas.

5.2.4 RNA extraction, microarray hybridization, and gene expression analyses

Two aliquots of 1-mL culture samples of CPC-Sbm cultivated anaerobically with glycerol or glucose as the major carbon sources were collected in the mid-exponential growth phase. Total RNA extraction was performed in duplicate for each sample using High Pure RNA Isolation Kit (Roche Diagnostics, Indianapolis, IN, USA) according to the manufacturer's instructions. The integrity of extracted total RNA

was verified by agarose gel electrophoresis, and the RNA quality was evaluated based on the concentration and the OD_{260/280} and OD_{260/230} ratios. Samples were adjusted to a final concentration of 1 µg µL⁻¹ total RNA. Duplicate aliquots of 100 µL of the total RNA samples were subjected to microarray transcriptomic analysis (conducted in the Centre for Applied Genomics at the Hospital for Sick Children, Toronto, Ontario, Canada) using Affymetrix *E. coli* Genome 2.0 GeneChips (Santa Clara, CA, USA). Statistical data analyses, bioinformatic annotation, and retrieval of hybridization intensity raw data from the microarray experiments were carried out using Bioconductor version 3.0 (www.bioconductor.org) and supporting R-Project Bioconductor statistical tools packages (CRAN-Comprehensive R Archive Network, www.cran.r-project.org) (203-205). Normalized gene expression values and expression summaries were generated for each array chip using the Bioconductor Robust Multichip Average (RMA) normalization package with default parameters for raw data background correction, quantile normalization, and signal summation. The ‘limma’ package of the Bioconductor project was used to identify differentially expressed genes. Annotation of the probe sets was performed using the Affymetrix ‘E. coli-2’ annotation file.

5.3 Results

5.3.1 Implementation of synthetic pathway for ketone production in *E. coli*

A prerequisite for *in vivo* butanone biosynthesis via our proposed pathway is the intracellular presence of propionyl-CoA. This can be provided by activation of the Sbm pathway for extended dissimilation of succinyl-CoA (**Figure 5.1**) (199). For molecular hetero-fusion of propionyl-CoA with acetyl-CoA to form 3-ketovaleryl-CoA, two promiscuous β-ketothiolase genes (i.e. *phaA* and *bktB* from *C. necator*) were expressed either individually (using pK-PhaA or pK-BktB) or in combination (using pK-PhaA-BktB) for CoA-dependent chain elongation. Note that PhaA and BktB have enzymatic specificity towards short-chain and long-chain CoA-molecules, respectively (200). On the other hand, β-ketothiolases can also mediate homo-fusion of two acetyl-CoA moieties into acetoacetyl-CoA. For subsequent ketone biosynthesis through thioester hydrolysis and decarboxylation of 3-ketovaleryl-CoA and acetoacetyl-CoA, we introduced the clostridial acetone-formation pathway by fusing the three relevant genes in the transcriptional order of *ctfA-ctfB-adc* in plasmid pCtfAB-Adc for episomal expression under the regulation of the P_{ini} promoter. Each of the β-ketothiolase expression plasmids (i.e. pK-PhaA, pK-BktB, and pK-PhaA-BktB) were co-transferred with pCtfAB-Adc into CPC-Sbm to generate ketogenic strains CPC-MEKCon1, CPC-MEKCon2 and CPC-MEK, respectively (**Table 5.1 and Figure 5.2**).

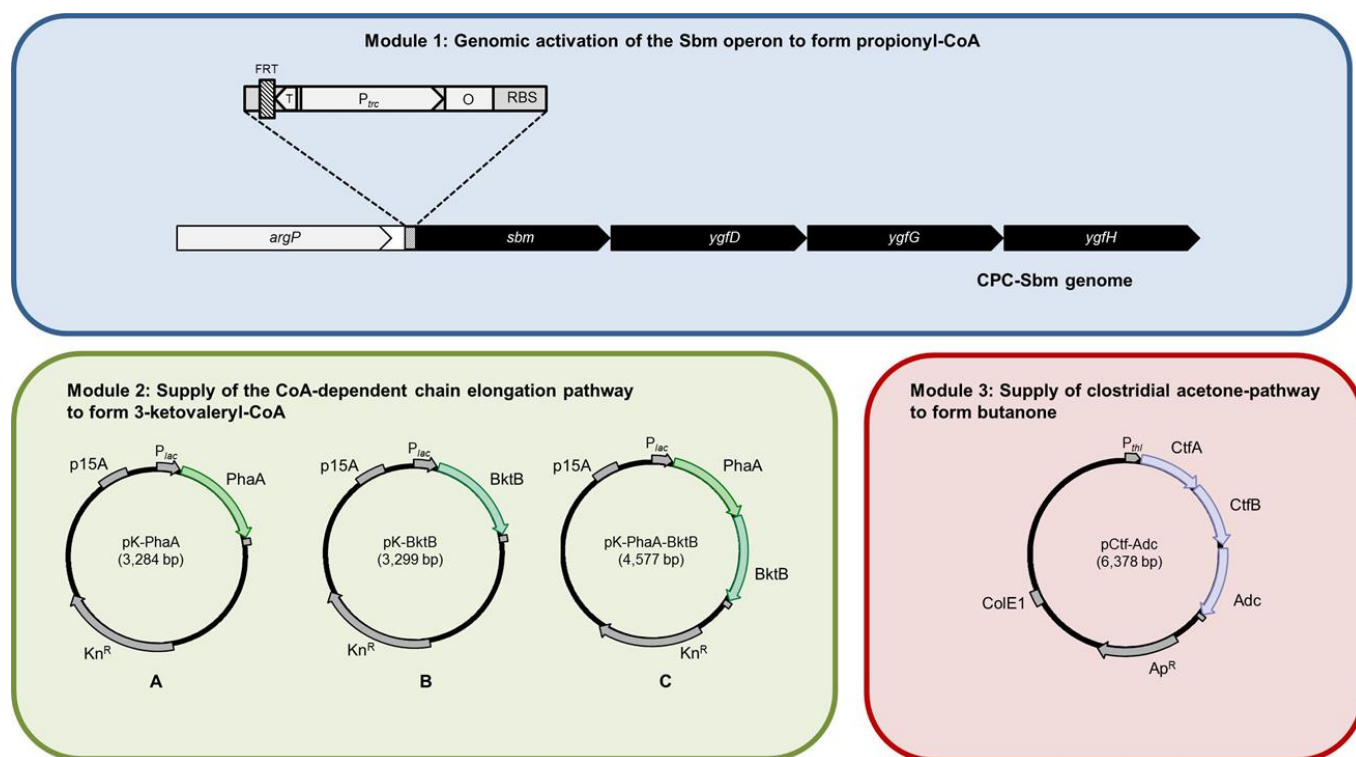


Figure 5.2: Synthetic biology strategies used for heterologous production of butanone in engineered *E. coli*.

The ketone biosynthetic pathway consisted of three modules: (1) the chromosomally activated Sbm pathway in CPC-Sbm for supply of propionyl-CoA, (2) a set of promiscuous β -ketothiolases (i.e. PhaA and BktB) expressed independently or in tandem to generate the CoA-dependent chain elongation pathway for either homo-fusion of acetyl-CoA or hetero-fusion of acetyl-CoA and propionyl-CoA, (3) the clostridial acetone-formation pathway (i.e. CtfAB-Adc) for thioester hydrolysis of the fused CoA-intermediate and subsequent decarboxylation. All three modules were assembled together to generate various ketone production strains, i.e. CPC-MEKCon1 contained modules 1, 2A, and 3, CPC-MEKCon2 contained modules 1, 2B, and 3, and CPC-MEK contained modules 1, 2C, and 3. The single-gene knockouts (i.e. *adhE*, *pta*, *glpD* and *dhaK*) are all variants of the parent ketogenic strain CPC-MEK.

To demonstrate ketone production, CPC-MEKCon1, CPC-MEKCon2, and CPC-MEK were cultivated in a bioreactor. However, culture conditions appear to critically affect ketone production. Previously, it was shown that glycerol, with a higher degree of reduction, outperformed glucose as the major carbon source for anaerobic cultivation of the propanogenic *E. coli* (199). Comparative transcriptomic analysis of the propanogenic strain CPC-Sbm cultivated with glucose or glycerol also indicated that most of the Sbm operon genes were upregulated when glycerol was used as the major carbon source (**Appendix A – Figure S1**). Nevertheless, glycerol dissimilation was significantly

hampered by anaerobiosis (199) and anaerobic cultivation conditions normally favor alcohologenesis. Given that ketones are less reduced than alcohols, their biosynthesis may require a more aerobic environment. Consequently, in addition to strict anaerobiosis, microaerobic and semi-aerobic conditions were also established by purging air at a low flow rate of 0.1 vvm into the headspace and the bulk culture, respectively, while all other cultivation parameters remained the same. These culture conditions were used to characterize CPC-MEKCon1, CPC-MEKCon2, and CPC-MEK for their ketone-producing capacity and the cultivation results are summarized in **Figure 5.3, Appendix A – Figure S2 and Table S2**.

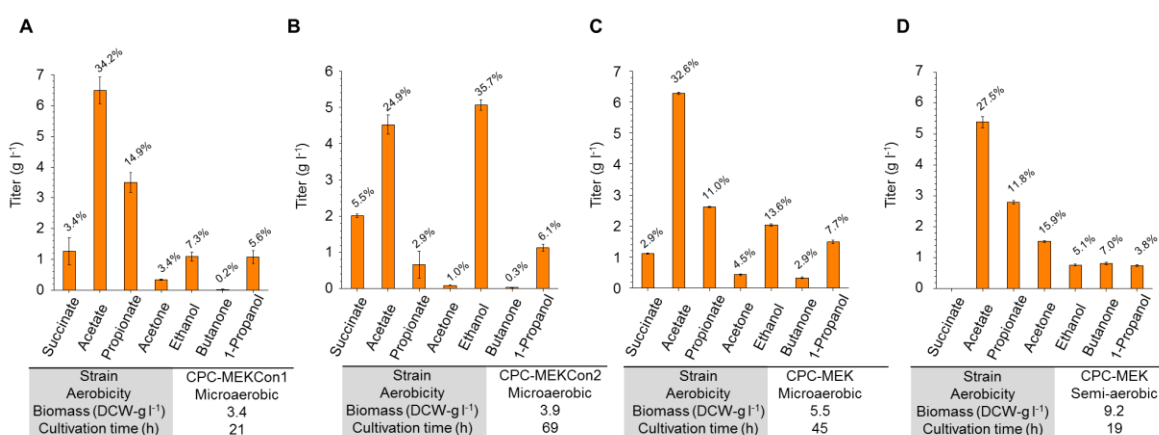


Figure 5.3: Constructing the biosynthetic pathway for ketone production in *E. coli*.

Final metabolite titers including acetone and butanone under microaerobic cultivations of the ketogenic strains (A) CPC-MEKCon1 and (B) CPC-MEKCon2 using 30 g l⁻¹ glycerol as the major carbon source. Final metabolite titers including acetone and butanone under (C) microaerobic cultivation and (D) semi-aerobic cultivation of the ketogenic strain CPC-MEK using 30 g l⁻¹ glycerol as the major carbon source. All of the strains were induced at the start of the batch cultivation with 0.1 mM IPTG. Error bars represent s.d. (n = 2). The metabolite distribution (denoted as the fraction of spent glycerol converted to a specific metabolite) is indicated above each bar.

Glycerol dissimilation and cell growth were low upon anaerobic cultivation of these *E. coli* strains (data not shown), but were much improved by introducing oxygenic conditions. While CPC-MEKCon1 and CPC-MEKCon2 were competent producers of acetone, only trace levels of butanone was detected in these strains under microaerobic cultivation conditions (Figure 5.3A-3B, Appendix A – Figure S2A, S2B and Table S2). Interestingly, heterologous expression of both β -ketothiolases, PhaA and BktB in CPC-MEK greatly augmented ketone production under microaerobic cultivation conditions with 0.43 g l⁻¹ acetone and 0.33 g l⁻¹ butanone (Figure 5.3C, Appendix A – Figure S2C and Table S2).

Semi-aerobic cultivation consumed 30 g l⁻¹ glycerol in 19 h compared to 45 h for microaerobic cultivation and had higher ketone titers (i.e. 1.53 g l⁻¹ acetone and 0.82 g l⁻¹ butanone, respectively) with the total ketone production accounting for ~23% of the dissimilated glycerol (**Figure 5.3D, S2D and Appendix A – Table S2**). More oxygenic conditions by further increasing the air-purging rate to 1 vvm into the bulk culture, however, impaired ketone production with most dissimilated glycerol being directed toward acidogenesis (namely the formation of acetate and propionate) and biomass formation (data not shown). Accordingly, unless otherwise specified, subsequent cultivations were conducted under semi-aerobic conditions using glycerol as the major carbon source. Note that no ketones or other major metabolites were detected when glycerol was not supplemented in the medium and no ketones were detected with CPC-MEKCon3 or CPC-MEKCon4, in which *ctfAB* or *adc* was expressed independently (**Table 5.1 and Appendix A – Table S2**), suggesting that all carbon among fermentative end-products are derived from glycerol and that all three enzymatic components of the clostridial acetone-formation pathway are required for ketone synthesis under these culture conditions. On the other hand, non-propanogenic *E. coli* BW- ΔdhA harboring pK-PhaA-BktB and pCtfAB-Adc produced trace amounts of acetone only, but not butanone (data not shown), implying that propionyl-CoA acts as a precursor for butanone biosynthesis. Lastly, for pK-PhaA-BktB, IPTG induction was critical for functional expression of β -ketothiolases in CPC-MEK (**Appendix A – Table S2**). These control experiments not only confirmed functional expression of the two heterologous β -ketothiolases of PhaA and BktB but also their synergistic effects on CoA-dependent chain elongation, particularly associated with the substrate of propionyl-CoA.

5.3.2 Engineering of *E. coli* to enhance ketone biosynthesis

5.3.2.1 Effect of blocking alcohologenesis

While cell growth and glycerol dissimilation were improved by introducing oxygenic conditions to favor ketone biosynthesis in CPC-MEK, the formation of ethanol and 1-propanol may represent competing pathways, particularly under microaerobic conditions. Hence, we further manipulated CPC-MEK by disrupting the *adhE* gene encoding alcohol dehydrogenase, and the ketone-producing capacity of the resulting mutant CPC-MEK $\Delta adhE$ was characterized (**Figure 5.4A, 5.4B, Appendix A – Figure S3A, S3B and Table S3**). As expected, inactivation of *adhE* abolished the formation of ethanol and 1-propanol without harming cell growth and glycerol dissimilation. Under microaerobic conditions, ketone production was significantly enhanced with abolished alcohologenesis, from 0.43 g l⁻¹ acetone and 0.33 g l⁻¹ butanone for CPC-MEK to 0.84 g l⁻¹ acetone and 0.94 g l⁻¹ butanone for CPC-MEK $\Delta adhE$. Such

improvement was less drastic under semi-aerobic conditions with ~30% increase in butanone titer, i.e. from 0.82 g l⁻¹ for CPC-MEK to 1.07 g l⁻¹ for CPC-MEKΔ*adhE*.

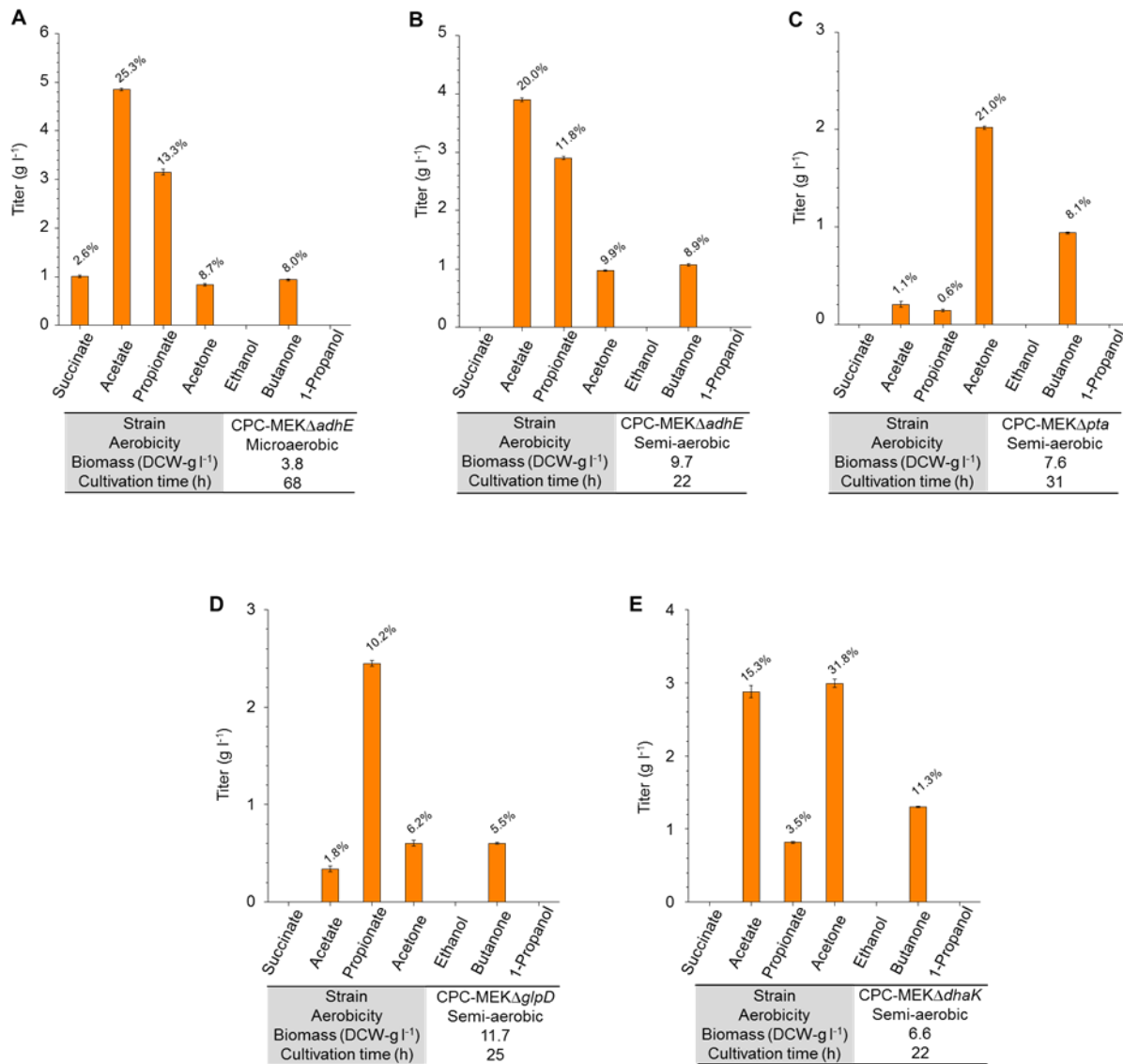


Figure 5.4: Enhancing ketone production in engineered *E. coli*.

Final metabolite titers for (A) microaerobic cultivation of CPC-SbmΔ*adhE* (B) semi-aerobic cultivation of CPC-SbmΔ*adhE* (C) semi-aerobic cultivation of CPC-SbmΔ*pta* (D) semi-aerobic cultivation of CPC-SbmΔ*glpD* (E) semi-aerobic cultivation of CPC-SbmΔ*dhaK* using 30 g l⁻¹ glycerol as the major carbon source. All of the strains were induced at the start of the batch cultivation with 0.1 mM IPTG. Error bars represent s.d. (n = 2). The metabolite distribution (denoted as the fraction of spent glycerol converted to a specific metabolite) is indicated above each bar.

5.3.2.2 Effect of blocking acidogenesis

While ketone-producing capacity for CPC-MEK was enhanced by introducing oxygenic conditions, this aeration strategy also elevated acidogenesis with the sum of the titers of acetate and propionate accounting for up to ~40% of dissimilated glycerol (**Appendix A – Table S2**), a phenotype also observed in the *adhE*-null mutant CPC-MEK Δ *adhE*. Accordingly, we inactivated the phosphotransacetylase (Pta)-acetate kinase (AckA) pathway in CPC-MEK, and the ketone-producing capacity of the resulting mutant CPC-MEK Δ *pta* was characterized (**Figure 4.4C, S3C and Appendix A – Table S3**). Inactivation of the Pta-AckA pathway significantly redistributed metabolites. While it was expected that knocking out *pta* would drastically reduce acidogenesis, alcohologenesis was also abolished in CPC-MEK Δ *pta*, resulting in the production of acetone (2.0 g l⁻¹) and butanone (0.94 g l⁻¹). However, these metabolic perturbations led to severe carbon loss, with the entire accumulated metabolites only accounting for 31% of dissimilated glycerol.

5.3.3 Manipulating glycerol dissimilation to enhance ketone biosynthesis

In *E. coli*, two alternative pathways, i.e. the respiratory GlpK-GlpD and fermentative GldA-DhaK pathways (206), mediate dissimilation of glycerol prior to their merging with the glycolytic trunk. We recently observed that, upon genomic activation of the Sbm operon, the pathway utilization for glycerol dissimilation can potentially affect carbon flux competition between the C2- and C3-fermentative pathways (199, 207). To assess the contribution of the two glycerol dissimilation pathways to the production of the C3-fermentative products, we first engineered CPC-Sbm by inactivating either of the two pathways, resulting in the derivation of two mutant strains, i.e. CPC-Sbm Δ *glpD* and CPC-Sbm Δ *dhaK* containing a single deletion in *glpD* and *dhaK*, respectively, and their cultivation performance were evaluated (**Appendix A – Figure S4A-C and Table S3**). Inactivating either pathway resulted in major changes in biomass formation, carbon flux distribution, and metabolite profile. In comparison to the parental strain CPC-Sbm, lower alcohologenesis and increased acidogenesis were observed for both knockout mutants with propionate titers of 5.2 g l⁻¹ for CPC-Sbm Δ *glpD* and 11.8 g l⁻¹ for CPC-Sbm Δ *dhaK*. The substantial increase in the C3:C2-fermentative product ratio as well as the propionate:acetate ratio for CPC-Sbm Δ *dhaK* compared to CPC-Sbm (**Appendix A – Figure S4D**) suggests that inactivating the fermentative glycerol dissimilation pathway could be used to modulate the “flux competition” between the C2- and C3-fermentative pathways. To potentially increase the level of propionyl-CoA, initial glycerol dissimilation should be channeled through the respiratory pathway.

To further evaluate the ketone-producing capacity of these mutant strains, CPC-Sbm Δ *glpD* and CPC-Sbm Δ *dhaK* were transformed with pK-PhaA-BktB and pCtfAB-Adc to generate strains CPC-MEK Δ *glpD* and CPC-MEK Δ *dhaK*, respectively. Semi-aerobic cultivations of these resulting strains were conducted and the results are summarized in **Figure 5.4D, 5.4E, Appendix A – Figure S5A, S5B and Table S3**. For both mutants with slightly reduced glycerol dissimilation rates compared to the parental strain CPC-MEK, alcohologenesis was completely abolished and acidogenesis was significantly reduced. The dissimilated glycerol was primarily directed toward biomass formation with limited ketone production (i.e. 0.60 g l⁻¹ acetone and 0.64 g l⁻¹ butanone) for CPC-MEK Δ *glpD*. However, higher-level ketogenesis was observed for CPC-MEK Δ *dhaK*, leading to co-production of 2.89 g l⁻¹ acetone and 1.3 g l⁻¹ butanone. The theoretical yields of acetone and butanone based on our proposed biosynthetic pathways with glycerol as the substrate are 0.315 g/g and 0.39 g/g, respectively. As a result, our reported data for CPC-MEK Δ *dhaK* cultivation (i.e. 0.0963 g-acetone/g-glycerol and 0.0433 g-butanone/g-glycerol) suggests that approximately 42% of glycerol was utilized toward ketone biosynthesis. To our knowledge, this also represents one of the highest reported butanone titers for microbial production.

5.4 Discussion

Implementing recursive pathways into genetically tractable microorganisms is particularly useful for the production of longer-chain chemicals, as the key bond-forming functional group of the substrate is regenerated in each reaction cycle (208). Herein, we further engineered propanogenic *E. coli* strains by episomally expressing; (1) a set of promiscuous β -ketothiolases (i.e. PhaA and BktB) from *C. necator* for CoA-dependent chain elongation for either homo-fusion of acetyl-CoA or hetero-fusion of acetyl-CoA and propionyl-CoA, and (2) a clostridial acetone-formation pathway for thioester hydrolysis of the fused CoA-intermediate and subsequent decarboxylation. Note that PhaA and BktB can synergistically enhance CoA-dependent chain elongation and, therefore, the strain's ketone-producing capacity. The genetic strategies led to the derivation of *E. coli* strains for the co-production of acetone and butanone.

Since the CoA-dependent chain elongation reaction catalyzed by β -ketothiolases can be a major kinetic barrier (209), ensuring the abundance of key precursors of acetyl-CoA and propionyl-CoA becomes crucial. Activation of the Sbm pathway not only directed dissimilated carbon flux toward the propionyl-CoA node but also established an intracellular flux competition between the C2- and C3-fermentative pathways. Carbon source also appears to critically affect such competition. Glycerol was more effective than glucose as the major carbon source for cultivation of *E. coli* CPC-Sbm for 1-propanol production (199), implying a more active Sbm pathway and a higher propionyl-CoA level under such

conditions. This observation was further corroborated by a comparative transcriptomic analysis of CPC-Sbm cultivated with glucose or glycerol (**Appendix A – Figure S1**). Compared to glucose, several of the Sbm operon genes and other glycolytic enzyme genes, such as *pckA* and *ppsA*, were upregulated in cells cultivated with glycerol. TCA cycle genes, including *sdhB*, *sucC*, *sucD*, *sucA*, and *sucB*, in the pathway toward the node of succinyl-CoA (i.e. the starting precursor into the Sbm pathway) were also upregulated. Furthermore, given that ketones are less reduced than alcohols, ketogenic *E. coli* should not be cultivated under strict anaerobic conditions, which not only impacts glycerol dissimilation but also favors alcohologenesis. Under slightly oxygenic (i.e. microaerobic or semi-aerobic) conditions, not only cell growth and glycerol dissimilation were improved but also cell's capacity for redox-balanced biosynthesis of metabolites through anaerobic fermentation was preserved. Our results suggest that ketone production was most effective under semi-aerobic conditions. Interestingly, both CtfAB and Adc enzymes from anaerobic clostridia appear to be active under such culture conditions.

Disruption of *adhE* completely abolished alcohologenesis and increased acetone and butanone titers by more than two fold under microaerobic conditions. In addition to carbon flux redirection, the enhanced ketogenesis can be associated with potential elimination of alcohol inhibition of clostridial CoA transferase (210). Our results also contrast an earlier observation that ethanol formation is necessary for respiro-fermentative utilization of glycerol (206). While such genetic effect on enhancing ketogenesis was limited under semi-aerobic conditions for acetone, the butanone titer was increased by ~30%. Also, note that the enhanced ketogenesis appeared to occur simultaneously with increased propionate titers and reduced acetate titers, suggesting that knocking out *adhE* can potentially enhance intracellular propionyl-CoA pool by limiting 1-propanol formation.

On the other hand, knocking out *pta* significantly reduced acidogenesis while completely abolishing alcohologenesis, resulting in an almost homo-ketogenic behavior. These results are similar to those of a previous study of semi-aerobic cultivation with glycerol as the major carbon source, in which the inactivation of the Pta-Ack pathway led to significant changes in the distribution of metabolites, namely reduced ethanol production and an overall increase in oxidized metabolites (206). Note that acetyl phosphate, the intermediate in the Pta-AckA pathway, serves as an important metabolite for global regulation of gene expression and other fundamental processes and inactivating this pathway can potentially induce metabolic complications (211). For instance, elimination of acetyl phosphate can lead to inadequate turnover of the sigma factor RpoS and an overall reduction in growth and metabolite formation (212, 213). Although this phenomenon is well known and its etiology is not fully understood, it

could be associated with the depletion of free intracellular CoA moieties caused by low rates of acetyl-CoA turnover (208). Furthermore, while the residual acetate can be produced via decarboxylation of pyruvate catalyzed by pyruvate oxidase (encoded by *poxB*) (206), whereas the residual propionate can be mediated by propionyl-CoA/succinyl-CoA transferase (encoded by *ygfH*), the homo-ketogenic behavior of this strain did not lead to higher ketone yields. Such low-level ketogenesis can be potentially associated with low acid production since, for acetone-butanol-ethanol (ABE) fermentation in clostridia, acetone production is coupled with acetate/butyrate uptake via CoA-transferase for continuous regeneration of acetyl-CoA/butyryl-CoA (214). It is thus difficult to decouple acidogenesis from ketogenesis without hampering cell growth and glycerol dissimilation. An alternative approach for coping with acetate/propionate accumulation can be recycling of excreted acetate/propionate to form acetyl-CoA in an ATP-dependent manner by overexpressing acetyl-CoA synthetase (encoded by *acs*) (215). Other strategies include establishing thioesterase-mediated ketone production platforms by relying on acetate-independent pathways (216) or fatty acid β -oxidation pathways (217).

Our results show that directing initial glycerol dissimilation through the respiratory GlpK-GlpD pathway can enhance butanone production, potentially due to an increased level of propionyl-CoA. A critical factor limiting biosynthesis based on the use of glycerol is the diversion of carbon flux at the phosphoenolpyruvate (PEP) node toward being a phosphate donor to support glycerol dissimilation via the fermentative GldA-DhaK pathway. Such competing need for PEP as a phosphate donor is eliminated in the mutant CPC-MEK Δ *dhaK*, ostensibly increasing the PEP pool. The increased PEP pool potentially enhances propionyl-CoA production as more carbon flux is diverted toward oxaloacetate (OAA) via the anaplerotic reactions catalyzed by the endogenous PEP carboxylase or PEP carboxykinase (encoded by *ppc* or *pckA*, respectively) (206, 218, 219). Similar to other Gram-negative bacteria that utilize glycerol (e.g. *Klebsiella pneumonia*), inactivating the fermentative GldA-DhaK pathway in *E. coli* also enhances acetate formation (206, 220). Inactivating *dhaK* is known to decrease the NADH/NAD⁺ ratio, thus reducing the biosynthesis of reduced products such as ethanol and 1-propanol. The cell potentially compensates for the NADH deficiency by enhancing acetate formation for ATP production (206, 220). An increase the PEP pool can also result in the decarboxylation of pyruvate to acetate catalyzed by PoxB (221). On the other hand, routing glycerol dissimilation through the fermentative GldA-DhaK pathway in mutant strain CPC-MEK Δ *glpD* can enhance such PEP competition and divert the carbon flux away from the C3-fermentative pathway, resulting in less butanone production. Also note that GlpD plays a role in balancing the intracellular PEP and OAA pools (219, 222), and such function appears to be critical for directing more carbon flux toward the propionyl-CoA node for butanone biosynthesis.

In summary, in this chapter we demonstrated the engineering *E. coli* for co-production of acetone and butanone was demonstrated with up to 42% of spent carbon source of glycerol being utilized toward ketone biosynthesis. While the current results appear to be promising, large-scale production will require derivation of superior ketogenic strains by targeting key steps in the ketone production pathway, eliminating latent metabolic bottlenecks and imbalances, and substantially reducing byproduct formation. For instance, 3-ketovaleryl-CoA and acetoacetyl-CoA are converted to 3-oxopentanoate and acetoacetate, respectively, via the clostridial CoA transferase with the use of acetate as the major CoA acceptor, resulting in recycling of acetyl-CoA. We are exploring several higher-chain CoA transferases (e.g. 3-oxoadipate: succinyl-CoA transferase), which can potentially use propionate or succinate as the CoA acceptor and promote recycling of propionyl-CoA. Note that butanone (and to a less extent acetone) can also be used as an intermediate for the biological conversion of other value-added products such as ethyl esters (223) and secondary alcohols such as 2-butanol (197) and isopropanol (224). Lastly, in addition to medium chain methyl ketones, CoA-dependent elongation pathways can also be applied for biosynthesis of several other long chain oleochemicals such as fatty acid ethyl-esters, fatty alcohols and amines, paraffins, and olefins (225, 226), thus expanding the scope of whole-cell biocatalytic platforms.

Chapter 6

Engineering propanogenic *E. coli* for direct biosynthesis of poly(3-hydroxybutyrate-co-3-hydroxyvalerate) using unrelated carbon sources

Chapter Abstract

In this chapter, we further expanded the utility of our developed propanogenic *E. coli* for the production of poly(3-hydroxybutyrate-co-3-hydroxyvalerate) [also referred to as PHBV or P(3HB-co-3HV)], a commercial biodegradable plastic from a single unrelated carbon source (i.e. glucose or glycerol). To enable P(3HB-co-3HV) biosynthesis in our propanogenic *E. coli*, two metabolic strategies were implemented. First, two acetyl-CoA moieties or acetyl-CoA and propionyl-CoA were condensed to generate the C4 and C5 thioesters 3-hydroxybutyryl-CoA and 3-ketovaleryl-CoA, respectively, by functionally expressing a set of β -ketothiolases from *C. necator* (i.e. PhaA and BktB). Next, the resulting intermediates were channeled into the *C. necator* PHA biosynthetic pathway, which was implemented by functionally expressing PhaB and PhaC, for subsequent thioester reduction and polymerization. In addition to the above synthetic approaches, various biochemical, genetic, and metabolic factors and cultivation strategies were also systematically explored to not only enhance total PHA content but also the 3HV monomer fraction in the copolymer. Using the derived polymer-accumulating *E. coli* strains for batch cultivation, we achieved 3HV fractions ranging from 3 mol% to 19 mol% in 3HV in total polymer, thus demonstrating the potential industrial applicability of these whole-cell biocatalysts.

6.1 Background

Since the 1970s, petroleum (mineral oil) derived plastics (i.e. traditional plastics) have been the most used material in the world, and are used extensively for myriad domestic, medical, and commercial applications (227, 228). On a global scale, it is estimated that approximately 200 million tons of polymeric material is now manufactured each year (228). Nevertheless, mounting concerns over fossil fuel prices, depletion, and climate change and environmental problems have created a renewed impetus in the search for more sustainable bio-based production platforms (227, 228). Another serious issue against unfettered use of traditional plastics is their recalcitrance with respect to environmental degradation (227). For these reasons, natural biodegradable bacterial polyesters such as polyhydroxyalkanoates (PHAs) have attracted considerable research interest as promising candidates to substitute for petroleum-based plastics. PHAs are produced by diverse Gram-negative and Gram-positive bacteria, including those from the genera *Cupriavidus*, *Pseudomonas*, and *Bacillus*, and exist as insoluble cytoplasmic granules for use as carbon storage and reducing potential (229-231). Being polyesters of various (*R*)-hydroxycarboxylic acids monomers, PHAs can exhibit properties ranging from thermoplastic elastomers to viscous liquids depending on their monomeric composition (231, 232).

The most well-characterized and naturally abundant member of PHAs is poly(3-hydroxybutyrate) (PHB) (231, 233). PHB is derived from acetoacetyl-CoA, a C4 biogenic intermediate that is formed via Claisen condensation of two acetyl-CoA moieties by the action of a β -ketothiolase (PhaA). Acetoacetyl-CoA is reduced to (*R*)-3-hydroxybutyryl-CoA (3HB-CoA) by an NADPH-dependent acetoacetyl-CoA reductase (PhaB) and subsequently incorporated into the growing polymer by PHA polymerase/synthase (PhaC) (230). Similar to other short-chain PHA homopolymers, PHB has a high degree of crystallinity and a high melting temperature. Therefore, it has a limited range of applicability as an industrial plastic material as it is too brittle and stiff to be processed (229, 234). Accordingly, there have been numerous attempts to develop bioprocess schemes based on incorporating longer chain (*R*)-hydroxycarboxylic acids monomers in PHB to generate copolymers with increased toughness, ductility and impact strength and lower stiffness and crystallinity (299).

Historically, the random copolymer poly(3-hydroxybutyrate-*co*-3-hydroxyvalerate) [P(3HB-*co*-3HV)] has been the most extensively studied 3HB-based copolymer and was commercially sold by Imperial Chemical Industries and later Monsanto under the tradename Biopol™ (235, 236). P(3HB-*co*-3HV) is a coalesce of monomers 3HB and (*R*)-3-hydroxyvalerate (3HV) and is synthesized from precursors acetyl-CoA and propionyl-CoA in an analogous manner to that of PHB (**Figure 6.1**) (235,

237). While Monsanto had several P(3HB-*co*-3HV)-based biodegradable products in the pipeline such as molded bottles, films, coatings, and even biochemical devices, the company withdrew from the biopolymer market in 1998 citing high production costs as a major deterrent to Biopol™ commercialization (231, 238). When P(3HB-*co*-3HV) was produced on an industrial-scale, the 3HV monomer fraction was generated *in vivo* by feeding glucose and a second related carbon source (i.e. propionate or valerate) to cultures of *C. necator*, a natural producer of PHAs (231, 235, 236). Although monomer composition of the copolymer can be controlled via exogenous supplementation of propionate or valerate to the cultivation medium, the addition of these related carbon sources is prohibitively expensive and can often negatively impact cell growth and culture performance (226). Thus, many recent metabolic engineering efforts have focused on expanding the chemical diversity of whole-cell biocatalysts for *de novo* synthesis of propionyl-CoA from single unrelated carbon sources (e.g. glucose or glycerol) for the production of P(3HB-*co*-3HV).

In this chapter, we describe the implementation of a metabolic pathway in the genetically tractable organism *E. coli* for direct propionate-independent biosynthesis of P(3HB-*co*-3HV) using glucose or glycerol as sole carbon sources. To generate the required 3HV monomer fraction for incorporation in PHB, we first introduced a facile and efficient catalytic node toward high-level production of the non-native precursor propionyl-CoA. Organisms more amenable to genetic manipulations such as *E. coli* or yeast do not possess metabolic enzymes or utilize alternative pathways for propionyl-CoA anabolism (239). However, a popular approach to enable propionyl-CoA metabolism has been via the extended dissimilation of 2-ketobutyrate, derived from the tricarboxylic acid cycle (TCA) intermediate oxaloacetate, and has served as the basis for the production of several unnatural odd-chain biofuels, organic acids, and also for the controlled biosynthesis of 3HV and P(3HB-*co*-3HV). In the previous chapters, we demonstrated the heterologous production of 1-propanol and propionate based on the genomic activation of the quiescent yet functional sleeping beauty mutase operon in *E. coli* (173, 199, 225) This four-gene operon (i.e. *sbm-ygfD-ygfG-ygfH*) encodes various enzymes involved in the cataplerotic conversion of the TCA intermediate succinyl-CoA to propionyl-CoA, resulting in the production of non-native C3-metabolites 1-propanol and propionate (**Figure 6.1**) (148). As a result, genomic activation of the Sbm pathway not only transforms *E. coli* to be propanogenic/propionogenic, but also introduces an intracellular “carbon flux competition” between the traditional C2-fermentative pathway (forming acetate and ethanol) and the novel C3-fermentative pathway (forming propionate and 1-propanol).

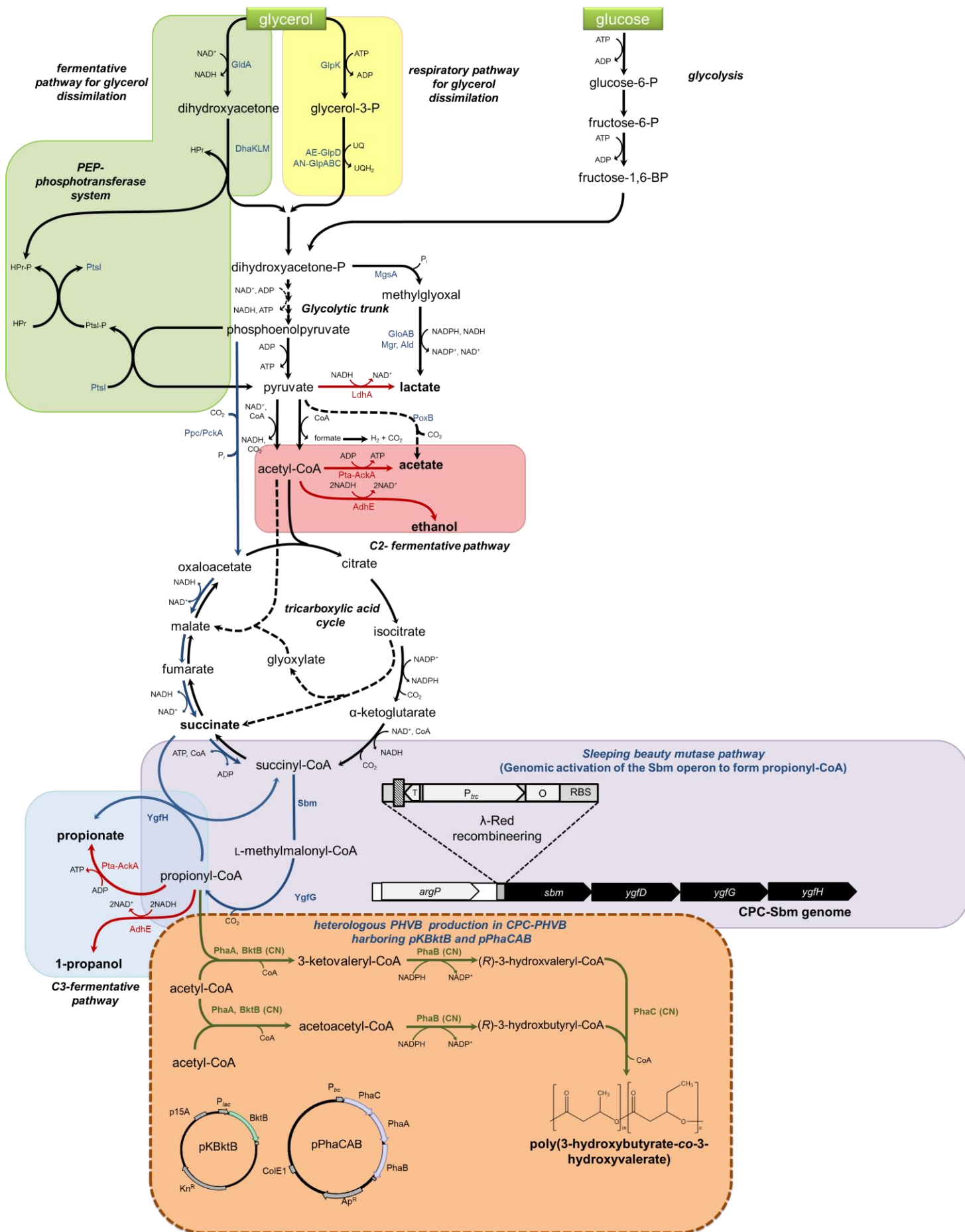


Figure 6.1: Schematic representation of the synthetic biology and metabolic strategies used to establish the P(3HB-co-3HV) biosynthetic pathway in engineered propanogenic/propionogenic *E. coli* (on previous page).

Heterologous enzymes from *Cupriavidus necator* (CN) are shown in green text. The fermentative pathway for glycerol dissimilation is presented in a light green box and the respiratory pathway for glycerol dissimilation is presented in a yellow box. The activated Sleeping beauty mutase (Sbm) pathway is presented in a purple box. Red and blue arrows represent the route to the C2- and C3-fermentative products, respectively. The C2-fermentative pathway is presented in a red box, while the C3-fermentative pathway is presented in a blue box. Relevant enzymes for production of various fermentative products as well as the enzymes of the respiratory and fermentative glycerol pathways and the Sbm pathway are in blue text.

For P(3HB-co-3HV) biosynthesis in propanogenic/propionogenic *E. coli*, two more metabolic approaches were implemented. First, to generate the required C4 and C5 precursors 3HB-CoA and 3HV-CoA, respectively, a CoA thioester-dependent chain elongation system was employed by functionally expressing a set of β -ketothiolases from *C. necator* (i.e. PhaA and BktB). Next, the resulting intermediates were channeled into the *C. necator* PHA biosynthetic pathway, which was implemented by functionally expressing PhaB and PhaC, for thioester reduction and polymerization (**Figure 6.1**). In addition to the above synthetic approaches, various biochemical, genetic, and metabolic factors and cultivation strategies were also systematically explored to not only enhance total PHA content but also the 3HV monomer fraction in the copolymer. The range of 3HV fractions obtained in our developed polymer-accumulating *E. coli* strains are similar to that used in BiopolTM (3 mol % to 19 mol %), thus demonstrating the potential industrial applicability of these whole-cell biocatalysts.

6.2 Methods

6.2.1 Bacterial strains and plasmids

E. coli strains, plasmids and DNA primers used in this study are listed in **Table 6.1**. Standard recombinant DNA technologies for molecular cloning were applied (150). *Pfu* and *Taq* DNA polymerases, T4 DNA ligase, and large (Klenow) fragment of DNA Polymerase I were obtained from New England Biolabs (Ipswich, MA, USA). All synthesized oligonucleotides were obtained from Integrated DNA Technologies (Coralville, IA, USA). DNA sequencing was conducted by the Centre for Applied Genomics at the Hospital for Sick Children (Toronto, Canada). *E. coli* BW25141 was the parental strain for derivation of all mutant strains in this study and *E. coli* HST08 was used for molecular cloning.

Activation of the genomic Sbm operon to form propanogenic/propionogenic *E. coli* CPC-Sbm was described previously (199). Briefly, the FRT-Cm^R-FRT cassette from pKD3 was PCR-amplified

Table 6.1: List of *E. coli* strains, plasmids, and oligonucleotides used in this study.

Name	Description, relevant genotype or primer sequence (5'→3')	Reference
<i>E. coli</i> host strains		
HST08	F ⁻ , <i>endA1</i> , <i>supE44</i> , <i>thi-1</i> , <i>recA1</i> , <i>relA1</i> , <i>gyrA96</i> , <i>phoA</i> , $\Phi 80d$ <i>lacZ</i> Δ <i>M15</i> , Δ (<i>lacZYA</i> – <i>argF</i>) <i>U169</i> , Δ (<i>mrr</i> – <i>hsdRMS</i> – <i>mcrBC</i>), Δ <i>mcrA</i> , λ^-	Takara Bio, Shiga, Japan
BW25141	F ⁻ , Δ (<i>araD-araB</i>)567, Δ <i>lacZ</i> 4787(:: <i>rrnB-3</i>), Δ (<i>phoB-phoR</i>)580, λ^- , <i>galU95</i> , Δ <i>uidA3</i> :: <i>pir+</i> , <i>recA1</i> , <i>endA9</i> (<i>del-ins</i>)::FRT, <i>rph-1</i> , Δ (<i>rhaD-rhaB</i>)568, <i>hsdR514</i>	Datsenko and Wanner(153)
BW25113	F ⁻ , Δ (<i>araD-araB</i>)567, Δ <i>lacZ</i> 4787(:: <i>rrnB-3</i>), λ^- , <i>rph-1</i> , Δ (<i>rhaD-rhaB</i>)568, <i>hsdR514</i>	Datsenko and Wanner(153)
BW- Δ ldhA	BW25113 Δ <i>ldhA</i> null mutant	Srirangan et al.(173)
CPC-Sbm-Cm ^R	BW- Δ ldhA, P _{<i>trc</i>} :: <i>sbm</i> (i.e. with the FRT-Cm ^R -FRT-P _{<i>trc</i>} cassette replacing the 204-bp upstream of the Sbm operon)	This study
CPC-Sbm	BW- Δ ldhA, P _{<i>trc</i>} :: <i>sbm</i> (i.e. with the FRT -P _{<i>trc</i>} cassette replacing the 204-bp upstream of the Sbm operon)	This study
CPC-Sbm Δ adhE	BW- Δ ldhA, Δ <i>adhE</i> , P _{<i>trc</i>} :: <i>sbm</i> (i.e. with the FRT -P _{<i>trc</i>} cassette replacing the 204-bp upstream of the Sbm operon),	This study
CPC-Sbm Δ pta	BW- Δ ldhA, Δ <i>pta</i> , P _{<i>trc</i>} :: <i>sbm</i> (i.e. with the FRT -P _{<i>trc</i>} cassette replacing the 204-bp upstream of the Sbm operon)	This study
CPC-Sbm Δ glpD	BW- Δ ldhA, Δ <i>glpD</i> , P _{<i>trc</i>} :: <i>sbm</i> (i.e. with the FRT -P _{<i>trc</i>} cassette replacing the 204-bp upstream of the Sbm operon)	This study
CPC-Sbm Δ dhaK	BW- Δ ldhA, Δ <i>dhaK</i> , P _{<i>trc</i>} :: <i>sbm</i> (i.e. with the FRT- P _{<i>trc</i>} cassette replacing the 204-bp upstream of the Sbm operon)	This study
CPC-PHB	BW- Δ ldhA/pPhaCAB and pKBktB	The study

CPC-PHBV	CPC-Sbm/pPhaCAB and pKBktB	This study
CPC-PHBVCon1	CPC-Sbm/pPhaCAB	This study
CPC-PHBV Δ adhE	CPC-Sbm Δ adhE/pPhaCAB and pKBktB	This study
CPC-PHBV Δ pta	CPC-Sbm Δ pta/pPhaCAB and pKBktB	This study
CPC-PHBV Δ glpD	CPC-Sbm Δ glpD/pPhaCAB and pKBktB	This study
CPC-PHBV Δ dhaK	CPC-Sbm Δ dhaK/pPhaCAB and pKBktB	This study
Plasmids		
pCP20	FLP ⁺ , λ cI857 ⁺ , λ p _R Rep(pSC101 ori) ^{ts} , Ap ^R , Cm ^R	Cherepanov and Wackernagel (155)
pKD46	RepA101 ^{ts} ori, Ap ^R , <i>araC</i> -P _{araB} : <i>gam-bet-exo</i>	Datsenko and Wanner (153)
pTrc99a	ColE1 ori, Ap ^R , P _{trc}	Amann et al. (180)
pKD3	R6K- γ ori, Ap ^R , FRT-Cm ^R -FRT	Datsenko and Wanner (2000)
pK184	p15A ori, Km ^R , P _{lac} : <i>lacZ</i> '	Jobling and Holmes (156)
pPhaCAB	From pTrc99a, P _{trc} : <i>phaCAB</i>	This study

pKBktB	From pK184, P _{lac} : <i>bktb</i>	This study
Primers		
v-ldhA	GATAACGGAGATCGGGAATGATTAA; GGTTTAAAAGCGTCGATGTCCAGTA	Srirangan et al. (173)
v-adhE	ATCAGGTGTCCTGAACTGTGCG; TTGACCAGCGCAAATAACCCGATGA	This study
v-pta	GGCATGAGCGTTGACGCAATCA; CAGCTGTACGCGGTGATACTCAGG	This study
v-dhaK	CATCGAGGATAAACAGCGCA; ATCTGATAAAGCTCTTCCAGTGT	This study
v-glpD	CGTCAATGCTATAGACCACATC; TATTATTGAAGTTTGTAAATATCCTTATCAC	This study
c-frt	AGATTGCAGCATTACACGTCTTGAG; CCAGCTGCATTAATGAATCGGGCCATGGTCCATATGAATATCCTCC	This study
c-ptrc	CCGATTCATTAATGCAGCTGG; GGTCTGTTTCCTGTGTGAAATTGTTA	This study
r-frt:ptrc	CTCGATTATGGTCACAAAGTCCTTCGTCAGGATTA AAGATTGCAGCATTACACGTCTTGA; GTTGGCAAGCTGTTGCCACTCCTGCACGTTAGACATGGTCTGTTTCCTGTGTGAAATTGT	This study
v-frt:ptrc	GCGCTCGACTATCTGTTTCGTCAGCTC; TCGACAGTTTTCTCCCGACGGCTCA	This study
g-phaCAB	CACACAGGAAACAGACATGGCGACCGGCAAAGGC; CGAGCTCGAATTCCATTCAGCCCATATGCAGGCC	This study
c-bktb	CATGATTACGAATTCGATGACGCGTGAAGTGGTAGTGGTGA; TACCGAGCTCGAATTCTCAGATGCGTTCGAAGATAGCGGCAA	This study

Notation for primers: v- verification primer, c- cloning primer, r- recombineering and g-Gibson DNA assembly primer. Restriction recognition sequences are underlined and homology arms for *in vivo* or *in vitro* recombination are in bold print

using the primer set c-frt, whereas the *trc* promoter-operator region was PCR-amplified using the c-ptrc primer set. The two DNA amplicons were fused together by splice overlap-extension (SOE) PCR (151) using the forward primer of the c-frt primer set and the reverse primer of the c-ptrc primer set to generate the FRT-Cm^R-FRT-P_{*trc*} cassette. To generate the DNA cartridge for genomic integration, the FRT-Cm^R-FRT-P_{*trc*} cassette was PCR-amplified using the r-frt:ptrc primer set containing the 5'- and 3'-36-bp homology arms, respectively. The homology arms were chosen so that the FRT-Cm^R-FRT-P_{*trc*} cassette was inserted precisely upstream of the *Sbm* operon. λ -Red genomic recombineering was carried out as described by Datsenko and Wanner (153).

Gene knockouts (i.e. *adhE*, *pta*, *glpD*, and *dhaK*) were introduced into CPC-Sbm by P1 phage transduction (150) using the appropriate Keio Collection strains (The Coli Genetic Stock Center, Yale University, New Haven, CT, USA) as donors (152). To eliminate the co-transduced FRT-Km^R-FRT cassette, the transductant mutants were transformed with pCP20 (155), a temperature sensitive plasmid expressing a flippase (Flp) recombinase. Upon Flp-mediated excision of the Km^R cassette, a single Flp recognition site (FRT “scar site”) was left behind. Plasmid pCP20 was then removed by growing cells at 42 °C. The genotypes of derived knockout strains were confirmed by whole-cell colony PCR using the appropriate “verification” primer sets listed in **Table 6.1**.

The DNA fragment containing the native *C. necator* PHA operon genes (*phaC-phaA-phaB*) was PCR-amplified from the genomic DNA of the wild-type *C. necator* strain (ATCC 43291) using the g-phaCAB primer set. The amplified DNA fragment was assembled using Gibson method (202) into vector pTrc99a. A clone with the correct transcriptional orientation of the *phaC-phaA-phaB* fragment with respect to the p_{*trc*} promoter was selected and verified by DNA sequencing, yielding pK-PhaCAB. Similarly, the β -ketothiolase gene was PCR-amplified from the genomic DNA of the wild-type *C. necator* strain (ATCC 43291) using primer set c-bktb. The resulting fragment was cloned into the *EcoRI* restriction site of pK184. A clone with the correct transcriptional orientation of the *bktB* fragment with respect to the P_{*lac*} promoter was selected and verified by DNA sequencing, yielding pKBktB.

6.2.2 Media and cultivation conditions

All media components were obtained from Sigma-Aldrich Co. (St Louis, MO, USA) except glucose, yeast extract, and tryptone which were obtained from BD Diagnostic Systems (Franklin Lakes, NJ, USA). Media was supplemented with antibiotics as required (30 $\mu\text{g mL}^{-1}$ and 12 $\mu\text{g mL}^{-1}$ of kanamycin and chloramphenicol, respectively). For PHA production, the recombinant *E. coli* strains (stored as glycerol stocks at -80 °C) were streaked on LB agar plates with appropriate antibiotics and incubated at 37 °C for

16 h. Single colonies were picked from LB plates to inoculate 30-mL SB medium (32 g l⁻¹ tryptone, 20 g l⁻¹ yeast extract, and 5 g l⁻¹ NaCl) with appropriate antibiotics in 125-mL conical flasks. Overnight cultures were shaken at 37 °C and 280 rpm in a rotary shaker (New Brunswick Scientific, NJ, USA) and used as seed cultures to inoculate 200 mL SB media at 1% (v/v) with appropriate antibiotics in 1-L conical flasks. This second seed culture was shaken at 37 °C and 280 rpm for approximately 16 h. Cells were then harvested by centrifugation at 6,000 × g and 20 °C for 15 min and resuspended in 100-mL fresh LB media. The suspended culture was used to inoculate a 1-L stirred-tank bioreactor (CelliGen 115, Eppendorf AG, Hamburg, Germany) operated microaerobically, semiaerobically, or aerobically at 30 °C and 430 rpm. The semi-defined production medium in the bioreactor contained 30 g l⁻¹ glycerol or 30 g l⁻¹ glucose, 0.23 g l⁻¹ K₂HPO₄, 0.51 g l⁻¹ NH₄Cl, 49.8 mg l⁻¹ MgCl₂, 48.1 mg l⁻¹ K₂SO₄, 1.52 mg l⁻¹ FeSO₄, 0.055 mg l⁻¹ CaCl₂, 2.93 g l⁻¹ NaCl, 0.72 g l⁻¹ tricine, 10 g l⁻¹ yeast extract, 10 mM NaHCO₃, 0.2 μM cyanocobalamin (vitamin B₁₂) and trace elements (2.86 g l⁻¹ H₃BO₃, 1.81 g l⁻¹ MnCl₂·4H₂O, 0.222 g l⁻¹ ZnSO₄·7H₂O, 0.39 g l⁻¹ Na₂MoO₄·2H₂O, 79 μg l⁻¹ CuSO₄·5H₂O, 49.4 μg l⁻¹ Co(NO₃)₂·6H₂O) (179), appropriate antibiotics, and supplemented with 0.1 mM isopropyl β-D-1-thiogalactopyranoside (IPTG). Microaerobic conditions were maintained by purging air into the headspace at 0.1 vvm. Semiaerobic conditions were maintained by purging air into the bulk culture at 0.1 vvm. Aerobic conditions were maintained by purging air into the bulk culture at 1 vvm. The pH of the production culture was maintained at 7.0 ± 0.1 with 30% (v/v) NH₄OH and 15% (v/v) H₃PO₄. All cultivation experiments were performed in triplicate.

6.2.3 Offline analyses and polymer extraction

Culture samples were appropriately diluted with saline for measuring the optical cell density (OD₆₀₀) using a spectrophotometer (DU520, Beckman Coulter, Fullerton, CA). Cell-free supernatant was collected and filter sterilized for titer analysis of glucose, glycerol, and the various excreted metabolites using an HPLC (LC-10AT, Shimadzu, Kyoto, Japan) with a refractive index detector (RID-10A, Shimadzu, Kyoto, Japan) and a chromatographic column (Aminex HPX-87H, Bio-Rad Laboratories, CA, USA). The column temperature was maintained at 65 °C and the mobile phase was 5 mM H₂SO₄ (pH 2.0) running at 0.6 mL min⁻¹. The RID signal was acquired and processed by a data processing unit (Clarity Lite, DataApex, Prague, The Czech Republic).

Intracellular polymer production was evaluated by gas chromatography as described by Braunegg (207). Briefly, culture samples harvested from the bioreactor cultivations were pelleted by centrifugation at 4000 × g for 20 min, then washed twice with distilled water, and finally dried at 100°C overnight. The

dried cell weight (DCW) was recorded before methanolysis in 2 ml chloroform and 1 ml PHA solution containing 4 g/L benzoic acid (as an internal standard) and 15% sulfuric acid in methanol. Methanolysis was carried out at 96°C for 6 h. The reaction was then cooled to room temperature, and after addition of 1 ml distilled water, the mixture was vortexed and allowed to separate into two phases. 1 µl of the chloroform phase was injected into Agilent 6890 series GC system (Agilent Technologies, Santa Clara, CA, USA) with a J & W Scientifics DB Wax column (30 m x 0.53 mm, film thickness 1 µm) (Agilent Technologies, Santa Clara, CA, USA). The oven program was set as following: initial temperature was set at 80°C for 5 min, then ramped to 230°C at 7.5°C/min, and continued to ramp to 260°C at a faster rate 10°C/min followed by maintaining that temperature for the analysis. Pure standards of methyl 3-hydroxybutyrate and methyl 3-hydroxyvalerate (Sigma-Aldrich Co., St Louis, MO, USA) were used to generate calibration curves for the methanolysis assay. The PHA content was defined as the ratio of PHA mass to dry cell mass (DCW) in a given sample, expressed as a percentage. The 3HV fraction was defined as the ratio of 3HV to 3HV plus 3HB in the copolymer, expressed in mole percent.

6.3 Results

6.3.1 Direct biosynthesis of P(3HB-co-3HV) in *E. coli*

A prerequisite to the formation of 3HV-CoA in *E. coli* is the intracellular presence of non-native propionyl-CoA as a precursor. Recently, we reported construction of propanogenic/propionogenic *E. coli* strains for heterologous production of 1-propanol (173, 199) and propionate (225) by activating the inherently silent sleeping beauty mutase (Sbm) operon in the host genome. The Sbm pathway serves as a direct route to propionyl-CoA through extended dissimilation of succinyl-CoA, a tricarboxylic acid cycle (TCA) intermediate (**Figure 6.1**). In this study, the resulting propanogenic/propionogenic *E. coli*, CPC-Sbm, and its derivatives were explored as host strains to produce P(3HB-co-3HV).

To implement relevant pathways for the production of P(3HB-co-3HV), a double plasmid expression system was employed (**Figure 6.1 and Table 1**). First, using a β -ketothiolase encoded by the *bktb* gene from *C. necator*, a CoA-dependent chain elongation system was established to carry out hetero-fusion of propionyl-CoA and acetyl-CoA and homo-fusion of two acetyl-CoA molecules to form biogenic intermediates 3-ketoaleryl-CoA and acetoacetyl-CoA, respectively. The *bktb* gene was cloned in a plasmid pK-BktB with a p15A replicon for its heterologous expression under the regulation of the *lac* promoter. Next, for reduction of 3-ketoaleryl-CoA and acetoacetyl-CoA to their corresponding 3-hydroxyacyl-CoA monomers, i.e. 3-HV-CoA and 3-HB-CoA, and subsequent polymerization of them, we

introduced the *C. necator* PHA biosynthetic operon in the transcriptional order *phaC-phaA-phaB* in a plasmid pPhaCAB with a ColE1 replicon for its heterologous expression under the regulation of the *trc*-promoter. To generate the PHA-producing strains CPC-PHBV and CPC-PHB, the two plasmids pK-BktB and pPhaCAB were co-transformed into the propanogenic strain CPC-Sbm and its non-propanogenic parental strain BW- Δ ldhA, respectively.

To demonstrate PHA production from an unrelated carbon source, CPC-PHB and CPC-PHBV were cultivated in a bioreactor under microaerobic conditions with 30 g/L glycerol as the sole carbon source (**Figure 6.2A-B**, **Appendix – B S1A-1B** and **Appendix – B Table S1**). For CPC-PHBV, the total PHA content accounted for 65% dry cell weight (DCW) with 4.7 mol% of the total PHA being 3HV. On the other hand, for the control strain CPC-PHB, the total PHA content accounted for only 57% DCW with no 3HV fraction. The results suggest competent production of P(3HB-*co*-3HV) for propanogenic CPC-PHBV, but not for non-propanogenic CPC-PHB. No PHA production was observed for the other control strains that do not harbor pPhaCAB (data not shown), indicating that the *C. necator* PHA biosynthetic operon was functionally expressed. The results also suggest that the presence of Sbm-derived propionyl-CoA can mediate P(3HB-*co*-3HV) biosynthesis from an unrelated carbon source. Upon comparing CPC-PHB and CPC-PHBV cultivations, activation of the Sbm operon ostensibly decreased both glycerol dissimilation rate and biomass yield, but with enhanced secretion of C2- and C3-fermentative metabolites.

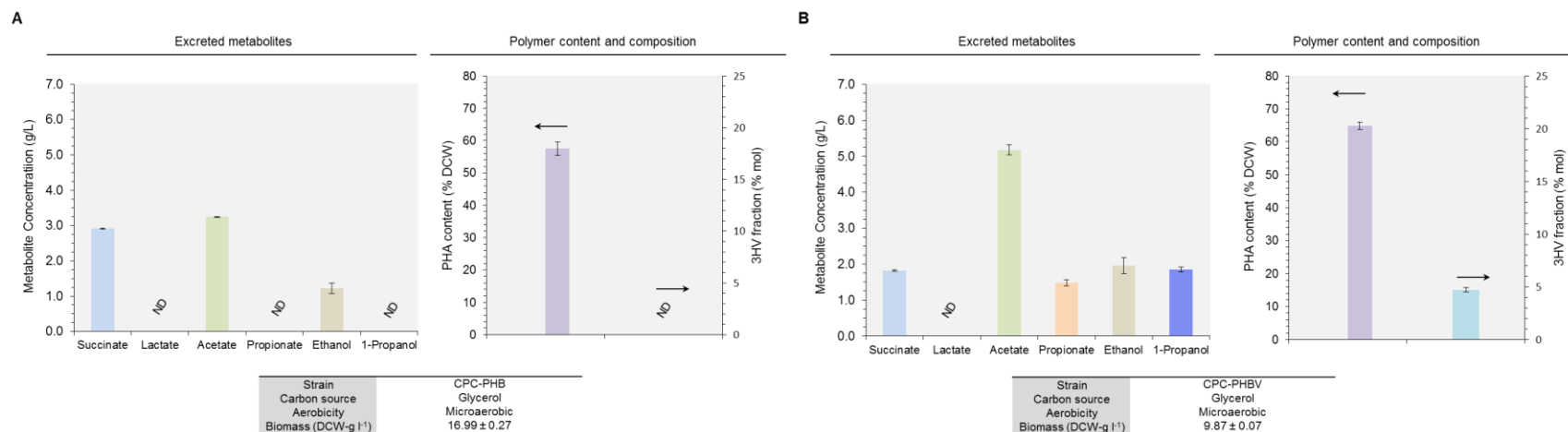


Figure 6.2.: Establishing the biosynthetic pathway for P(3HB) and P(3HB-co-3HV) copolymer formation in propanogenic/propionogenic *E. coli*.

Major metabolite titers, total PHA content (% DCW) and 3HV in total polymer (% mol) during microaerobic cultivations of strains (A) CPC-PHB and (B) CPC-PHBV using glycerol as the major carbon source. Culture performance (i.e. overall glycerol consumption and final biomass and metabolite concentrations) and time profiles are given in **Table S1** and **Appendix – B Figure S1**.

6.3.2 Cultivation conditions for P(3HB-*co*-3HV) biosynthesis

With the established pathway for direct biosynthesis of P(3HB-*co*-3HV) in CPC-PHBV, the effects of bioreactor conditions (i.e. carbon source and aerobicity) on culture performance and copolymer formation were investigated (**Figure 6.3A–D**, **Appendix – B S2A–2D** and **Appendix – B Table S1**). While the carbon dissimilation rate for glucose culture was much faster than that for glycerol microaerobic culture (i.e. taking ~54 h and ~21 h to consume 30 g/L glycerol and glucose, respectively), the biomass yield was reduced by 24% and the PHA yield was reduced by 10% (i.e. 5.8 g/L for glucose culture vs. 6.4 g/L for glycerol culture). Most importantly, the 3HV fraction of the produced PHA was also reduced (i.e. 3.2 mol% for glucose culture vs. 4.7 mol% for glycerol culture). While the titers of the C2-fermentative metabolites (i.e. ethanol and acetate) for the two cultures remained similar, more C3-fermentative metabolites (i.e. 1-propanol and propionate) were produced for glycerol culture. Also, note that, though CPC-PHBV has a Δ *ldhA* genetic background, an unusually high lactate spill was observed for glucose culture. These results corroborate with our previous observations that glycerol, with a higher reductance, appears to be a more effective carbon source than glucose to drive more carbon flux towards the C3-fermentative pathways when the *Sbm* operon is activated (199, 225).

On the other hand, introducing more oxygenic semiaerobic conditions into the culture significantly increased glycerol dissimilation rate (i.e. taking ~21 h and ~54 h to consume 30 g/L glycerol for semiaerobic and microaerobic cultivations, respectively) and enhanced cultivation performance. With a slightly higher PHA yield (i.e. 6.8 g/L for semiaerobic culture vs. 6.4 g/L for microaerobic culture), semiaerobic cultivation also dramatically increased the 3HV fraction of the produced PHA (i.e. 7.2 mol% for semiaerobic culture vs. 4.7 mol% for microaerobic culture). Note that semiaerobic cultivation resulted in a higher level of acidogenesis with the sum of the titers of acetate and propionate accounting for up to 40% of dissimilated glycerol. Nevertheless, such operational change increased the C3/C2 fermentative metabolite ratio (i.e. 0.31 for semiaerobic culture vs. 0.11 for microaerobic culture), implying that the *Sbm* operon remained active under semiaerobic conditions. Further increasing the air-purging rate at 1 vvm into the bulk culture (i.e. aerobic cultivation conditions), however, impaired P(3HB-*co*-3HV) production with most dissimilated glycerol being directed toward biomass formation (**Figure 6.3C**). Based on these characterization results, it appears that semiaerobic cultivation using glycerol as the major carbon source is most suitable for P(3HB-*co*-3HV) production and, therefore, all subsequent cultivations were conducted under this culture condition

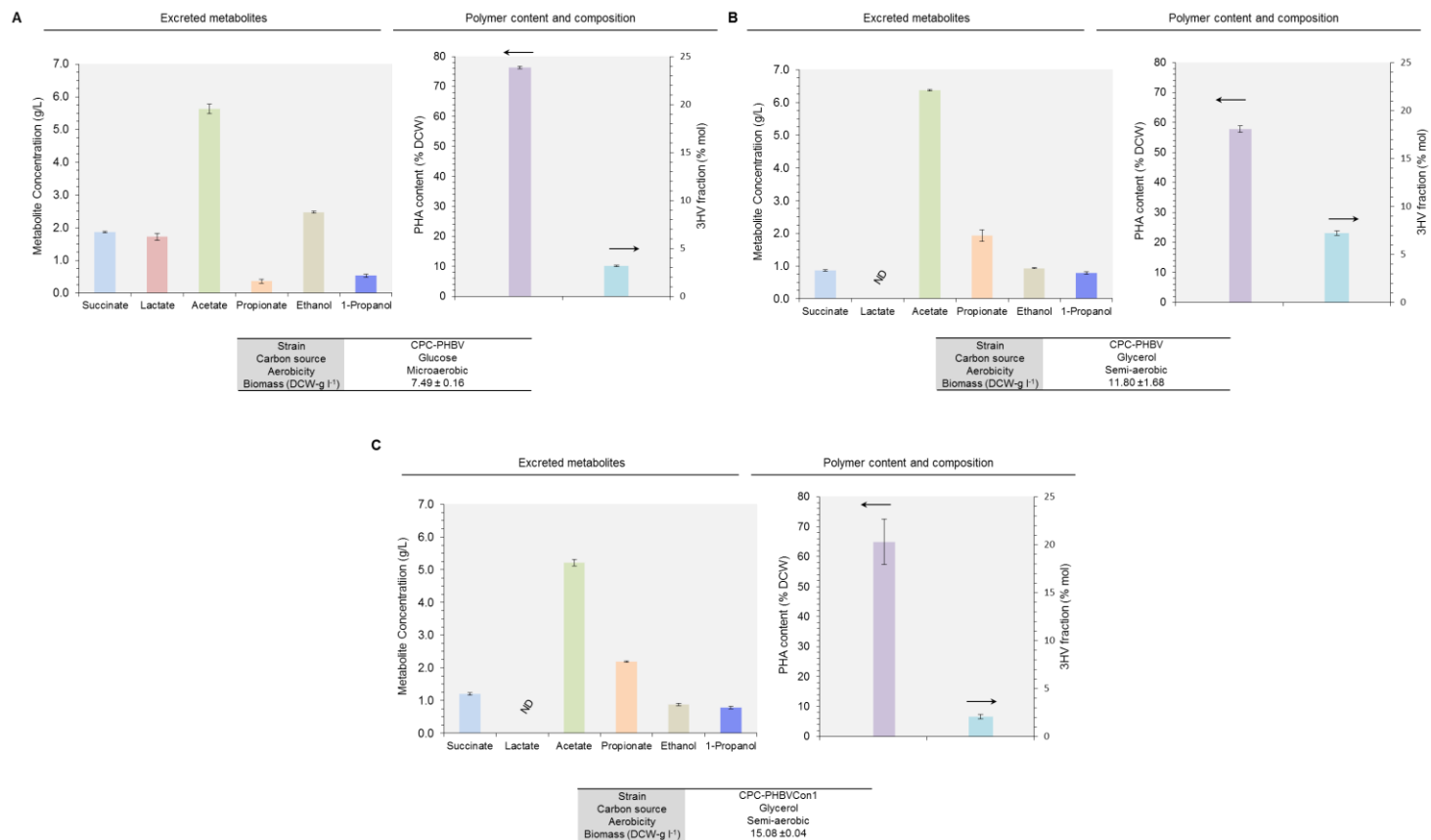


Figure 6.3.: Cultivation conditions for enhancing 3HV incorporation in the copolymer.

Major metabolite titers, total PHA content (% DCW) and 3HV in total polymer (% mol) during (A) microaerobic cultivation of CPC-PHBV using glucose as the major carbon source or (B) semiaerobic cultivation of CPC-PHBV using glycerol as the major carbon source. (C) Major metabolite titers, total PHA content (% DCW) and 3HV in total polymer (% mol) during aerobic cultivation of CPC-PHBV using glycerol as the major carbon source. (D) Major metabolite titers, total PHA content (% DCW) and 3HV in total polymer (% mol) during semiaerobic cultivation of CPC-PHBVCon1 using glycerol as the major carbon source. Culture performance (i.e. overall glycerol or glucose consumption and final biomass and metabolite concentrations) and time profiles are given in **Table S1** and **Appendix – B Figure S2**.

Note that BktB has been previously shown to have a higher substrate specificity toward C5 thioesters, compared to PhaA which is a short-chain-specific thiolase (200, 240). Eliminating expression of *bktb* in strain CPC-PHBVCon1 drastically reduced the 3HV monomer fraction in copolymer, compared with that obtained in the control strain CPC-PHBV (i.e. 2.0 mol% and 7.2 mol% for CPC-PHBVCon1 and CPC-PHBV, respectively) under semiaerobic conditions. Thus, simultaneous expression of the two biosynthetic thiolases of PhaA and BktB was considered synergistically ideal for P(3HB-*co*-3HV) production.

6.3.3 Metabolic engineering of fermentative pathways to enhance P(3HB-*co*-3HV) biosynthesis

While culture performance in P(3HB-*co*-3HV) production was markedly improved for CPC-PHBV under semiaerobic conditions, high-level acidogenesis was observed with an excessive accumulation of acetate and propionate in the culture medium. Such acidogenesis can potentially exacerbate carbon spill and reduce P(3HB-*co*-3HV) yield. Accordingly, we blocked acidogenesis by inactivating the phosphotransacetylase (Pta)-acetate kinase (AckA) pathway in CPC-PHBV and culture performance of the resultant mutant CPC-PHBV Δ pta was evaluated (**Figures 6.4B, Appendix – B S3B and Appendix – B Table S1**). While the overall glycerol dissimilation rate for CPC-PHBV Δ pta was slightly slower than that for CPC-PHBV (i.e. taking ~29 h and ~21 h to consume 30 g/L glycerol for CPC-PHBV Δ pta and CPC-PHBV, respectively), the level of acidogenesis was significantly reduced with an abolished succinate production. In addition, the biomass yield for CPC-PHBV Δ pta was 48% higher than that for CPC-PHBV with a concomitant increase in total PHA content (i.e. 66% DCW and 57% DCW for CPC-PHBV Δ pta and CPC-PHBV, respectively). Most importantly, the 3HV fraction of the produced PHA was increased (i.e. 8.5 mol% and 7.2 mol% for CPC-PHBV Δ pta and CPC-PHBV, respectively). These results suggest that blocking acidogenesis can potentially lead to more effective production of P(3HB-*co*-3HV).

While the level of solventogenesis was not high for CPC-PHBV, the carbon spill associated with alcohol formation can potentially limit P(3HB-*co*-3HV) biosynthesis. Therefore, we blocked solventogenesis in CPC-PHBV by inactivating the *adhE* gene encoding the fermentative bifunctional acetaldehyde/alcohol dehydrogenase and culture performance of the resulting mutant CPC-PHBV Δ adhE was evaluated (**Figures 6.4C, Appendix – B S3C, and Appendix – B Table S1**). Compared to the control strain CPC-PHBV, the overall glycerol dissimilation rate for CPC-PHBV Δ adhE was slower (i.e. taking ~33 h and ~21 h to consume 30 g/L glycerol for CPC-PHBV Δ adhE and CPC-PHBV, respectively), whereas the

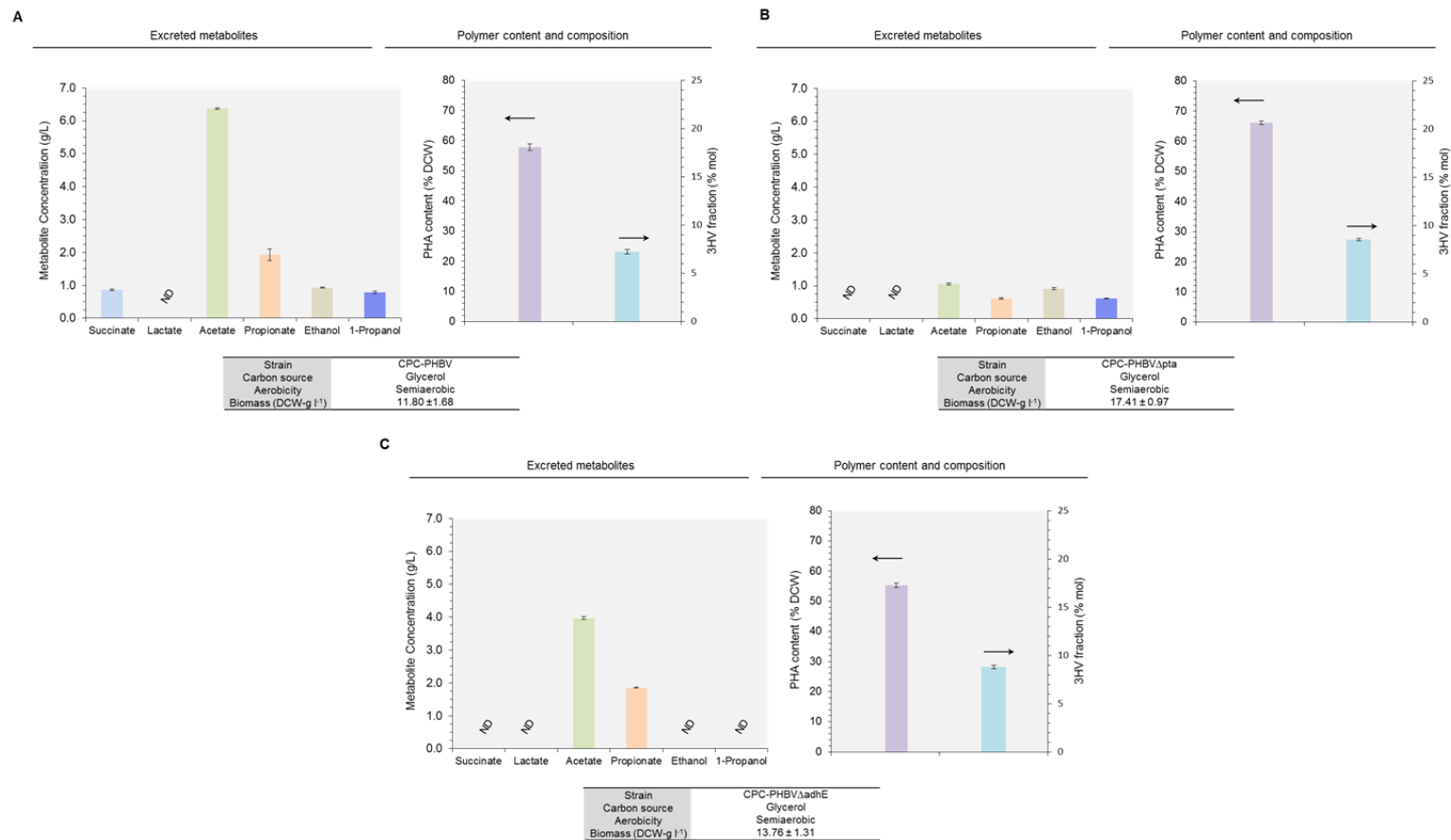


Figure 6.4.: Metabolic engineering strategies enhance copolymer formation.

Major metabolite titers, total PHA content (% DCW) and 3HV in total polymer (% mol) during semiaerobic cultivations of (A) CPC-PHBV, (B) CPC-PHBVΔadhE and (C) CPC-PHBVΔpta using glycerol as the major carbon source. Culture performance (i.e. overall glycerol consumption and final biomass and metabolite concentrations) and time profiles are given in **Table S1** and **Appendix – B Figure S3**.

biomass yield was 17% higher. The higher biomass yield resulted in a higher PHA yield (i.e. 7.7 g/L and 6.8 g/L for CPC-PHBV Δ adhE and CPC-PHBV, respectively). Most importantly, the 3HV fraction of the produced PHA was increased (i.e. 8.8 mol% and 7.2 mol% for CPC-PHBV Δ adhE and CPC-PHBV, respectively). These results suggest that blocking solventogenesis can lead to more effective production of P(3HB-*co*-3HV) though the carbon spill as secretion of acetate and propionate accounted for 28% of dissimilated glycerol.

6.3.4 Manipulation of glycerol dissimilation to enhance P(3HB-*co*-3HV) biosynthesis

In *E. coli*, glycerol is dissimilated via two routes to form the glycolytic intermediate dihydroxyacetone phosphate (DHAP), i.e. (i) the GldA-DhaK route under fermentative conditions and (ii) the GlpK-GlpD/GlpABC route under respiratory conditions (206) (**Figure 6.1**). Manipulation of various genes involved in the respiratory and fermentative pathways for glycerol dissimilation appears to be an effective method to drive more carbon flux toward the propionyl-CoA node (225). Among these trials, inactivation of either the fermentative dihydroxyacetone kinase (Δ *dhaK*) or respiratory glycerol-3-phosphate dehydrogenase (Δ *gldA*) pathway almost abolished solventogenesis with more carbon flux being shifted toward the C3-fermentative pathway. Accordingly, for better understanding of the effects of glycerol dissimilation on P(3HB-*co*-3HV) biosynthesis, we further engineered CPC-PHBV by inactivating either of the two pathways, resulting in the derivation of two mutant strains, i.e. CPC-PHBV Δ dhaK and CPC-PHBV Δ glpD containing a single deletion in *dhaK* and *glpD*, respectively, and their culture performance was evaluated (**Figures 6.5B–C, Appendix – B S4B–3C and Appendix – B Table S1**).

Compared to the control strain CPC-PHBV, inactivation of the fermentative GldA-DhaK route slightly reduced glycerol dissimilation rate (i.e. taking 27 h and 21 h to consume 30 g/L glycerol for CPC-PHBV Δ dhaK and CPC-PHBV, respectively) with a slight increase in both biomass yield (i.e. 66% DCW and 57% DCW for CPC-PHBV Δ dhaK and CPC-PHBV, respectively) and total PHA content (i.e. 8.4 g/L and 6.8 g/L for CPC-PHBV Δ dhaK and CPC-PHBV, respectively). While the inactivation minimally affected metabolite profiling, the 3HV fraction of the produced PHA was significantly increased by 36% (i.e. 9.8 mol% and 7.2 mol% for CPC-PHBV Δ pta and CPC-PHBV, respectively).

On the other hand, compared to the control strain CPC-PHBV, though inactivation of the aerobic GlpK-GlpD/GlpABC route significantly hampered glycerol dissimilation (i.e. taking 41 h and 21 h to consume 30 g/L glycerol for CPC-PHBV Δ glpD and CPC-PHBV, respectively), the biomass yield was significantly increased by 58%. The gene inactivation potentially reduced carbon spill by completely blocking solventogenesis and significantly reducing acidogenesis. As a result, the total amount of PHA

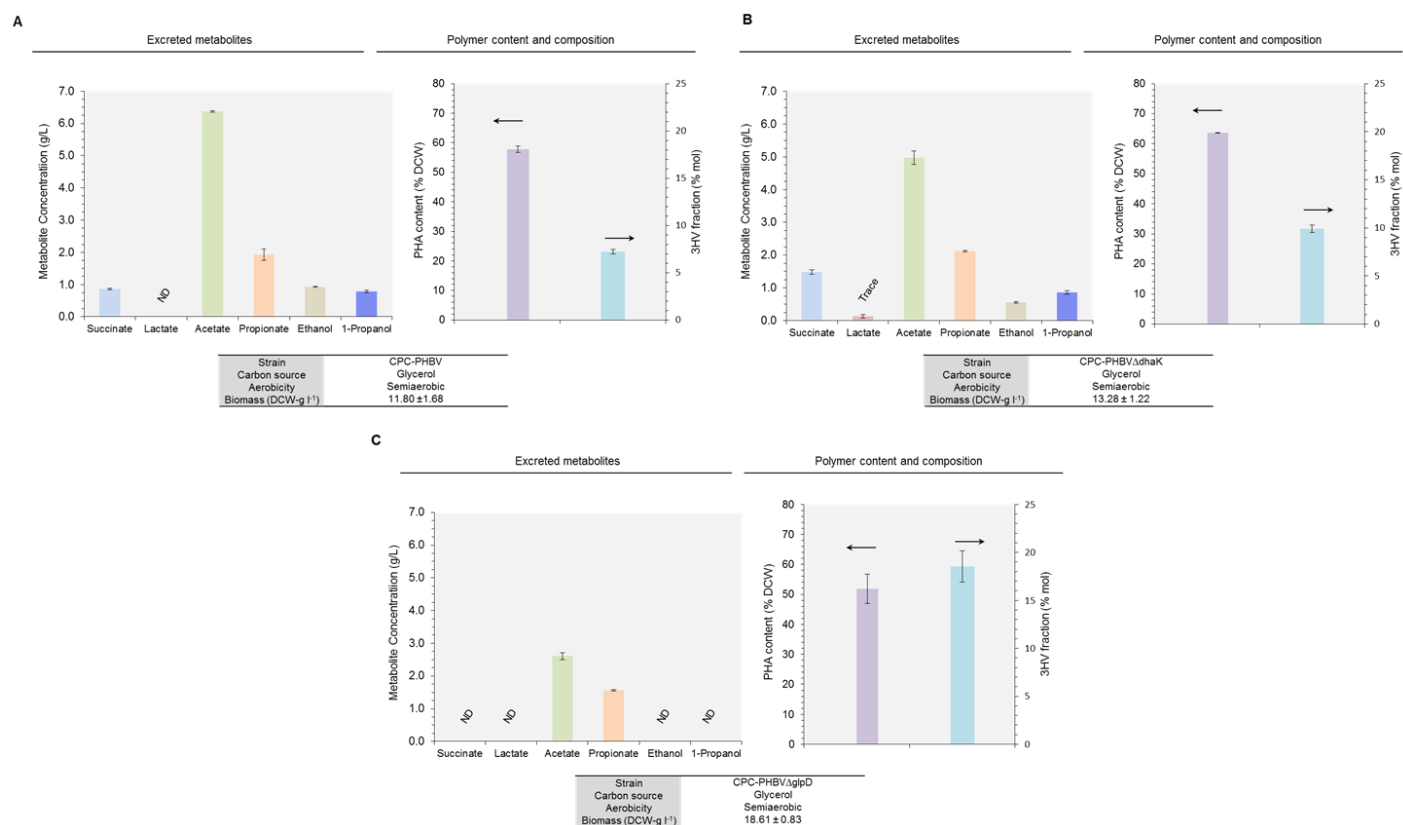


Figure 6.5.: Linking glycerol metabolism to P(3HB-co-3HV) biosynthesis in propanogenic/proprionogenic *E. coli*.

Major metabolite titers, total PHA content (% DCW) and 3HV in total polymer (% mol) during semiaerobic cultivations of (A) CPC-PHBV, (B) CPC-PHBVΔdhaK and (C) CPC-PHBVΔglpD using glycerol as the major carbon source. Culture performance (i.e. overall glycerol consumption and final biomass and metabolite concentrations) and time profiles are given in **Table S1** and **Appendix – B Figure S4**.

production was significantly increased (i.e. 9.6 g/L and 6.8 g/L for CPC-PHBV Δ glpD and CPC-PHBV, respectively). Most importantly, the 3HV fraction reached to an extremely high level of 18.5 mol%, which, to the best of our knowledge, represents the highest reported level for *E. coli*-based P(3HB-*co*-3HV) biosynthesis using an unrelated carbon source.

6.4 Discussion

Biological synthesis is an attractive option as a renewable method for producing value-added chemicals that is in part limited by the availability of natural pathways for molecules of interest. Expanding the chemical diversity of whole-cell biocatalysts thus requires the *de novo* construction of novel biosynthetic routes. For instance, implementing carbon-carbon bond forming chemistry via chain elongation pathways in tractable hosts such as *E. coli* provides a unique way to extend the boundaries of metabolic engineering for the biosynthesis of a myriad of structurally diverse and industrially important chemicals such as unnatural advanced alcohols, methyl ketones and polyesters (208, 212, 213). Herein, we further engineered our previously developed propanogenic/propionogenic *E. coli* by episomally expressing a set of promiscuous β -ketothiolases (i.e. PhaA and BktB) from *C. necator* for CoA-dependent Claisen condensation of either two acetyl-CoA moieties or acetyl-CoA and Sbm-derived propionyl-CoA. The resulting C4 and C5 biogenic thioesters (i.e. acetoacetyl-CoA and 3-ketovaleryl-CoA, respectively) were then channeled via the *C. necator* PHA synthesis pathway (i.e. PhaB and PhaC) for subsequent reduction and polymerization. Note that β -ketothiolases PhaA and BktB can synergistically enhance molecular fusion for CoA-dependent chain elongation and therefore, the strains' polymer-producing capacity. These metabolic and genetic strategies led to the development of several propanogenic/propionogenic *E. coli* capable of high-level direct biosynthesis of P(3HB-*co*-3HV) from unrelated carbon sources glucose and glycerol. P(3HB-*co*-3HV) is far more ductile, flexible, and tougher than its homopolymer counterpart P(3HB) and thus considered an attractive substitute to petrochemical-based polymers and plastics (241, 242).

There has been considerable work towards synthesizing P(3HB-*co*-3HV) from unrelated carbon sources in natural and recombinant microbes (13, 226, 241, 243, 244) and even planta (245-247). However, most of these metabolic approaches rely on the extended dissimilation of either intracellular intermediate citramalate or the α -amino acid L-threonine to generate the required propionyl-CoA pool (i.e. the so-called canonical 2-keto-acid biosynthesis pathways). While the 2-keto-acid-based pathways have been extensively utilized for high-level production of several important commodity chemicals, such as biofuels (134, 248) and organic acids (249, 250), their application for direct P(3HB-*co*-3HV) synthesis is

limited as the 3HV fractions obtained from these strategies are far below levels deemed sufficient for industrial adoption. For the production of higher chain compounds, accumulation of key biogenic precursors of acetyl-CoA and propionyl-CoA is critical to overcome the large thermodynamic barrier of the condensation reactions catalyzed by the β -ketothiolases (i.e. PhaA and BktB) (209). Based on evidence presented here, the Sbm pathway seems far more conducive in accumulating propionyl-CoA as relatively high levels of 3HV monomer fractions were produced with either glucose or glycerol as sole carbon sources. This may in part be explained by the fact that the Sbm pathway serves as a direct route toward propionyl-CoA from the glycolytic intermediate PEP, making it potentially more efficient than the 2-keto-acid-based pathways. The Sbm pathway is also devoid of amino acid biosynthetic intermediates and therefore not subjected to complex feedback regulations and extensive crosstalk between different metabolic pathway pathways. Perturbing amino acid metabolism by rerouting intracellular flux via amino acid intermediates toward propionyl-CoA can also result in growth retardation and low protein production (226, 251).

Although economic production of P(3HB-*co*-3HV) becomes feasible as exogenous supplementation of expensive related carbon sources (i.e. propionate or valerate) is no longer required, the physicochemical and mechanical properties of P(3HB-*co*-3HV) are highly contingent on the 3HV monomer fraction in the copolymer (13, 252). Therefore, it is often crucial to control the copolymer composition to produce P(3HB-*co*-3HV) suitable for a wide spectrum of applications. In most examples, producing P(3HB-*co*-3HV) with different compositions in engineered *E. coli* have used the same strategy as that used with *C. necator*; that is, varying the propionate or valerate concentration in the feed to modulate the 3HV fraction. While copolymer composition can easily be fine-tuned by adjusting the ratio of these related carbon sources (253), this is often difficult when P(3HB-*co*-3HV) is made from a single unrelated carbon source (e.g. glucose or glycerol). Previously, Keasling and colleagues described a “dial-a-composition” system whereby copolymer composition was altered and to some extent controlled at a fixed carbon concentration by varying the level of induction of critical pathway genes in polymer-accumulating recombinant *Salmonella* (13, 254). A notable finding of this work was the observation that a similar dial-a-composition strategy is possible with propanogenic/propionogenic CPC-PHBV cultures. For instance, by varying the aeration regime of the batch fermentation (i.e. microaerobic, semiaerobic or aerobic cultivation conditions) at fixed glucose or glycerol concentrations, copolymers with 3HV fractions ranging from ~3 mol% to ~7.5 mol% can be obtained. Moreover, in mutant host strains CPC-PHBV Δ adhE, CPC-PHBV Δ pta, CPC-PHBV Δ glpD, the platform P(3HB-*co*-3HV) pathway developed

herein also has the flexibility to produce copolymers with even higher 3HV fractions ranging from ~8 mol% to ~19 mol% under semiaerobic cultivation conditions using glycerol as the sole carbon source.

The 3HV incorporation is highly dependent on the oxygenic level of the culture since various intracellular reactions associated with P(3HB-*co*-3HV) biosynthesis have different preferences in aerobicity. For example, while polymerization is growth-associated and therefore can be favored by aerobiosis, the derivation of reduced propionyl-CoA precursor for 3HV production requires more anaerobic growth conditions (255-258). Nevertheless, anaerobic conditions tend to exacerbate carbon spill as fermentative metabolites, negatively affecting P(3HB-*co*-3HV) biosynthesis. Also, activation of the *Sbm* operon introduces an intracellular competition in carbon flux between the C2-fermentative pathway (with acetyl-CoA as a local hub) and the C3-fermentative one (with propionyl-CoA as a local hub). With glycerol as the major carbon source, it was shown that its dissimilation can be critical for such flux competition (225). Although glycerol is a favorable carbon source supporting biosynthesis via the activated *Sbm* pathway (225), it is considered as a recalcitrant feedstock for *E. coli* cultivation, particularly under limited oxygenic conditions (199). Accordingly, to take advantage of the high degree of reduction of glycerol, we used well-defined microaerobic and semiaerobic conditions, in which oxygen acts as a terminal electron acceptor, to convert glycerol into P(3HB-*co*-3HV) while preserving cell growth and minimizing formation of fermentative end-products. Our results suggest that incorporation of 3HV monomer fraction into the copolymer was optimal under semiaerobic conditions.

Further enhancement of 3HV monomer fraction in the copolymer was achieved by metabolic inactivation of host pathways that may potentially compete with copolymer-formation for acetyl-CoA, propionyl-CoA and NADH. Knocking out the *adhE* gene encoding alcohol dehydrogenase in strain CPC-PHBV Δ *adhE* completely abolished alcohol formation but only slightly improved 3HV formation with minimal increase in biomass and total polymer production. On the hand, inactivating the phosphotransacetylase (Pta)-acetate kinase (AckA) pathway in CPC-PHBV Δ *pta* significantly reduced acidogenesis and alcohologenesis and increased 3HV formation and total biomass formation by 1.2-fold and 1.5-fold, respectively. However, the glycerol dissimilation rate for the *pta* mutant was slightly slower than that for CPC-PHBV. Although the reason is not clear, this observation appears to be due to decreased carbon flux towards acetyl phosphate, an intermediate in the Pta-AckA pathway that serves as an important regulator in *E. coli* affecting global gene expression and metabolism (211). Excreted acetate and propionate serve as carbon sources for precursors for acetyl-CoA and propionyl-CoA, and therefore can also be converted via parallel assimilating pathways into the cell to minimize carbon loss and redox

imbalance. In most examples of pathway design for recycling of acetyl-CoA, acetate consumption is enhanced either by episomally expressing the ATP-dependent Acs (acetyl-CoA synthetase) pathway (259) or the ATP-independent AldB–MhpF (two acetaldehyde dehydrogenases) pathway (260). Note *E. coli* also possess several genes involved in propionyl-CoA degradation such as *prpC* encoding 2-methylcitrate synthase and the Sbm-operon gene *ygfH* encoding propionyl-CoA:succinate CoA transferase (226, 261, 262). However, attempts to further engineer host metabolism by inactivation of either *prpC* or *ygfH* genes have generally resulted in markedly slower growth rates accompanied by an overall decrease in PHA content (226).

Our results suggest while both GldA-DhaK and GlpK-GlpD/GlpABC pathways were active under respiro-fermentative culture conditions to enhance glycerol dissimilation, the physiological scenario was not optimal for biomass formation and P(3HB-*co*-3HV) biosynthesis. Note during aerobic glycerol metabolism, quinones serve as electron acceptors, whereas in the absence of oxygen, glycerol is oxidized into dihydroxyacetone using NAD⁺ as the electron acceptor (**Figure 6.1**) (219). It was previously established that for production of reduced metabolites, the cell preferentially utilizes the GldA-DhaK fermentative route as higher energy NADH is generated when glycerol is consumed via GldA rather than through the reduced quinone GlpD/GlpABC route (263, 264). Indeed, metabolic manipulation to direct initial glycerol dissimilation through the respiratory GldA-DhaK pathway significantly enhanced both biomass formation and incorporation of 3HV monomer fraction into the copolymer. These results are also especially encouraging as inactivating *glpD* concomitantly reduced acidogenesis and completely abolished alcohologenesis. The exact metabolic mechanism involved in the increased biomass and decreased acido- and alcohologenic flux is not clear, and contrasts that of an earlier observation in which disruption of the genes *glpK* or *glpD* prevented cell growth under respiro-fermentative conditions (206). Nevertheless, these results highlight the importance not only of this gene manipulation strategy but also the respiratory pathway of glycerol metabolism for enhancing 3HV formation. Alternatively, channeling initial glycerol metabolism through the aerobic GlpK-GlpD/GlpABC arm moderately increases 3HV monomer fraction in P(3HB-*co*-3HV), although the fermentation still appears to lean toward acidogenesis. Nonetheless, CPC- CPC-PHBV Δ dhaK indeed produced higher levels of C3 metabolites (i.e. propionate and 1-propanol) compared to that of CPC-PHBV. The GldA-DhaK pathway requires phosphoenolpyruvate (PEP) as a cofactor and therefore serves as an important mediator in the interconversion of PEP and pyruvate (206, 219). Eliminating such need for PEP in CPC-PHBV Δ dhaK increases the intracellular PEP pool, potentially diverting more flux toward propionyl-CoA by way of oxaloacetate (OAA) via the reductive TCA arm. Accordingly, an effective way to fully harness the GlpK-

GlpD/GlpABC route and generate higher levels of propionyl-CoA can be to overexpress phosphoenolpyruvate carboxylase (encoded by *ppc*) to create an efficient glycolytic node for the conversion of PEP to OAA (265, 266).

Chapter 7

Original contributions and recommendations

7.1 Original contributions

7.1.1 Activation of the Sbm operon for the production of 1-propanol

The endogenous Sbm operon genes were episomally activated in engineered *E. coli* to demonstrate *in vivo* production of 1-propanol. In addition to the Sbm operon genes, the triple-plasmid expression system also consisted of the genes encoding bifunctional aldehyde/alcohol dehydrogenases (ADHs) from several microbial sources, and the native *sucCD* gene encoding succinyl-CoA synthetase. In this initial study, other parameters (e.g. effect of cyanocobalamin concentration on 1-propanol production and optimal cell-density for shaker-based 1-propanol production) were also investigated. In summary, we demonstrated that the Sbm pathway in engineered *E. coli* is indeed functional and can be used as a novel route towards propionyl-CoA biosynthesis. Using these engineered *E. coli* strains under anaerobic conditions, production titers up to 150 mg/L of 1-propanol were obtained in lab-scale shake-flask growths.

7.1.2 Identification of glycerol as an efficient carbon source for the production of 1-propanol and the development of a plasmid-free propanogenic *E. coli* strain

From our initial report in Chapter 3, we further enhanced 1-propanol production via various biochemical, genetic and metabolic engineering strategies. Most importantly, 1-propanol production was significantly enhanced in a bioreactor under anaerobic conditions by using glycerol as a carbon source using a single-plasmid system solely expressing the Sbm operon genes. Also, plasmid-induced metabolic burden was alleviated in the engineered strain by activating the Sbm operon on the genome. This plasmid-free propanogenic *E. coli* strain showed high levels of solventogenesis accounting for up to 85 % of dissimilated carbon. Anaerobic fed-batch cultivation of CPC-PrOH₃ with glycerol as the major carbon source produced high titers of nearly 7 g/L 1-propanol. This host strain was the basis of our work for the development of other engineered *E. coli* strains capable of producing high-level propionate (225), butanone, and P(3HB-co-3HV).

7.1.3 Extending the Sbm pathway in engineered *E. coli* for the production of butanone

In this portion of our study we further extended the utility of our developed propanogenic *E. coli* strain for co-production of acetone and butanone. For microbial production of butanone, the following synthetic biology strategies were applied: First, a set of novel microbial β -ketothiolases were expressed for intracellular fusion of propionyl-CoA and acetyl-CoA to form 3-ketovaleryl-CoA. The nascent 3-ketovaleryl-CoA was then channeled via the canonical clostridia acetone-formation pathway for subsequent thioester hydrolysis and decarboxylation. It was also identified that channeling glycerol metabolism via GlpK-GlpD/GlpABC glycerol dissimilation pathway greatly enhanced ketogenesis while minimizing by-product formation (i.e. acidogenesis/alcohologenesis). Using the GlpK-GlpD/GlpABC glycerol dissimilation pathway, we demonstrated that up to 42% of spent carbon source of glycerol can be utilized toward ketone biosynthesis.

7.1.4 Extending the Sbm pathway in engineered *E. coli* for direct biosynthesis of poly(3-hydroxybutyrate-co-3-hydroxyvalerate)

In the last major chapter of this thesis, we demonstrated the direct biosynthesis of poly(3-hydroxybutyrate-co-3-hydroxyvalerate) from non-related carbon sources glycerol and glucose. For P(3HB-co-3HV) biosynthesis, we first generated C4 and C5 precursors 3-hydroxybutyryl-CoA and 3-ketovaleryl-CoA using the CoA thioester-dependent chain elongation system was previously employed in chapter 5 (i.e. by functionally expressing a set of β -ketothiolases from *C. necator*). Next, the resulting C4 and C5 intermediates were channeled into the *C. necator* PHA biosynthetic pathway (i.e. PhaB and PhaC) for thioester reduction and polymerization. Using various aeration regimes and host-gene deletions, copolymer with 3HV fractions ranging from ~3 mol% to ~19 mol% can be obtained using glycerol as the sole carbon source. In contrast to butanone production, metabolic manipulation to direct glycerol metabolism via the GldA-DhaK pathway significantly enhanced both biomass formation and incorporation of 3HV monomer fraction into the copolymer.

7.2 Recommendations and future prospects

As documented in this thesis, modulating propionyl-CoA metabolism in *E. coli* has opened an avenue for novel biomanufacturing, including odd-chain alcohols and organic acids, ketones and PHA-based copolymers. Future research efforts should focus on identification and integration of metabolic pathways not only for propionyl-CoA biogenesis but also subsequent novel biosynthesis of other products of industrial relevance (**Figure 7.1**). Because propionyl-CoA is a key precursor to all these products, the

engineered *E. coli* strain with its genomic *Sbm* operon being activated (199, 225) can be effective for such production purposes.

It has been shown that the alcohol *O*-acyltransferase (ATF) class of enzymes can be used for heterologous fusion of acyl-CoA and alcohols to form low-molecular-weight volatile esters (267, 268). Volatile esters are currently produced through traditional chemical-based acid-catalyzed esterification of organic acids and alcohols for their extensive use as flavor and fragrance products in the food, beverage, and cosmetics industries (269). Nevertheless, the presence of different acyl-CoA and alcohol formation pathways enables biosynthesis of a wide variety of short- and long-chain esters using whole-cell biocatalysts. Similar to acetyl-CoA as the starter molecular for microbial production of small volatile esters (260), propionyl-CoA and its biogenic C5 counterpart valeryl-CoA can be potentially used to generate propionate and valerate esters (**Figure 7.1A**). Likewise, C2-C4 alk(a/e)nes (**Figure 7.1B**) and advanced ketones (**Figure 7.1C**) can be potentially derived with propionyl-CoA or its biogenic C5/C7 counterparts as precursors. Short-chain alk(a/e)nes are attractive hydrocarbon fuels due to facile phase separation, which not only enables effective recovery of fuels from the bulk culture but also minimizes product toxicity and inhibition on producing cells (270). Several cyanobacteria of the genera *Synechococcus* and *Synechocystis* can convert CoA-derived aldehydes into long- and short-chain (C1-C17) alk(a/e)nes via endogenous aldehyde decarboxylases (271, 272). While the biological role of alk(a/e)ne production and the catalytic mechanism of the cryptic aldehyde decarboxylases in these cyanobacteria remain largely unknown, the production of gaseous olefins appears to result from cleavage of non-cognate substrates (273). Such a method for alkane production was recently adopted for biosynthesis of propane from acetyl-CoA-derived butyraldehyde in engineered *E. coli* (274). Presumably, the same chemistry can be extended to larger CoA thioesters, such as propionyl-CoA and valeryl-CoA for the production of eth(a/e)ne and but(a/e)ne, respectively (**Figure 7.1B**). As mentioned in chapter 5, the production of advanced aliphatic commodity ketones in engineered microbial systems has gained significant attention recently (197, 275, 276).

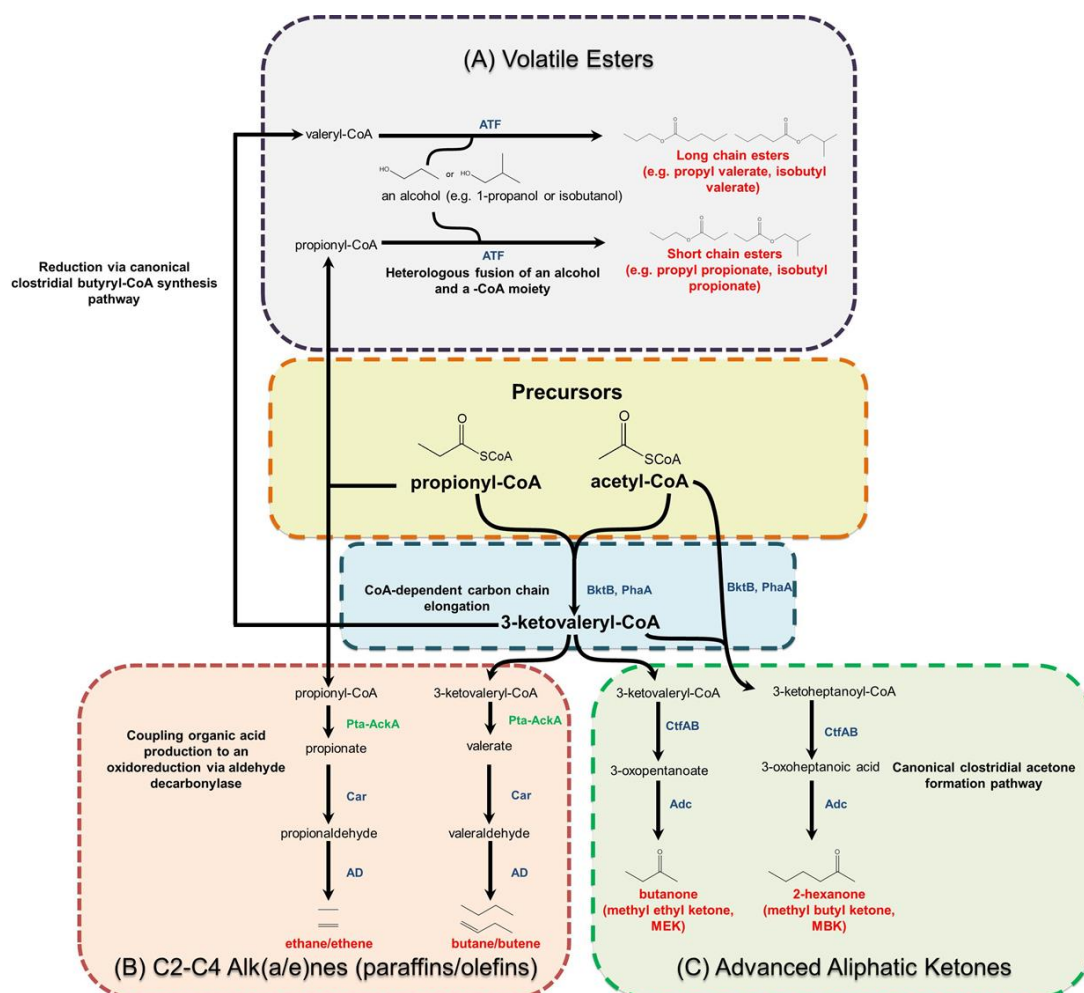


Figure 7.1: Putative metabolic pathways for the production of small chain volatile esters, C2-C4 alk(a/e)nes, and advanced ketones using propionyl-CoA as a key precursor.

(A) Propionyl-CoA or its five-carbon biogenic counterpart, valeryl-CoA can be fused with a linear or branched alcohol (e.g. 1-propanol or isobutanol) via ATF, an alcohol-O-acetyl transferase from *Saccharomyces cerevisiae* for the production of various volatile esters. (B) Similarly, using the acid-formation pathway (i.e. Pta-AckA, phosphotransacetylase-acetate kinase) of *E. coli*, propionyl-CoA or 3-ketovaleryl-CoA can also be converted into non-activated organic acids propionate or valerate, respectively. Next, through the action of a carboxylic acid reductase (CAR) from *Mycobacterium marinum* and a cryptic aldehyde reductase (AD) from *Synechocystis* sp, propionate and valerate can be reduced into their respective aldehydes and alk(a/n)es. (C) Lastly, propionyl-CoA derived C5 and C7 biogenic precursors 3-ketovaleryl-CoA and 3-ketoheptanoyl-CoA, respectively, can also be channeled into the canonical clostridial acetone-formation pathway (i.e. CtfAB-Adc, acetoacetyl-CoA: acetate/butyrate: CoA transferase and acetoacetate decarboxylase from *C. acetobutylicum*) for thioester hydrolysis and decarboxylation to form the advanced ketones. Heterologous enzymes are represented in blue, whereas native *E. coli* enzymes are represented in green.

Larger-chain ketones, such as butanone, are widely used as general solvents in the printing and textile industries and components of synthetic rubber (194). In the canonical clostridial-acetone pathway, the C4 thioester acetoacetyl-CoA (formed via the homo-fusion of two acetyl-CoA moieties) is converted to acetone via acetoacetyl-CoA:acetate/butyrate:CoA transferase (CtfAB) and acetoacetate decarboxylase (Adc) (201). *In vitro* studies suggest that CtfAB has a wide range of substrate specificities to various short- and long-chain CoA derivatives and organic acids (210). Accordingly, this pathway can be potentially applied not only for butanone production (as demonstrated in chapter 5) but also for other high-chain ketones such as 2-hexanone using long-chain CoA derived from propionyl-CoA (e.g. 3-ketoheptanoyl-CoA) as a substrate (**Figure 7.1C**).

On a final note, the implementation of auxiliary CoA-dependent chain elongation pathways for hetero-fusion of propionyl-CoA (or longer CoA moieties) and acetyl-CoA is critical in mediating the production of these longer-chain products. Despite the success presented in this thesis in implementing these recursive elongation pathways for butanone formation and P(3HB-*co*-3HV) biosynthesis, these applications have yet to be fully realized due to a major challenge of striking a flux balance between the C2 and C3 fermentative pathways with acetyl-CoA and propionyl-CoA as the major metabolic hubs. Other potential challenges include utilization of unrelated carbon sources, cofactor engineering, effective supply of metabolic energy for biosynthetic pathways, and identification of latent metabolic bottlenecks. For instance, targeted gene knockdown and/or knockout studies are still required to improve the productivity of products derived from propionyl-CoA whilst minimizing carbon flux toward the acetyl-CoA (i.e. the C2 metabolic node)-derived pathways (i.e. the ethanogenic and acetate-forming pathways).

Appendix A

Chapter 5 supplementary materials

Supplementary Table 1: Nucleotide sequence of the oligonucleotides used in Chapter 5

Supplementary Table 2: Growth and metabolic parameters of CPC-MEK and its control counterparts in a bioreactor under microaerobic or semi-aerobic cultivation conditions. The metabolite distribution (i.e. the fraction of dissimilated glycerol to form a metabolite) is defined as the ratio of the glycerol equivalent titer of the metabolite (calculated based on the stoichiometric mass ratio of metabolite/substrate, i.e.: 1.28 g succinate/ g glycerol, 0.65 g acetate/ g glycerol, 0.80 g propionate/ g glycerol, 0.32 g acetone/ g glycerol, 0.5 g ethanol/ g glycerol, 0.39 g butanone/ g glycerol, 0.65 g 1-propanol/ g glycerol) to the total consumed glycerol. The glycerol efficiency toward metabolite synthesis is calculated as the sum of all metabolite distributions. All of the strains were induced at the start of the batch cultivation with 0.1 mM IPTG (except the control cultivation of CPC-MEK presented in the final column). Error bars represent s.d. (n = 2).

Supplementary Table 3: Summary of cultivation of CPC-Sbm, CPC-Sbm Δ glpD, CPC-Sbm Δ dhaK, and various mutants of CPC-MEK in a bioreactor under microaerobic or semi-aerobic cultivation conditions. The metabolite distribution (i.e. the fraction of supplemented glycerol to form a metabolite) is defined as the ratio of the glycerol equivalent titer of the metabolite (calculated based on the stoichiometric mass ratio of metabolite/substrate, i.e.: 1.28 g succinate/ g glycerol, 0.65 g acetate/ g glycerol, 0.80 g propionate/ g glycerol, 0.32 g acetone/ g glycerol, 0.5 g ethanol/ g glycerol, 0.39 g butanone/ g glycerol, 0.65 g 1-propanol/ g glycerol) to the total consumed glycerol. The glycerol efficiency toward metabolite synthesis is calculated as the sum of all metabolite distributions. All of the strains were induced at the start of the batch cultivation with 0.1 mM IPTG. Error bars represent s.d. (n = 2).

Supplementary Table 1 Nucleotide sequence of the oligonucleotides

Primer name	Sequence (5' to 3')	Reference
v-ldhA	GATAACGGAGATCGGGAATGATTAA; GGTTTAAAAGCGTCGATGTCCAGTA	Srirangan et al. (173)
v-adhE	ATCAGGTGTCCTGAACTGTGCG; TTGACCAGCGCAAATAACCCGATGA	This study
v-pta	GGCATGAGCGTTGACGCAATCA; CAGCTGTACGCGGTGATACTCAGG	This study
v-dhaK	CATCGAGGATAAACAGCGCA; ATCTGATAAAGCTCTTCCAGTGT	This study
v-glpD	CGTCAATGCTATAGACCACATC; TATTATTGAAGTTTGTAAATATCCTTATCAC	This study
c-frt	AGATTGCAGCATTACACGTCTTGAG; CCAGCTGCATTAATGAATCGGGCCATGGTCCATATGAATATCCTCC	This study
c-ptrc	CCGATTCATTAATGCAGCTGG; GGTCTGTTTCCTGTGTGAAATTGTTA	This study
r-frt:ptrc	CTCGATTATGGTCACAAAGTCCTTCGTCAGGATTAAAGATTGCAGCATTACACGTCTTGA; GTTGGCAAGCTGTTGCCACTCCTGCACGTTAGACATGGTCTGTTTCCTGTGTGAAATTGT	This study
v-frt:ptrc	GCGCTCGACTATCTGTTTCGTCAGCTC; TCGACAGTTTTCTCCCGACGGCTCA	This study
c-phaA1	ACACAGGAAACAGCTATGACATGACTGACGTTGTCATCGTATCC; GAGCTCGAATTCGTAATCATTTATTTGCGCTCGACTGCCA	This study
c-bktb1	ACACAGGAAACAGCTATGACATGACGCGTGAAGTGGTAGTG GAGCTCGAATTCGTAATCATTCAGATACGCTCGAAGATGG	This study
c-pK184	GTCATAGCTGTTTCCTGTGTG; ATGATTACGAATTCGAGCTC	This study

c-phaA2	CATGATTAC <u>GAATTC</u> GATGACTGACGTTGTCATCGTATCCGCCGCC; TACCACTTCACGCGTCATGGTATATCTCCTTTATTTGCGCTCGACTGCCAGCGCC	This study
c-bktb2	AGGAGATATACCATGACGCGTGAAGTGGTAGTGGTGA; TACCGAGCTC <u>GAATTC</u> CAGATGCGTTCGAAGATAGCGGCAA	This study
c-ctf	CGCGTTGGTGCG <u>GATATC</u> GGTCGACTGTGGATGGAGTTAAGTC; TACCGAGCTC <u>GAATTC</u> CACACAGGAAACAGCTATGACCATG	This study
c-ctf-c3	GTTGGTGCG <u>GATATC</u> TTCGACTTTTTAAACAAAATATATTG; TACCGAGCTC <u>GAATTC</u> CCTAAACAGCCATGGGTCTAAG	This study
c-adc-c4A	GTTGGTGCG <u>GATATC</u> TATTGAATAAAAGATATGAGAGATTTATC; CCTTTAACATTTAATCCCTCCTTTTAAATTC	This study
c-adc-c4B	GGGATTAAATGTTAAAGGATGAAGTAATTA AAC ; TACCGAGCTC <u>GAATTC</u> TTACTTAAGATAATCATATATAACTTCAGC;	This study

Notation for primers: **v**- verification primer, **c**- cloning primer, and **r**- recombineering. Restriction recognition sequences are underlined and recombination homology arms for *in vivo* or *in vitro* recombination are in bold print

Supplementary Table 2 Summary of cultivation of CPC-MEK and its control counterparts

Strain	Aerobicity (Cultivation time ^a)	Glycerol ^b	Biomass ^c	Succinate ^d	Acetate ^d	Propionate ^d	Acetone ^d	Ethanol ^d	Butanone ^d	1-Propanol ^d
CPC-MEKCon1	Microaerobic (21)	29.66 ± 0.14 (68.9%)	3.40 -	1.27 ± 0.44 (3.4%)	6.50 ± 0.43 (34.2%)	3.50 ± 0.33 (14.9%)	0.33 ± 0.02 (3.4%)	1.08 ± 0.14 (7.3%)	0.02 ± 0.01 (0.2%)	1.07 ± 0.21 (5.6%)
CPC-MEKCon2	Microaerobic (69)	29.40 ± 1.23 (76.5%)	3.90 -	2.01 ± 0.05 (5.5%)	4.53 ± 0.27 (24.9%)	0.66 ± 0.37 (2.9%)	0.09 ± 0.01 (1.0%)	5.07 ± 0.13 (35.7%)	0.03 ± 0.01 (0.3%)	1.13 ± 0.09 (6.1%)
CPC-MEK	Microaerobic (45)	29.75 ± 1.11 (75.3%)	5.51 -	1.09 ± 0.02 2.9%	6.21 ± 0.04 (32.6%)	2.61 ± 0.02 (11.0%)	0.43 ± 0.03 (4.5%)	2.03 ± 0.04 (13.6%)	0.33 ± 0.03 (2.9%)	1.49 ± 0.05 (7.7%)
	Semi-aerobic (19)	29.98 ± 0.15 (71.1%)	9.24 -	ND -	5.27 ± 0.18 (27.5%)	2.79 ± 0.06 (11.8%)	1.53 ± 0.03 (15.9%)	0.77 ± 0.03 (5.1%)	0.82 ± 0.01 (7.0%)	0.75 ± 0.02 (3.8%)
CPC-MEKCon3	Semi-aerobic (21)	29.98 ± 0.66 (59.8%)	8.85 -	0.62 ± 0.04 (1.6%)	7.49 ± 0.16 (39.8%)	2.14 ± 0.40 (9.2%)	ND -	0.90 ± 0.02 (6.1%)	ND -	0.59 ± 0.11 (3.1%)
CPC-MEKCon4	Semi-aerobic (22)	28.82 ± 0.17 (69.0%)	7.86 -	1.01 ± 0.03 (2.7%)	8.66 ± 0.06 (46.9%)	1.14 ± 0.66 (5.0%)	ND -	1.16 ± 0.67 (8.1%)	ND -	0.51 ± 0.03 (2.7%)
CPC-MEK ^e	Semi-aerobic (17)	0 -	8.75 -	ND -	ND -	ND -	ND -	ND -	ND -	ND -
CPC-MEK	Semi-aerobic (13)	15.01 ± 0.30 (63.6%)	6.33 -	ND -	4.11 ± 0.26 (42.2%)	1.12 ± 0.05 (9.4%)	0.23 ± 0.01 (4.8%)	0.17 ± 0.11 (2.3%)	0.08 ± 0.02 (1.4%)	0.30 ± 0.02 (3.1%)
CPC-MEK ^f	Semi-aerobic (22)	29.81 ± 0.06 (63.1%)	8.44 -	Trace -	7.76 ± 0.06 (41.2%)	2.05 ± 0.02 (9.4%)	ND -	1.05 ± 0.22 (7.2%)	ND -	0.81 ± 0.04 (4.5%)

^a cultivation time of batch fermentation (h)

^b glycerol consumption (g), glycerol efficiency is presented in parentheses under the carbon source consumption value

^c biomass accumulation (g-DCW l⁻¹)

^d metabolite titers (g l⁻¹), the metabolite distribution is presented in parentheses under each titer

^e cultivation performed without glycerol supplementation

^f cultivation performed without IPTG induction

ND not detected

Supplementary Table 3 Summary of cultivation of various mutants of CPC-MEK and CPC-Sbm

Strain	Aerobicity (Cultivation time ^a)	Glycerol ^b	Biomass ^c	Succinate ^d	Acetate ^d	Propionate ^d	Acetone ^d	Ethanol ^d	Butanone ^d	1-Propanol ^d
CPC- MEK Δ <i>adhE</i>	Microaerobic (68)	29.90 ± 0.54 (58.0%)	3.8 -	1.06 ± 0.05 (2.6%)	4.85 ± 0.07 (25.3%)	3.15 ± 0.06 (13.3%)	0.84 ± 0.01 (8.7%)	ND -	0.94 ± 0.03 (8.0%)	ND -
	Semi-aerobic (22)	30.62 ± 0.07 (50.6%)	9.7 -	ND -	3.91 ± 0.04 (20.0%)	2.87 ± 0.04 (11.8%)	0.97 ± 0.01 (9.9%)	ND -	1.06 ± 0.01 (8.9%)	ND -
CPC- MEK Δ <i>pta</i>	Semi-aerobic (31)	29.96 ± 0.07 (30.8%)	7.6 -	ND -	0.20 ± 0.01 (1.1%)	0.14 ± 0.01 (0.6%)	2.01 ± 0.03 (21%)	ND -	0.94 ± 0.01 (8.1%)	ND -
CPC-Sbm	Microaerobic (27)	30.45 ± 3.01 (53.1%)	4.20 -	0.46 ± 0.09 (1.2%)	3.68 ± 0.33 (19.0%)	1.84 ± 0.24 (7.7%)	ND -	2.25 ± 0.05 (14.8%)	ND -	2.05 ± 0.11 (10.4%)
CPC- Sbm Δ <i>glpD</i>	Microaerobic (38)	30.14 ± 0.12 (75.73%)	6.70 -	0.49 ± 0.10 (1.27%)	7.88 ± 0.15 (40.80%)	5.22 ± 0.04 (21.82%)	ND -	1.03 ± 0.10 (6.84%)	ND -	0.98 ± 0.04 5.00%
CPC- Sbm Δ <i>dhaK</i>	Microaerobic (38)	30.03 ± 0.05 (73.94%)	6.56 -	0.48 ± 0.09 (1.24%)	4.44 ± 0.16 (23.04%)	11.83 ± 0.09 (49.66%)	ND -	ND -	ND -	ND -
CPC- MEK Δ <i>glpD</i>	Semi-aerobic (25)	30.2 ± 0.40 (23.7%)	11.8 -	ND -	0.34 ± 0.04 (1.8%)	2.4 ± 0.09 (10.2%)	0.60 ± 0.01 (6.2%)	ND -	0.64 ± 0.01 (5.5%)	ND -
CPC- MEK Δ <i>dhaK</i>	Semi-aerobic (22)	29.45 ± 0.04 (61.9%)	6.56 -	ND -	2.9 ± 0.08 (15.3%)	0.81 ± 0.01 (3.5%)	3.0 ± 0.06 (31.8%)	ND -	1.30 ± 0.07 (11.3%)	ND -

^a cultivation time of batch fermentation (h)

^b glycerol consumption (g), glycerol efficiency is presented in parentheses under the carbon source consumption value

^c biomass accumulation (g-DCW l⁻¹)

^d metabolite titers (g l⁻¹), the metabolite distribution is presented in parentheses under each titer

ND not detected

Appendix A - Supplementary Figures

Supplementary Fig. 1 DNA microarray transcriptomic analysis of strain CPC-Sbm using glycerol or glucose as the major carbon source. Numerical values represent the ratios of the transcript levels of central metabolic pathway genes of the glycerol culture to those of the glucose culture (i.e. in fold). Green boxes represent up-regulation of genes during glycerol cultivation whereas red boxes represent down-regulation. The sleeping beauty mutase pathway is shown in blue.

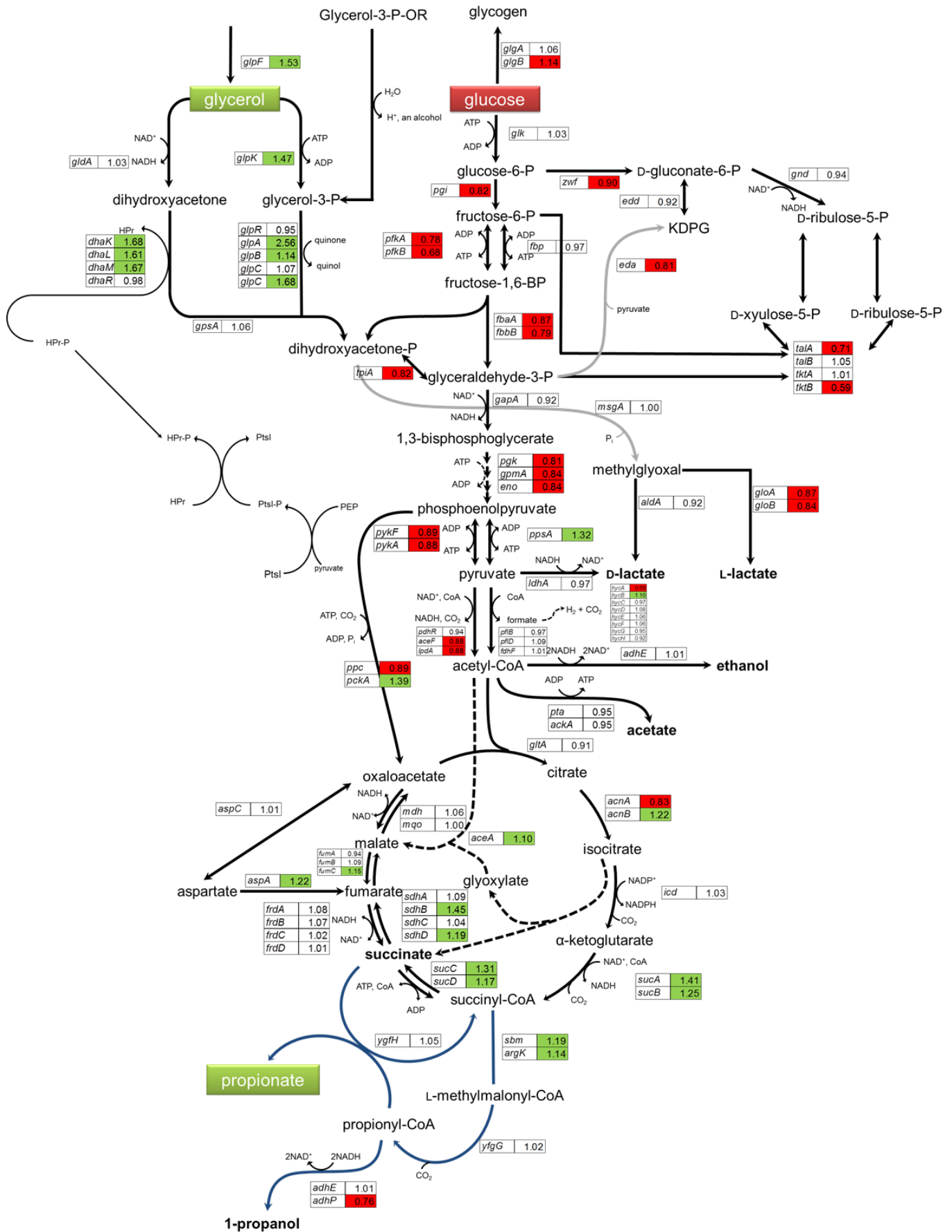
Supplementary Fig. 2 Time profiles of CPC-MEK and select control counterparts. Time profiles of glycerol, biomass, and major metabolites during (A) microaerobic batch cultivation of CPC-MEKCon1 (B) microaerobic batch cultivation of CPC-MEKCon2 (C) microaerobic batch cultivation of CPC-MEK and (D) semi-aerobic batch cultivation of CPC-MEK. All of the strains were induced at the start of the batch cultivation with 0.1 mM IPTG. Error bars represent s.d. (n = 2)

Supplementary Fig. 3 Time profiles of glycerol, biomass, and major metabolites during (A) microaerobic batch cultivation of CPC-MEK $\Delta adhE$ (B) semi-aerobic batch cultivation of CPC-MEK $\Delta adhE$ (C) semi-aerobic batch cultivation of CPC-MEK Δpta . All of the strains were induced at the start of the batch cultivation with 0.1 mM IPTG. Error bars represent s.d. (n = 2)

Supplementary Fig. 4 Time profiles of glycerol, biomass, and major metabolites during microaerobic batch cultivation of (A) CPC-Sbm (B) CPC-Sbm $\Delta glpD$ and (C) CPC-Sbm $\Delta dhaK$. (D) Metabolic distribution ratios of C3:C2 fermentative products (i.e.: propionate + 1-propanol: acetate + ethanol), overall acid: alcohol production (i.e.: propionate + acetate: 1-propanol + ethanol) as well as propionate: acetate production for each of the batch cultivations, ratios are calculated from the fractions of dissimilated glycerol. All of the strains were induced at the start of the batch cultivation with 0.1 mM IPTG. Error bars represent s.d. (n = 2)

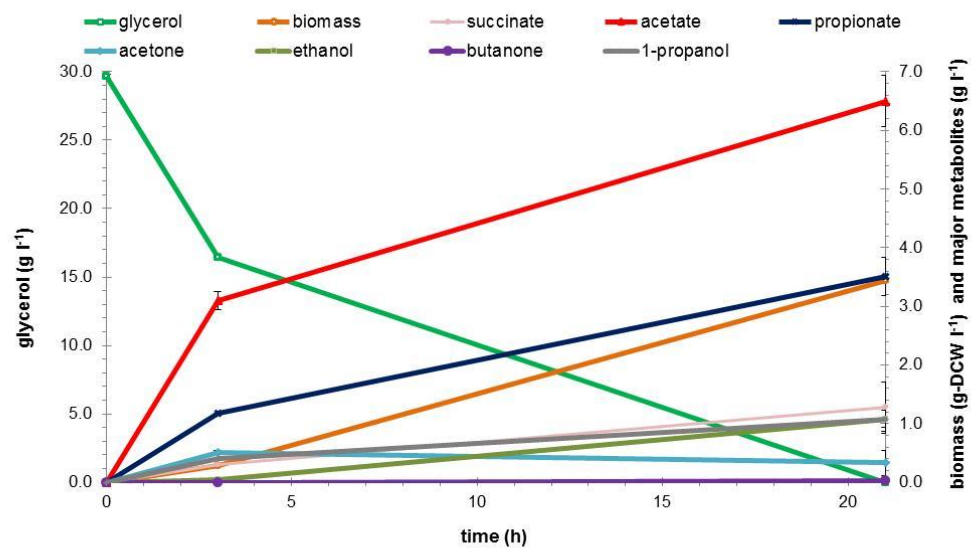
Supplementary Fig. 5 Time profiles of glycerol, biomass, and major metabolites during semi-aerobic batch cultivation of (A) CPC-MEK $\Delta glpD$ and (B) CPC-MEK $\Delta dhaK$. All of the strains were induced at the start of the batch cultivation with 0.1 mM IPTG. Error bars represent s.d. (n = 2)

Supplementary Figure 1

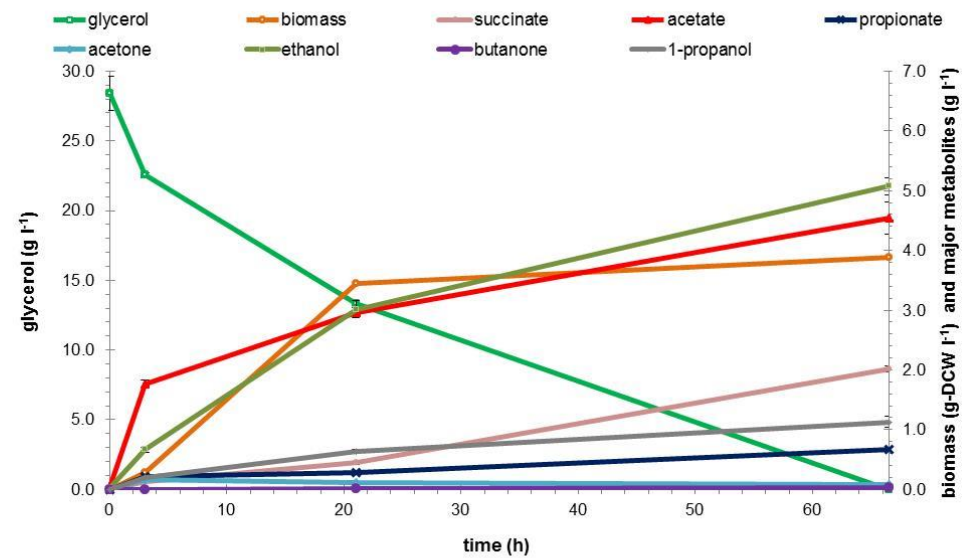


Supplementary Figure 2

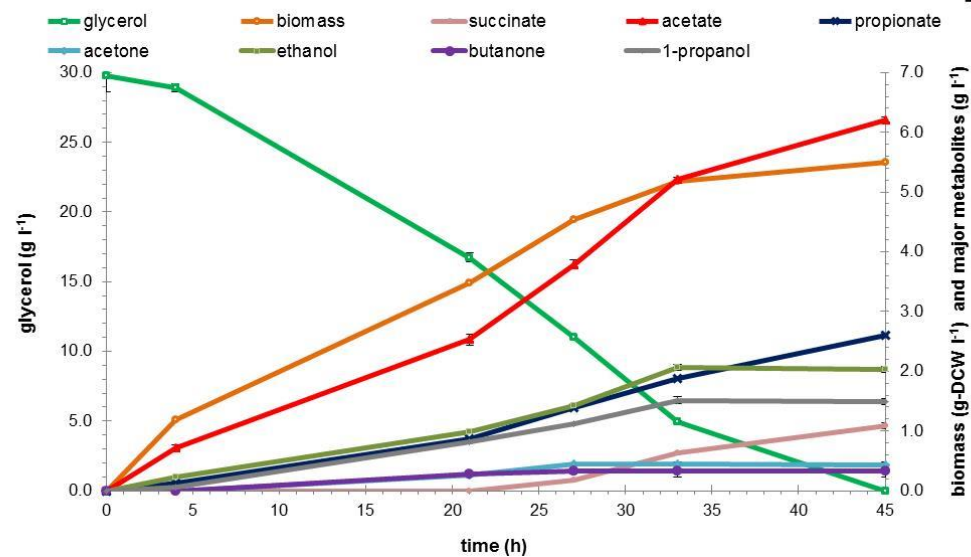
A



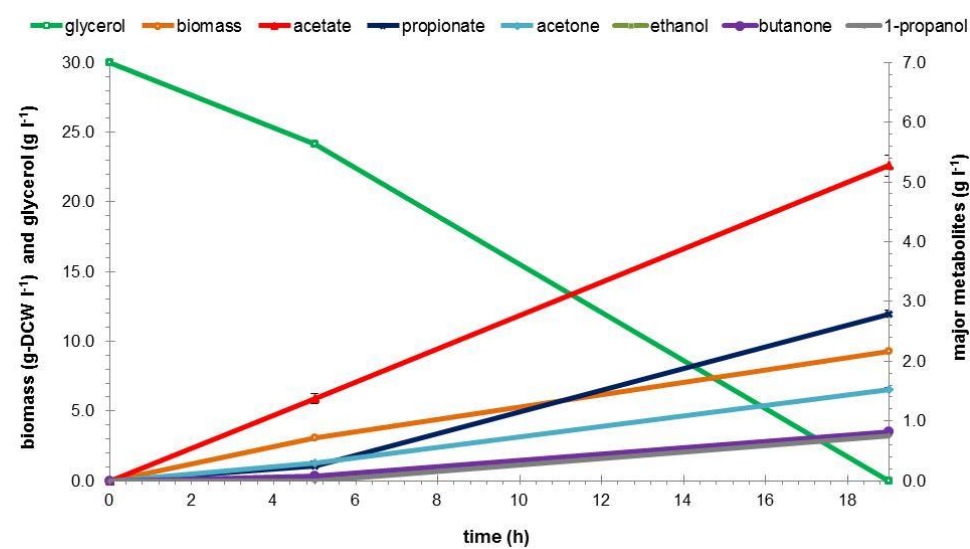
B



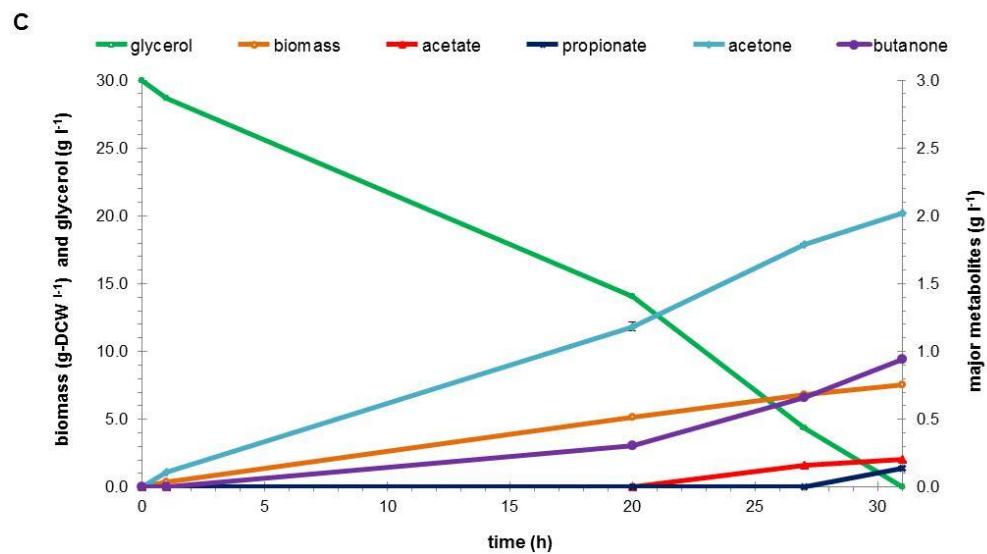
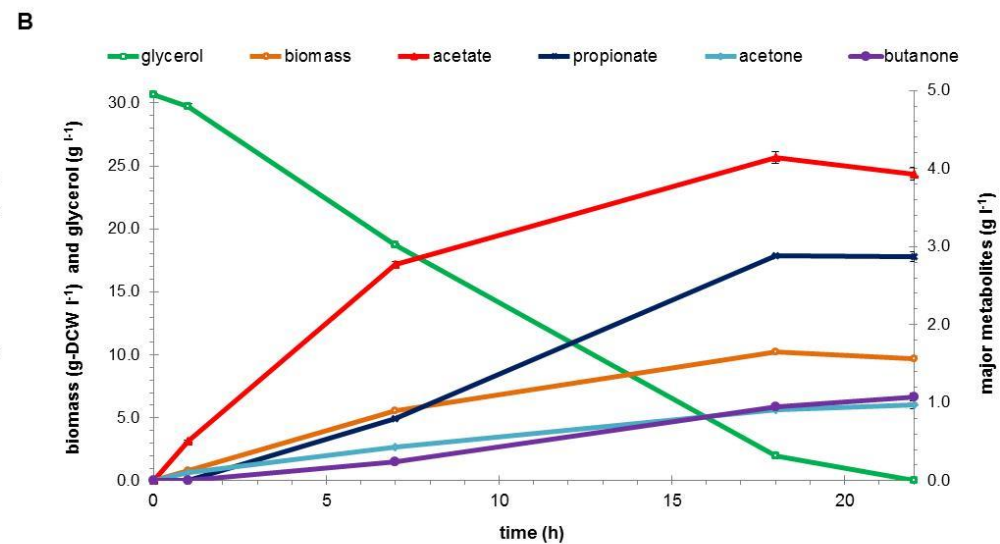
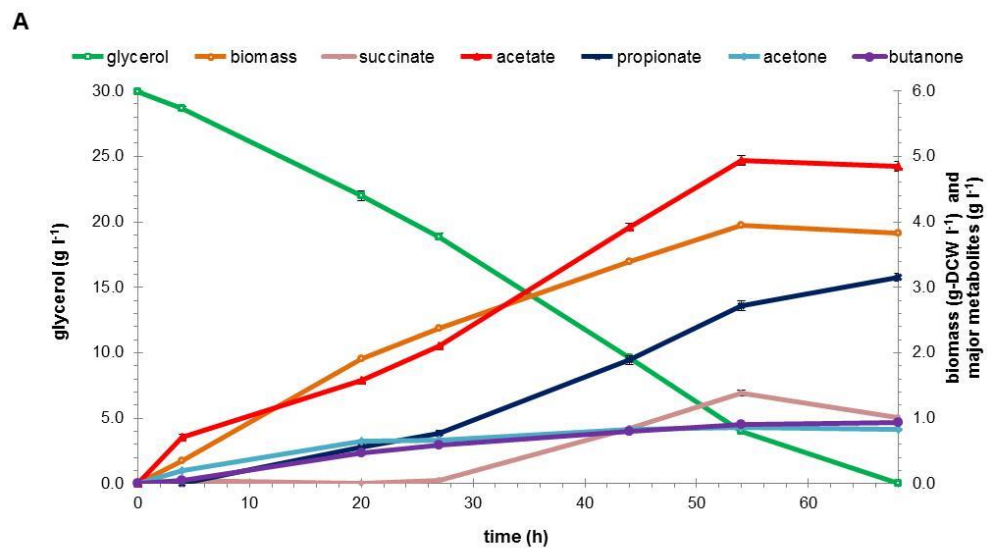
C



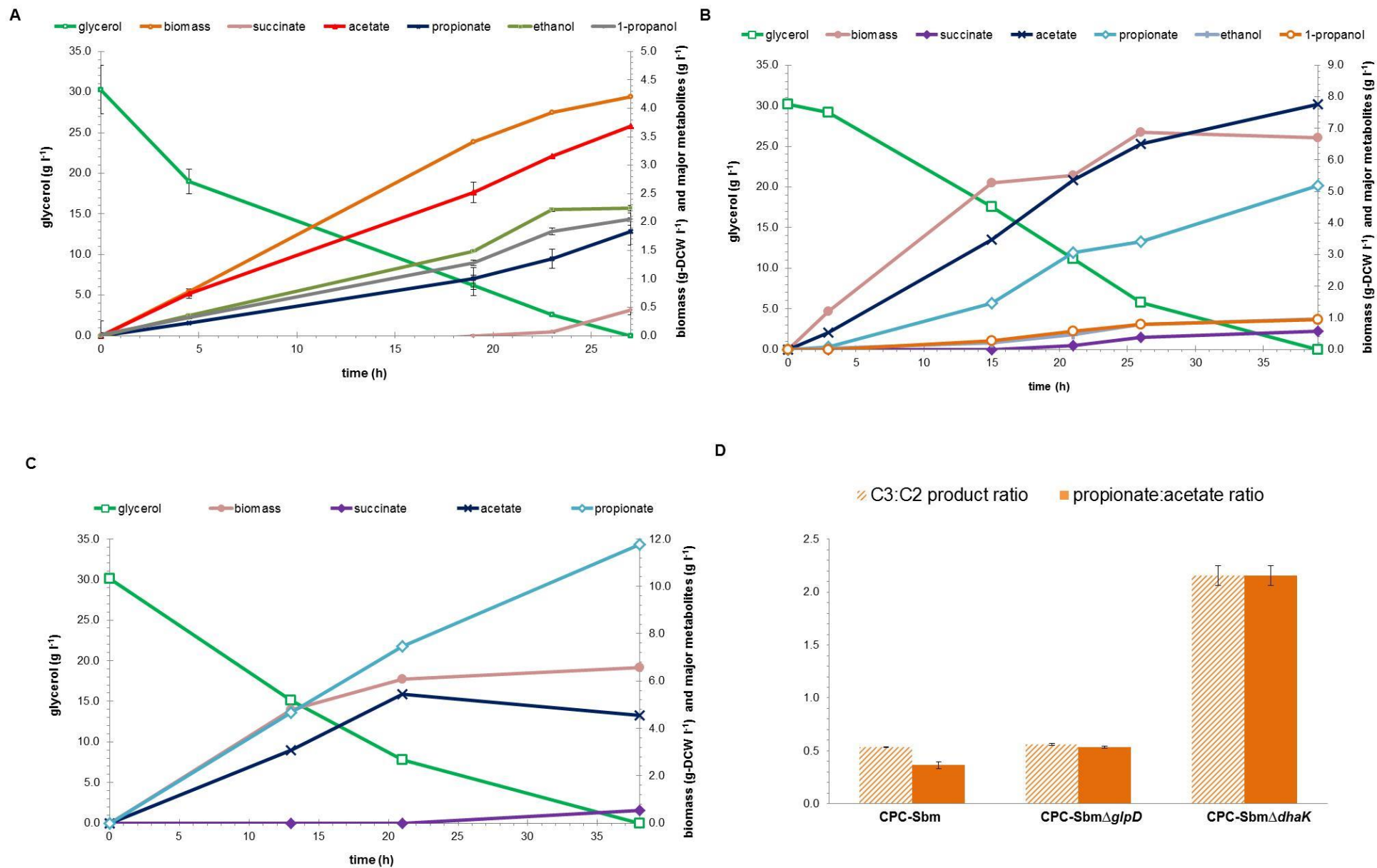
D



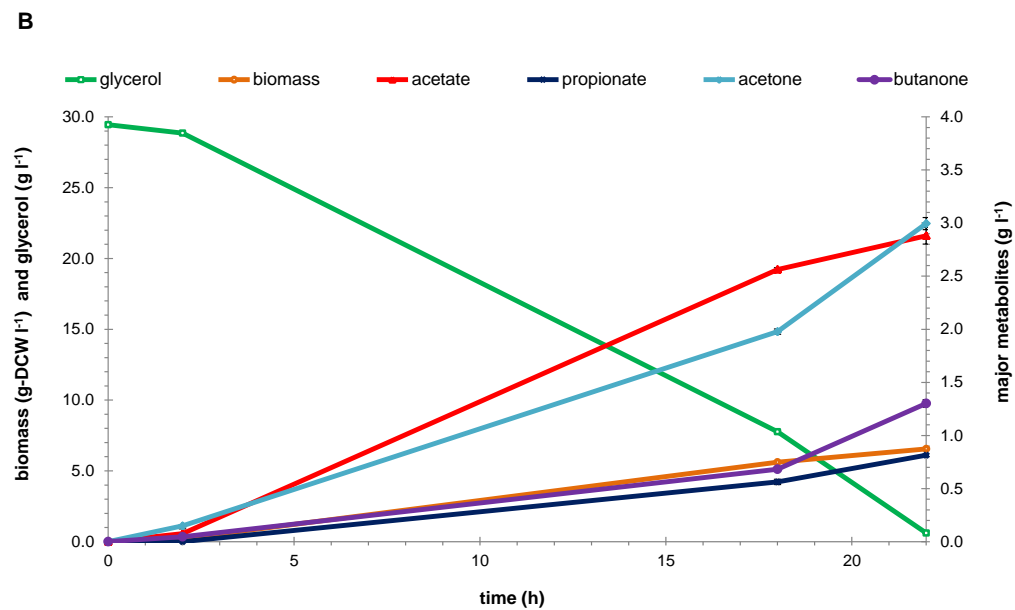
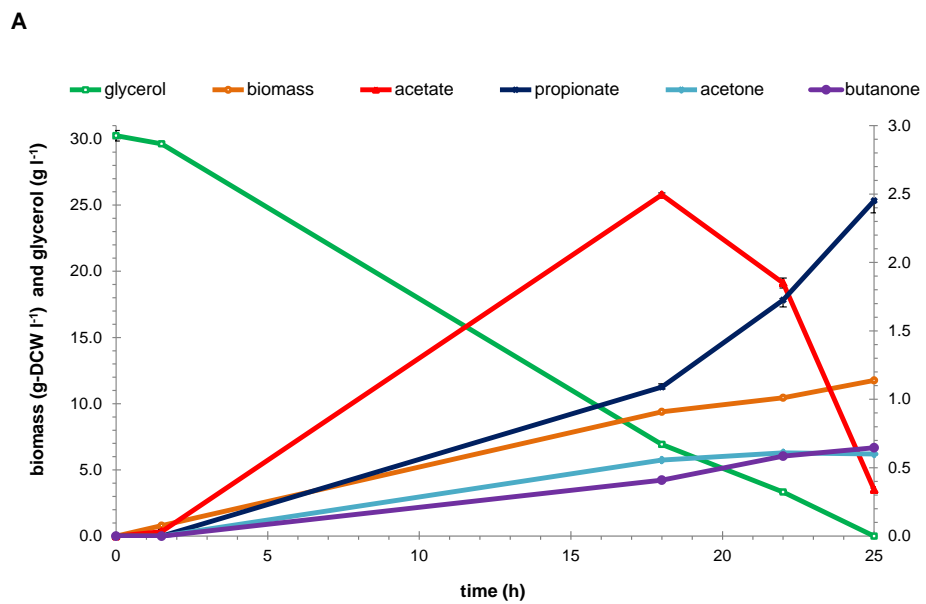
Supplementary Figure 3



Supplementary Figure 4



Supplementary Figure 5



Appendix B

Chapter 6 supplementary materials

Supplementary Table 1: Culture performance (i.e. overall glycerol or glucose consumption and final biomass and excreted metabolite concentrations) of CPC-PHB, CPC-PHBV and its control and mutant counterparts) in a bioreactor under microaerobic or semiaerobic cultivation conditions. All of the strains were induced at the start of the batch cultivation with 0.1 mM IPTG. Error bars represent s.d. (n = 2)

Supplementary Table 1

Strain	Aerobicity	Glucose ^a	Glycerol ^a	Biomass ^b	Lactate ^c	Succinate ^c	Acetate ^c	Propionate ^c	Ethanol ^c	1-Propanol ^c
CPC-PHB	Microaerobic	-	29.01 ± 0.29	16.99 ± 0.27	ND	2.91 ± 0.02	3.45 ± 0.16	ND	1.27 ± 0.45	ND
	Microaerobic	-	29.67 ± 0.44	9.87 ± 0.07	ND	1.82 ± 0.22	5.17 ± 0.13	1.48 ± 0.08	1.96 ± 0.22	1.87 ± 0.07
CPC-PHBV	Microaerobic	33.61 ± 0.32	-	7.49 ± 0.16	1.72 ± 0.11	1.87 ± 0.12	5.62 ± 0.11	0.36 ± 0.06	2.41 ± 0.03	0.53 ± 0.44
	Semiaerobic	-	30.12 ± 0.44	11.80 ± 1.68	ND	0.87 ± 0.02	6.37 ± 0.10	1.92 ± 0.17	0.92 ± 0.01	0.78 ± 0.04
	Aerobic	-	29.45 ± 0.25	34.2 ± 0.28	ND	0.15 ± 0.04	3.76 ± 0.08	1.14 ± 0.06	0.62 ± 0.06	0.46 ± 0.06
CPC-PHBVCon1	Semiaerobic	-	30.05 ± 0.84	15.04 ± 0.03	ND	1.19 ± 0.04	5.13 ± 0.11	2.19 ± 0.22	0.88 ± 0.45	0.74 ± 0.36
CPC-PHBVΔpta	Semiaerobic	-	29.66 ± 0.07	17.41 ± 0.97	ND	ND	1.05 ± 0.03	0.62 ± 0.02	0.91 ± 0.03	0.62 ± 0.01
CPC-PHBVΔadhE	Semiaerobic	-	29.5 ± 0.02	13.76 ± 1.31	ND	ND	3.91 ± 0.05	1.85 ± 0.01	ND	ND
CPC-PHBVΔdhaK	Semiaerobic	-	30.14 ± 0.04	13.26 ± 1.22	0.13 ± 0.06	1.45 ± 0.06	4.97 ± 0.21	2.12 ± 0.02	0.56 ± 0.02	0.86 ± 0.05
CPC-PHBVΔglpD	Semiaerobic	-	29.67 ± 0.44	18.61 ± 0.83	ND	ND	2.67 ± 0.12	1.5 ± 0.02	ND	ND

^a glycerol/glucose consumption (g l⁻¹)

^b biomass accumulation (g-DCW l⁻¹)

^c metabolite concentrations (g l⁻¹)

ND not detected

Appendix B – Supplementary Figure Legends

Supplementary Fig. 1 Time profiles of glycerol, biomass, and major metabolites during (A) microaerobic batch cultivation of CPC-PHB and (B) CPC-PHBV using glycerol as the major carbon source. All of the strains were induced at the start of the batch cultivation with 0.1 mM IPTG. Error bars represent s.d. (n = 2)

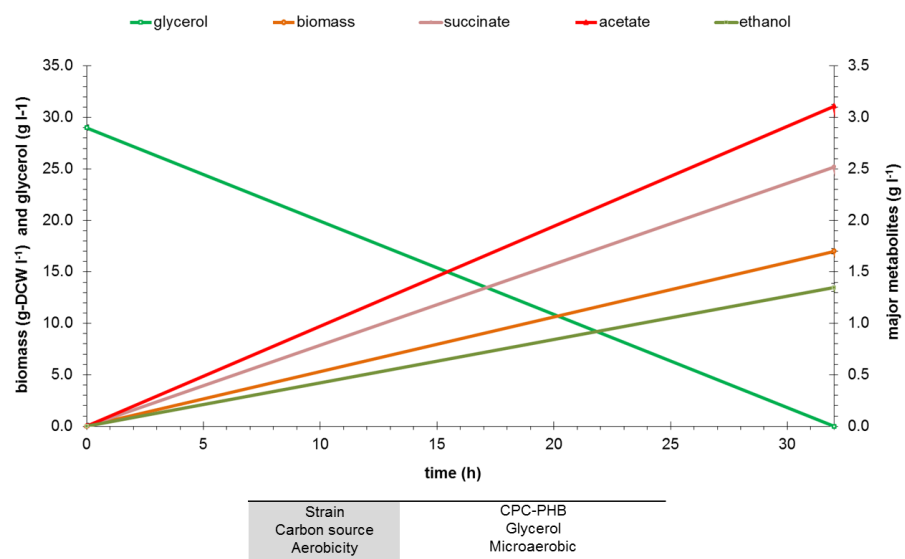
Supplementary Fig. 2 (A) Time profiles of glucose, biomass, and major metabolites during microaerobic batch cultivation of CPC-PHBV using glucose as the major carbon source. Time profiles of glycerol, biomass, and major metabolites during (B) semiaerobic and (C) aerobic batch cultivation of CPC-PHBV. (D) Time profiles of glycerol, biomass, and major metabolites during semiaerobic batch cultivation of CPC-PHBVCon1 using glycerol as the major carbon source. All of the strains were induced at the start of the batch cultivation with 0.1 mM IPTG. Error bars represent s.d. (n = 2)

Supplementary Fig. 3 Time profiles of glycerol, biomass, and major metabolites during semiaerobic batch cultivation of (A) CPC-PHBV, (B) CPC-PHBV Δ adhE and (C) CPC-PHBV Δ pta using glycerol as the major carbon source. All of the strains were induced at the start of the batch cultivation with 0.1 mM IPTG. Error bars represent s.d. (n = 2)

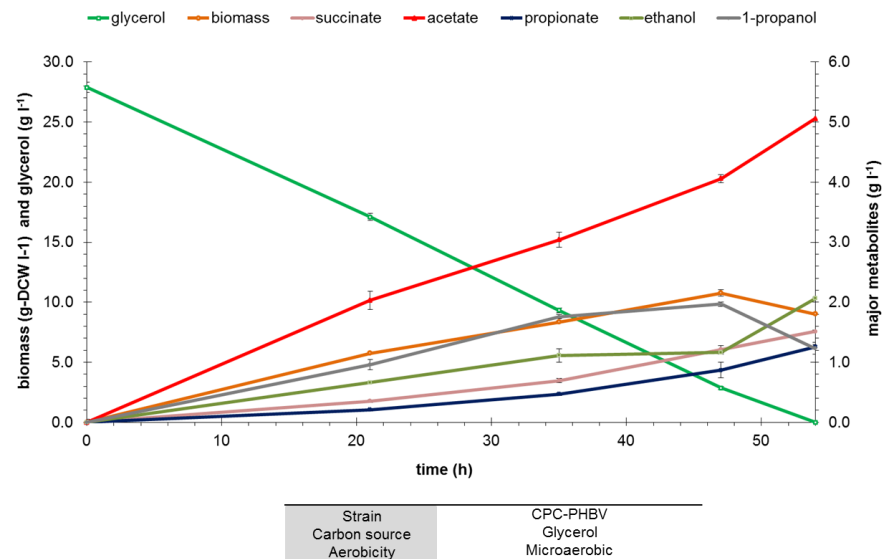
Supplementary Fig. 4 Time profiles of glycerol, biomass, and major metabolites during semiaerobic batch cultivation of (A) CPC-PHBV, (B) CPC-PHBV Δ dhaK and (C) CPC-PHBV Δ glpD using glycerol as the major carbon source. All of the strains were induced at the start of the batch cultivation with 0.1 mM IPTG. Error bars represent s.d. (n = 2)

Supplementary Fig. 1

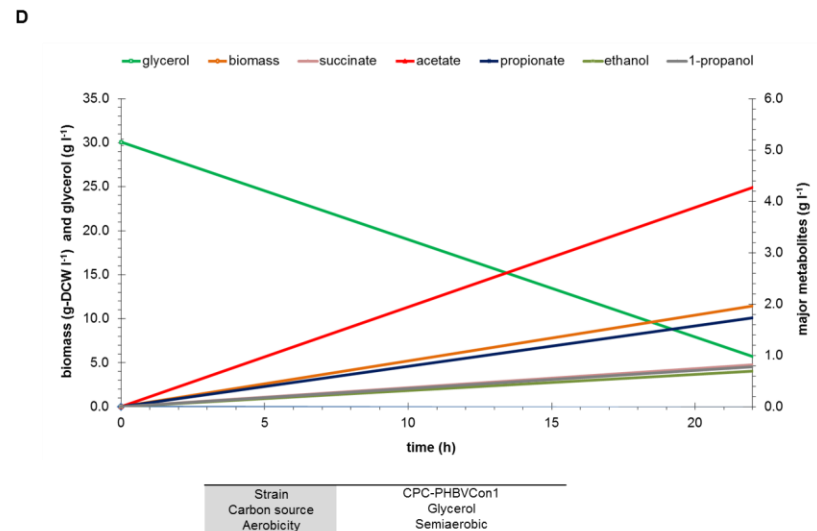
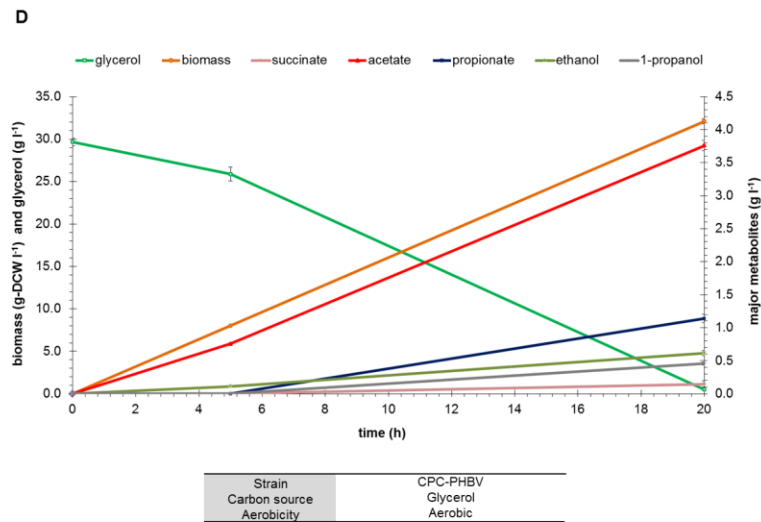
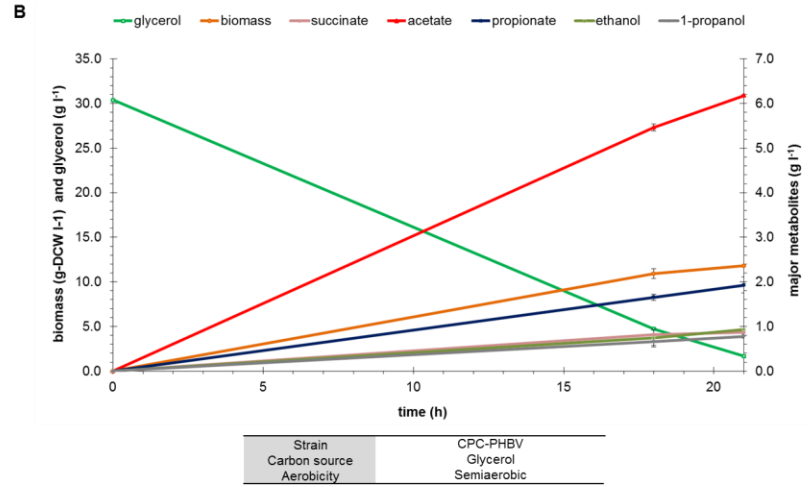
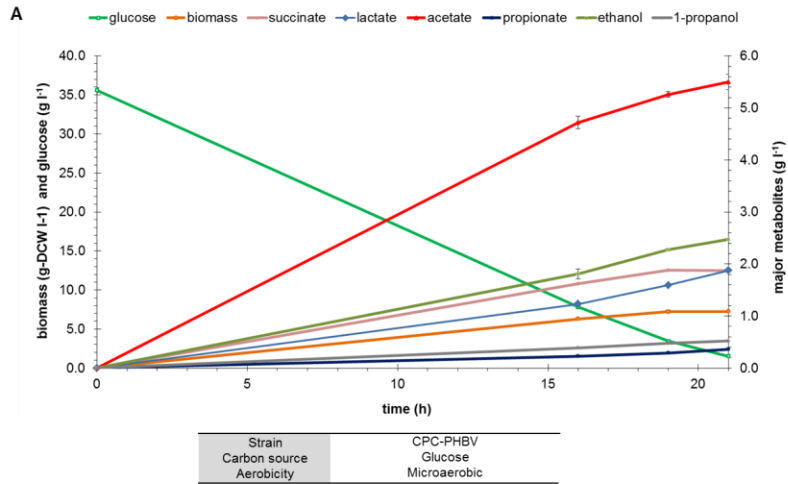
A



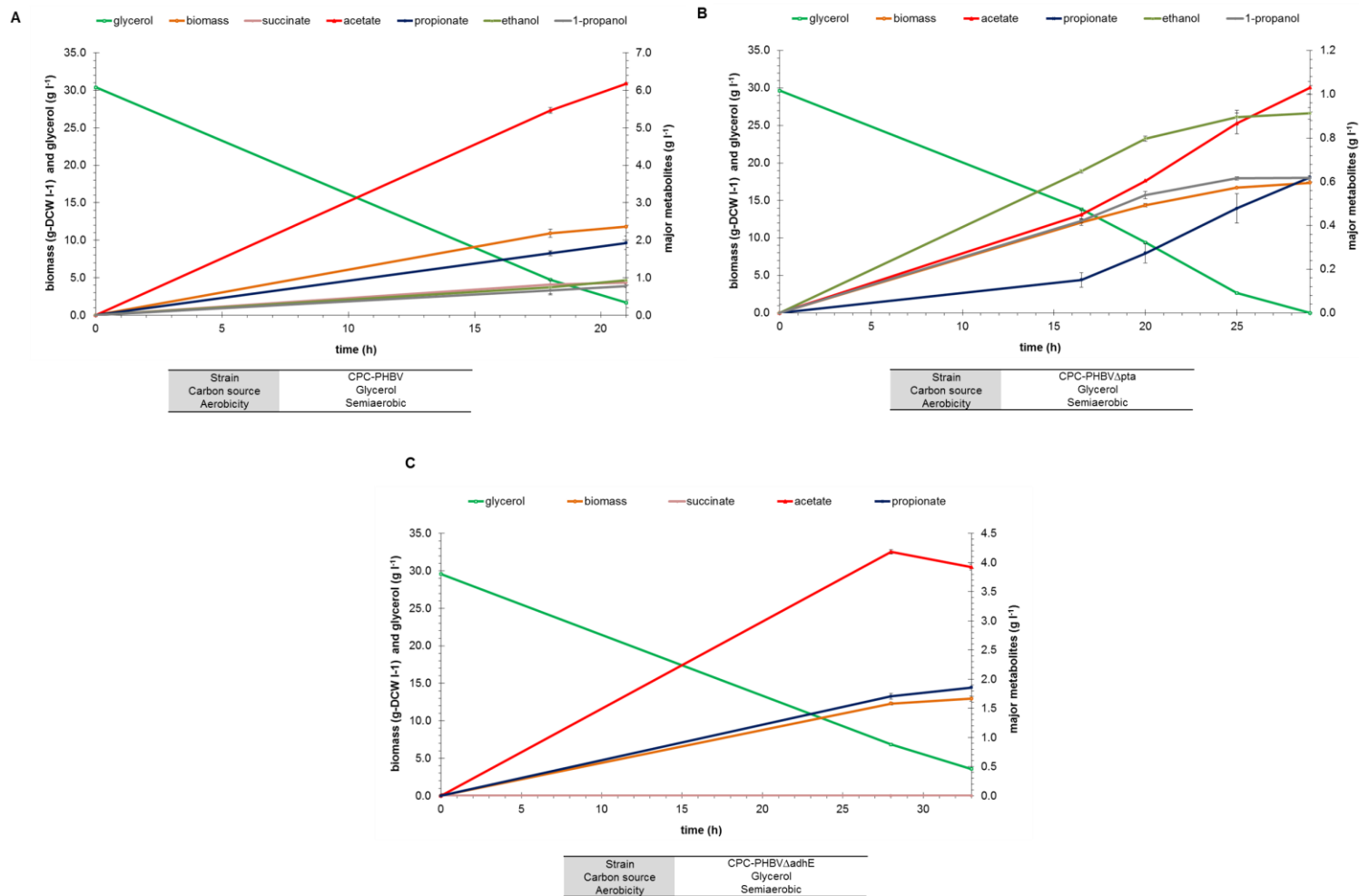
B



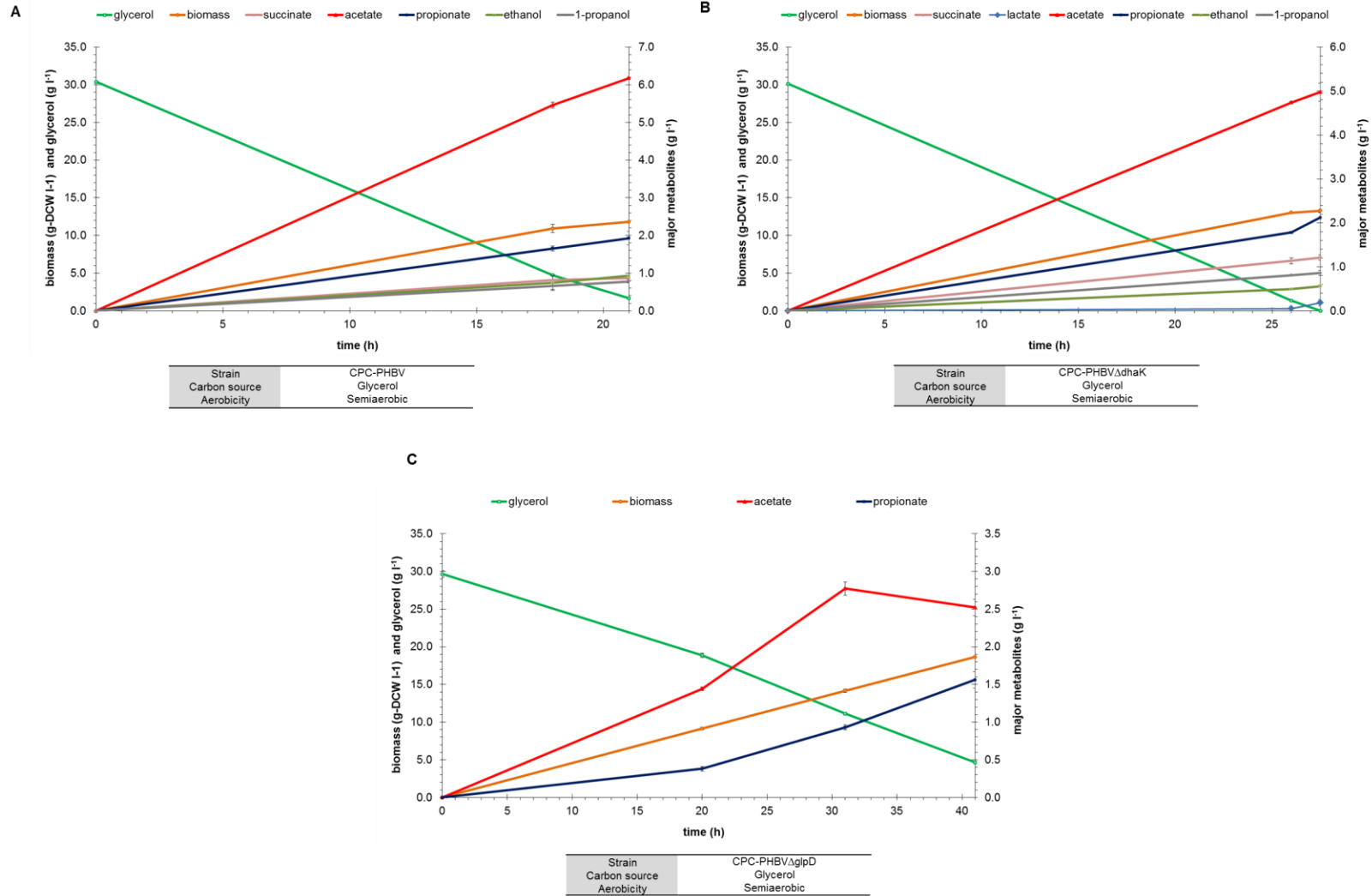
Supplementary Fig. 2



Supplementary Fig. 3



Supplementary Fig. 4



Bibliography

1. **Jones JA, Toparlak ÖD, Koffas MAG.** 2015. Metabolic pathway balancing and its role in the production of biofuels and chemicals. *Current Opinion in Biotechnology* **33**:52-59.
2. **Srirangan K, Akawi L, Moo-Young M, Chou CP.** 2012. Towards sustainable production of clean energy carriers from biomass resources. *Applied Energy* **100**:172-186.
3. **Nielsen J.** 2001. Metabolic engineering. *Applied Microbiology and Biotechnology* **55**:263-283.
4. **Aristidou A, Penttilä M.** 2000. Metabolic engineering applications to renewable resource utilization. *Current Opinion in Biotechnology* **11**:187-198.
5. **Lee SK, Chou H, Ham TS, Lee TS, Keasling JD.** 2008. Metabolic engineering of microorganisms for biofuels production: from bugs to synthetic biology to fuels. *Current Opinion in Biotechnology* **19**:556-563.
6. **Krivoruchko A, Zhang Y, Siewers V, Chen Y, Nielsen J.** 2015. Microbial acetyl-CoA metabolism and metabolic engineering. *Metabolic Engineering* **28**:28-42.
7. **Oliver DJ, Nikolau BJ, Wurtele ES.** 2009. Acetyl-CoA—life at the metabolic nexus. *Plant science* **176**:597-601.
8. **Brock M.** 2010. Role of Cellular Control of Propionyl-CoA Levels for Microbial Pathogenesis, p. 3279-3291, *Handbook of Hydrocarbon and Lipid Microbiology*. Springer.
9. **Zhang Y-Q, Brock M, Keller NP.** 2004. Connection of propionyl-CoA metabolism to polyketide biosynthesis in *Aspergillus nidulans*. *Genetics* **168**:785-794.
10. **Atsumi S, Hanai T, Liao JC.** 2008. Non-fermentative pathways for synthesis of branched-chain higher alcohols as biofuels. *Nature* **451**:86-89.
11. **McEwen JT, Atsumi S.** 2012. Alternative biofuel production in non-natural hosts. *Current Opinion in Biotechnology* DOI:10.1016/j.copbio.2011.12.019.
12. **Atsumi S, Cann AF, Connor MR, Shen CR, Smith KM, Brynildsen MP, Chou KJY, Hanai T, Liao JC.** 2008. Metabolic engineering of *Escherichia coli* for 1-butanol production. *Metabolic Engineering* **10**:305-311.
13. **Aldor IS, Kim SW, Prather KLJ, Keasling JD.** 2002. Metabolic engineering of a novel propionate-independent pathway for the production of poly (3-hydroxybutyrate-co-3-hydroxyvalerate) in recombinant *Salmonella enterica* serovar typhimurium. *Applied and Environmental Microbiology* **68**:3848-3854.
14. **Kannan SM.** 2008. Studies on methylmalonyl-CoA mutase from *Escherichia coli*. University of Westminster.
15. **Leadlay PF.** 1981. Purification and characterization of methylmalonyl-CoA epimerase from *Propionibacterium shermanii*. *Biochemical Journal* **197**:413-419.
16. **Haller T, Buckel T, Rétey J, Gerlt JA.** 2000. Discovering new enzymes and metabolic pathways: conversion of succinate to propionate by *Escherichia coli*. *Biochemistry* **39**:4622-4629.
17. **Weiland P.** 2010. Biogas production: current state and perspectives. *Applied Microbiology and Biotechnology* **85**:849-860.
18. **Lucian LA, Argyropoulos DS, Adamopoulos L, Gaspar AR.** 2007. Chemicals, materials, and energy from biomass: a review, p. 2-30. *In* Argyropoulos DS (ed.), *ACS Symposium Series 954: Materials, Chemicals, and Energy for Forest Biomass*, vol. 954. American Chemical Society, Washington.
19. **Klass DL.** 1998. Biomass for renewable energy, fuels, and chemicals. Academic Press, San Diego.
20. **An H, Wilhelm WE, Searcy SW.** 2011. Biofuel and petroleum-based fuel supply chain research: a literature review. *Biomass and Bioenergy* **35**:3763-3774.

21. **Kamm B, Kamm M.** 2004. Principles of biorefineries. *Applied microbiology and biotechnology* **64**:137-145.
22. **Volsky R, Smithhart R.** 2011. A brief perspective on biomass for bioenergy and biofuels. *Journal of Tropical Forestry and Environment* **1**:1-13.
23. **Abdeshanian P, Dashti MG, Kalil MS, Yusoff WMW.** 2010. Production of biofuel using biomass as a sustainable biological resource. *Biotechnology* **9**:274-282.
24. **Gupta RB, Demirbas A.** 2010. Gasoline, diesel and ethanol biofuels from grasses and plants. Cambridge University Press, Cambridge.
25. **Haberl H, Beringer T, Bhattacharya SC, Erb K-H, Hoogwijk M.** 2010. The global technical potential of bio-energy in 2050 considering sustainability constraints. *Current Opinion in Environmental Sustainability* **2**:394-403.
26. **Alexander BR, Mitchell RE, Gur TM.** 2012. Experimental and modeling study of biomass conversion in a solid carbon fuel cell. *Journal of the Electrochemical Society* **159**:B347-B354.
27. **Berndes G, Hoogwijk M, van den Broek R.** 2003. The contribution of biomass in the future global energy supply: a review of 17 studies. *Biomass and Bioenergy* **25**:1-28.
28. **Worldwatch-Institute.** 2007. Biofuels for transport: global potential and implications for sustainable energy and agriculture. Earthscan, London.
29. **Cherubini F.** 2010. The biorefinery concept: Using biomass instead of oil for producing energy and chemicals. *Energy Conversion and Management* **51**:1412-1421.
30. **Torney F, Moeller L, Scarpa A, Wang K.** 2007. Genetic engineering approaches to improve bioethanol production from maize. *Current Opinion in Biotechnology* **18**:193-199.
31. **Rooney WL, Blumenthal J, Bean B, Mullet JE.** 2007. Designing sorghum as a dedicated bioenergy feedstock. *Biofuels, Bioproducts and Biorefining* **1**:147-157.
32. **Saballos A.** 2008. Development and utilization of sorghum as a bioenergy crop
p. 211-248. *In* Vermerris W (ed.), *Genetic Improvement of Bioenergy Crops*. Springer New York.
33. **El Bassam N.** 2010. Handbook of bioenergy crops: a complete reference to species, development and applications. Earthscan, London.
34. **Murphy DJ.** 2012. Oil crops as potential sources of biofuels
p. 269-284. *In* Gupta SK (ed.), *Technological innovations in major world oil crops, vol. 2*. Springer New York.
35. **Juan JC, Kartika DA, Wu TY, Hin T-YY.** 2011. Biodiesel production from jatropha oil by catalytic and non-catalytic approaches: An overview. *Bioresource Technology* **102**:452-460.
36. **Shahid EM, Jamal Y.** 2011. Production of biodiesel: A technical review. *Renewable and Sustainable Energy Reviews* **15**:4732-4745.
37. **Margeot A, Hahn-Hagerdal B, Edlund M, Slade R, Monot F.** 2009. New improvements for lignocellulosic ethanol. *Current Opinion in Biotechnology* **20**:372-380.
38. **Nigam PS, Singh A.** 2011. Production of liquid biofuels from renewable resources. *Progress in Energy and Combustion Science* **37**:52-68.
39. **Balat M.** 2011. Production of bioethanol from lignocellulosic materials via the biochemical pathway: A review. *Energy Conversion and Management* **52**:858-875.
40. **Ghosh D, Hallenbeck PC.** 2012. Advanced bioethanol production
p. 165-181. *In* Hallenbeck PC (ed.), *Microbial Technologies in Advanced Biofuels Production*. Springer US, New York.
41. **Nitayavardhana S, Khanal SK.** 2012. Biofuel residues/wastes: ban or boon? *Crit Rev Environ Sci Technol* **42**:1-43.

42. **Demirbaş A.** 2001. Biomass resource facilities and biomass conversion processing for fuels and chemicals. *Energy Conversion and Management* **42**:1357-1378.
43. **Carere C, Sparling R, Cicek N, Levin D.** 2008. Third generation biofuels via direct cellulose fermentation. *International Journal of Molecular Sciences* **9**:1342-1360.
44. **Loeser M, Redfern MA.** 2008, p 1-4. Universities Power Engineering Conference, 43rd International.
45. **McKendry P.** 2002. Energy production from biomass (part 2): conversion technologies. *Bioresource Technology* **83**:47-54.
46. **Balat M, Balat M, Kirtay E, Balat H.** 2009. Main routes for the thermo-conversion of biomass into fuels and chemicals. Part 2: gasification systems. *Energy Conversion and Management* **50**:3158-3168.
47. **Kirubakaran V, Sivaramakrishnan V, Nalini R, Sekar T, Premalatha M, Subramanian P.** 2009. A review on gasification of biomass. *Renewable and Sustainable Energy Reviews* **13**:179-186.
48. **Kumar A, Jones D, Hanna M.** 2009. Thermochemical biomass gasification: a review of the current status of the technology. *Energies* **2**:556-581.
49. **Tijmensen MJA, Faaij APC, Hamelinck CN, van Hardeveld MRM.** 2002. Exploration of the possibilities for production of Fischer Tropsch liquids and power via biomass gasification. *Biomass and Bioenergy* **23**:129-152.
50. **Damartzis T, Zabaniotou A.** 2011. Thermochemical conversion of biomass to second generation biofuels through integrated process design: a review. *Renewable and Sustainable Energy Reviews* **15**:366-378.
51. **Cao Y, Wang Y, Riley JT, Pan W-P.** 2006. A novel biomass air gasification process for producing tar-free higher heating value fuel gas. *Fuel Processing Technology* **87**:343-353.
52. **Balat M, Balat M, Kirtay E, Balat H.** 2009. Main routes for the thermo-conversion of biomass into fuels and chemicals. Part 1: pyrolysis systems. *Energy Conversion and Management* **50**:3147-3157.
53. **Goyal HB, Seal D, Saxena RC.** 2008. Bio-fuels from thermochemical conversion of renewable resources: a review. *Renewable and Sustainable Energy Reviews* **12**:504-517.
54. **Mohan D, Pittman CU, Steele PH.** 2006. Pyrolysis of wood/biomass for bio-oil: a critical review. *Energy and Fuels* **20**:848-889.
55. **Zhang Q, Chang J, Wang T, Xu Y.** 2007. Review of biomass pyrolysis oil properties and upgrading research. *Energy Conversion and Management* **48**:87-92.
56. **Balat M.** 2008. Mechanisms of thermochemical biomass conversion processes. Part 3: reactions of liquefaction. *Energy Sources, Part A: Recovery, Utilization, and Environmental Effects* **30**:649-659.
57. **Demirbaş A.** 2000. Mechanisms of liquefaction and pyrolysis reactions of biomass. *Energy Conversion and Management* **41**:633-646.
58. **Zhang L, Xu C, Champagne P.** 2010. Overview of recent advances in thermo-chemical conversion of biomass. *Energy Conversion and Management* **51**:969-982.
59. **Behrendt F, Neubauer Y, Oevermann M, Wilmes B, Zobel N.** 2008. Direct liquefaction of biomass. *Chemical Engineering and Technology* **31**:667-677.
60. **Toor SS, Rosendahl L, Rudolf A.** 2011. Hydrothermal liquefaction of biomass: A review of subcritical water technologies. *Energy* **36**:2328-2342.
61. **Foresti E.** 2001. Perspectives on anaerobic treatment in developing countries. *Water Science and Technology* **44**:144-148.
62. **Guiot SR, Frigon J-C.** 2012. Anaerobic digestion as an effective biofuel production technology

- M, p. 143-161. *In* Hallenbeck PC (ed.), *Microbial Technologies in Advanced Biofuels Production*. Springer US, New York.
63. **Braber K.** 1995. Anaerobic digestion of municipal solid waste: A modern waste disposal option on the verge of breakthrough. *Biomass and Bioenergy* **9**:365-376.
 64. **Gunaseelan VN.** 1997. Anaerobic digestion of biomass for methane production: A review. *Biomass and Bioenergy* **13**:83-114.
 65. **Mata-Alvarez J, Macé S, Llabrés P.** 2000. Anaerobic digestion of organic solid wastes. An overview of research achievements and perspectives. *Bioresource Technology* **74**:3-16.
 66. **Sialve B, Bernet N, Bernard O.** 2009. Anaerobic digestion of microalgae as a necessary step to make microalgal biodiesel sustainable. *Biotechnology Advances* **27**:409-416.
 67. **Ward AJ, Hobbs PJ, Holliman PJ, Jones DL.** 2008. Optimisation of the anaerobic digestion of agricultural resources. *Bioresource Technology* **99**:7928-7940.
 68. **Chen Y, Yang G, Sweeney S, Feng Y.** 2010. Household biogas use in rural China: A study of opportunities and constraints. *Renewable and Sustainable Energy Reviews* **14**:545-549.
 69. **Zeng X, Ma Y, Ma L.** 2007. Utilization of straw in biomass energy in China. *Renewable and Sustainable Energy Reviews* **11**:976-987.
 70. **Banks CJ, Salter AM, Chesshire M.** 2006. Potential of anaerobic digestion for mitigation of green house gas emissions and production of renewable energy from agriculture: Barriers and incentives to widespread adoption in Europe. *Water Science and Technology* **55**:165-173.
 71. **Claassen PAM, van Lier JB, Lopez Contreras AM, van Niel EWJ, Sijtsma L, Stams AJM, de Vries SS, Weusthuis RA.** 1999. Utilisation of biomass for the supply of energy carriers. *Applied Microbiology and Biotechnology* **52**:741-755.
 72. **Knowles J, Lehtovaara P, Teeri T.** 1987. Cellulase families and their genes. *Trends in Biotechnology* **5**:255-261.
 73. **Wen F, Nair NU, Zhao H.** 2009. Protein engineering in designing tailored enzymes and microorganisms for biofuels production. *Current Opinion in Biotechnology* **20**:412-419.
 74. **Bhat MK.** 2000. Cellulases and related enzymes in biotechnology. *Biotechnology Advances* **18**:355-383.
 75. **Carmen S.** 2009. Lignocellulosic residues: Biodegradation and bioconversion by fungi. *Biotechnology Advances* **27**:185-194.
 76. **Martinez D, Berka RM, Henrissat B, Saloheimo M, Arvas M, Baker SE, Chapman J, Chertkov O, Coutinho PM, Cullen D, Danchin EGJ, Grigoriev IV, Harris P, Jackson M, Kubicek CP, Han CS, Ho I, Larrondo LF, de Leon AL, Magnuson JK, Merino S, Misra M, Nelson B, Putnam N, Robbertse B, Salamov AA, Schmoll M, Terry A, Thayer N, Westerholm-Parvinen A, Schoch CL, Yao J, Barabote R, Nelson MA, Detter C, Bruce D, Kuske CR, Xie G, Richardson P, Rokhsar DS, Lucas SM, Rubin EM, Dunn-Coleman N, Ward M, Brettin TS.** 2008. Genome sequencing and analysis of the biomass-degrading fungus *Trichoderma reesei* (syn. *Hypocrea jecorina*). *Nature Biotechnology* **26**:553-560.
 77. **Percival Zhang YH, Himmel ME, Mielenz JR.** 2006. Outlook for cellulase improvement: screening and selection strategies. *Biotechnology Advances* **24**:452-481.
 78. **Escovar-Kousen J, Wilson D, Irwin D.** 2004. Integration of computer modeling and initial studies of site-directed mutagenesis to improve cellulase activity on Cel9A from *Thermobifida fusca*. *Applied Biochemistry and Biotechnology* **113**:287-297.
 79. **Nakazawa H, Okada K, Onodera T, Ogasawara W, Okada H, Morikawa Y.** 2009. Directed evolution of endoglucanase III (Cel12A) from *Trichoderma reesei*. *Applied Microbiology and Biotechnology* **83**:649-657.
 80. **Bayer EA, Lamed R, Himmel ME.** 2007. The potential of cellulases and cellulosomes for cellulosic waste management. *Current Opinion in Biotechnology* **18**:237-245.

81. **Sticklen M.** 2006. Plant genetic engineering to improve biomass characteristics for biofuels. *Current Opinion in Biotechnology* **17**:315-319.
82. **Wingren A, Galbe M, Zacchi G.** 2003. Techno-economic evaluation of producing ethanol from softwood: comparison of SSF and SHF and identification of bottlenecks. *Biotechnology Progress* **19**:1109-1117.
83. **Lynd LR, Zyl WHv, McBride JE, Laser M.** 2005. Consolidated bioprocessing of cellulosic biomass: an update. *Current Opinion in Biotechnology* **16**:577-583.
84. **Dellomonaco C, Rivera C, Campbell P, Gonzalez R.** 2010. Engineered respiro-fermentative metabolism for the production of biofuels and biochemicals from fatty acid-rich feedstocks. *Applied and Environmental Microbiology* **76**:5067-5078.
85. **Dellomonaco C, Fava F, Gonzalez R.** 2010. The path to next generation biofuels: successes and challenges in the era of synthetic biology. *Microbial Cell Factories* **9**:1-15.
86. **Lin Y, Tanaka S.** 2006. Ethanol fermentation from biomass resources: current state and prospects. *Applied Microbiology and Biotechnology* **69**:627-642.
87. **Zaldivar J, Nielsen J, Olsson L.** 2001. Fuel ethanol production from lignocellulose: a challenge for metabolic engineering and process integration. *Applied Microbiology and Biotechnology* **56**:17-34.
88. **Jeffries TW, Jin YS.** 2004. Metabolic engineering for improved fermentation of pentoses by yeasts. *Applied Microbiology and Biotechnology* **63**:495-509.
89. **Ma M, Liu Z, Moon J.** 2012. Genetic engineering of inhibitor-tolerant *Saccharomyces cerevisiae* for improved xylose utilization in ethanol production. *BioEnergy Research* DOI: **10.1007/s12155-011-9176-9**.
90. **Katahira S, Ito M, Takema H, Fujita Y, Tanino T, Tanaka T, Fukuda H, Kondo A.** 2008. Improvement of ethanol productivity during xylose and glucose co-fermentation by xylose-assimilating *S. cerevisiae* via expression of glucose transporter Sut1. *Enzyme and Microbial Technology* **43**:115-119.
91. **Zhang M, Eddy C, Deanda K, Finkelstein M, Picataggio S.** 1995. Metabolic engineering of a pentose metabolism pathway in ethanologenic *Zymomonas mobilis*. *Science* **267**:240-243.
92. **Agrawal M, Mao Z, Chen RR.** 2011. Adaptation yields a highly efficient xylose-fermenting *Zymomonas mobilis* strain. *Biotechnology and Bioengineering* **108**:777-785.
93. **Tao H, Gonzalez R, Martinez A, Rodriguez M, Ingram LO, Preston JF, Shanmugam KT.** 2001. Engineering a homo-ethanol pathway in *Escherichia coli*: increased glycolytic flux and levels of expression of glycolytic genes during xylose fermentation. *Journal of Bacteriology* **183**:2979-2988.
94. **Ohta K, Beall DS, Mejia JP, Shanmugam KT, Ingram LO.** 1991. Metabolic engineering of *Klebsiella oxytoca* M5A1 for ethanol production from xylose and glucose. *Applied and environmental microbiology* **57**:2810-2815.
95. **Golias H, Dumsday GJ, Stanley GA, Pamment NB.** 2002. Evaluation of a recombinant *Klebsiella oxytoca* strain for ethanol production from cellulose by simultaneous saccharification and fermentation: comparison with native cellobiose-utilising yeast strains and performance in co-culture with thermotolerant yeast and *Zymomonas mobilis*. *Journal of Biotechnology* **96**:155-168.
96. **Carraretto C, Macor A, Mirandola A, Stoppato A, Tonon S.** 2004. Biodiesel as alternative fuel: experimental analysis and energetic evaluations. *Energy* **29**:2195-2211.
97. **Gerhard K.** 2010. Biodiesel and renewable diesel: a comparison. *Progress in Energy and Combustion Science* **36**:364-373.
98. **Kalscheuer R, Stölting T, Steinbüchel A.** 2006. Microdiesel: *Escherichia coli* engineered for fuel production. *Microbiology* **152**:2529-2536.

99. **Elbahloul Y, Steinbüchel A.** 2010. Pilot-scale production of fatty acid ethyl esters by an engineered *Escherichia coli* strain harboring the p(Microdiesel) plasmid. *Applied and Environmental Microbiology* **76**:4560-4565.
100. **Steen EJ, Kang Y, Bokinsky G, Hu Z, Schirmer A, McClure A, del Cardayre SB, Keasling JD.** 2010. Microbial production of fatty-acid-derived fuels and chemicals from plant biomass. *Nature* **463**:559-562.
101. **Cohen E, Arad S.** 1989. A closed system for outdoor cultivation of *Porphyridium*. *Biomass* **18**:59-67.
102. **Ugwu CU, Aoyagi H, Uchiyama H.** 2008. Photobioreactors for mass cultivation of algae. *Bioresource Technology* **99**:4021-4028.
103. **Brennan L, Owende P.** 2010. Biofuels from microalgae—A review of technologies for production, processing, and extractions of biofuels and co-products. *Renewable and Sustainable Energy Reviews* **14**:557-577.
104. **Wijffels RH, Barbosa MJ.** 2010. An outlook on microalgal biofuels. *Science* **329**:796-799.
105. **Schmidt JE, Mladenovska Z, Lange M, Ahring BK.** 2000. Acetate conversion in anaerobic biogas reactors: traditional and molecular tools for studying this important group of anaerobic microorganisms. *Biodegradation* **11**:359-364.
106. **Börjesson P, Mattiasson B.** 2008. Biogas as a resource-efficient vehicle fuel. *Trends in Biotechnology* **26**:7-13.
107. **Persson M, Jönsson O, Wellinger A.** 2006. Biogas upgrading to vehicle fuel standards and grid injection. IEA Bioenergy, Task 37 – Energy from Biogas and Landfill Gas.
108. **Lütke-Eversloh T, Bahl H.** 2011. Metabolic engineering of *Clostridium acetobutylicum*: recent advances to improve butanol production. *Current Opinion in Biotechnology* **22**:634-647.
109. **Dürre P.** 2011. Fermentative production of butanol: the academic perspective. *Current Opinion in Biotechnology* **22**:331-336.
110. **Patakova P, Linhova M, Rychtera M, Paulova L, Melzoch K.** 2012. Novel and neglected issues of acetone–butanol–ethanol (ABE) fermentation by clostridia: *Clostridium* metabolic diversity, tools for process mapping and continuous fermentation systems. *Biotechnology Advances* DOI:10.1016/j.biotechadv.2012.01.010.
111. **Jiang Y, Xu C, Dong F, Yang Y, Jiang W, Yang S.** 2009. Disruption of the acetoacetate decarboxylase gene in solvent-producing *Clostridium acetobutylicum* increases the butanol ratio. *Metabolic Engineering* **11**:284-291.
112. **Lee JY, Jang Y-S, Lee J, Papoutsakis ET, Lee SY.** 2009. Metabolic engineering of *Clostridium acetobutylicum* M5 for highly selective butanol production. *Biotechnology Journal* **4**:1432-1440.
113. **Sillers R, Chow A, Tracy B, Papoutsakis ET.** 2008. Metabolic engineering of the non-sporulating, non-solventogenic *Clostridium acetobutylicum* strain M5 to produce butanol without acetone demonstrate the robustness of the acid-formation pathways and the importance of the electron balance. *Metabolic Engineering* **10**:321-332.
114. **López-Contreras AM, Smidt H, van der Oost J, Claassen PAM, Mooibroek H, de Vos WM.** 2001. *Clostridium beijerinckii* cells expressing neocallimastix patriciarum glycoside hydrolases show enhanced lichenan utilization and solvent production. *Applied and Environmental Microbiology* **67**:5127-5133.
115. **Tomas CA, Welker NE, Papoutsakis ET.** 2003. Overexpression of groESL in *Clostridium acetobutylicum* results in increased solvent production and tolerance, prolonged Metabolism, and changes in the cell's transcriptional program. *Applied and Environmental Microbiology* **69**:4951-4965.

116. **Inui M, Suda M, Kimura S, Yasuda K, Suzuki H, Toda H, Yamamoto S, Okino S, Suzuki N, Yukawa H.** 2008. Expression of *Clostridium acetobutylicum* butanol synthetic genes in *Escherichia coli*. *Applied Microbiology and Biotechnology* **77**:1305-1316.
117. **Shen CR, Lan EI, Dekishima Y, Baez A, Cho KM, Liao JC.** 2011. Driving forces enable high-titer anaerobic 1-butanol synthesis in *Escherichia coli*. *Applied and Environmental Microbiology* **77**:2905-2915.
118. **Nielsen DR, Leonard E, Yoon S-H, Tseng H-C, Yuan C, Prather KLJ.** 2009. Engineering alternative butanol production platforms in heterologous bacteria. *Metabolic Engineering* **11**:262-273.
119. **Berezina O, Zakharova N, Brandt A, Yarotsky S, Schwarz W, Zverlov V.** 2010. Reconstructing the clostridial n-butanol metabolic pathway in *Lactobacillus brevis*. *Applied Microbiology and Biotechnology* **87**:635-646.
120. **Steen E, Chan R, Prasad N, Myers S, Petzold C, Redding A, Ouellet M, Keasling J.** 2008. Metabolic engineering of *Saccharomyces cerevisiae* for the production of n-butanol. *Microbial Cell Factories* **7**:1-36.
121. **Balat H, Kirtay E.** 2010. Hydrogen from biomass – present scenario and future prospects. *International Journal of Hydrogen Energy* **35**:7416-7426.
122. **Kapdan IK, Kargi F.** 2006. Bio-hydrogen production from waste materials. *Enzyme and Microbial Technology* **38**:569-582.
123. **Navarro RM, Sanchez-Sanchez MC, Alvarez-Galvan MC, Valle Fd, Fierro JLG.** 2009. Hydrogen production from renewable sources: biomass and photocatalytic opportunities. *Energy and Environmental Science* **2**:35-54.
124. **Ni M, Leung DY, Leung MKH, Sumathy K.** 2006. An overview of hydrogen production from biomass. *Fuel Processing Technology* **87**:461-472.
125. **Srirangan K, Pyne ME, Chou CP.** 2011. Biochemical and genetic engineering strategies to enhance hydrogen production in photosynthetic algae and cyanobacteria. *Bioresource Technology* **102**:8589-8604.
126. **Zhang K, Sawaya MR, Eisenberg DS, Liao JC.** 2008. Expanding metabolism for biosynthesis of nonnatural alcohols. *Proceedings of the National Academy of Sciences of the United States of America*:20653–20658.
127. **Dewick PM.** 1999. The biosynthesis of C5-C25 terpenoid compounds. *Natural Product Reports* **16**.
128. **Jojima T, Inui M, Yukawa H.** 2008. Production of isopropanol by metabolically engineered *Escherichia coli*. *Applied Microbiology and Biotechnology* **77**:1219-1224.
129. **Inokuma K, Liao JC, Okamoto M, Hanai T.** 2010. Improvement of isopropanol production by metabolically engineered *Escherichia coli* using gas stripping. *J Biosci Bioeng* **110**:696-701.
130. **Hanai T, Atsumi S, Liao JC.** 2007. Engineered synthetic pathway for isopropanol production in *Escherichia coli*. *Applied and Environmental Microbiology* **73**:7814-7818.
131. **Wang Z, Sun J, Zhang A, Yang ST.** 2013. Propionic acid fermentation. *Bioprocessing Technologies in Biorefinery for Sustainable Production of Fuels, Chemicals, and Polymers*:331-350.
132. **McKie N, Keep N, Patchett M, Leadlay P.** 1990. Adenosylcobalamin-dependent methylmalonyl-CoA mutase from *Propionibacterium shermanii*. Active holoenzyme produced from *Escherichia coli*. *Biochemical Journal* **269**:293-298.
133. **Otzen C, Bardl B, Jacobsen ID, Nett M, Brock M.** 2014. *Candida albicans* Utilizes a Modified β -Oxidation Pathway for the Degradation of Toxic Propionyl-CoA. *Journal of Biological Chemistry* **289**:8151-8169.

134. **Jun Choi Y, Hwan Park J, Yong Kim T, Yup Lee S.** 2012. Metabolic engineering of *Escherichia coli* for the production of 1-propanol. *Metabolic Engineering* **14**:477-486.
135. **Smallwood I.** 2012. Handbook of organic solvent properties. Butterworth-Heinemann.
136. **Shen CR, Liao JC.** 2008. Metabolic engineering of *Escherichia coli* for 1-butanol and 1-propanol production via the keto-acid pathways. *Metabolic Engineering* **10**:312-320.
137. **Janssen PH.** 2004. Propanol as an end product of threonine fermentation. *Archives of Microbiology* **182**:482-486.
138. **Howell DM, Xu HM, White RH.** 1999. (R)-citramalate synthase in methanogenic archaea. *Journal of Bacteriology* **181**:331-333.
139. **Atsumi S, Liao JC.** 2008. Directed evolution of *Methanococcus jannaschii* citramalate synthase for biosynthesis of 1-propanol and 1-butanol by *Escherichia coli*. *Applied and Environmental Microbiology* **74**:7802-7808.
140. **Shen CR, Liao JC.** 2013. Synergy as design principle for metabolic engineering of 1-propanol production in *Escherichia coli*. *Metabolic Engineering* **17**:12-22.
141. **Rahman M, Hasan MR, Oba T, Shimizu K.** 2006. Effect of rpoS gene knockout on the metabolism of *Escherichia coli* during exponential growth phase and early stationary phase based on gene expressions, enzyme activities and intracellular metabolite concentrations. *Biotechnology and Bioengineering* **94**:585-595.
142. **Shen C, Liao J.** 2008. Metabolic engineering of *Escherichia coli* for 1-butanol and 1-propanol production via the keto-acid pathways. *Metabolic Engineering* **10**:312-320.
143. **Jain R, Yan Y.** 2011. Dehydratase mediated 1-propanol production in metabolically engineered *Escherichia coli*. *Microbial Cell Factories* **10**:1-10.
144. **Deng Y, Fong SS.** 2011. Metabolic engineering of *Thermobifida fusca* for direct aerobic bioconversion of untreated lignocellulosic biomass to 1-propanol. *Metabolic Engineering* **13**:570-577.
145. **Shen C, Liao J.** 2013. Synergy as design principle for metabolic engineering of 1-propanol production in *Escherichia coli*. *Metabolic Engineering* **17** 12–22.
146. **Di Masi DR, White JC, Schnaitman CA, Bradbeer C.** 1973. Transport of vitamin B₁₂ in *Escherichia coli*: Common receptor sites for vitamin B₁₂ and the E Colicins on the outer membrane of the cell envelope. *Journal of Bacteriology* **115**:506-513.
147. **Raux E, Lanois A, Levillayer F, Warren MJ, Brody E, Rambach A, Thermes C.** 1996. *Salmonella typhimurium* cobalamin (vitamin B₁₂) biosynthetic genes: functional studies in *S. typhimurium* and *Escherichia coli*. *Journal of Bacteriology* **178**:753-767.
148. **Froese D, Dobson C, White A, Wu X, Padovani D, Banerjee R, Haller T, Gerlt J, Surette M, Gravel R.** 2009. Sleeping beauty mutase *sbm* is expressed and interacts with *ygfD* in *Escherichia coli*. *Microbiological research* **164**:1-8.
149. **Clark DP.** 1989. The fermentation pathways of *Escherichia coli*. *FEMS Microbiology Letters* **63**:223-234.
150. **Miller JH.** 1992. A short course in bacterial genetics: a laboratory manual and handbook for *Escherichia coli* and related bacteria, vol. 1. Cold Spring Harbor Laboratory Pr.
151. **Barnard RT.** 2005. Chimerization of multiple antibody classes using splice overlap extension PCR. *Biotechniques* **38**:181-182.
152. **Baba T, Ara T, Hasegawa M, Takai Y, Okumura Y, Baba M, Datsenko KA, Tomita M, Wanner BL, Mori H.** 2006. Construction of *Escherichia coli* K-12 in-frame, single-gene knockout mutants: the Keio collection. *Molecular systems biology* **2**:1-11.
153. **Datsenko KA, Wanner BL.** 2000. One-step inactivation of chromosomal genes in *Escherichia coli* K-12 using PCR products. *Proceedings of the National Academy of Sciences* **97**:6640-6645.

154. **Casadaban MJ.** 1976. Transposition and fusion of the lac genes to selected promoters in *Escherichia coli* using bacteriophage lambda and Mu. *Journal of Molecular Biology* **104**:541-555.
155. **Cherepanov PP, Wackernagel W.** 1995. Gene disruption in *Escherichia coli*: Tc^R and Km^R cassettes with the option of Flp-catalyzed excision of the antibiotic-resistance determinant. *Gene* **158**:9-14.
156. **Jobling MG, Holmes RK.** 1990. Construction of vectors with the p15A replicon, kanamycin resistance, inducible lacZ α and pUC18 or pUC19 multiple cloning sites. *Nucleic Acids Research* **18**:5315-5316.
157. **Kovach ME, Elzer PH, Steven Hill D, Robertson GT, Farris MA, Roop II RM, Peterson KM.** 1995. Four new derivatives of the broad-host-range cloning vector pBBR1MCS, carrying different antibiotic-resistance cassettes. *Gene* **166**:175-176.
158. **Atsumi S, Wu T-Y, Eckl E-M, Hawkins SD, Buelter T, Liao JC.** 2010. Engineering the isobutanol biosynthetic pathway in *Escherichia coli* by comparison of three aldehyde reductase/alcohol dehydrogenase genes. *Applied microbiology and biotechnology* **85**:651-657.
159. **Schomburg I, Chang A, Ebeling C, Gremse M, Heldt C, Huhn G, Schomburg D.** 2004. BRENDA, the enzyme database: updates and major new developments. *Nucleic Acids Research* **32**:D431-D433.
160. **Membrillo-Hernández J, Echave P, Cabisco E, Tamarit J, Ros J, Lin EC.** 2000. Evolution of the *adhE* gene product of *Escherichia coli* from a functional reductase to a dehydrogenase. *Journal of Biological Chemistry* **275**:33869-33875.
161. **Dürre P.** 2007. Biobutanol: an attractive biofuel. *Biotechnology Journal* **2**:1525-1534.
162. **Dayem LC, Carney JR, Santi DV, Pfeifer BA, Khosla C, Kealey JT.** 2002. Metabolic engineering of a methylmalonyl-CoA mutase-epimerase pathway for complex polyketide biosynthesis in *Escherichia coli*. *Biochemistry* **41**:5193-5201.
163. **Havemann GD, Sampson EM, Bobik TA.** 2002. PduA is a shell protein of polyhedral organelles involved in coenzyme B₁₂-dependent degradation of 1,2-propanediol in *Salmonella enterica* serovar *Typhimurium* LT2. *Journal of Bacteriology* **184**:1253-1261.
164. **Skraly FA, Lytle BL, Cameron DC.** 1998. Construction and characterization of a 1,3-propanediol operon. *Applied and environmental microbiology* **64**:98-105.
165. **Neidhardt FC, Ingraham JL, Schaechter M.** 1990. *Physiology of the bacterial cell: a molecular approach*. Sinauer Associates Sunderland, MA.
166. **Sánchez AM, Bennett GN, San K-Y.** 2005. Novel pathway engineering design of the anaerobic central metabolic pathway in *Escherichia coli* to increase succinate yield and productivity. *Metabolic Engineering* **7**:229-239.
167. **Moon SY, Hong SH, Kim TY, Lee SY.** 2008. Metabolic engineering of *Escherichia coli* for the production of malic acid. *Biochemical Engineering Journal* **40**:312-320.
168. **Hidber E, Brownie ER, Hayakawa K, Fraser ME.** 2007. Participation of Cys123 of *Escherichia coli* succinyl-CoA synthetase in catalysis. *Acta Crystallographica Section D: Biological Crystallography* **63**:876-884.
169. **Fiege H, Voges H, Hamamoto T.** 2002. *Ullmann's encyclopedia of industrial chemistry*. Federal Republic of Germany, AG Bayer **19**:324.
170. **Fernando S, Adhikari S, Kota K, Bandi R.** 2007. Glycerol based automotive fuels from future biorefineries. *Fuel* **86**:2806-2809.
171. **Rase HF.** 2000. *Handbook of commercial catalysts: heterogeneous catalysts*. CRC press, Boca Raton, Florida.

172. **Jarboe LR, Zhang X, Wang X, Moore JC, Shanmugam K, Ingram LO.** 2010. Metabolic engineering for production of biorenewable fuels and chemicals: contributions of synthetic biology. *Journal of Biomedicine and Biotechnology* **2010**:1-18.
173. **Srirangan K, Akawi L, Liu X, Westbrook A, Blondeel EJ, Aucoin MG, Moo-Young M, Chou CP.** 2013. Manipulating the sleeping beauty mutase operon for the production of 1-propanol in engineered *Escherichia coli*. *Biotechnology for Biofuels* **6**:139.
174. **Jones KL, Kim S-W, Keasling J.** 2000. Low-copy plasmids can perform as well as or better than high-copy plasmids for metabolic engineering of bacteria. *Metabolic Engineering* **2**:328-338.
175. **Ow DS-W, Nissom PM, Philp R, Oh SK-W, Yap MG-S.** 2006. Global transcriptional analysis of metabolic burden due to plasmid maintenance in *Escherichia coli* DH5 α during batch fermentation. *Enzyme and Microbial Technology* **39**:391-398.
176. **Glick BR.** 1995. Metabolic load and heterologous gene expression. *Biotechnology Advances* **13**:247-261.
177. **Sukhija K, Pyne M, Ali S, Orr V, Abedi D, Moo-Young M, Chou CP.** 2012. Developing an extended genomic engineering approach based on recombineering to knock-in heterologous genes to *Escherichia coli* genome. *Molecular Biotechnology* **51**:109-118.
178. **Hanahan D.** 1983. Studies on transformation of *Escherichia coli* with plasmids. *Journal of Molecular Biology* **166**:557-580.
179. **Neidhardt FC, Bloch PL, Smith DF.** 1974. Culture medium for enterobacteria. *Journal of Bacteriology* **119**:736-747.
180. **Amann E, Ochs B, Abel K-J.** 1988. Tightly regulated *tac* promoter vectors useful for the expression of unfused and fused proteins in *Escherichia coli*. *Gene* **69**:301-315.
181. **Jantama K, Zhang X, Moore J, Shanmugam K, Svoronos S, Ingram L.** 2008. Eliminating side products and increasing succinate yields in engineered strains of *Escherichia coli* C. *Biotechnology and Bioengineering* **101**:881-893.
182. **da Silva GP, Mack M, Contiero J.** 2009. Glycerol: a promising and abundant carbon source for industrial microbiology. *Biotechnology Advances* **27**:30-39.
183. **Clomburg JM, Gonzalez R.** 2011. Metabolic engineering of *Escherichia coli* for the production of 1,2-propanediol from glycerol. *Biotechnology and Bioengineering* **108**:867-879.
184. **van de Walle M, Shiloach J.** 1998. Proposed mechanism of acetate accumulation in two recombinant *Escherichia coli* strains during high density fermentation. *Biotechnology and Bioengineering* **57**:71-78.
185. **Korz D, Rinas U, Hellmuth K, Sanders E, Deckwer W-D.** 1995. Simple fed-batch technique for high cell density cultivation of *Escherichia coli*. *Journal of Biotechnology* **39**:59-65.
186. **Cintolesi A, Clomburg JM, Rigou V, Zygorakis K, Gonzalez R.** 2012. Quantitative analysis of the fermentative metabolism of glycerol in *Escherichia coli*. *Biotechnology and Bioengineering* **109**:187-198.
187. **Dharmadi Y, Murarka A, Gonzalez R.** 2006. Anaerobic fermentation of glycerol by *Escherichia coli*: a new platform for metabolic engineering. *Biotechnology and Bioengineering* **94**:821-829.
188. **Murarka A, Dharmadi Y, Yazdani SS, Gonzalez R.** 2008. Fermentative utilization of glycerol by *Escherichia coli* and its implications for the production of fuels and chemicals. *Applied and Environmental Microbiology* **74**:1124-1135.
189. **Song H, Lee SY.** 2006. Production of succinic acid by bacterial fermentation. *Enzyme and Microbial Technology* **39**:352-361.
190. **Chao Y, Patnaik R, Roof W, Young R, Liao J.** 1993. Control of gluconeogenic growth by *pps* and *pck* in *Escherichia coli*. *Journal of Bacteriology* **175**:6939-6944.

191. **Brock M, Maerker C, Schütz A, Völker U, Buckel W.** 2002. Oxidation of propionate to pyruvate in *Escherichia coli*. *European Journal of Biochemistry* **269**:6184-6194.
192. **Bond-Watts BB, Bellerose RJ, Chang MC.** 2011. Enzyme mechanism as a kinetic control element for designing synthetic biofuel pathways. *Nature Chemical Biology* **7**:222-227.
193. **Lee JW, Na D, Park JM, Lee J, Choi S, Lee SY.** 2012. Systems metabolic engineering of microorganisms for natural and non-natural chemicals. *Nature Chemical Biology* **8**:536-546.
194. **Hoell D, Mensing T, Roggenbuck R, Sakuth M, Sperlich E, Urban T, Neier W, Strehlke G.** 2000. 2-Butanone. Wiley-VCH Verlag, Weinheim.
195. **Mueller A, Koepke M, Liew F.** 2013. Recombinant microorganisms and uses therefor. United States Patent: 0330809 A1.
196. **Yoneda H, Tantillo DJ, Atsumi S.** 2014. Biological Production of 2-Butanone in *Escherichia coli*. *ChemSusChem* **7**:92-95.
197. **Ghiaci P, Norbeck J, Larsson C.** 2014. 2-Butanol and Butanone production in *Saccharomyces cerevisiae* through combination of a B₁₂ dependent dehydratase and a secondary alcohol dehydrogenase using a TEV-based expression system. *PLoS ONE* **9**:e102774.
198. **Pfeifer BA, Admiraal SJ, Gramajo H, Cane DE, Khosla C.** 2001. Biosynthesis of complex polyketides in a metabolically engineered strain of *E. coli*. *Science* **291**:1790-1792.
199. **Srirangan K, Liu X, Westbrook A, Akawi L, Pyne M, Moo-Young M, Chou CP.** 2014. Biochemical, genetic, and metabolic engineering strategies to enhance coproduction of 1-propanol and ethanol in engineered *Escherichia coli*. *Applied Microbiology and Biotechnology* **98**:9499-9515.
200. **Slater S, Houmiel KL, Tran M, Mitsky TA, Taylor NB, Padgett SR, Gruys KJ.** 1998. Multiple β -ketothiolases mediate poly (β -hydroxyalkanoate) copolymer synthesis in *Ralstonia eutropha*. *Journal of Bacteriology* **180**:1979-1987.
201. **Bermejo LL, Welker NE, Papoutsakis ET.** 1998. Expression of *Clostridium acetobutylicum* ATCC 824 Genes in *Escherichia coli* for acetone production and acetate peroxidation. *Applied and Environmental Microbiology* **64**:1079-1085.
202. **Gibson DG, Young L, Chuang R-Y, Venter JC, Hutchison CA, Smith HO.** 2009. Enzymatic assembly of DNA molecules up to several hundred kilobases. *Nature Methods* **6**:343-345.
203. **Bolstad BM, Irizarry RA, Åstrand M, Speed TP.** 2003. A comparison of normalization methods for high density oligonucleotide array data based on variance and bias. *Bioinformatics* **19**:185-193.
204. **Gautier L, Cope L, Bolstad BM, Irizarry RA.** 2004. affy—analysis of Affymetrix GeneChip data at the probe level. *Bioinformatics* **20**:307-315.
205. **Irizarry RA, Hobbs B, Collin F, Beazer-Barclay YD, Antonellis KJ, Scherf U, Speed TP.** 2003. Exploration, normalization, and summaries of high density oligonucleotide array probe level data. *Biostatistics* **4**:249-264.
206. **Durnin G, Clomburg J, Yeates Z, Alvarez PJJ, Zygorakis K, Campbell P, Gonzalez R.** 2009. Understanding and harnessing the microaerobic metabolism of glycerol in *Escherichia coli*. *Biotechnology and Bioengineering* **103**:148-161.
207. **Braunegg G, Sonnleitner By, Lafferty R.** 1978. A rapid gas chromatographic method for the determination of poly- β -hydroxybutyric acid in microbial biomass. *Applied Microbiology and Biotechnology* **6**:29-37.
208. **Felnagle EA, Chaubey A, Noey EL, Houk KN, Liao JC.** 2012. Engineering synthetic recursive pathways to generate non-natural small molecules. *Nature Chemical Biology* **8**:518-526.
209. **Weber AL.** 1991. Origin of fatty acid synthesis: thermodynamics and kinetics of reaction pathways. *Journal of Molecular Evolution* **32**:93-100.

210. **Wiesenborn DP, Rudolph F, Papoutsakis E.** 1989. Coenzyme A transferase from *Clostridium acetobutylicum* ATCC 824 and its role in the uptake of acids. Applied and Environmental Microbiology **55**:323-329.
211. **McCleary WR, Stock JB, Ninfa AJ.** 1993. Is acetyl phosphate a global signal in *Escherichia coli*? Journal of Bacteriology **175**:2793-2798.
212. **Pfleger BF, Gossing M, Nielsen J.** 2015. Metabolic engineering strategies for microbial synthesis of oleochemicals. Metabolic Engineering **29**:1-11.
213. **Marcheschi RJ, Li H, Zhang K, Noey EL, Kim S, Chaubey A, Houk K, Liao JC.** 2012. A synthetic recursive “+ 1” pathway for carbon chain elongation. ACS Chemical Biology **7**:689-697.
214. **Bermejo LL, Welker NE, Papoutsakis ET.** 1998. Expression of *Clostridium acetobutylicum* ATCC 824 Genes in *Escherichia coli* for acetone production and acetate detoxification. Applied and Environmental Microbiology **64**:1079-1085.
215. **Brown TDK, Jones-Mortimer MC, Kornberg HL.** 1977. The enzymic interconversion of acetate and acetyl-coenzyme A in *Escherichia coli*. Journal of General Microbiology **102**:327-336.
216. **May A, Fischer R-J, Thum SM, Schaffer S, Verseck S, Dürre P, Bahl H.** 2013. A modified pathway for the production of acetone in *Escherichia coli*. Metabolic Engineering **15**:218-225.
217. **Mifune J, Nakamura S, Fukui T.** 2010. Engineering of pha operon on *Cupriavidus necator* chromosome for efficient biosynthesis of poly (3-hydroxybutyrate-co-3-hydroxyhexanoate) from vegetable oil. Polym Degrad and Stabil **95**:1305-1312.
218. **Shams Yazdani S, Gonzalez R.** 2008. Engineering *Escherichia coli* for the efficient conversion of glycerol to ethanol and co-products. Metabolic Engineering **10**:340-351.
219. **Zhang X, Shanmugam KT, Ingram LO.** 2010. Fermentation of glycerol to succinate by metabolically engineered strains of *Escherichia coli*. Applied and Environmental Microbiology **76**:2397-2401.
220. **Seo M-Y, Seo J-W, Heo S-Y, Baek J-O, Rairakhwada D, Oh B-R, Seo P-S, Choi MH, Kim CH.** 2009. Elimination of by-product formation during production of 1, 3-propanediol in *Klebsiella pneumoniae* by inactivation of glycerol oxidative pathway. Applied Microbiology and Biotechnology **84**:527-534.
221. **Causey T, Shanmugam K, Yomano L, Ingram L.** 2004. Engineering *Escherichia coli* for efficient conversion of glucose to pyruvate. Proceedings of the National Academy of Sciences of the United States of America **101**:2235-2240.
222. **Mazumdar S, Clomburg JM, Gonzalez R.** 2010. *Escherichia coli* strains engineered for homofermentative production of D-Lactic acid from glycerol. Applied and Environmental Microbiology **76**:4327-4336.
223. **Kotani T, Yurimoto H, Kato N, Sakai Y.** 2007. Novel acetone metabolism in a propane-utilizing bacterium, *Gordonia* sp. strain TY-5. Journal of Bacteriology **189**:886-893.
224. **Hanai T, Atsumi S, Liao J.** 2007. Engineered synthetic pathway for isopropanol production in *Escherichia coli*. Applied and Environmental Microbiology **73**:7814-7818.
225. **Akawi L, Srirangan K, Liu X, Moo-Young M, Chou CP.** 2015. Engineering *Escherichia coli* for high-level production of propionate. Journal of Industrial Microbiology and Biotechnology **42**:1057-1072.
226. **Yang JE, Choi YJ, Lee SJ, Kang K-H, Lee H, Oh YH, Lee SH, Park SJ, Lee SY.** 2014. Metabolic engineering of *Escherichia coli* for biosynthesis of poly (3-hydroxybutyrate-co-3-hydroxyvalerate) from glucose. Applied Microbiology and Biotechnology **98**:95-104.
227. **Keshavarz T, Roy I.** 2010. Polyhydroxyalkanoates: bioplastics with a green agenda. Current Opinion in Microbiology **13**:321-326.

228. **Schenck HU.** 2003, p 19-24. Macromolecular Symposia.
229. **Luo R, Chen J, Zhang L, Chen G.** 2006. Polyhydroxyalkanoate copolyesters produced by *Ralstonia eutropha* PHB-4 harboring a low-substrate-specificity PHA synthase PhaC2 Ps from *Pseudomonas stutzeri* 1317. *Biochemical Engineering Journal* **32**:218-225.
230. **Dennis DE, Klomparens K.** 1992. Polyhydroxybutyrate, a biodegradable thermoplastic, produced in transgenic plants. *Science* **256**:520.
231. **Chen G-Q.** 2010. Industrial production of PHA, p. 121-132, *Plastics from bacteria*. Springer.
232. **Sin MC, Tan IKP, Annuar MSM, Gan SN.** 2012. Thermal behaviour and thermodegradation kinetics of poly (vinyl chloride) plasticized with polymeric and oligomeric medium-chain-length poly (3-hydroxyalkanoates). *Polymer Degradation and Stability* **97**:2118-2127.
233. **Rincones J, Zeidler AF, Grassi MCB, Carazzolle MF, Pereira GA.** 2009. The golden bridge for nature: the new biology applied to bioplastics. *Journal of Macromolecular Science* **49**:85-106.
234. **Noda I, Lindsey SB, Caraway D.** 2010. Nodax™ class PHA copolymers: their properties and applications, p. 237-255, *Plastics from Bacteria*. Springer.
235. **Guo M, Stuckey D, Murphy R.** 2013. Is it possible to develop biopolymer production systems independent of fossil fuels? Case study in energy profiling of polyhydroxybutyrate-valerate (PHBV). *Green Chemistry* **15**:706-717.
236. **Du C, Sabirova J, Soetaert W, Ki Carol Lin S.** 2012. Polyhydroxyalkanoates production from low-cost sustainable raw materials. *Current Chemical Biology* **6**:14-25.
237. **Tseng H-C, Harwell CL, Martin CH, Prather KL.** 2010. Biosynthesis of chiral 3-hydroxyvalerate from single propionate-unrelated carbon sources in metabolically engineered *E. coli*. *Microbial Cell Factories* **9**:96.
238. **Ahankari SS, Mohanty AK, Misra M.** 2011. Mechanical behaviour of agro-residue reinforced poly (3-hydroxybutyrate-co-3-hydroxyvalerate),(PHBV) green composites: A comparison with traditional polypropylene composites. *Composites Science and Technology* **71**:653-657.
239. **Brock M.** 2010. 71 Role of Cellular Control of Propionyl-CoA Levels for Microbial Pathogenesis.
240. **Mifune J, Nakamura S, Fukui T.** 2010. Engineering of pha operon on *Cupriavidus necator* chromosome for efficient biosynthesis of poly (3-hydroxybutyrate-co-3-hydroxyhexanoate) from vegetable oil. *Polymer Degradation and Stability* **95**:1305-1312.
241. **Lau N-S, Ch'ng DH-E, Chia K-H, Wong Y-M, Sudesh K.** 2014. Advances in Polyhydroxyalkanoate (PHA): Unraveling the Development and New Perspectives. *Journal of Biobased Materials and Bioenergy* **8**:118-129.
242. **Snell KD, Peoples OP.** 2009. PHA bioplastic: A value-added coproduct for biomass biorefineries. *Biofuels, Bioproducts and Biorefining* **3**:456-467.
243. **Wang Q, Liu X, Qi Q.** 2014. Biosynthesis of poly (3-hydroxybutyrate-co-3-hydroxyvalerate) from glucose with elevated 3-hydroxyvalerate fraction via combined citramalate and threonine pathway in *Escherichia coli*. *Applied Microbiology and Biotechnology* **98**:3923-3931.
244. **Heinrich D, Raberg M, Steinbüchel A.** 2015. Synthesis of poly (3-hydroxybutyrate-co-3-hydroxyvalerate) from unrelated carbon sources in engineered *Rhodospirillum rubrum*. *FEMS Microbiology Letters* **362**:fnnv038.
245. **Slater S, Mitsky TA, Houmiel KL, Hao M, Reiser SE, Taylor NB, Tran M, Valentin HE, Rodriguez DJ, Stone DA.** 1999. Metabolic engineering of *Arabidopsis* and *Brassica* for poly (3-hydroxybutyrate-co-3-hydroxyvalerate) copolymer production. *Nature Biotechnology* **17**:1011-1016.
246. **Snell KD, Peoples OP.** 2002. Polyhydroxyalkanoate Polymers and Their Production in Transgenic Plants. *Metabolic Engineering* **4**:29-40.

247. **Batool N, Ilyas N.** 2014. Polyhydroxyalkanoates from Plants and Microorganisms. *International Journal of Biosciences* **5**:298-307.
248. **Tseng H-C, Prather KL.** 2012. Controlled biosynthesis of odd-chain fuels and chemicals via engineered modular metabolic pathways. *Proceedings of the National Academy of Sciences of the United States of America* **109**:17925-17930.
249. **Tseng HC, Harwell CL, Martin CH, Prather KL.** 2010. Biosynthesis of chiral 3-hydroxyvalerate from single propionate-unrelated carbon sources in metabolically engineered *E. coli*. *Microbial Cell Factories* **9**:96.
250. **Tseng HC, Martin CH, Nielsen DR, Prather KL.** 2009. Metabolic engineering of *Escherichia coli* for enhanced production of (R)- and (S)-3-hydroxybutyrate. *Applied and Environmental Microbiology* **75**:3137-3145.
251. **Brenner K, You L, Arnold FH.** 2008. Engineering microbial consortia: a new frontier in synthetic biology. *Trends in Biotechnology* **26**:483-489.
252. **Cox M.** 1994. Properties and applications of polyhydroxyalkanoates. *Studies in Polymer Science* **12**:120-120.
253. **Leong YK, Show PL, Ooi CW, Ling TC, Lan JC-W.** 2014. Current trends in polyhydroxyalkanoates (PHAs) biosynthesis: Insights from the recombinant *Escherichia coli*. *Journal of Biotechnology* **180**:52-65.
254. **Aldor I, Keasling J.** 2001. Metabolic engineering of poly (3-hydroxybutyrate-co-3-hydroxyvalerate) composition in recombinant *Salmonella enterica serovar typhimurium*. *Biotechnology and Bioengineering* **76**:108-114.
255. **Hungund B, Shyama V, Patwardhan P, Saleh A.** 2013. Production of Polyhydroxy alkanoate from *Paenibacillus durus* BV-1 Isolated from Oil Mill Soil. *J Microb Biochem Tech* **5**:013-017.
256. **Chanprateep S, Katakura Y, Visetkoop S, Shimizu H, Kulpreecha S, Shioya S.** 2008. Characterization of new isolated *Ralstonia eutropha* strain A-04 and kinetic study of biodegradable copolyester poly (3-hydroxybutyrate-co-4-hydroxybutyrate) production. *Journal of Industrial Microbiology & Biotechnology* **35**:1205-1215.
257. **Yardley-Jones A, Anderson D, Jenkinson P.** 1988. Effect of occupational exposure to benzene on phytohaemagglutinin (PHA) stimulated lymphocytes in man. *British journal of industrial medicine* **45**:516-522.
258. **Thakur P, Borah B, Baruah S, Nigam J.** 2001. Growth-associated production of poly-3-hydroxybutyrate by *Bacillus mycooides*. *Folia Microbiologica* **46**:488-494.
259. **Kumari S, Beatty CM, Browning DF, Busby SJ, Simel EJ, Hovel-Miner G, Wolfe AJ.** 2000. Regulation of acetyl coenzyme A synthetase in *Escherichia coli*. *Journal of Bacteriology* **182**:4173-4179.
260. **Tashiro Y, Desai SH, Atsumi S.** 2015. Two-dimensional isobutyl acetate production pathways to improve carbon yield. *Nature Communications* **6**.
261. **Textor S, Wendisch VF, De Graaf AA, Müller U, Linder MI, Linder D, Buckel W.** 1997. Propionate oxidation in *Escherichia coli*: evidence for operation of a methylcitrate cycle in bacteria. *Archives of Microbiology* **168**:428-436.
262. **Claes WA, Pühler A, Kalinowski J.** 2002. Identification of two prpDBC gene clusters in *Corynebacterium glutamicum* and their involvement in propionate degradation via the 2-methylcitrate cycle. *Journal of Bacteriology* **184**:2728-2739.
263. **Yazdani SS, Gonzalez R.** 2008. Engineering *Escherichia coli* for the efficient conversion of glycerol to ethanol and co-products. *Metabolic Engineering* **10**:340-351.
264. **Blankschien MD, Clomburg JM, Gonzalez R.** 2010. Metabolic engineering of *Escherichia coli* for the production of succinate from glycerol. *Metabolic Engineering* **12**:409-419.

265. **Chao Y-P, Liao JC.** 1993. Alteration of growth yield by overexpression of phosphoenolpyruvate carboxylase and phosphoenolpyruvate carboxykinase in *Escherichia coli*. *Applied and Environmental Microbiology* **59**:4261-4265.
266. **Millard CS, Chao Y-P, Liao JC, Donnelly MI.** 1996. Enhanced production of succinic acid by overexpression of phosphoenolpyruvate carboxylase in *Escherichia coli*. *Applied and Environmental Microbiology* **62**:1808-1810.
267. **Stergiou P-Y, Foukis A, Filippou M, Koukouritaki M, Parapouli M, Theodorou LG, Hatziloukas E, Afendra A, Pandey A, Papamichael EM.** 2013. Advances in lipase-catalyzed esterification reactions. *Biotechnology advances* **31**:1846-1859.
268. **Fujii T, Nagasawa N, Iwamatsu A, Bogaki T, Tamai Y, Hamachi M.** 1994. Molecular cloning, sequence analysis, and expression of the yeast alcohol acetyltransferase gene. *Applied and Environmental Microbiology* **60**:2786-2792.
269. **Sakamuri R.** 2000. Esters, Organic, Kirk-Othmer Encyclopedia of Chemical Technology. John Wiley & Sons, Inc.
270. **Davis R, Biddy M, Tan E, Tao L, Jones S.** 2013. Biological conversion of sugars to hydrocarbons technology pathway. Golden, Colorado and Richland, Washington, USA: National Renewable Energy Laboratory and Pacific Northwest National Laboratory.
271. **Li N, Nørgaard H, Warui DM, Booker SJ, Krebs C, Bollinger Jr JM.** 2011. Conversion of fatty aldehydes to alkanes and formate by a cyanobacterial aldehyde decarbonylase: cryptic redox by an unusual dimetal oxygenase. *Journal of the American Chemical Society* **133**:6158-6161.
272. **Tornabene T.** 1982. Microorganisms as hydrocarbon producers, p. 49-52, *New Trends in research and utilization of solar energy through biological systems*. Springer.
273. **van Leeuwen BN, van der Wulp AM, Duijnste I, van Maris AJ, Straathof AJ.** 2012. Fermentative production of isobutene. *Appl Microbiol Biotechnol* **93**:1377-1387.
274. **Kallio P, Pásztor A, Thiel K, Akhtar MK, Jones PR.** 2014. An engineered pathway for the biosynthesis of renewable propane. *Nature Communications* **5**.
275. **Yoneda H, Tantillo DJ, Atsumi S.** 2014. Biological Production of 2-Butanone in *Escherichia coli*. *ChemSusChem* **7**:92-95.
276. **Lan EI, Dekishima Y, Chuang DS, Liao JC.** 2013. Metabolic engineering of 2-pentanone synthesis in *Escherichia coli*. *AIChE Journal* **59**:3167-3175.